

Report No. NS-67-1

**FINAL REPORT**

Project No. 231-001-01X

**TEST AND EVALUATION OF THE RADAR VIDEO DATA PROCESSOR**

AD658337

230  
570



JUNE 1967

ADDC  
RECEIVED  
SEP 20 1967  
RECEIVED

**DEPARTMENT OF TRANSPORTATION  
FEDERAL AVIATION ADMINISTRATION  
National Aviation Facilities Experimental Center  
Atlantic City, New Jersey 08405**

Reproduced by the  
CLEARINGHOUSE  
for Federal Scientific & Technical  
Information Springfield Va. 22151

180

**FINAL REPORT**

**TEST AND EVALUATION OF THE RADAR VIDEO DATA PROCESSOR**

**PROJECT NO. 231-001-01X  
REPORT NO. NS-67-1**

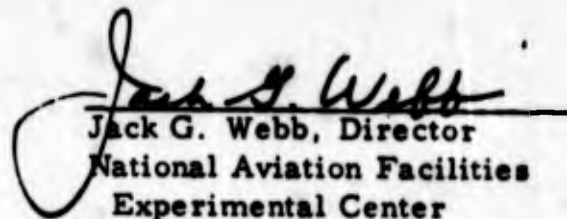
**Prepared by:**

**ALBERT A. LUPINETTI  
ROY P. SCHINDLER**

**Test and Evaluation Division**

**JUNE 1967**

**Distribution of this document is unlimited. This document does not necessarily reflect Federal Aviation Administration policy in all respects and it does not, in itself, constitute a standard, specification, or regulation.**

  
**Jack G. Webb, Director  
National Aviation Facilities  
Experimental Center**

**DEPARTMENT OF TRANSPORTATION  
Federal Aviation Administration  
National Aviation Facilities Experimental Center  
Atlantic City, New Jersey**

## FOREWORD

The testing, analysis and improvement of video digitizers is a dynamic process. As our knowledge of the digitizing phenomena is extended and as the state-of-the-art advances, more mature judgment can be exercised in selecting the optimum in digitizer design and testing.

This test program taught us much about the technical characteristics of digitizers and the art of testing digitizers. Instrumentation was developed to test parameters that had never been thoroughly tested before. Faster and more efficient data reduction and analysis techniques using digital computers evolved. And, as is generally the case in test programs with new devices, we learned that much remains to be done.

No claim is made that this document completely describes all technical aspects of the Radar Video Data Processor (RVDP). In some areas, the data may appear incomplete or insufficient. Nevertheless, the data are presented as collected and analyzed. Many of the important characteristics of the RVDP and digitizers in general are fully described. We feel that in spite of any limitations that the report may have, it is, nonetheless, a clear indication that digitizers are here to stay--that they can be made to adequately perform the functions of target detection and data transmission.

The program presently underway to test and evaluate the AN/FYQ-40 (Common Digitizer) is part of the continuing process to better understand the capabilities and limitations of digitizers. The degree of maturity that has been achieved in the testing of the RVDP will be present in the Common Digitizer test program

## TABLE OF CONTENTS

	Page
ABSTRACT	ix
SUMMARY	x
INTRODUCTION	1
Purpose	1
Background	1
Brief Description of RVDP	2
Test Program	2
DISCUSSION	4
Primary Radar Detection	4
Video Quantization	4
Description	5
Reference Level Control	7
Performance	10
Statistical Detection	11
Sliding Window Detector	11
Automatic Clutter Eliminator	14
Run Length Discriminator	14
Detector Performance with Controlled Inputs	19
Detector Performance On-Line	25
Beacon Detection	36
Pulse Detection	36
Amplitude Threshold	36
Pulse Width Threshold	37
Noise Response	37
Pulse Resolution	40
Bracket Detection	42
Target Detection	46
Description	46
Probability of Detection with Controlled Inputs	48
On-Line Tests of Probability of Detection	48
False Target Detection	50
Radar Reinforced Beacon Targets	55

## TABLE OF CONTENTS (continued)

	Page
Code Detection	56
Code Sampling	57
Garble Sensing	60
Emergency Code Detection	62
Code Validation	64
On-Line Tests of Code Detection	68
RVDP Performance Using Defruited Beacon Video	72
Probability of Detection	72
Code Validation	74
Mode Generation and Detection	78
Accuracy	79
Accuracy Checks with Controlled Inputs	79
Primary Radar Azimuth Accuracy	79
Beacon Azimuth Accuracy	80
Primary Radar Range Accuracy	82
Beacon Range Accuracy	84
On-Line Accuracy Tests	84
Range and Azimuth Accuracy	84
Accuracy as a Function of Range	87
Resolution	92
Resolution Checks with Controlled Inputs	92
Azimuth Resolution	92
Range Resolution	93
On-Line Resolution Tests	96
Target Split Rate	101
Data Transfer Capacity	104
Message Transfer Rate	104
Message Time-In-Storage	106
SUMMARY OF RESULTS	109
CONCLUSIONS	112
RECOMMENDATIONS	113
REFERENCES	115
ACKNOWLEDGMENT	116

**TABLE OF CONTENTS (continued)**

- APPENDIX I Radar Video Data Processor - System Design (8 pages)**
- APPENDIX II Modifications to the RVDP (4 pages)**
- APPENDIX III RVDP Maintainability and Availability (5 pages)**
- APPENDIX IV Test Environment (22 pages)**
- APPENDIX V Beacon System Description (5 pages)**
- APPENDIX VI Beacon Fruit Environment (6 pages)**
- APPENDIX VII Derivation of Azimuth Bias and Resolution Equation (4 pages)**

## LIST OF ILLUSTRATIONS

Figure		Page
1	Radar Video Quantizer Block Diagram	6
2	Percent Noise Vs. Video Noise Level	8
3	Voltage Waveforms at Quantizer Test Points	9
4	Probability of Quantizing Signal Plus Noise Vs. Percent Noise	12
5	Detector Block Diagram	13
6	Function Generator Transfer Characteristic	15
7	Run Length Distributions of Aircraft Targets	17
8	Run Length Distributions of Clutter Targets	18
9	Probability of Detection Vs. Percent Noise	20
10	False Target Rate Vs. Percent Noise	22
11	Probability of Detection Vs. False Target Rate	24
12	Primary Radar Sensitivity Curves	26
13	Primary Radar Sensitivity at Maximum Range	28
14	Comparison Between Digital Channel and Video Channel for Target Detection Within Areas of Weather Clutter	30
15	Digital Channel Display Presentation of Aircraft Targets and Weather Clutter Targets	32
16	Video Channel Display Presentation of Aircraft Targets and Weather Clutter	33
17	Digital Channel Display Presentation of Aircraft Targets and Weather Clutter Targets After One Antenna Scan	34

## LIST OF ILLUSTRATIONS (continued)

Figure		Page
18	Video Channel Display Presentation of Aircraft Targets and Weather Clutter After One Antenna Scan	35
19	Beacon Quantizer Amplitude Threshold Characteristics	38
20	Beacon Quantizer Noise Response	39
21	Beacon Quantizer Pulse Resolution	41
22	Unresolved Pulse Separation	43
23	Resolved Pulse Separation	44
24	Bracket Detection Characteristics	45
25	Beacon Sliding Window Block Diagram	47
26	Beacon Probability of Detection	49
27	Beacon Sensitivity at Maximum Range	51
28	Digital Channel Display Presentation (200 Mile Range) - Beacon	52
29	Video Channel Display Presentation (200 Mile Range) - Beacon	53
30	Beacon False Target Detection	54
31	Beacon Reply Processing Block Diagram	58
32	Beacon Code Acceptance Zones	59
33	SPI Pulse Acceptance Zone	61
34	Beacon Code Garble Sensing Zones	63
35	Emergency Code Detection/Inhibit Zones	65

## LIST OF ILLUSTRATIONS (continued)

Figure		Page
36	Beacon Code Validation as a Function of Fruit Density	67
37	Probability of Declaring False SPI Pulses	69
38	Results of Code Validation Tests for Mode A/3 Interrogations	70
39	Results of Code Validation Tests for Mode C Interrogations	71
40	Beacon Probability of Detection Using Defruited Video	73
41	Beacon Code Validation Using Normal and Defruited Video	76
42	Probability of Declaring False SPI Pulses Using Normal and Defruited Video	77
43	RVDP Azimuth Bias	81
44	Distributions of Declared Range	83
45	Beacon Declared Range Difference (Short Range)	85
46	Beacon Declared Range Difference (Long Range)	86
47	Distributions of RVDP Range Errors	89
48	Distribution of RVDP Azimuth Errors	90
49	RVDP Accuracy as a Function of Range	91
50	Primary Radar Azimuth Resolution	94
51	Reported Vs. Actual Pulse Separation	95
52	Range Resolution for Primary Radar	98
53	Range Resolution for Beacon	99

**LIST OF ILLUSTRATIONS (continued)**

<b>Figure</b>		<b>Page</b>
54	<b>Azimuth Resolution - Primary Radar and Beacon</b>	<b>100</b>
55	<b>Digital Channel Display Presentation - Beacon</b>	<b>102</b>
56	<b>Video Channel Display Presentation - Beacon</b>	<b>103</b>
57	<b>Distributions of Message Transfer Rates</b>	<b>105</b>
58	<b>Distributions of Message Time-In-Storage</b>	<b>107</b>

## LIST OF TABLES

Table		Page
I	Moving Target Indicator (MTI) Sensitivity	27
II	RVDP Accuracy Data	88
III	Azimuth Resolution Test Conditions	92

## ABSTRACT

The Radar Video Data Processor (RVDP) processes primary and secondary raw radar information to derive aircraft position and to extract identity and altitude code information. The processed data are in digital format and are remoted over narrow-band telephone lines.

Detailed tests of the RVDP detection criteria did not reveal any unexplainable deviations from detection theory. The on-line tests indicated that system sensitivity and track-thru-clutter capability compared favorably with unprocessed radar data remoted by conventional wide-band systems. In the course of the test program certain modifications were incorporated into the RVDP, and at the conclusion of the test program other modifications were recommended.

It is concluded that the RVDP represents a suitable design for the reliable detection and processing of primary and secondary radar information for the National Airspace System.

It is recommended that the modified RVDP be integrated into the NAFEC System Support Facility for the National Airspace System for operational testing as a component of that system.

## SUMMARY

The Radar Video Data Processor (RVDP) digitizes primary radar returns and beacon (secondary surveillance radar) replies to derive aircraft positional information and extract beacon code information. A single digital message is prepared for each target for each scan of the antenna. This message is transmitted from the remote site to the computer complex at the control center via voice bandwidth telephone lines.

A comprehensive test program was undertaken to determine the performance characteristics of the RVDP in order to provide data related to the design specifications and the development of the AN/FYQ-40 (Common Digitizer), and to provide preliminary data relevant to the application of the RVDP as a component of the System Support Facility for the National Airspace System (NAS).

The test program consisted of a series of static and dynamic tests. The static tests were performed using controlled laboratory generated input signals which simulate live inputs. The dynamic tests were to verify the findings of the static tests with the use of live inputs from test aircraft.

The primary radar detection process consists of video quantization and statistical detection. The video quantization tests were performed by applying various levels and durations of input signals with several values of percent noise into the radar quantizer. The statistical detection process, which consists of storing returns until selected leading and trailing edge thresholds have been reached, was tested using well defined input signals and a wide range of threshold settings. The effectiveness of the Automatic Clutter Eliminator (ACE) and the run length discriminator functions were also tested. The rate of false target detection as a function of percent noise and threshold settings was also determined. A series of graphs were plotted which describe the results of the static tests. From these graphs, the performance of the primary radar detection processes can be determined.

Dynamic tests of radar detection were performed with test aircraft flying in prescribed patterns while data were recorded on magnetic tape. The tapes were analyzed using a computer program to tabulate and print out the desired information. These tests produced curves which describe the RVDP performance with live inputs including performance in areas of clutter.

The beacon detection process is performed in four basic steps: pulse detection, bracket detection, target detection and code detection. The pulse detection tests were performed by applying various levels and durations of input signals into the beacon quantizer. The effect of receiver noise and closely spaced pulses was also tested. The bracket detection process of recognizing the presence of a beacon reply was tested by varying the bracket spacing of the input signal over its complete range of detection. The target detection process, as in radar detection, consists of storing replies until selected leading and trailing edge thresholds have been reached. This was tested by applying input signals, which simulated live inputs, including effects of the signal environment such as the presence of non-synchronous replies or fruit. Several values of leading edge thresholds were checked. The rate of false target detection as a function of fruit density and threshold settings was also determined. The code detection process consists of code pulse sampling, garble sensing, and code validation. The code pulse sampling zone for each code pulse was determined by varying each code pulse over its entire range of detection. Varying the relative positions of two code trains determined the garble sensing characteristics of the RVDP. The emergency code sensing characteristics were also determined by varying each code pulse of the emergency codes over its range of detection. The code validation process is performed by comparing presently-received code with the previously-stored code for each interrogation mode. This process was tested as a function of fruit density to determine performance characteristics. Dynamic tests, using test aircraft and targets of opportunity, were performed to verify the static tests results. All the static and dynamic tests results were plotted and the resulting graphs describe the performance of the RVDP under the specified conditions for each process.

An additional series of beacon target detection and code detection tests were performed to determine the effect of using a defruiter to remove most of the non-synchronous beacon replies.

The RVDP's capability to generate modes A/3, 2 and C interrogation pulse pairs was also tested.

The total system accuracy in both range and azimuth is a function of the primary radar and beacon systems supplying the inputs to the RVDP. Tests with controlled inputs were conducted to determine to what extent the RVDP itself could contribute to system error. The range and azimuth error distributions for both primary radar and beacon inputs that resulted, describe the correction bias that is necessary within the RVDP under various conditions. Flight tests

were conducted to verify the static test results. These tests employed an independent aircraft position determining system for comparison. Data reduction, comparison and analysis were performed using computer programs.

The capability of the RVDP to resolve targets whose returns occur in close proximity is also a function of the primary radar and beacon systems supplying the inputs as well as the RVDP itself. A series of static tests were performed to determine if the range and azimuth resolution characteristics of the RVDP were as predicted. This was performed for both primary radar and beacon. Dynamic tests were also performed to include the effects of live inputs. It was determined that the range and azimuth resolution functions perform as expected.

The data obtained during flight tests were analyzed to determine if range and azimuth splits might be a problem. When a split occurs, more than one message output is generated for a single target, indicating falsely that more than one target exists. Scope photographs of this phenomenon were also obtained.

Further analysis of flight test data yielded information concerning the amount of delay or time-in-storage encountered by target messages awaiting transmission over telephone lines. This information was used to produce distributions of time-in-storage as a function of target density including clutter conditions.

During many of the flight tests, especially when weather clutter was present, a count of total messages processed per scan was maintained at the RVDP output. A series of graphs were produced showing distribution of message transfer rates for various clutter conditions.

Several modifications were made to the RVDP during the course of the test program. Five of these were made to functionally make the RVDP more resemble the CD. Four more modifications were incorporated to improve the performance of the RVDP and came about as a result of information obtained from the test program.

During the course of the test program, a maintenance log was kept on the Elwood, N. J., RVDP to determine the nature and the extent of malfunctions encountered. Availability data were collected and tabulated for the RVDP located at Suitland, Maryland.

The testing of a complex device such as the RVDP presents many problems of instrumentation. Many times, to effect the configurations

necessary to perform the tests, a great deal of time and test equipment were required. To facilitate testing, three special test instruments were developed and built by the project team. The Digital Target Generator Test Set is a device which can simulate a controlled radar or beacon signal environment with three independently variable test targets. The Beacon Reply Counter is a device which was built to count live beacon replies and provide a direct recording of the azimuthal distribution of those replies. This recording describes the beacon environment that exists at a site. The Digital Data Recorder was built to record and print out message outputs from the RVDP. This system was used at the site.

The tests of the RVDP detection criteria did not reveal any unexplainable deviations from detection theory. The on-line tests indicated that system sensitivity and track-thru-clutter capability compared favorably with unprocessed radar data remoted by conventional wide-band systems.

It is concluded that the RVDP represents a suitable design approach for the reliable detection and processing of primary and secondary radar information for the National Airspace System.

It is recommended that the modified RVDP be integrated into the NAFEC System Support Facility for the National Airspace System for operational testing as a component of that system.

**BLANK PAGE**

## INTRODUCTION

### Purpose

The purpose of this project was to determine the performance characteristics of the Radar Video Data Processor (RVDP) to provide data related to the design specifications and the development of the Common Digitizer, and to provide preliminary data relevant to the application of the RVDP as a component of the National Aviation Facilities Experimental Center (NAFEC) System Support Facility for the National Airspace System (NAS).

### Background

The RVDP digitizes primary radar and beacon (secondary surveillance radar) data at the radar site so that the radar information may be remoted via voice bandwidth telephone lines. Studies of a similar United States Air Force (USAF) radar data processor, the AN/FST-2, established the cost advantage of using a narrow-band data transmission system.<sup>1, 2</sup>

By direction of the Administrator,<sup>3</sup> it has become the Agency policy to "(1) adopt the principle of digitizing radar and radar-beacon data when such digitized data is required by virtue of the design of processing and display systems utilizing such data; (2) digitize this data at the radar sites and transmit it by voice-bandwidth channels when remoting is required; and, (3) follow these principles in development and implementation programs." This policy is constrained to the extent that such digitizing, processing, and display functions will not, at any time, result in an increase in air traffic separation minimums or a decrease in data reliability and system availability provided all system elements are operating within design limits.

In accordance with Contract FA-WA-4693, the RVDP was developed by the Burroughs Corporation from design criteria specified by the Federal Aviation Agency (FAA). Four units were purchased for use in the System Support Facility of the NAS at NAFEC. Two units are operating with terminal radars--one at NAFEC (ASR-5) and one at

- . . . .

1 Reference 1

2 Reference 2

3 Reference 3

Philadelphia International Airport (ASR-6); and two are operating with enroute radars--one with an ARSR-2 at Elwood, New Jersey, and one with an ARSR-1E at Suitland, Maryland. The outputs of the Elwood, Suitland and Philadelphia units are remoted to NAFEC via Class 4A telephone lines. Only the enroute RVDP's (Elwood, N. J., and Suitland, Md.) were tested during the execution of this project.

### Brief Description of RVDP

The RVDP was designed to derive aircraft positional information from primary radar and beacon inputs. Beacon code replies for mode A/3 (identity), mode 2 (military identity), and mode C (altitude) are processed and reported with the associated positional information.

Input to the RVDP consisted of primary radar video, beacon video, radar pre-trigger, and antenna position data from an Air Route Surveillance Radar (ARSR-2) and an Air Traffic Control Beacon Interrogator (ATCBI-3). After detection and processing of radar targets by the RVDP, target-report messages (digital) were transferred from the data-transmission group at the remote site to the data-receiver group at NAFEC. Three voice-quality Class 4A telephone lines terminated at both ends with data transmitters and receivers (modems), type 26B manufactured by the Lenkurt Electric Company, were used to accomplish the data transfer. Each line was driven at a 2400 bit-per-second rate for a total capacity of 7200 bits per second.

A more complete description of the RVDP is given in Appendix I.

### Test Program

Before any tests had been performed on the RVDP, a joint FAA/DOD (Department of Defense) decision was made to procure the AN/FYQ-40, or Common Digitizer (CD), for joint USAF-FAA use. In order to gain the maximum benefit from the test and evaluation program, the RVDP at Elwood, N. J., was modified to more closely resemble the CD. These modifications and additional improvement modifications are discussed briefly in Appendix II. Subsequent experimentation was all performed on the modified Elwood RVDP. The enroute RVDP at Suitland, Maryland, was not modified and was operated 24 hours a day to collect reliability data. These data are presented in Appendix III. The test and evaluation of the RVDP began on March 23, 1965, when the last modification was completed. On June 7, 1965, the unmodified RVDP at Suitland was put on 24-hour operation. The formal test program was completed on March 1, 1966.

The test plan was prepared by the FAA (Test and Evaluation Division, NAFEC) and coordinated with the USAF (416M SPO, ESD, Hanscom Field, Massachusetts) to insure that the tests performed would be acceptable to both agencies involved in the CD development program. As each test called for in the test plan was completed, a data report was written containing the results of the test. A memorandum report was issued which summarized the results of the flight-test phase of the project.<sup>4</sup> These preliminary reports were written so that all available information relative to the CD development program could be supplied to those responsible for that program. This report summarizes the information included in these reports.

.....  
<sup>4</sup> Reference 4

## DISCUSSION

### Primary Radar Detection

The detection of primary radar targets is accomplished in two steps. In the first step, video quantization, the analog radar video signal is quantized in range and amplitude. The RVDP divides the radar trigger period into discrete range cells. The size of the range cell is approximately equal to the pulse width of the radar and, in the case of the ARSR-2, it is 3.09 microseconds (1/4 nautical mile). The radar video signal is compared to an amplitude threshold so that each range cell may be represented by a one or a zero depending on whether or not this amplitude threshold has been exceeded. Thus, further target processing and actual target detection may be accomplished using digital techniques.

The digital processing of the quantizer output is the second step in the detection process and is termed statistical detection. A sufficient number of consecutive radar trigger periods which have been thus quantized are stored in the memory of the RVDP to represent the 3 dB (decibel) beamwidth of the radar. For the ARSR-2, thirteen radar trigger periods are stored in this manner. Each range cell is then examined to determine whether the amplitude threshold has been exceeded for a sufficient number of radar trigger periods to indicate that a target is present at that range. During each succeeding radar trigger period, the oldest radar trigger period stored in memory is replaced by the current trigger period and each range cell is again examined for the presence of a target. This radar detection process is termed a sliding window detector and, in theory, will perform almost as well as an ideal linear integrator.<sup>5</sup>

In the following sections, this basic detection process will be described in detail along with the results of specific tests.

Video Quantization: The quantizer performs the amplitude and range quantization function. It consists of a slicer which provides a "one" logic level when the input video signal exceeds the amplitude threshold reference level and timing circuitry for range orientation of the output. Separate quantizers are provided for the normal and Moving Target Indicator (MTI) channels. These quantizers are identical and the description provided is valid for both.

- - - -

<sup>5</sup> Reference 5

Description - The clock signal used by the quantizer is a 2.59 Mc/s (megacycle per second) signal from the Azimuth Range and Timing Group (ARTG) of the RVDP. This clock is shock started with every radar pretrigger and so provides a clock signal whose period is 0.386 microseconds (1/32 nautical mile) synchronous with the radar generated time base. The clock is counted down by 8 to generate the 1/4 nautical mile (nmi) range cells of the RVDP.

To help discriminate against impulse noise, the output of the quantizer is subjected to a minimum width criterion. The video signal must remain above the amplitude threshold for a minimum of two clock times before it is accepted for further processing. Since the radar pulse is approximately the same width as the range cell, most radar returns would occur in portions of two range cells. To reduce the incidence of a single radar return being reported in two range cells, the output of the quantizer is suppressed for a fixed number of clock counts after the first clock period quantized. This is termed the range discrimination function. Suppression for eleven clock counts from the leading edge of the quantized pulse was required to assure that fewer than 5% of the target returns were reported in more than one range cell. Radar video would have to remain above threshold for from 3.86 to 4.25 microseconds to be processed in more than one range cell. (The exact period is determined by the relative phasing of the quantizer output and the clock.)

During periods of no clutter, the quantizer amplitude reference is set for a fixed probability of quantizing receiver noise. On the RVDP this control is termed percent noise ( $P_N$ ). To compensate for minor changes in the level of receiver noise this clip level is under the control of a slow feedback loop (Figure 1). Quantizer hits are applied to a noise metering circuit where they are integrated and compared to a manually selectable reference voltage. An error signal is derived which is fed back to the quantizer clip level reference input after further integration in a long-time-constant amplifier (the overall time constant is approximately one second).

When clutter is present it is desirable to raise the quantizer amplitude reference in proportion to average clutter amplitude. A separate reference voltage, used only when clutter is present, is derived from filtered video as shown in Figure 1 (fast feedback loop). The time constant of the low-pass filter is approximately 10 microseconds, which allows this reference voltage to respond quickly to clutter amplitude changes. The presence of clutter is sensed at the output of a three bit sliding window integrated over five range cells.

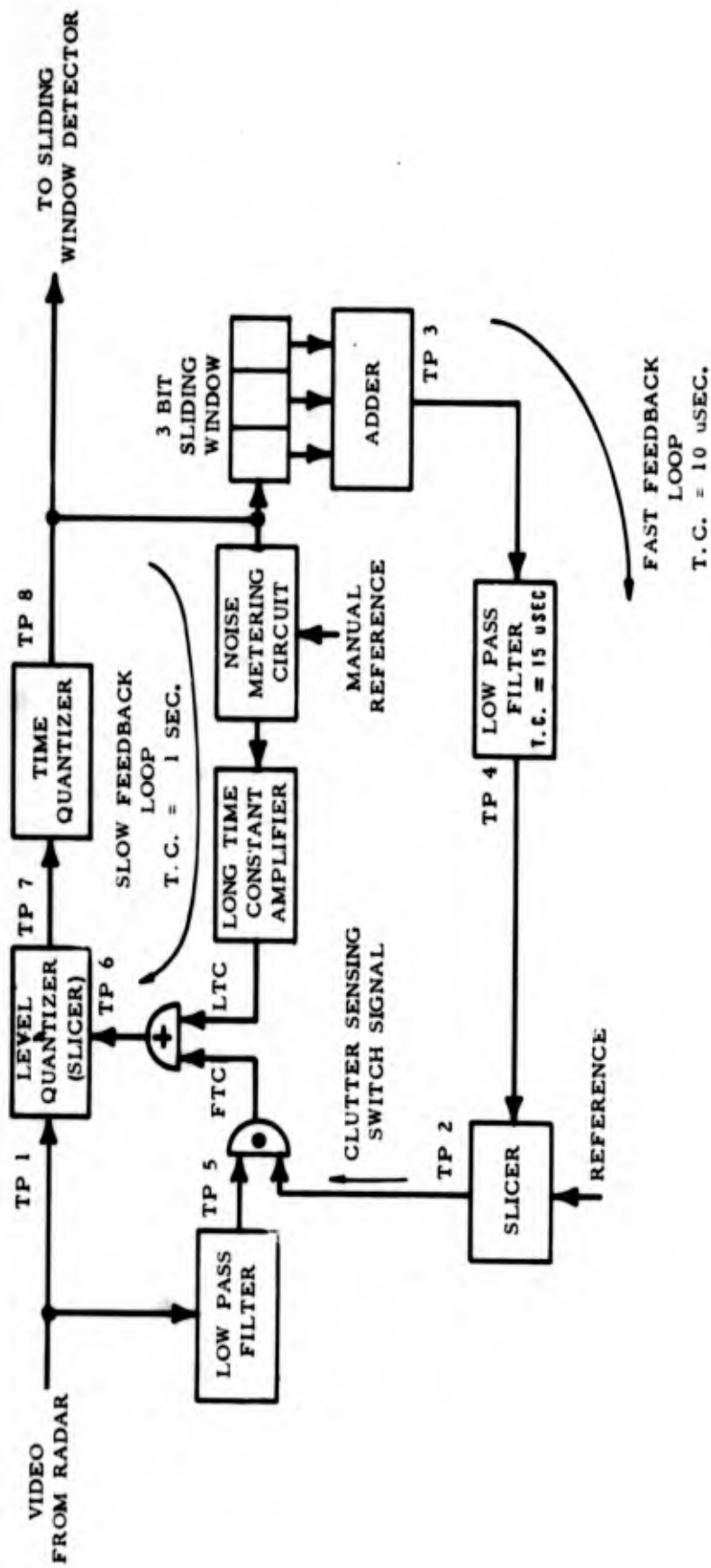


FIG. 1 RADAR VIDEO QUANTIZER BLOCK DIAGRAM

Tests of the quantizer included checks of the reference level control system and tests of quantizer performance with controlled video inputs.

### Reference Level Control

A. Test Procedure - The operation of the slow feedback loop was checked by varying the input video noise level from its nominal 0.3 volts up to 0.7 volts with the percent noise control set at 4%, 8%, and 12%. The actual percent noise was monitored by counting the quantizer output.

The operation of the fast feedback loop and the clutter sensing system used to switch between the slow and fast feedback loops was checked by photographing waveforms at the test points indicated in Figure 1. The input signal was a 70 microsecond radio frequency (RF) pulse applied to the radar waveguide directional coupler. This 70 microsecond pulse was varied in amplitude and represented a crude simulation of a ring of clutter of varying strength.

B. Test Results - The results of the slow feedback loop check are shown in Figure 2. The measured percent noise decreased slightly as the noise level was raised. This indicates that there was a slight overcorrection in the slow feedback circuit. The indicated overcorrection would not seriously affect the probability of false alarm or the probability of detection.

The photographs of the waveforms of Figure 3 are the results of the check on the fast feedback loop and reference switching logic. These waveforms were present at the indicated test points when the simulated clutter, described in the test procedures section, was applied to the radar input. The test points refer to the block diagram in Figure 1. The test signal amplitude is given in terms of dB relative to the radar minimum discernible signal (MDS). The upper trace on all oscilloscope photographs is the input video signal (TP-1). The output of the quantizer is actually applied to two sliding window detectors. The target detection sliding window detector is discussed in detail in the following section. The three bit sliding window of Figure 1 is the clutter detection sliding window. The output of the adder (TP-3) is the sum of the quantizer outputs for the current range cell for the past three radar trigger periods. It can be seen that only four levels are possible at this point corresponding to the sum of 0, 1, 2, and 3 hits in the three cells added. This sum is integrated in range by a low-pass filter whose time constant is approximately five range cells (15 microseconds). Thus,

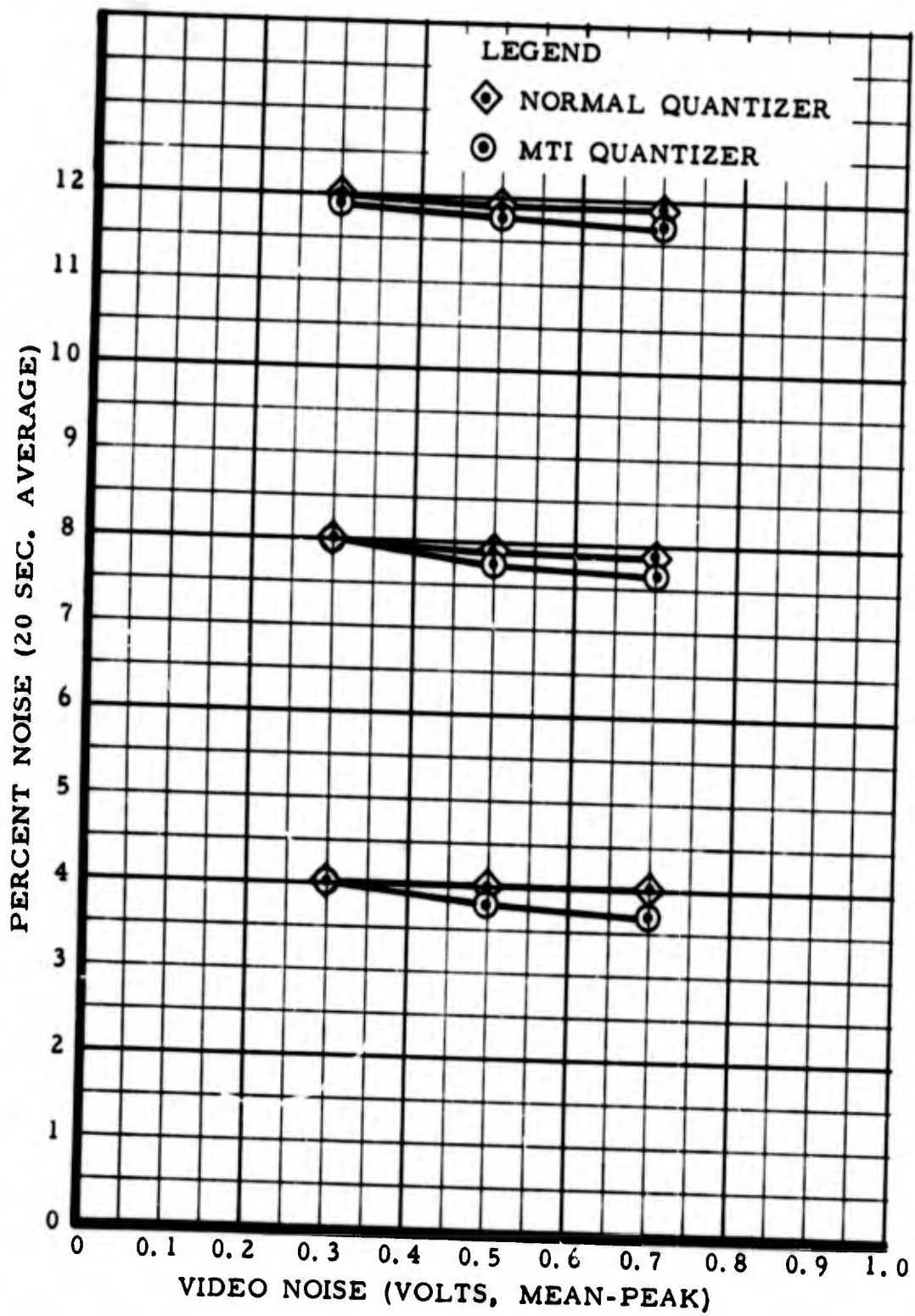


FIG. 2 PERCENT NOISE VS. VIDEO NOISE LEVEL

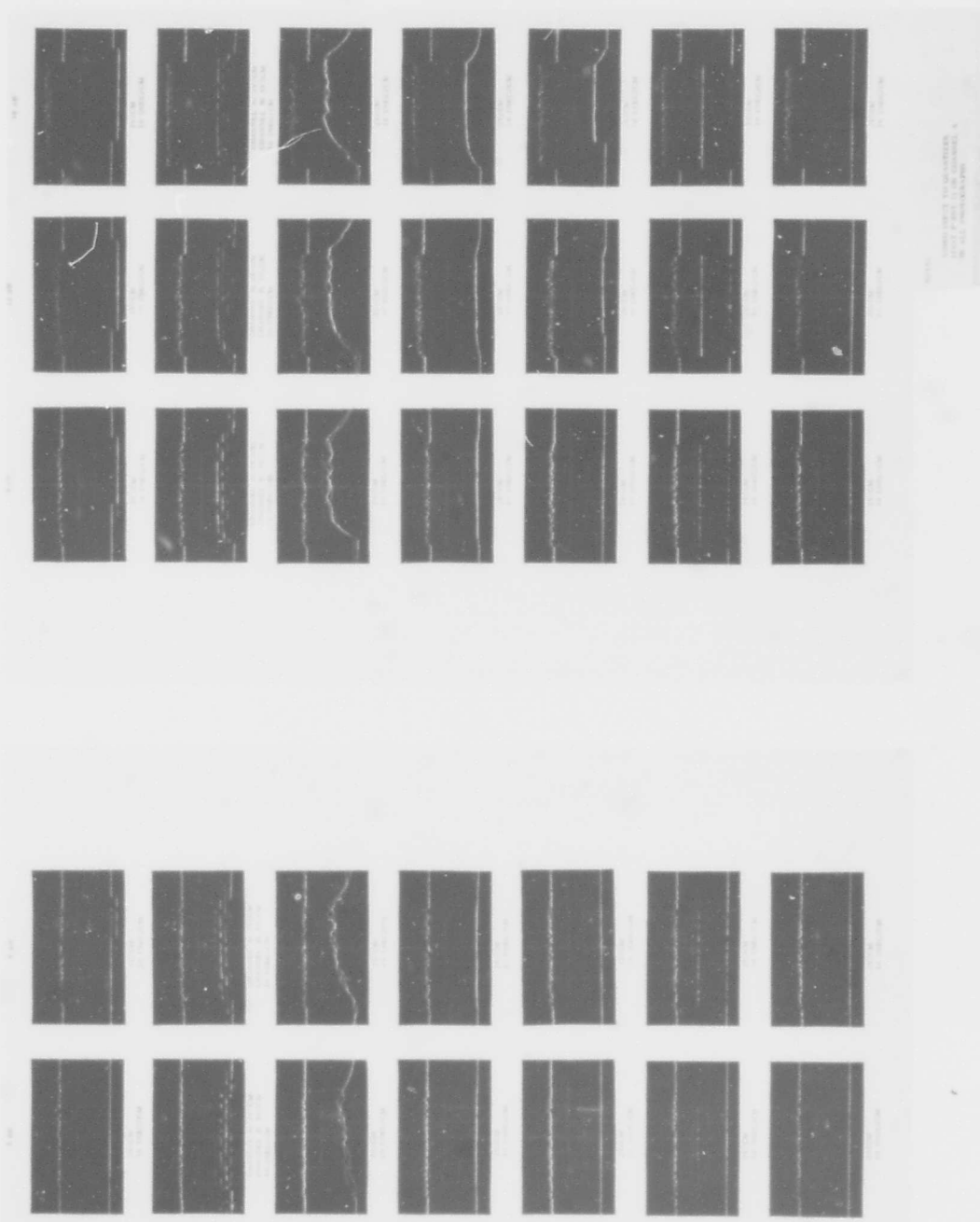


FIG. 3 VOLTAGE WAVEFORMS AT QUANTIZER TEST POINTS

the integrated output (TP-4) is proportional to the number of hits in a range-azimuth window which is five range cells long and three radar triggers wide. When this output exceeds a pre-set threshold, a level change (TP-2) allows the fast feedback quantizer amplitude reference (TP-5) to control the video quantizer threshold (TP-6). The output of a similar slicer is used to disable the long time constant feedback loop while clutter is being quantized. Thus, the long time constant reference is prevented from rising in the presence of clutter, and a suitable amplitude reference for use at ranges where there is no clutter is maintained.

Performance - As a check on quantizer performance, a test was performed to determine the probability of declaring a hit (probability of quantizing) in a particular range cell as a function of percent noise setting and target power.

A. Test Procedure - With the radar receiver input terminated in a dummy load a continuous ring of RF pulses, 2 microseconds in width, was introduced into the waveguide directional coupler. The resulting quantizer hits were bracketed by a 3.09 microsecond gate (equivalent to a 1/4 nmi range cell) and only these gated hits were counted with an electronic counter.

For each combination of percent noise setting and signal power (expressed in dB above radar MDS\*) chosen, five 10-second counts were made and recorded with a Hewlett-Packard counter-printer combination. This procedure was followed for both the MTI and normal quantizers.

The average 10-second counts were divided by the maximum possible counts over that period (radar pulse repetition frequency times 10) to obtain the probability of quantizing.

B. Test Results - The data so derived are shown in Figure 4. A sample theoretical curve, derived from the amplitude distribution developed by S. O. Rice<sup>6</sup> for a peak signal to root-mean-square (rms) noise ratio of 2, is also shown. The experimental curves agree with the theoretical curve in shape and reasonably well in magnitude.

The range discrimination function installed in the RVDP precludes the possibility of reaching 100% probability of quantizing. Since the quantizer output is inhibited for the equivalent of 1.3 range cells after

\* Radar MDS was the minimum power level of a test target signal which was discernible on an "A" scope display. This measurement was normally done by the site radar technician.

- - - -  
6  
Reference 6

a hit, noise hits, occasionally occurring late in the previous range cell, blank would-be target hits. This is borne out by the fact that a 9.5 dB curve approaches saturation short of 100%.

The probability of quantizing curves for the MTI channel is generally lower than for the normal video channel. Weak signals show little degradation while strong signals are degraded markedly. This type of degradation is characteristic of the MTI channel and is due to the action of the MTI canceler on a non-coherent signal source. Successive returns of a non-coherent target may add or subtract in the canceler, depending on their relative phases which are completely random and independent. A weak target with a low probability of quantizing would have an increased probability of quantizing on those occasions when the returns add in the canceler and a decreased probability of quantizing when the returns subtract in the canceler. A strong target with a high probability of quantizing would have its probability of quantizing increased very little when returns add in the canceler because this probability is limited, as shown by the curves for the normal channel in Figure 4, while there would be a decreased probability of quantizing when the returns subtract in the canceler.

Statistical Detection: Statistical detection is accomplished through the use of a ferrite core memory where the output of the quantizer is temporarily stored. Targets are detected and located in range and azimuth on the basis of the hits stored in this detection memory. Detection memory (termed Memory I in the RVDP) has a capacity of 1,024 fifty-one bit words.

Sliding Window Detector - For detection purposes the 200 nmi range of the ARSR-2 radar (and associated beacon system) is divided into 800 one-quarter nmi range cells. Each of these 800 range cells is assigned to a specific word location in detection memory. When the radar output pulse is transmitted, each range cell in detection memory is sequentially addressed so that when a radar signal from a particular range is quantized, the word in memory representing that particular range cell has been addressed and is available in a register. The portion of the word used as the sliding window detector functions as a shift register (Figure 5) with the latest quantizer output for that range cell being shifted into the left side of the register, moving all the rest of the bits one shift to the right and causing the oldest bit in the register to be lost. Before the word is transferred back to detection memory, a digital-to-analog (D/A) converter sums the hits in the sliding window.

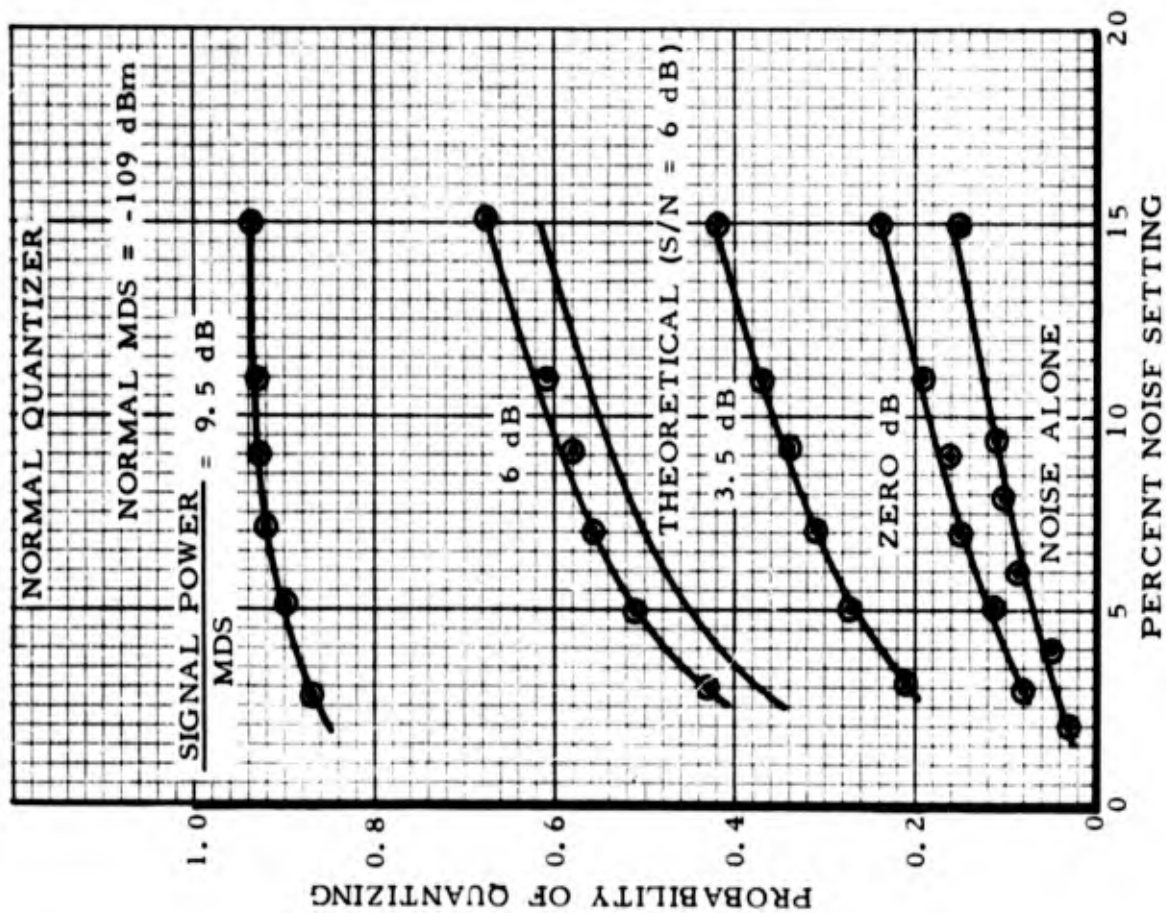
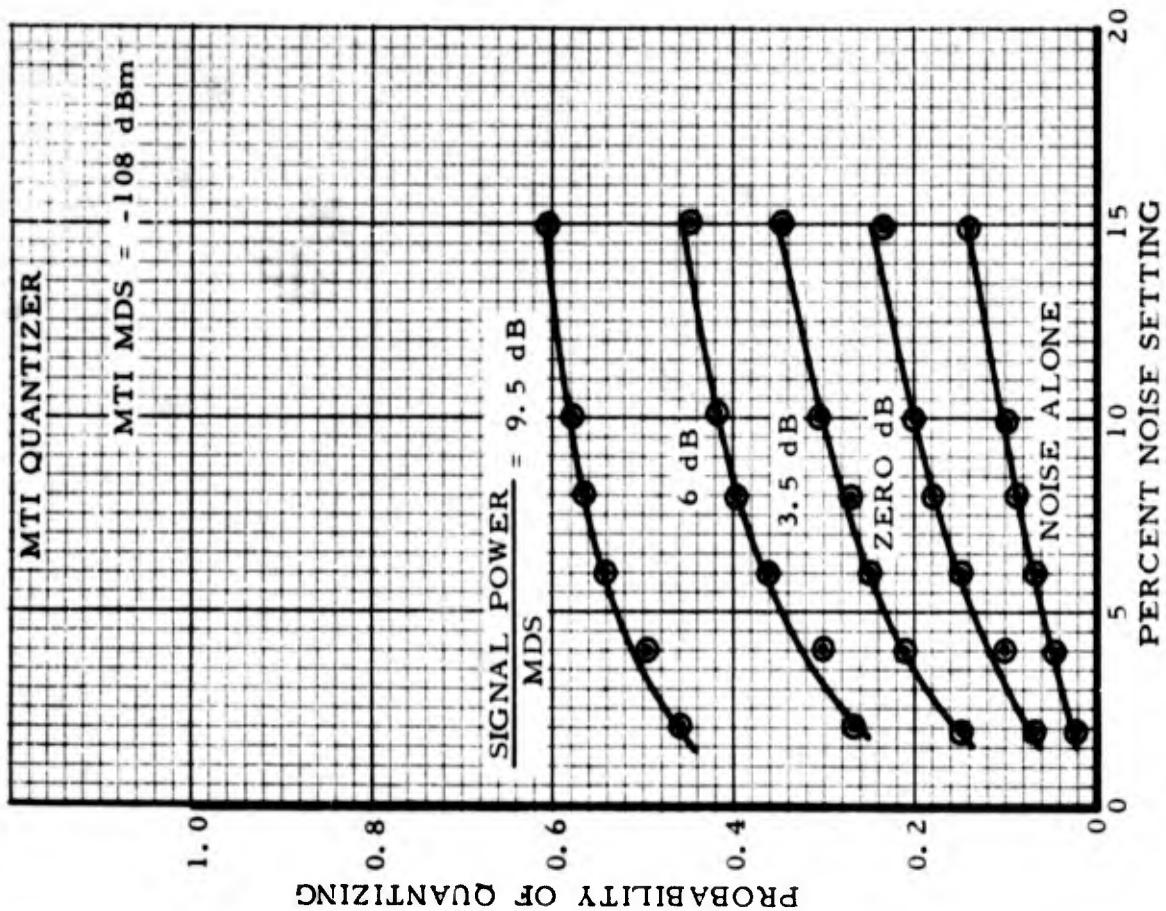


FIG. 4 PROBABILITY OF QUANTIZING SIGNAL PLUS NOISE VS. PERCENT NOISE

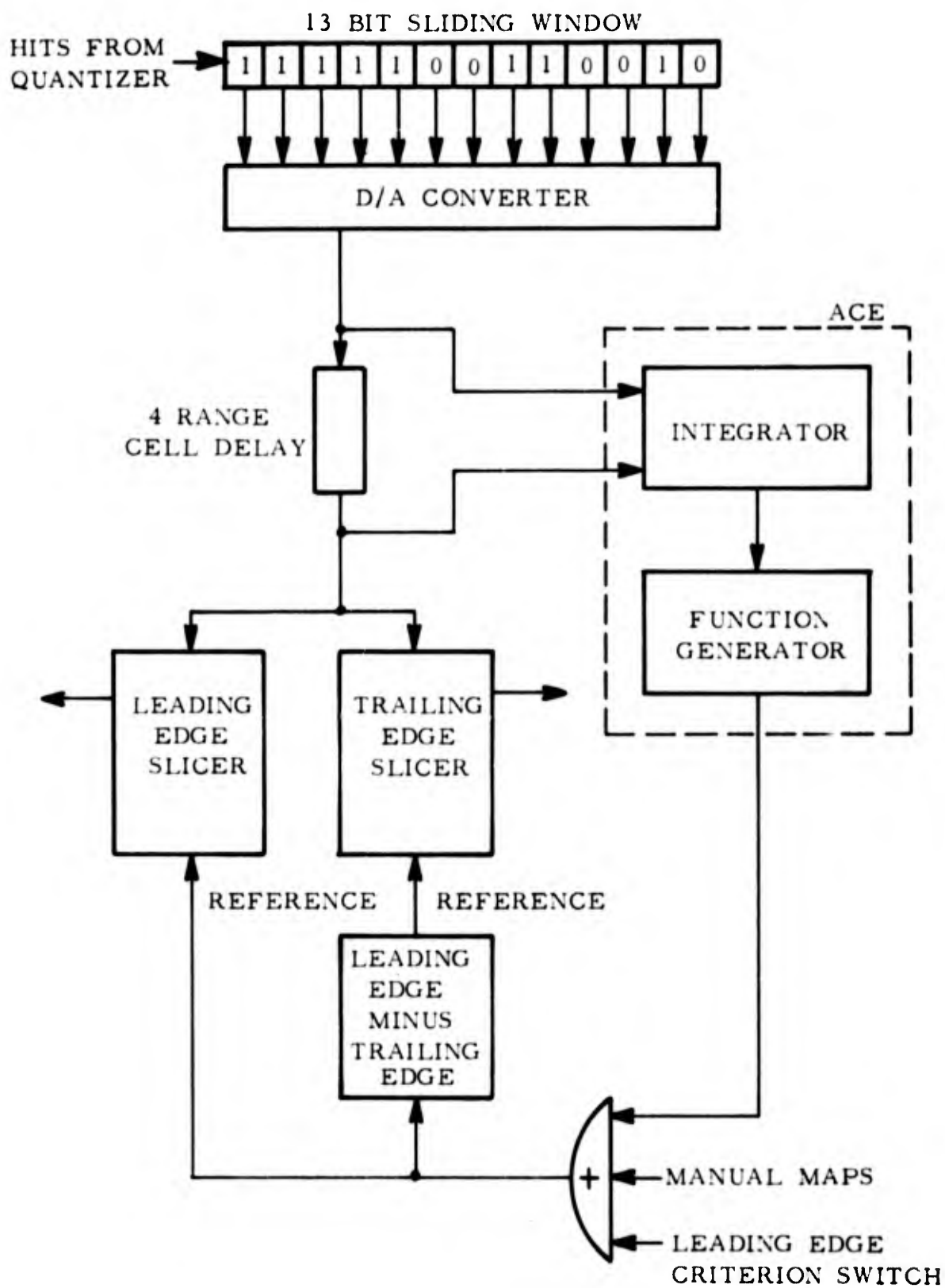


FIG. 5 DETECTOR BLOCK DIAGRAM

After a delay of 12.3 microseconds, to permit operation of the automatic clutter eliminator (ACE), the signal is applied to the target leading and trailing edge slicers. When the summed hits exceed the leading edge slicer reference, a target is declared in process and a target run length count begins. When the summed hits fall below the trailing edge slicer reference voltage, the target is declared complete, run-length count is terminated, and the information is transferred out of detection memory. Upon leaving memory, one-half the run length is subtracted from the current azimuth count for center azimuth determination.

A range accuracy determination is made at the time of target-leading-edge declaration. For this purpose the 1/4 nmi range cell is subdivided into four 1/16 nmi segments, and the segment containing the leading edge of the quantized pulse is recorded with two bits in the word in Memory I assigned to this range cell. Thus 1/16 nmi range precision is achieved in what is basically a 1/4 nmi system.

The fundamental leading edge criterion is determined by a manual switch setting which is set for a reasonable compromise between probability of detection and false target rate (false targets per scan).

Automatic Clutter Eliminator (ACE)- In the presence of clutter it is desirable to raise the leading edge criterion ( $T_L$ ) to reduce the number of false (clutter) targets. To perform this function, the D/A converter output (representing the number of hits in the sliding window) is also applied to an ACE circuit which consists of an integrator and a function generator (Figure 5). The output of the integrator is proportional to the percent hits in a sliding window 13 radar triggers wide and approximately 7 range cells deep. For every value of percent hits a value of  $T_L$  to use to prevent the probability of false alarm due to clutter from exceeding any specific value may be calculated from the binomial distribution. The function generator transposes its input signal (proportional to the percent hits) to the  $T_L$  which maintains the probability of false alarm due to clutter at  $10^{-3}$ . Figure 6 is the function generator curve for the RVDP. This function generator characteristic will maintain the design value of probability of false alarm only when the hits are located randomly in the range-azimuth window. If the hits are correlated concentrically, the probability of declaring a false alarm would be higher; and, if the hits are correlated radially, the probability of declaring a false alarm would be lower.

Run Length Discriminator - Run length discrimination was added to the RVDP as a modification to perform additional discrimination

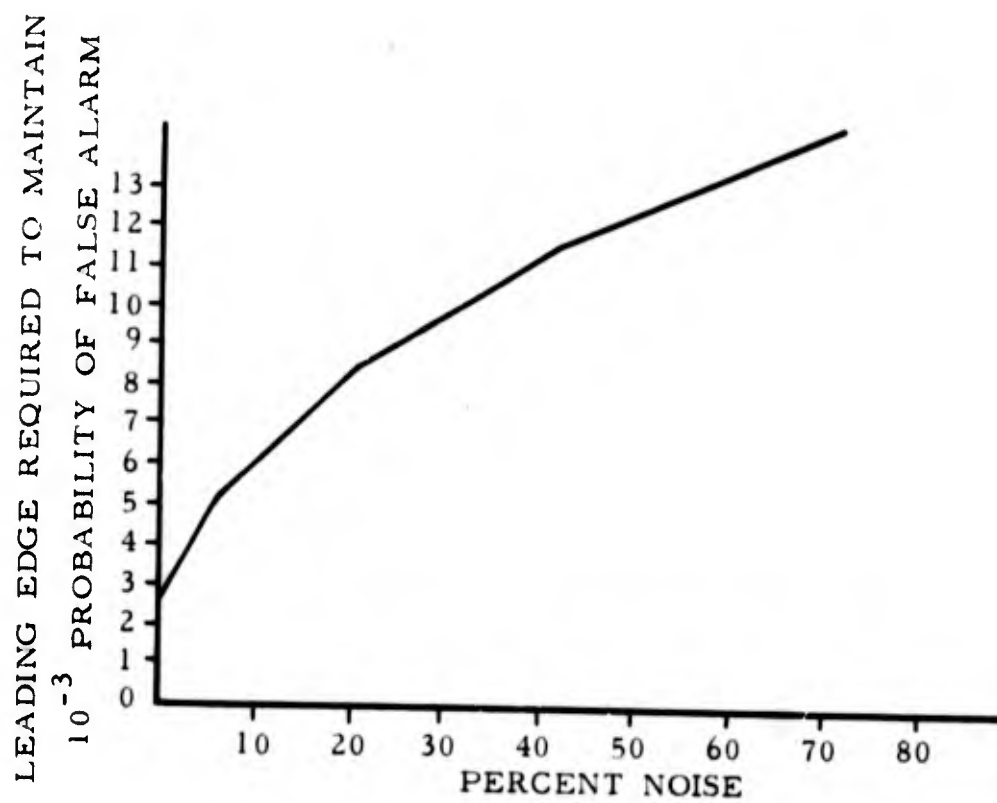


FIG. 6 FUNCTION GENERATOR TRANSFER CHARACTERISTIC

against primary radar clutter targets. With this modification it is possible to suppress targets with run lengths shorter than some preset minimum and/or longer than some preset maximum. The run length measure used is the number of azimuth change pulses (ACP's) between  $T_L$  and  $T_T$  (target trailing edge).

An aircraft target is essentially a point-source target and, as such, the return signal due to an aircraft target approximates a pulse train modulated by the radar two-way antenna pattern. Radar returns due to clutter would not, in general, be well defined but more noise-like in nature. (Actually, each individual raindrop acts as a point-source target; but, when these returns add up at the radar, the result is a noise-like signal.) The run length discrimination technique is designed to take advantage of the deviation that the noise-like signal causes from a normal Gaussian distribution. Its success as a clutter suppression device depends on how much difference there is between the run length statistics of aircraft targets and clutter targets.

A. Test Procedure - To establish what minimum and maximum run length criteria could be used without suppressing aircraft targets, it was necessary to measure the run lengths of aircraft targets. Since run length is a function of signal strength, the data were grouped according to range. To measure the effectiveness of various run length criteria, run lengths of weather clutter targets were also measured.

Run length distributions of weather clutter targets and aircraft targets were measured using the run length discriminator. The RVDP was gated so that only targets from a selected area would be detected. Counts were maintained of targets detected and targets rejected by the run length discriminator for various settings of the run length discriminator.

B. Test Results - Distributions of aircraft target run lengths are shown in Figure 7, while distributions of weather clutter target run lengths are shown in Figure 8. The weather clutter run length data were taken April 12, 1966. The Weather Bureau reported light rain and rain showers in the area in which the data were taken. Data for the two distributions were taken about two hours apart.

Safe minimum and maximum settings of the run length criteria may be derived from the aircraft run length distributions. The sample run length data indicate that suppressing targets with run lengths longer than 37 would not degrade target detection, while suppressing targets with run lengths shorter than 5 would cause fewer than 10% of the target returns from 150 to 200 miles to be lost.

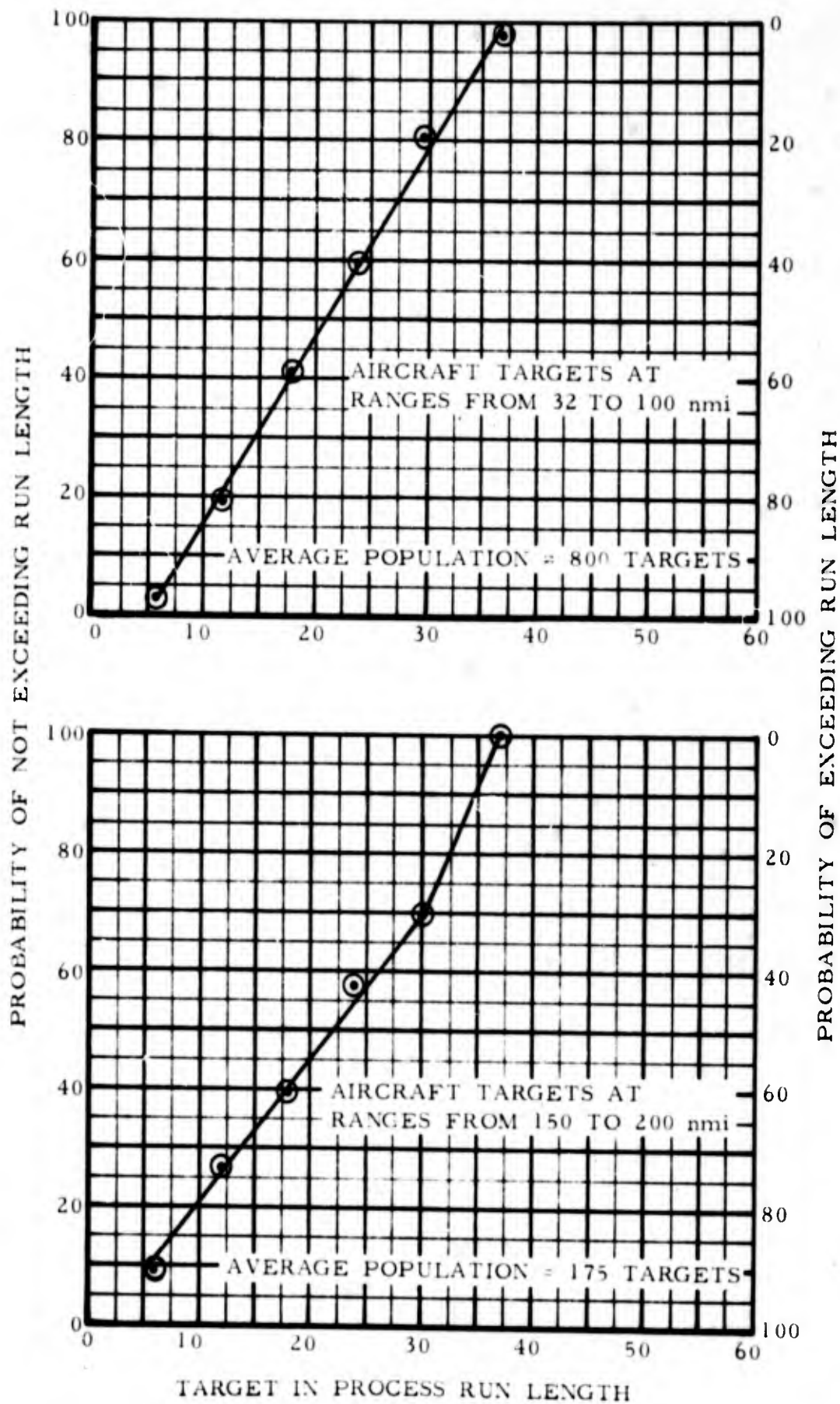


FIG. 7 RUN LENGTH DISTRIBUTIONS OF AIRCRAFT TARGETS

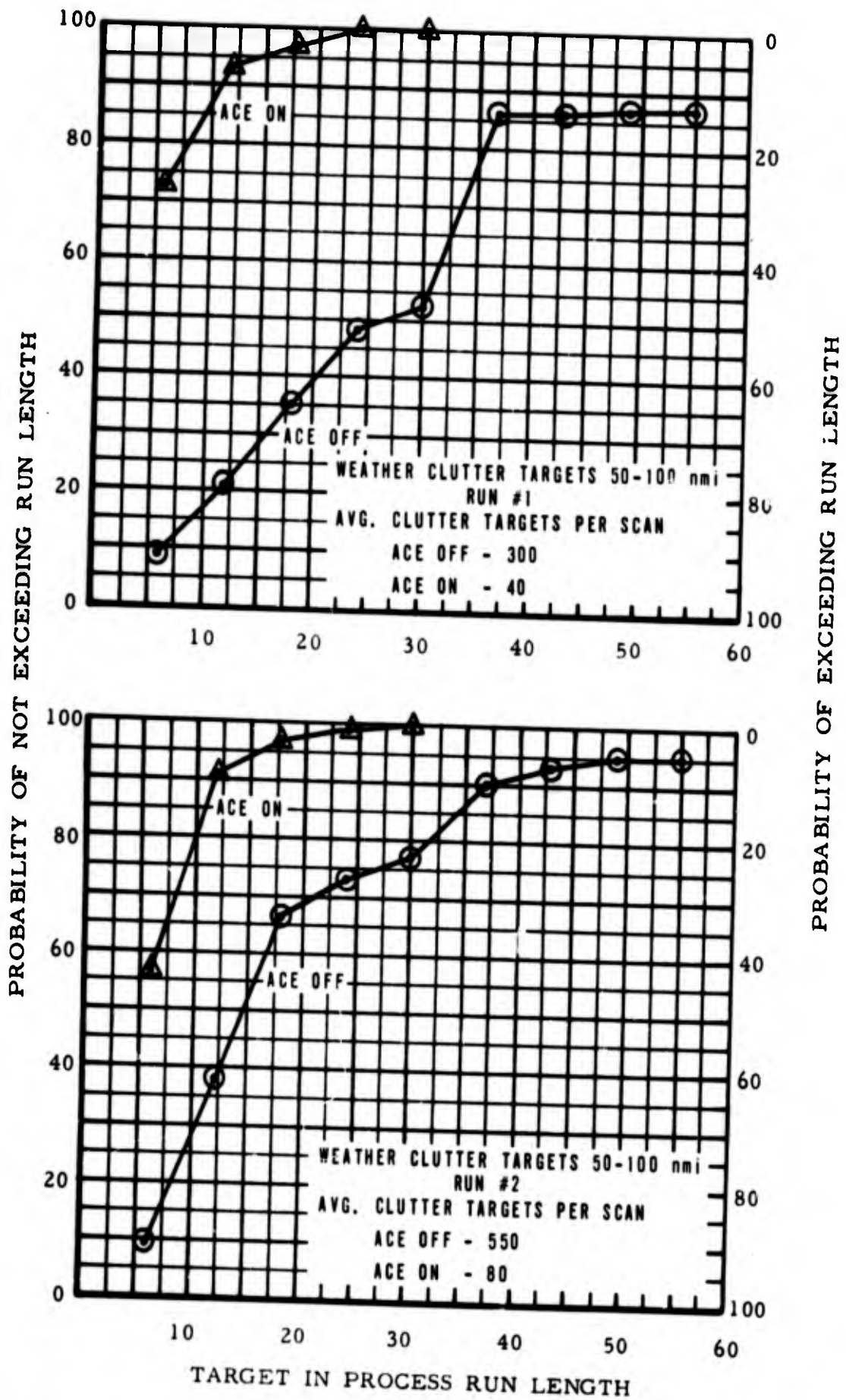


FIG. 8 RUN LENGTH DISTRIBUTIONS OF CLUTTER TARGETS

The clutter run length data indicate that, when the ACE circuit is functioning, the clutter target maximum run lengths are very little different from the maximum aircraft target run lengths, with ACE off 10% to 15% of the weather clutter targets represented by these samples would have been suppressed by setting the maximum run length criterion at 37. With ACE off, the clutter target minimum run lengths are similar to aircraft target minimum run lengths; while with ACE functioning, 55% to 70% of the weather clutter targets represented by the samples would have been suppressed by setting the minimum run length criterion at 5.

Detector Performance with Controlled Inputs - Detector performance was checked over a wide range of detection threshold settings with well defined input signals. This was done to permit comparison of the performance of the detector with what was theoretically expected and to collect data which would allow intelligent setting of these detection thresholds in a live environment. In setting detection threshold it is desirable to minimize false target detection and maximize the probability of detection of true targets. The results of this test series establish the trade off available in false target detection and probability of detection of valid targets through selection of detection thresholds.

A. Target Detection - The probability of detection was determined for signals of various levels as a function of percent noise and  $T_L$  with ACE "off" and then repeated with ACE "on."

1. Test Procedure - The radar receiver input was terminated with a dummy load. The Digital Target Generator Test Set (DTGTS) was used to generate three rings of RF test targets with 32 thirteen hit targets per ring at ranges of 64, 128, and 192 nmi. These signals were applied to the radar directional coupler. A repetitive range-azimuth decode, synchronized with the test targets and wired to the Random Access Plan Position Indicator (RAPPI) display register, was used to discriminate against false targets while obtaining the counts of valid target detections. This decode effectively placed a range-azimuth gate around the center of each test target which was 1 range cell deep and 8 ACP's wide. The output of this gate was counted for 5 scans for a total of 480 samples per data point.

2. Test Results - The results of these tests are shown in Figure 9. Signal amplitude is given in dB referred to the radar MDS. The probability of detection with ACE "on" is lower than the probability of detection with ACE "off" whenever the percent noise as measured by the ACE integrator circuit indicates that a higher  $T_J$ , than that set

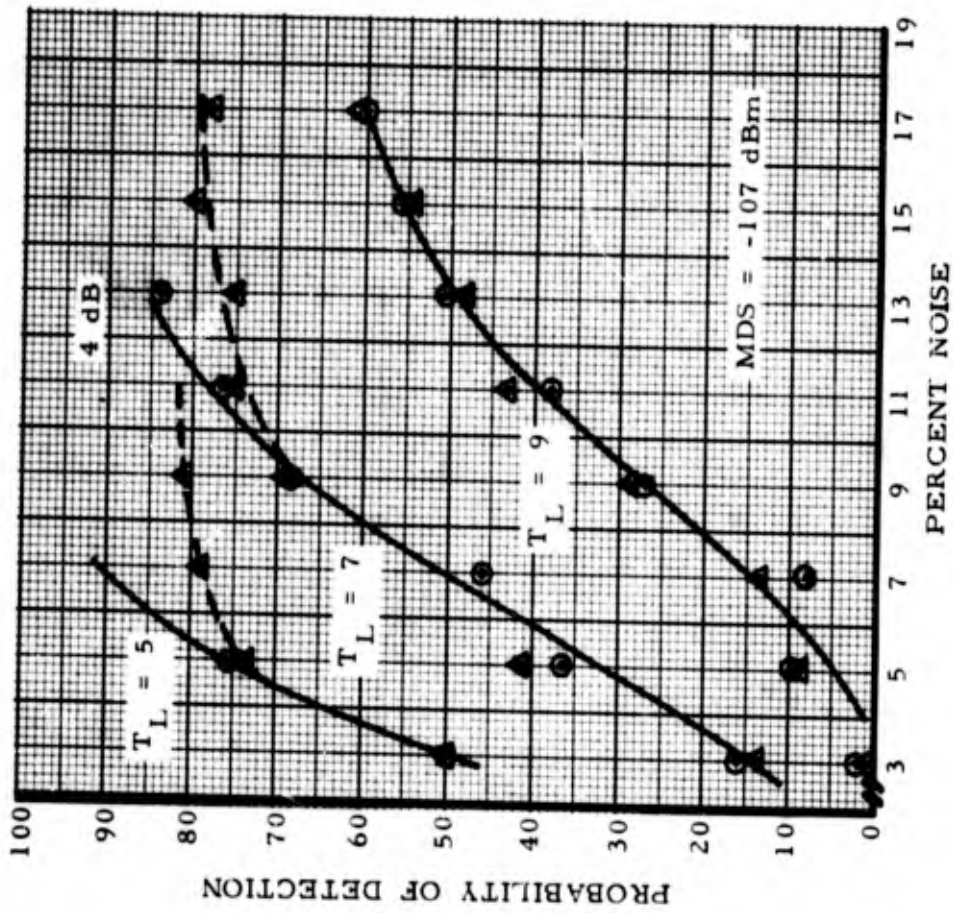
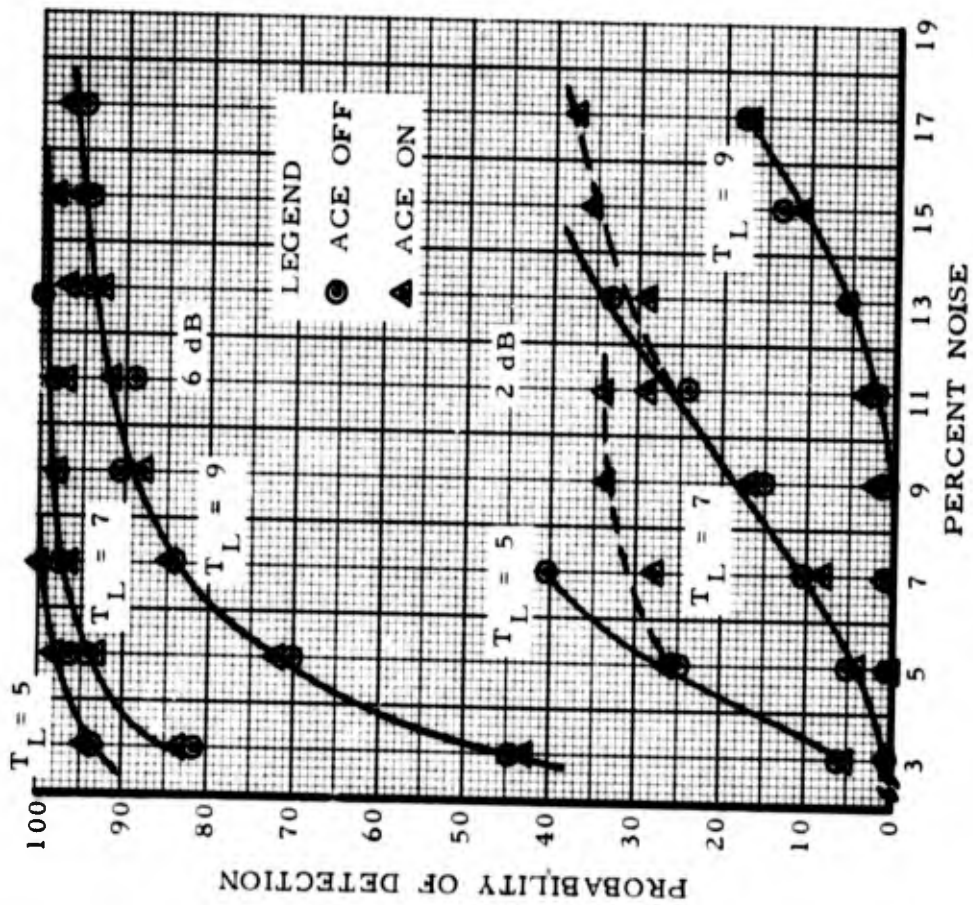


FIG. 9 PROBABILITY OF DETECTION VS. PERCENT NOISE

manually is required to maintain the  $10^{-3}$  probability of false alarm. The ACE curve (Figure 6) indicates that this will occur at a percent noise of 6% for a manual  $T_L$  of 5, a percent noise of 13% for a manual  $T_L$  of 7, and a percent noise of 23% for a manual  $T_L$  of 9. These test results indicate that the operation of the ACE circuit was normal. As in the false alarm tests, data could be taken only for percent noise and  $T_L$  combinations which did not cause data overflow in the Data Transmission Group (DTG) buffer.

B. False Target Detection - The probability of false alarm was determined as a function of percent noise and the manual setting of  $T_L$  with ACE "off" and then repeated with ACE "on."

1. Test Procedure - The radar transmitter was turned off and the input to the radar receiver was terminated with a dummy load. The percent noise was varied by adjusting the percent noise setting while a count of false targets detected was monitored. The test was repeated for various settings of  $T_L$ , with the ACE function "off" and "on," and for both the normal and MTI channels. Theoretical curves were calculated to permit comparison with the experimental results. These curves were based on the assumption that the input signal was random noise. Data taking for the experimental curves was terminated when the DTG indicated a buffer overflow.

2. Test Results - The results of these tests are shown in Figure 10. On the normal channel the probability of false alarm is approximately a factor of ten lower than that predicted by theory. In addition, the probability of false alarm with ACE "on" levels off at approximately  $10^{-4}$  rather than  $10^{-3}$ . Apparently, the quantized hits with receiver noise as an input are not completely random in range and azimuth. Radial correlation of hits is indicated. It is felt that the most likely cause of radial correlation was the presence of low level 60 cycle interference on the video line to the RVDP. At times, the peak-to-peak interference was as much as 10% of the mean peak noise voltage. This interference raised the level of noise slightly every 16.7 milliseconds (1/60 second); however, the overall percent noise was maintained at a fixed value by the slow feedback loop whose time constant was much longer than this. Thus, the output of the quantizer tended to occur in groups every 16.7 milliseconds. The sliding window encompassed about 37 milliseconds (13 radar trigger periods) allowing only two (possibly three) groups of hits to be included per window. Since the leading edge criterion was always much higher than three, this grouping of hits within the detection window resulted in a false alarm rate lower than would be predicted theoretically for a given percent noise and leading edge threshold.

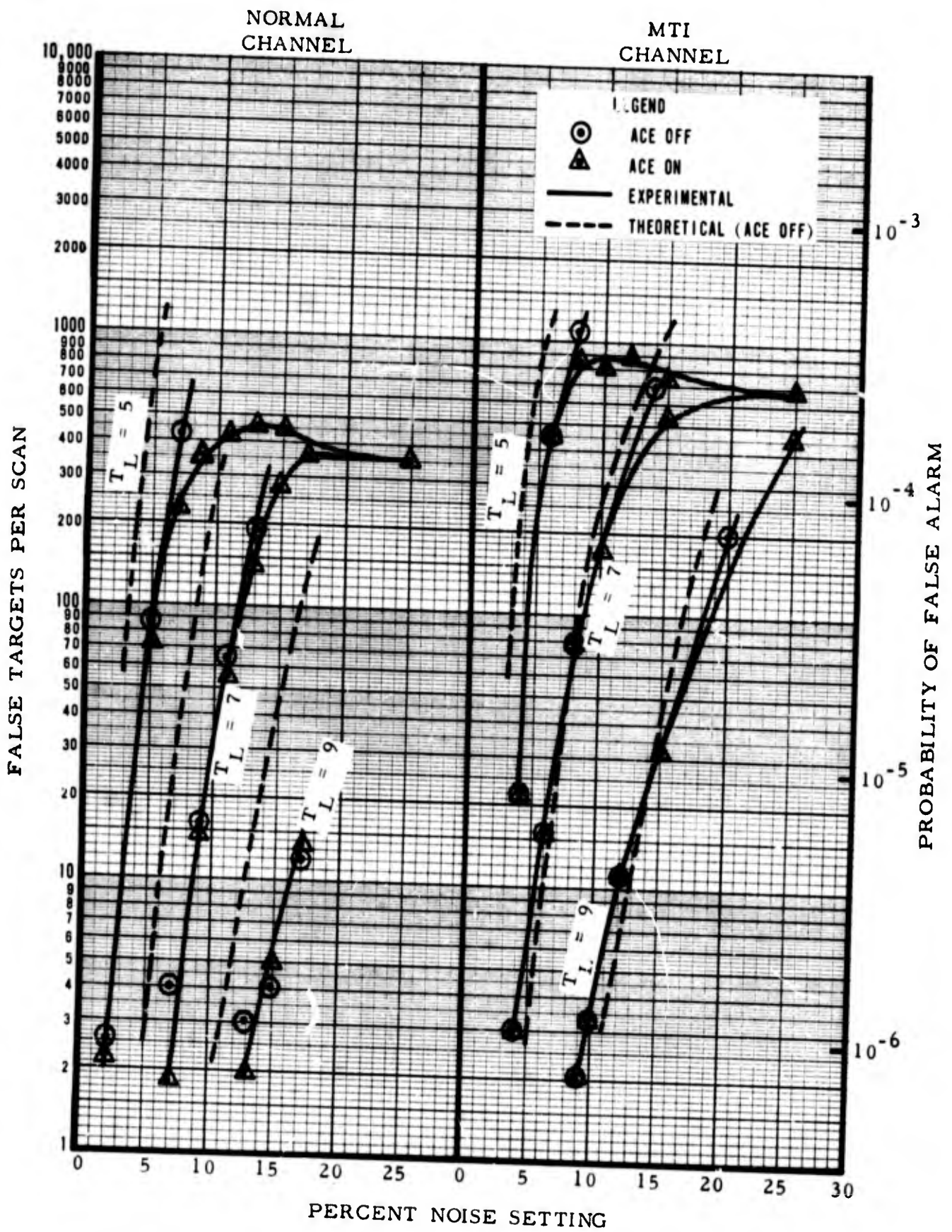


FIG. 10 FALSE TARGET RATE VS. PERCENT NOISE

The curves for false alarm rates on the MTI channel are somewhat closer to the theoretically predicted values. The MTI canceler circuit provides a limited amount of concentric correlation. Any noise peak is automatically distributed over three radar trigger periods at precisely the same range through the action of the double canceler. The range correlation produced by canceler action partially offsets the effect of hum on the MTI channel. Residual MTI rings also contributed to the false alarm rate.

Actual clutter returns display concentric correlation. The concentric correlation is primarily a function of the antenna beamwidth, scan-rate, radar pulse period, and turbulence. Since beamwidth, scan-rate and pulse period are fixed parameters, the amount of correlation is essentially a function of turbulence. This assumes, of course, that the radar receiver is not saturated. Concentric correlation of clutter returns was indicated by actual count of false returns in clutter areas when ACE was operating. In the normal radar channel where radial correlation restricted the ACE maintained probability of false alarm to  $10^{-4}$ , the probability of false alarm in actual clutter (which was due to light rain over a large area) was approximately  $2 \times 10^{-3}$ .

C. Composite Performance - The data on false alarm characteristics and the data on the probability of detection were combined to produce the composite curves of Figure 11. These curves were used to select the setting of percent noise and  $T_L$  for operational testing of the RVDP.

It has been determined theoretically by Swerling<sup>5</sup> that the optimum  $T_L$  for a window size of from 10 to 20 radar triggers is approximately one half the window size. The composite curves verify this theoretical determination. Swerling also demonstrated that the probability of detection is not a very sensitive function of the probability of false alarm. A change in  $T_L$  or percent noise which would drastically affect the false alarm rate should affect the probability of detection to a much smaller degree. The composite curves also verify this theoretical determination.

D. Sensitivity - From the composite performance data a leading edge threshold ( $T_L$ ) of seven, a percent noise of 8% for the normal quantizer, and a percent noise of 5% for the MTI quantizer were selected and the sensitivity of the primary radar detector was measured.

- - - - -  
<sup>5</sup>Reference 5

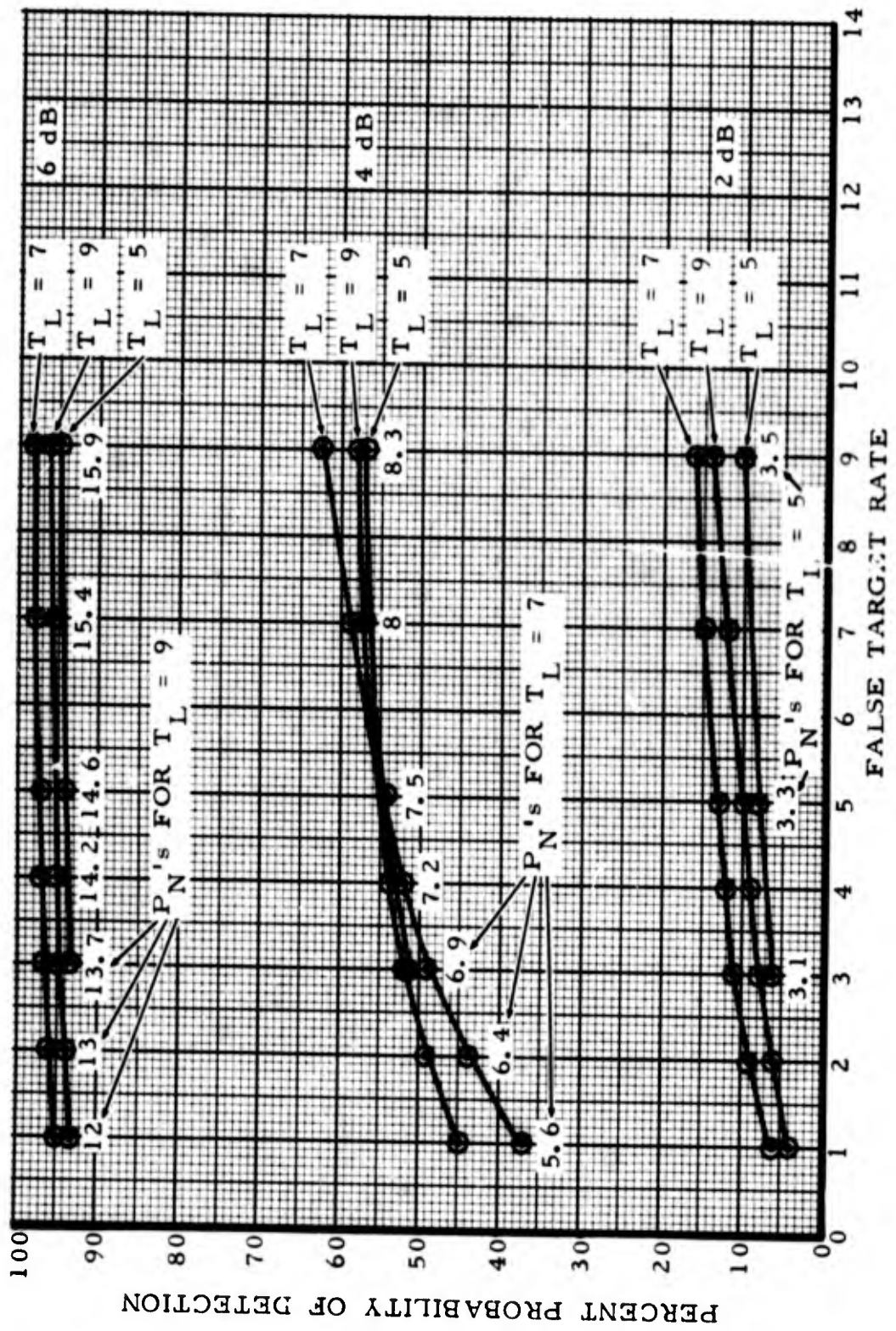


FIG. 11 PROBABILITY OF DETECTION VS. FALSE TARGET RATE

1. Test Procedure - A two microsecond test target was applied at the input of the radar receiver (waveguide directional coupler) and the run length of the test target was varied with the target generator test set. An electronic counter, in conjunction with a range/azimuth decoding gate, was used to obtain a count of the times the test target was detected by the RVDP over a period of 20 antenna scans. The target signal strength was reduced in 1 dB steps until the target was not detected over the 20-scan period. The primary radar MDS was measured for both normal and MTI video to establish the performance level of the radar alone.

2. Test Results - The relationship between signal strength and the probability of detection for various target run lengths is shown in Figure 12 for both normal and MTI video. Examination of the curves for a target run length of 13 indicates a difference of 7 dB at the 90% blip/scan point. This difference was due, in part, to the difference in the radar sensitivity for normal and MTI video, and partially due to the interaction between the MTI canceler and the RVDP quantizer. This interaction was noted and discussed in the previous section (Video Quantization).

### Detector Performance On-Line

A. Probability of Detection - Normal Channel - The detector performance on the normal channel was checked at maximum range by having test aircraft fly out to the maximum range of the radar coverage area while recording the percent of scans the target was detected. The detector performance was compared to the performance of the normal broad band radar system

1. Test Procedure - The test aircraft was flown out-bound on a selected radial that was relatively clear of other traffic. An altitude of 26,000 feet was used for this flight to assure that the aircraft would still be within line-of-sight at maximum range. Air Traffic Control (ATC) specialists observed the displayed output of the RVDP and the normal radar Plan Position Indicator (PPI) display and a "hit" or a "miss" was recorded for each channel every antenna scan. This was continued until the target was lost on both channels, at which time the test aircraft reversed its course allowing data collection to continue on the inbound run.

A description of the flight test configuration and the test flight procedures is included in Appendix IV.

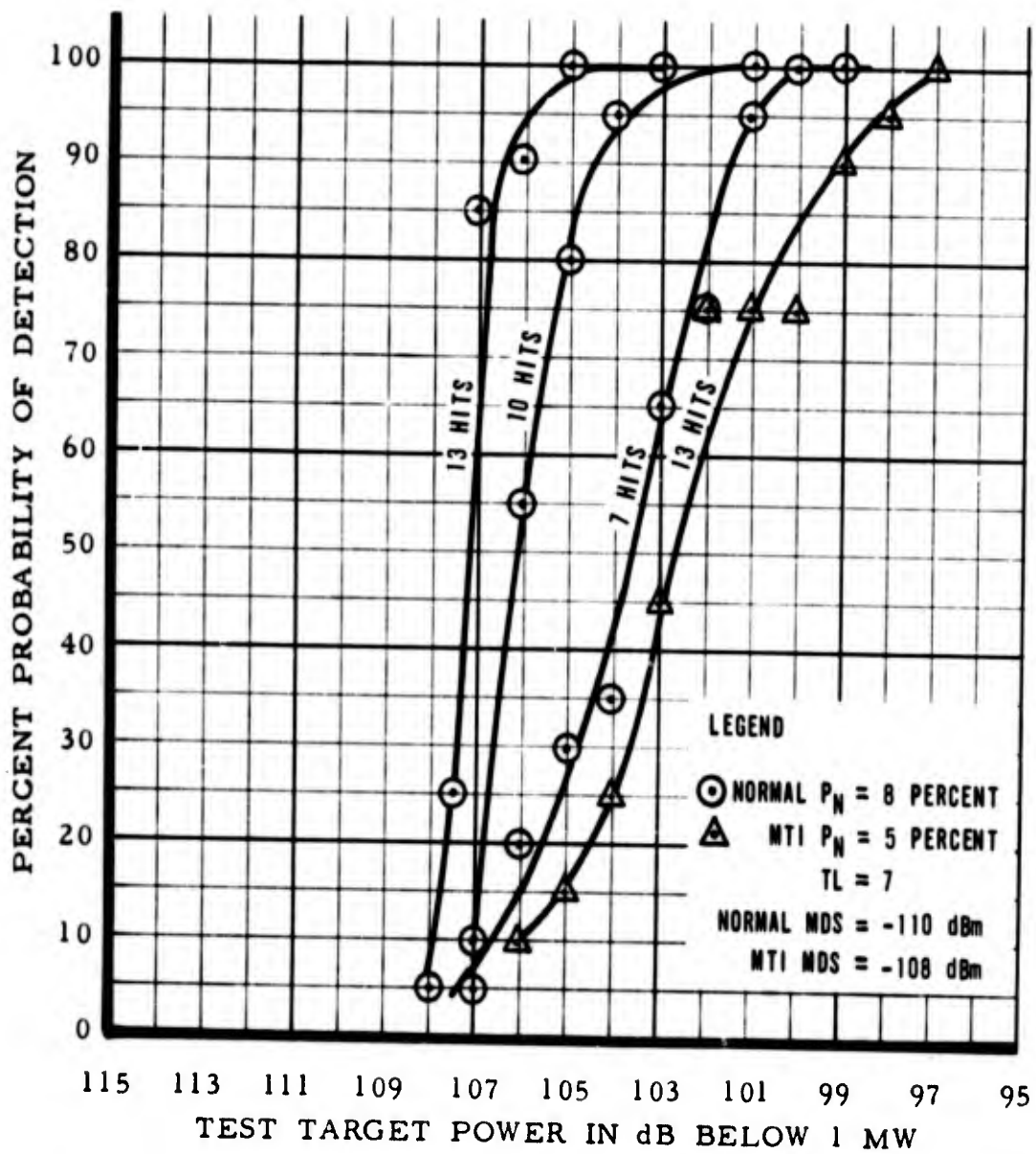


FIG. 12 PRIMARY RADAR SENSITIVITY CURVES

2. Test Results - The results of this test are presented in Figure 13. The results are grouped in 10 nmi intervals. Each data point represents the average percentage of scans in which the test aircraft was detected for that 10 nmi interval. The digital detector produced a slightly higher detection probability than the normal broad band radar system (video channel). These data represent radar returns from a relatively small target since the aircraft was proceeding out-bound (or inbound) along a selected radial.

B. Probability of Detection - MTI Channel - The MTI channel is used only at short range and, in general, the signals are quite strong. However, radar returns from aircraft with a low radial component of velocity (with respect to the radar site) tend to be reduced in amplitude by the MTI circuits. To check the performance of the RVDP in the MTI region, the output messages were recorded and analyzed using the TAD Program (Track Analysis and Display Program - see Appendix IV). The percent of scans in which each aircraft was detected for nine separate aircraft flights (targets of opportunity) through the MTI region is shown in Table I. The RVDP/MTI crossover point was set at 50 miles. The overall detection probability for all nine aircraft was 0.88.

TABLE I  
MOVING TARGET INDICATOR (MTI) SENSITIVITY

Aircraft	No. of Scans	RANGE		AZIMUTH		Percent of Scans in which Aircraft was Detected
		Start (nautical miles)	End	Start (degrees)	End	
1.	32	26	23	357	348	78%
2.	34	21	24	237	265	91%
3.	12	25	28	275	279	100%
4.	32	50	34	254	252	88%
5.	31	26	11	250	234	87%
6.	22	18	21	306	294	82%
7.	25	29	25	269	260	84%
8.	35	13	33	263	249	91%
9.	19	32	38	313	317	100%

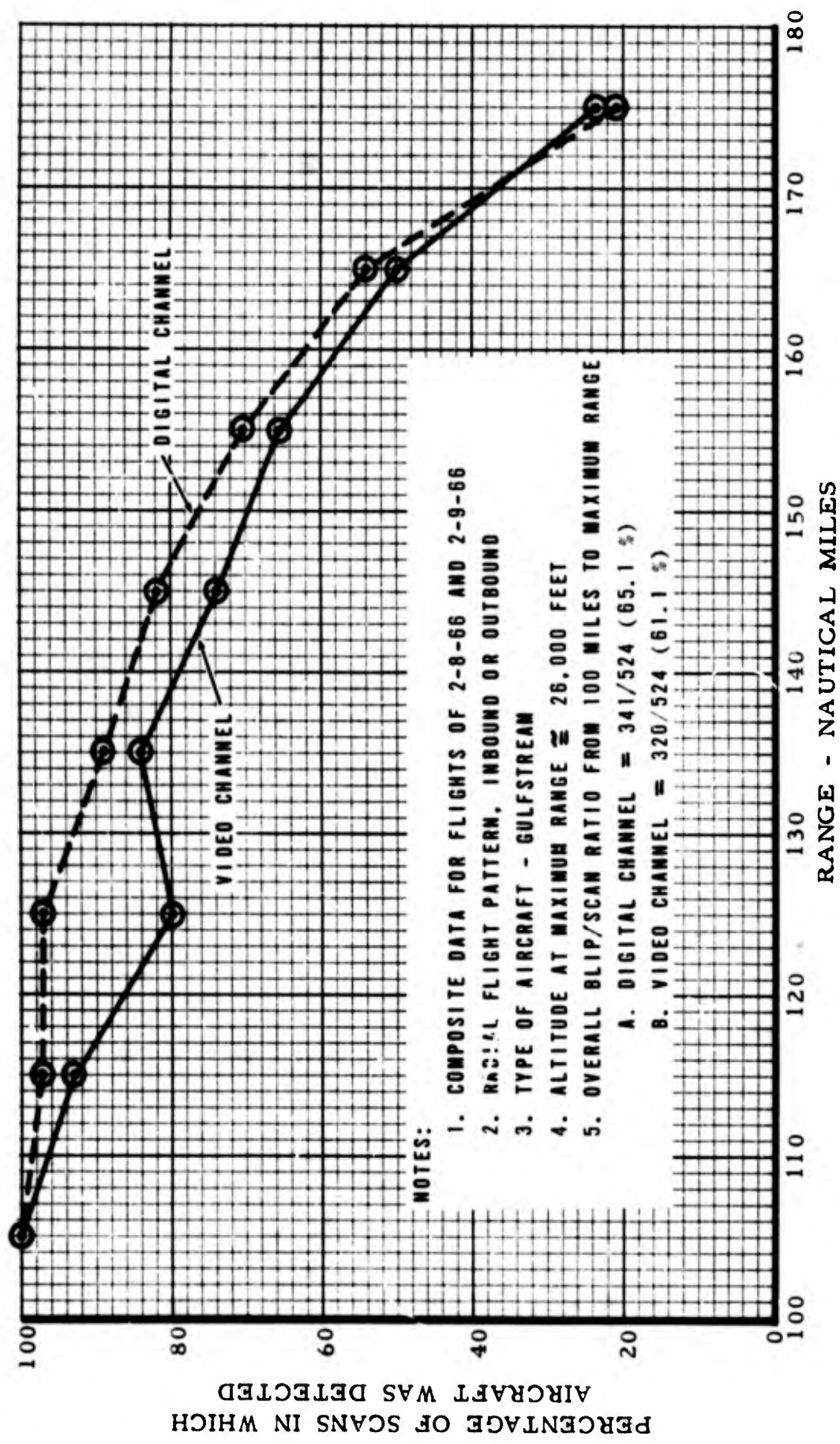


FIG. 13 PRIMARY RADAR SENSITIVITY AT MAXIMUM RANGE

C. Target Detection in Areas of Weather Clutter - When weather clutter is present, the target detection thresholds are automatically modified as described in the sections on video quantization and statistical detection. The RVDP performance in weather clutter was compared to the performance of the normal broad band radar system.

1. Test Procedure - By observation of the displays for the digital and video channels, ATC specialists recorded a "hit" or a "miss" during each antenna scan while tracking a single aircraft through areas of weather clutter. The initiation and termination of each data run were accomplished concurrently on both the digital and video channel displays for selected targets of opportunity. Two additional ATC specialists assisted in the recording of the observed information and the time-of-day reference. The ATC specialists who were performing the tracking function were permitted, at their discretion, to adjust the RBDE-5 display for optimum trail data and to use a manually-controlled symbol as a tracking aid.

2. Test Results - During the test, the Atlantic City Weather Bureau Airport Station was reporting radar weather returns for a radius of approximately 80 miles from Atlantic City. Throughout the data-collection period, all weather stations within a 50-mile radius were reporting precipitation in intensities varying from very light drizzle to light rain.

Aircraft-tracking data were obtained for 17 aircraft (targets of opportunity) which were in or near the areas of weather clutter, and the ratio of detected targets to the number of scans observed (blip/scan ratio) for each run is shown in Figure 14. Except for data runs 7 and 8, all data were collected with the ARSR-2 facility operating in the linear polarization mode. The RVDP ACE function was on during this test, the Run Length Discrimination (RLD) minimum setting was 5, and the RLD maximum setting was 30.

For ten of the data runs, a higher blip/scan ratio was obtained on the video channel, whereas five of the runs produced a higher blip/scan ratio for the digital channel. The overall blip/scan ratios for all data runs indicated a difference of approximately 2% between the video channel and the digital channel. A statistical test for difference between the blip/scan ratios for the digital and video channels indicated no significant difference at the .05 level of significance.

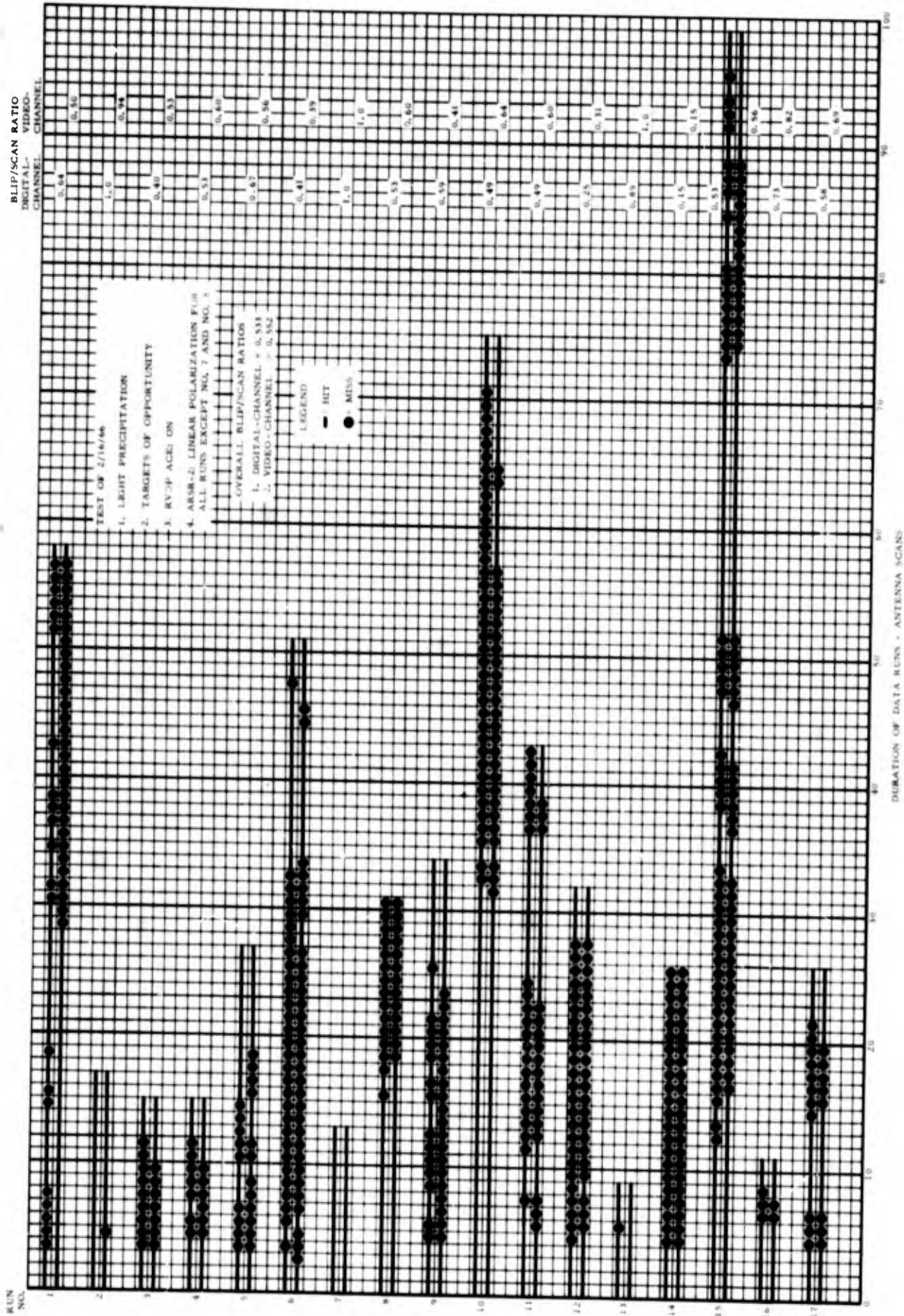


FIG. 14 COMPARISON BETWEEN DIGITAL CHANNEL AND VIDEO CHANNEL FOR TARGET DETECTION WITHIN AREAS OF WEATHER CLUTTER

It was noted that the ATC specialists observing the digital-channel display elected to use a higher storage factor than the controllers who were observing the video-channel display. During the debriefing period, the controllers stated that the longer trails were necessary on the digital-channel display to assist in tracking the aircraft targets through the weather-clutter areas, whereas more storage tube erasures were desired on the video-channel display to minimize the saturating effect that the weather clutter had on the scan-converter tube. Clutter returns on the digital-channel display cannot be distinguished from aircraft targets on the basis of intensity or size as they can be on the video channel.

The photographs shown in Figures 15 and 16 were taken at the conclusion of data run number 2 to illustrate the type of presentation viewed by the ATC specialists during the weather-clutter tests.

D. Weather Clutter Targets - Counts of false targets due to weather clutter were taken to check the effectiveness of the RVDP ACE system. A series of photographs was taken to obtain a count of the number of weather clutter targets processed in approximately one antenna scan under weather-clutter conditions. The photograph of a single scan of the digital-channel display (Figure 17) illustrates the weather-clutter targets that were processed for the type of weather clutter shown on the single scan of the video-channel display (Figure 18). Fourteen weather clutter targets (false alarms) were counted for a ten-degree segment (120 to 130 degrees) between the 25-mile and 50-mile range marks (Figure 17). This is quite close to the theoretical value of ten targets for a like area ( $10^4$  space bits) for a probability of false alarm of  $10^{-3}$ . It is possible that the count of 14 includes a few aircraft targets which would make the measured false alarm rate even closer to the design value.

The ACE was designed to inhibit the processing of all targets in areas where weather clutter is so intense that it is impossible to maintain a probability of false alarm of  $10^{-3}$  or less. The effect of this blanking function is depicted in the photograph of the digital-channel display (Figure 17) where no targets were processed for the most dense areas of weather clutter shown on the video-channel display (Figure 18).

During these tests it would have been desirable to adjust the probability of false alarm to determine the optimum balance between missed aircraft targets and false alarms. The RVDP does not have this capability.

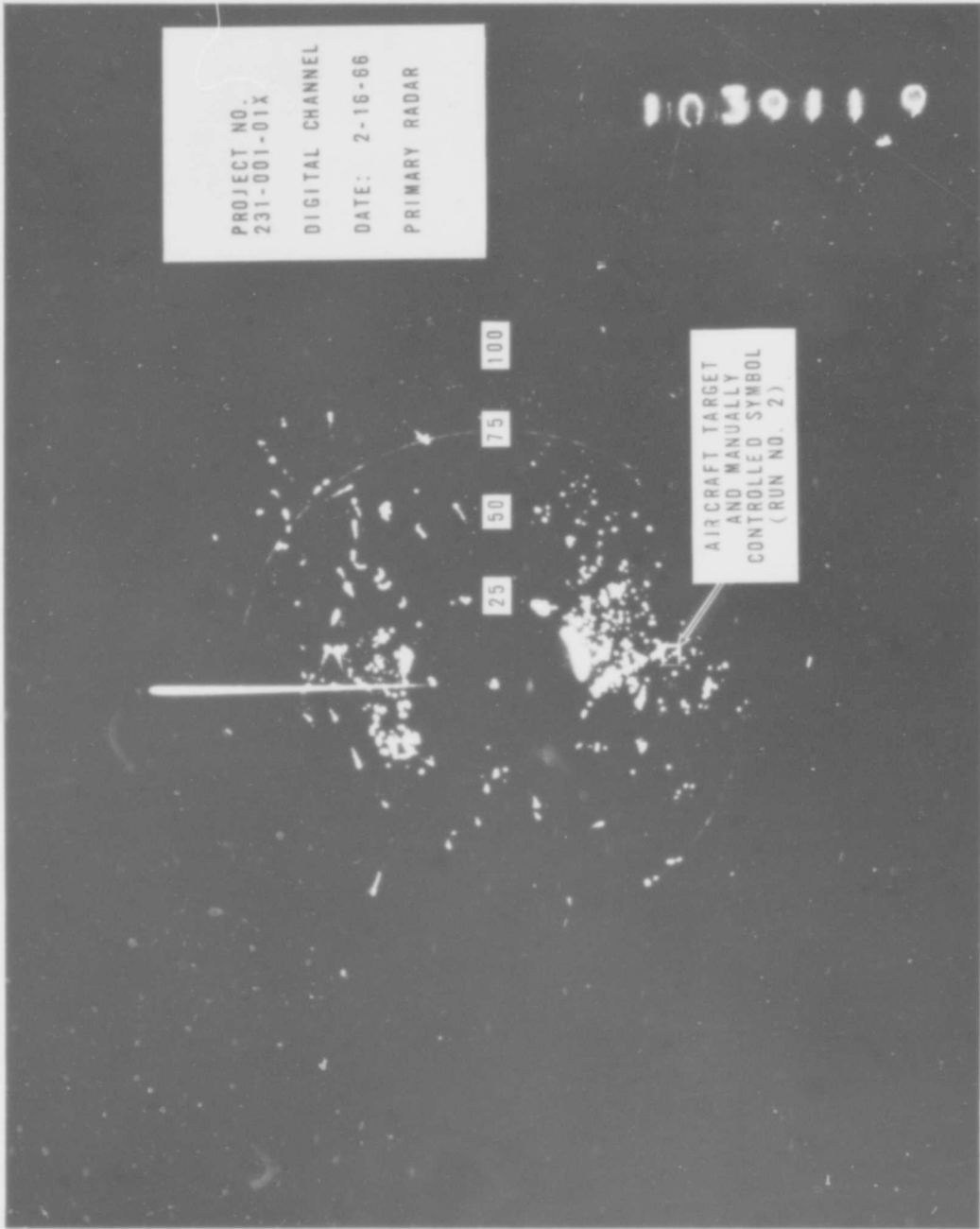


FIG. 15 DIGITAL CHANNEL DISPLAY PRESENTATION OF AIRCRAFT TARGETS AND WEATHER CLUTTER TARGETS

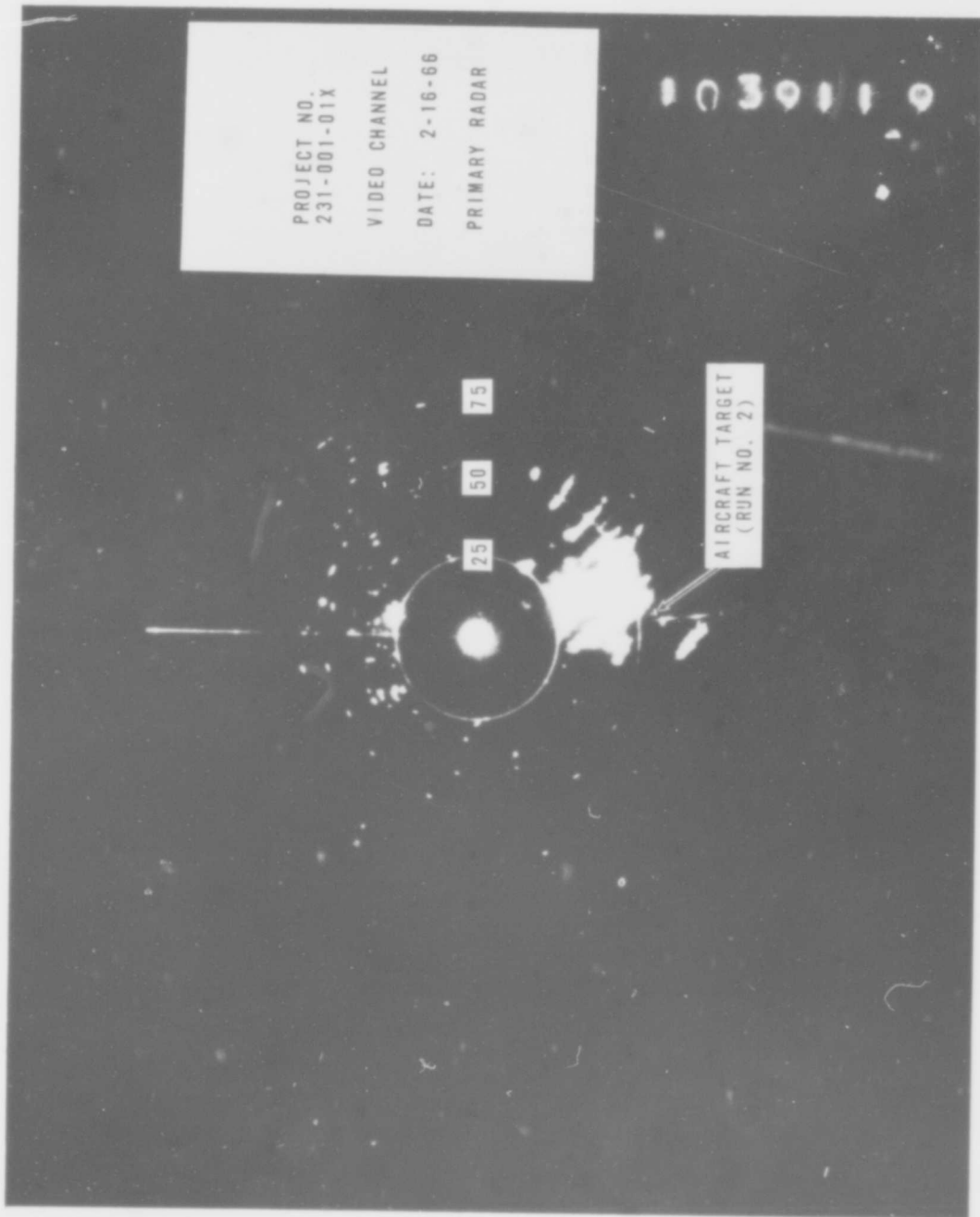


FIG. 16 VIDEO CHANNEL DISPLAY PRESENTATION OF AIRCRAFT TARGETS AND WEATHER CLUTTER

PROJECT NO.  
231-001-01X

DIGITAL CHANNEL

DATE: 2/24/66

PRIMARY RADAR

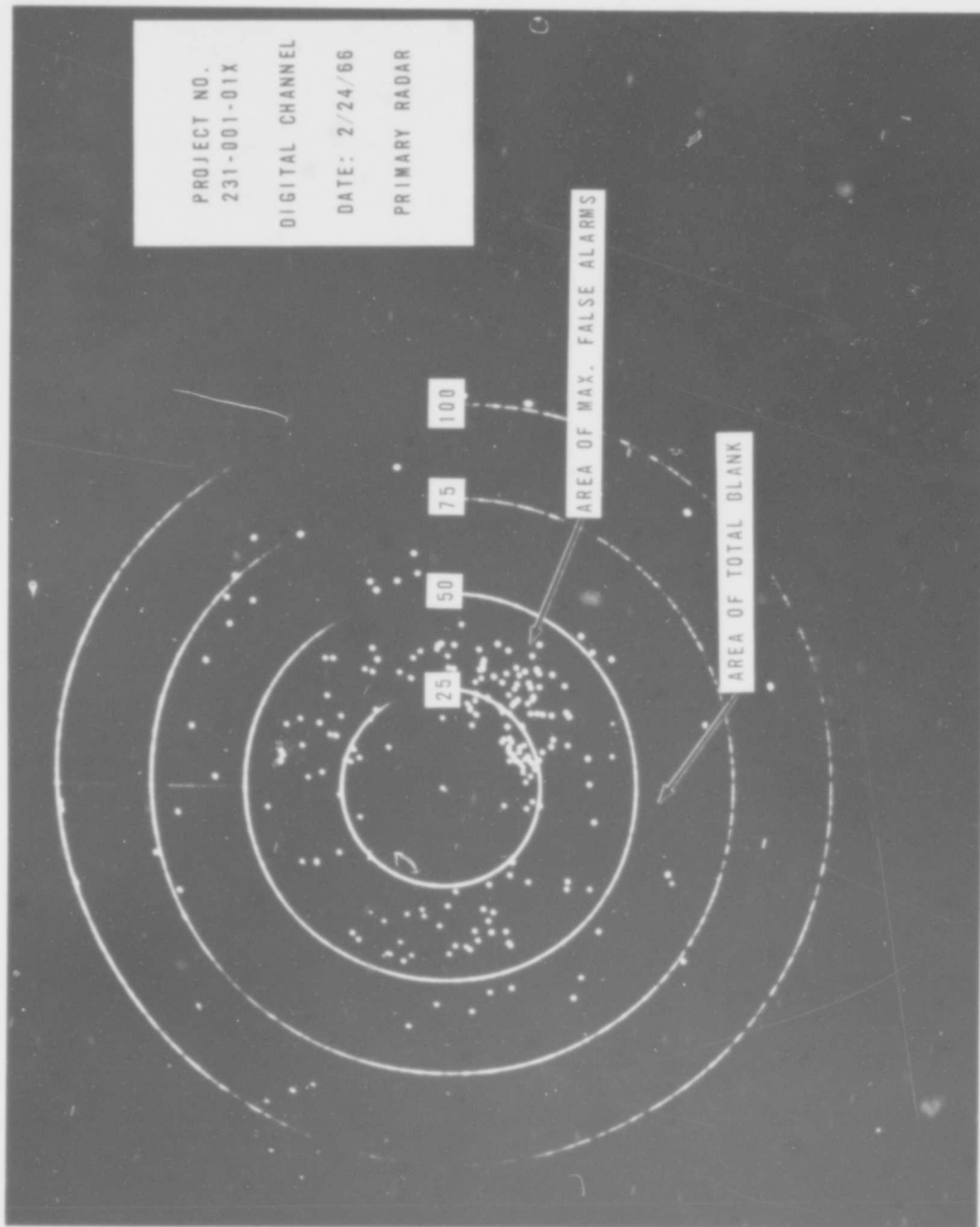


FIG. 17 DIGITAL CHANNEL DISPLAY PRESENTATION OF AIRCRAFT TARGETS AND WEATHER CLUTTER TARGETS AFTER ONE ANTENNA SCAN

PROJECT NO.  
231-001-01X  
VIDEO CHANNEL  
DATE: 2/24/66  
PRIMARY RADAR

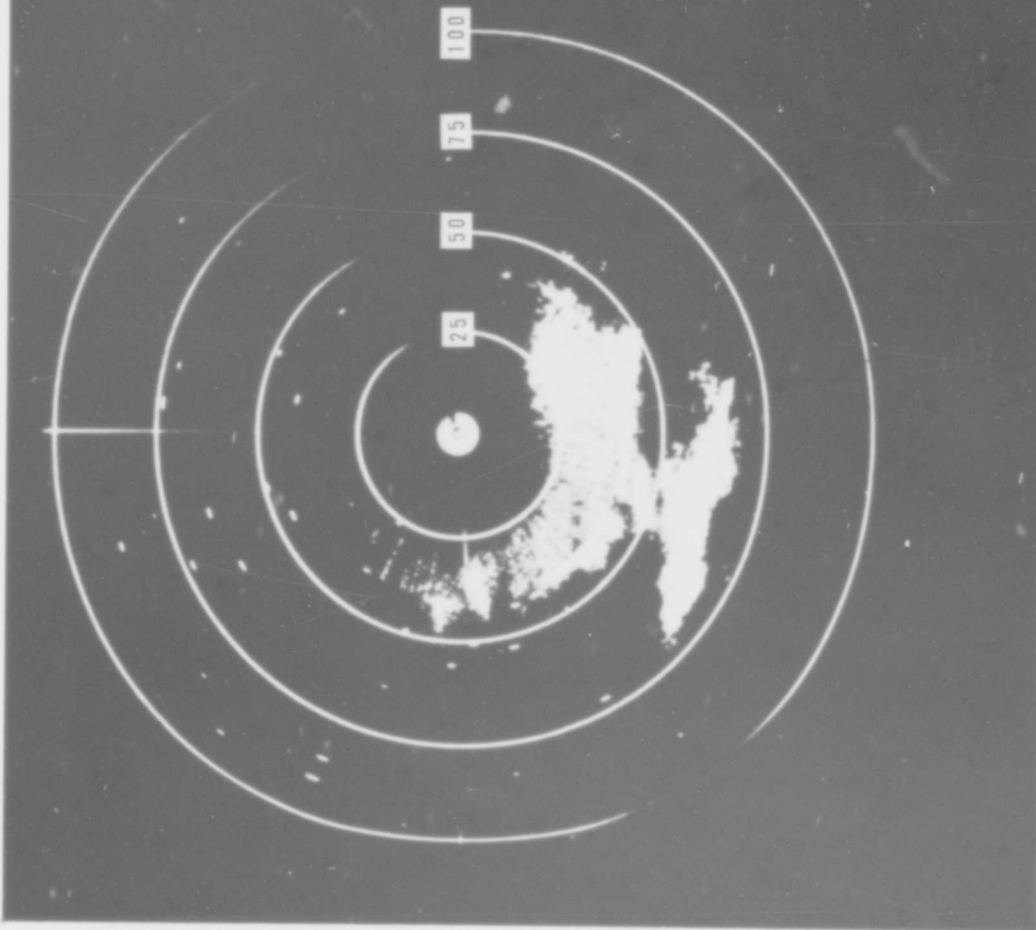


FIG. 18 VIDEO CHANNEL DISPLAY PRESENTATION OF AIRCRAFT TARGETS AND WEATHER CLUTTER AFTER ONE ANTENNA SCAN

## Beacon Detection

The RVDP detects and processes beacon transponder replies generated by ground interrogated aircraft and prepares a single digital message output for each such aircraft every antenna scan. The digital message contains all the information that was obtainable concerning the aircraft such as position (range and azimuth), beacon code, beacon altitude and special message control functions.

To prepare the output message, the RVDP must detect all the available information and attempt to determine its validity. The beacon detection process is actually performed in four steps.

1. Pulse Detection - The transponder coded replies in serial video form are applied to the beacon quantizer where the reply pulses are each inspected according to criteria of minimum amplitude and duration.

2. Bracket Detection - The code train is then inspected for the presence of bracket pulses at the proper spacing.

3. Target Detection - Bracket detection pulses, as a result of mode A/3 replies, are then stored at a memory location representing the range at which the bracket detection occurred. When a sufficient number of bracket detections have occurred from the transponder replies generated by the same aircraft, the target has been detected. This number of required bracket detection pulses is a threshold setting which must be equalled or exceeded within a given period of time (or number of interrogation periods). Also, the series of bracket detection pulses must occur at the same range (memory location) in order for target detection to take place.

4. Code Detection - At the same time that the bracket detection pulses are stored in memory for target detection, the code content of the transponder reply is strobed in parallel and temporarily stored. The code is inspected for possible garble with an interfering code train and is then stored in a second memory. Additional reply codes are compared with the stored code and, if comparison occurs, the code is considered validated. The validated code is held in memory to await the completion of the target detection process.

### Pulse Detection:

Amplitude Threshold - Incoming signals are amplitude compared with a reference voltage which determines the amplitude above

which the signal will be accepted and below which the signal will be rejected. Figure 19, **Beacon Quantizer Amplitude Threshold Characteristics**, shows the probability of quantizing versus the input pulse amplitude for nominal pulse widths and for minimum pulse widths required for 100% detection. As would be expected, both curves show a narrow gray zone between the 0% and 100% detection points.

**Pulse Width Threshold** - To test a beacon reply pulse for minimum width, it is first delayed by an amount equal to the minimum acceptable pulse width and then compared to the undelayed pulse for coincidence. If coincidence occurs, the pulse has met the minimum width criterion and is accepted. If no coincidence occurs, the pulse width is less than the minimum and is discarded. All measurements of pulse width are done between the 50% amplitude points of the leading and trailing edges. The test results determined that the pulse width at which 100% acceptance occurs is 0.285 microseconds and the point at which 0% acceptance occurs is 0.280 microseconds. All other pulse parameters such as amplitude, rise time, and decay time were maintained at nominal values. Since the minimum pulse width that is generated by the transponder is 0.35 microseconds, the performance of the RVDP beacon quantizer is such that all valid reply pulses will be accepted and noise transients that exceed the amplitude threshold will be rejected.

**Noise Response** - The response of the beacon quantizer to various levels of beacon receiver noise is shown in Figure 20. The average count of pulses per scan at the quantizer output is not significant for the noise level normally used in operating conditions (0.5 volt average peak). At the 0.6 V (volt) level, the average count still may be acceptable. However, above this value, the average count becomes significant. Few of these pulses would be at the proper spacing to generate bracket coincidence pulses, and the few that were would occur randomly and would not produce false targets. However, these pulses could appear as part of reply code trains, thus producing erroneous code information.

It is important to maintain the beacon quantizer noise input at the normal operating level (0.5 V average peak). Also, the quantizer 0% acceptance threshold must not be allowed to fall below 0.5 V.

It was also determined that no significant change in the amplitude and pulse-width detection limits of the quantizer occurred when pulses of nominal parameters were applied to the RVDP input in the presence of the normal operating level of receiver noise.

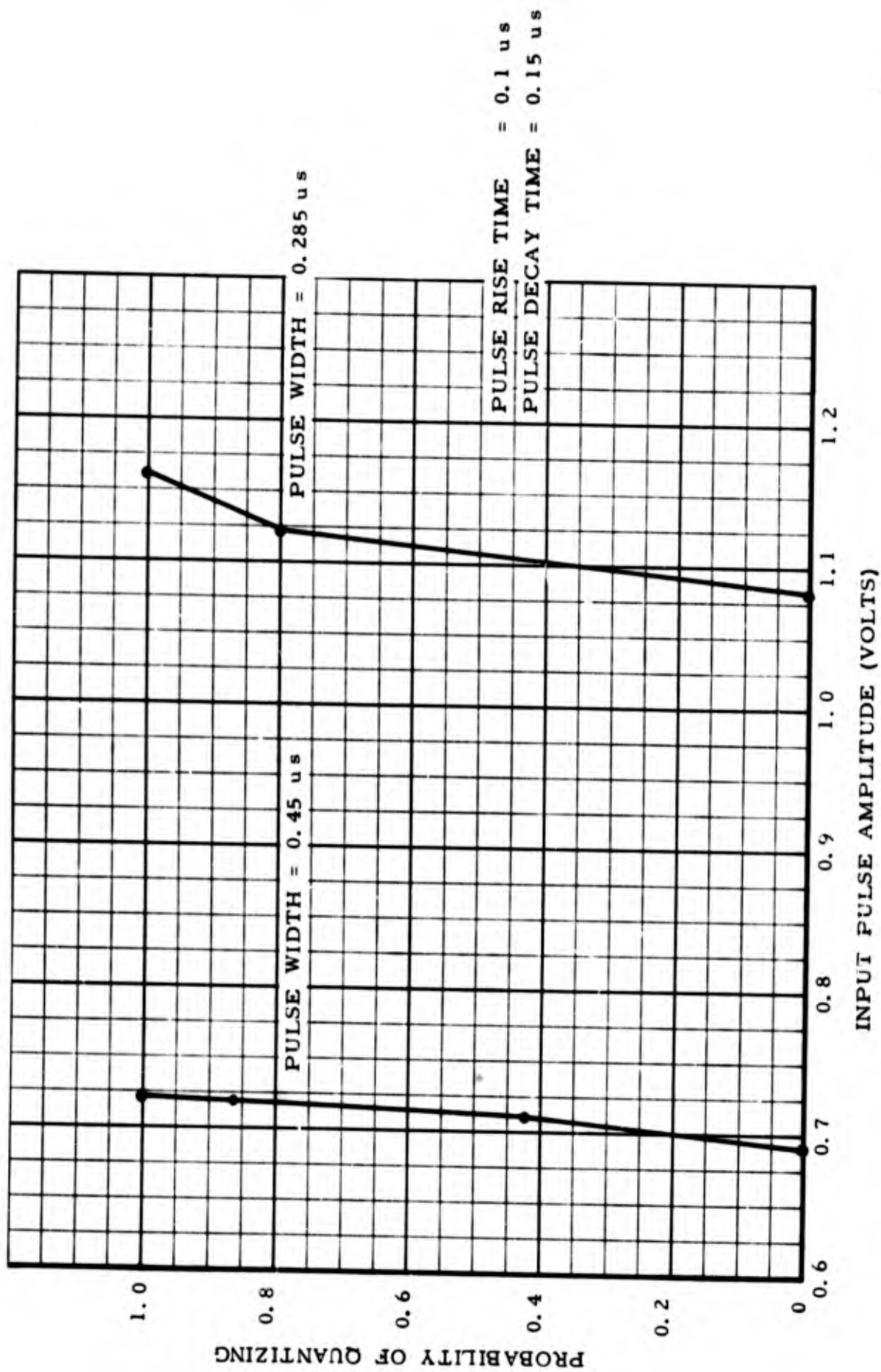


FIG. 19 BEACON QUANTIZER AMPLITUDE THRESHOLD CHARACTERISTICS

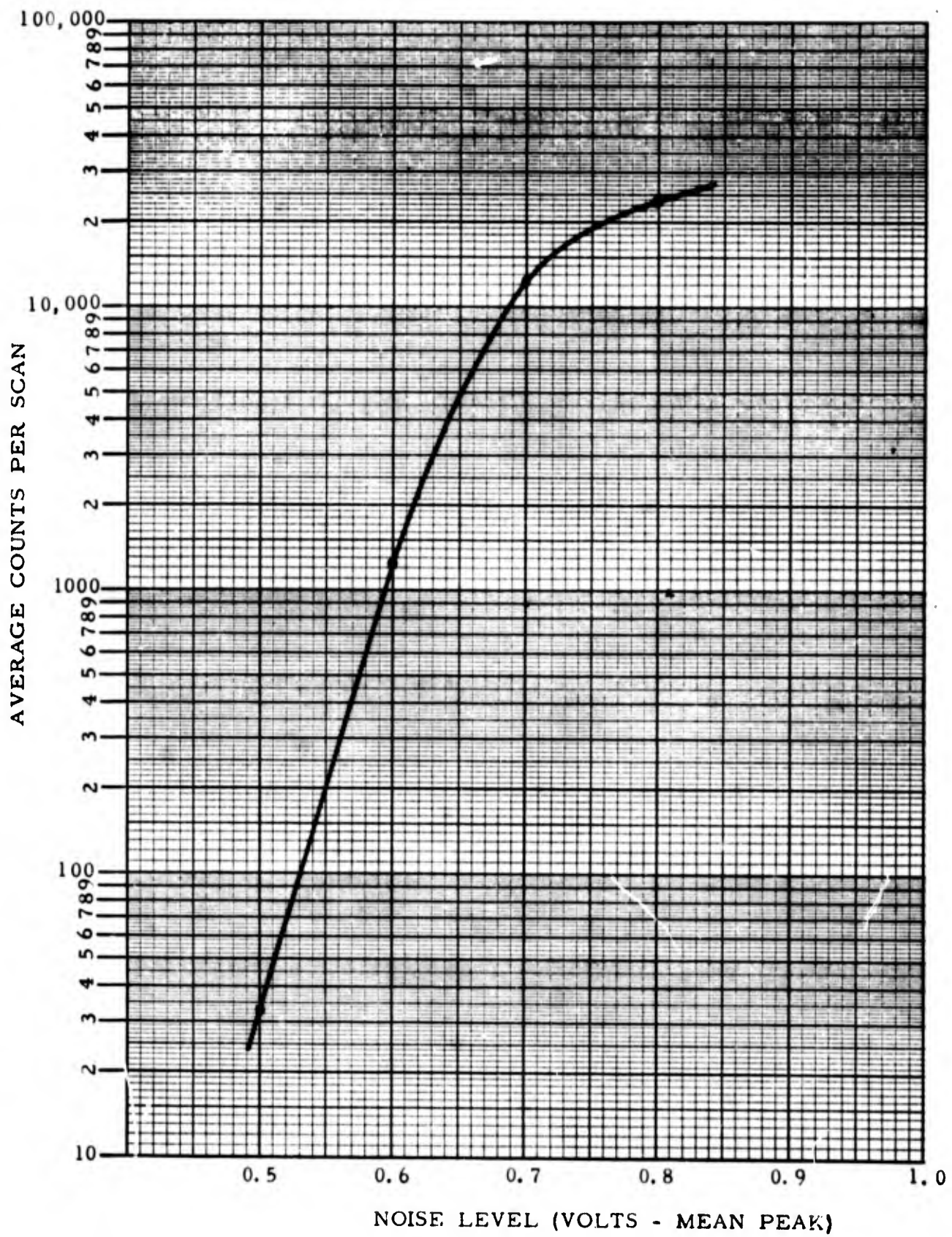


FIG. 20 BEACON QUANTIZER NOISE RESPONSE

Pulse Resolution - Figure 21 shows a series of photographs of the input and output of the beacon quantizer as the spacing of two pulses was varied from direct overlap to the point of 100% resolution. Figure 21A shows the input as two pulses completely overlapped and the output as a single pulse recognized by the quantizer. Figure 21B shows that as one pulse is moved slightly, a point is reached where neither pulse is accepted by the quantizer. This is because the combination of the two pulses' rise times exceeds the criteria for acceptance. Although the composite rise time does not appear to be excessive, it must be pointed out that the rise time sampling in the quantizer is done between the 50% and the 90% amplitude points of the pulse leading edge. This, then, makes the composite rise time of Figure 21B unacceptable. This effect of rise time rejection had been predicted and the rise time criterion of the beacon quantizer had been removed. It was replaced for this test only to document the effect and was again removed at the conclusion of this test.

Figure 21C shows that a wide output pulse is produced which roughly corresponds to the width of the composite input pulse. The two pulses which make up the composite pulse are separated slightly more than in Figure 21B.

Figure 21D shows the two input pulses separated enough so that the trailing edge of one and the leading edge of the other are just discernible. However, the quantizer does not yet recognize that there are two pulses and produces a single wide output pulse.

Figure 21E shows that the input pulses are separated slightly more than in Figure 21D. Although the output is still a single pulse, its width now approximates that of one input pulse. This is apparently due to the fact that at this point of pulse separation the quantizer recognizes the leading and trailing edges of the first pulse but, with the small separation that exists, cannot recognize the leading edge of the second pulse.

Figure 21F shows the two input pulses separated slightly more, so that the second pulse is now produced approximately 50% of the time.

Finally, Figure 21G shows the two input pulses separated to the point where both pulses are resolved 100% by the beacon quantizer. This separation from the trailing edge of the first pulse to the leading edge of the second pulse (measured at the 50% amplitude point) is about 0.05 microseconds.

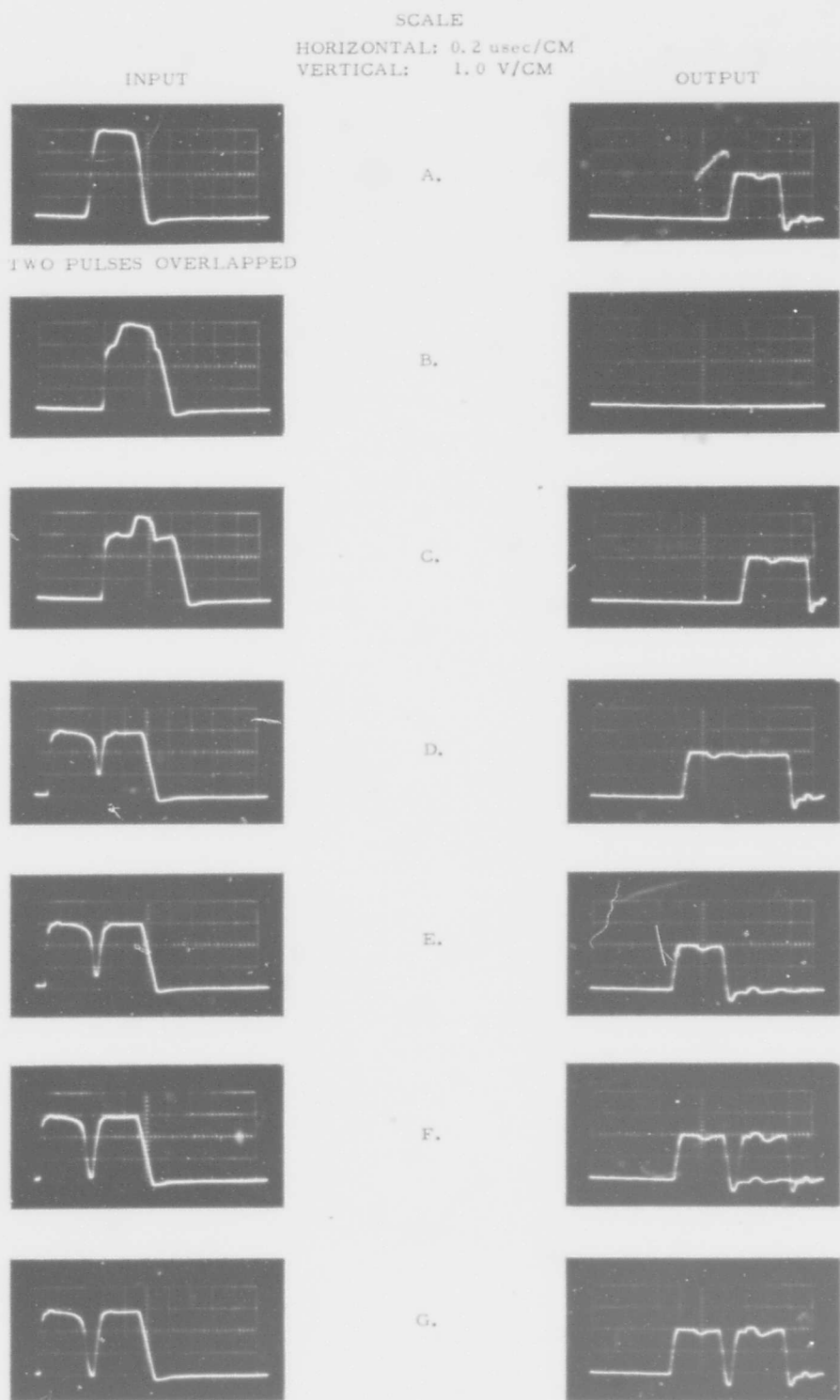


FIG. 21 BEACON QUANTIZER PULSE RESOLUTION

Figure 22 is a series of photographs which shows two input pulses separated to the point where only one output pulse is produced by the quantizer. The series of photographs of the input shows that one pulse was held constant in amplitude while the other was varied in 1-volt steps.

Figure 23 is a series of photographs which shows two input pulses separated to the point where both pulses are resolved 100% of the time. Here again, the series of photographs of the input shows that one pulse was held constant in amplitude while the other was varied in 1-volt steps.

### Bracket Detection

Description - Every reply code transmitted by the aircraft transponder to interrogations by the ground equipment is framed by a pair of bracket pulses spaced 20.3 microseconds apart. All the data pulses are contained within the bracket pulses and they are spaced in multiples of 1.45 microseconds. A complete description of an idealized pulse train reply is contained in Appendix V.

Bracket detection is the process of recognizing a pair of framing, or bracket, pulses (designated F1 and F2 for leading and trailing brackets, respectively) whose nominal separation is 20.3 microseconds. To accomplish bracket detection, the RVDP utilizes a coincidence principle whereby two points in a lumped-constant delay line are continuously monitored. The function of the delay line is to accept and store the individual pulses in a pulse train for a period of time long enough to ensure that the two pulses of interest (F1 and F2) can be detected simultaneously. On this basis, a coincidence criterion is established which, when satisfied, affords the required detection function.

Performance - Figure 24 shows the RVDP Bracket Detection Characteristics as the bracket spacing was varied over the complete range of bracket detection. This was performed for three values of bracket pulse widths.

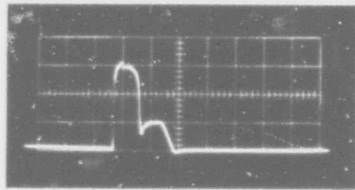
Detection of any pair of pulses separated by 20.3 microseconds is not, by itself, conclusively indicative of the presence of a valid reply code train. Conceivable spatial distributions of aircraft antenna illuminated by the ground beacon antenna during a single beacon radar interval include patterns of replies which may interfere in a

SCALE

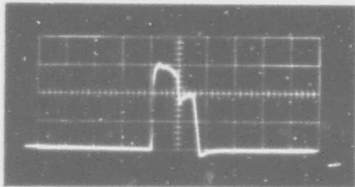
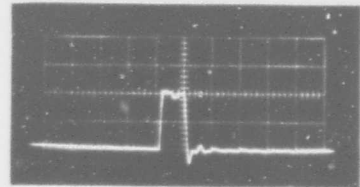
HORIZONTAL: 0.5  $\mu$  SEC/CM  
VERTICAL: A-D 1.0 V/CM  
E 2.0 V/CM

INPUT

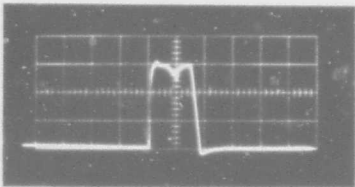
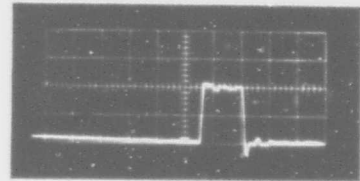
OUTPUT



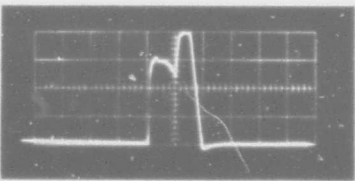
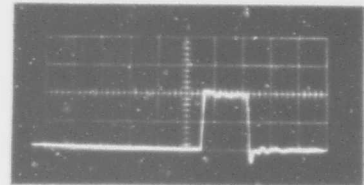
A



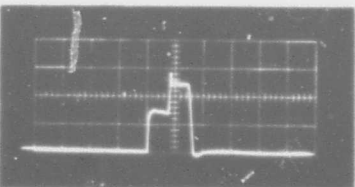
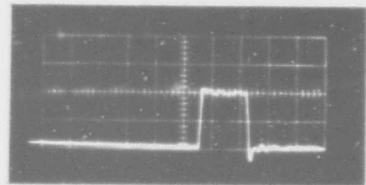
B



C



D



E

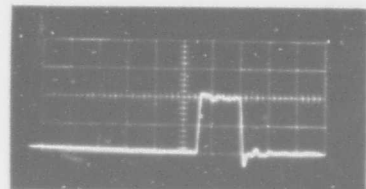


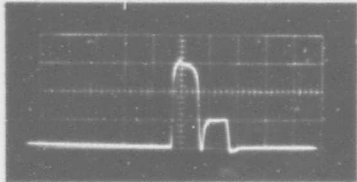
FIG. 22 UNRESOLVED PULSE SEPARATION

SCALE

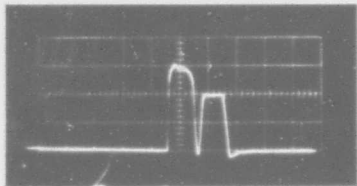
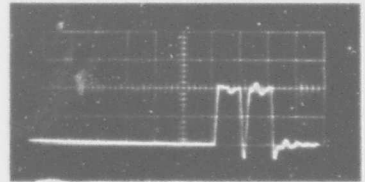
HORIZONTAL: 0.5  $\mu$  SEC/CM  
VERTICAL: A-D 1.0 V/CM  
E 2.0 V/CM

INPUT

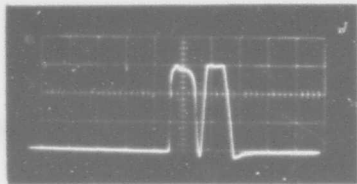
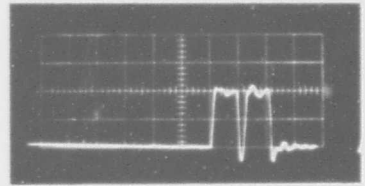
OUTPUT



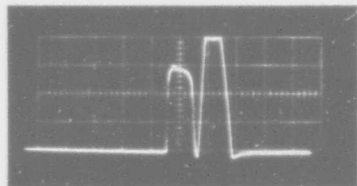
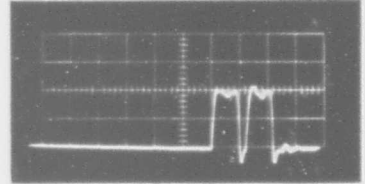
A



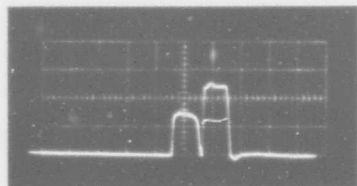
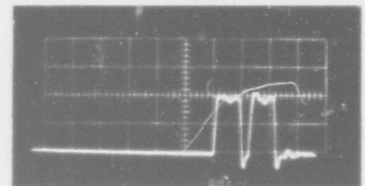
B



C



D



E

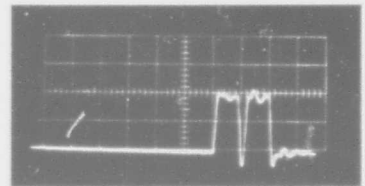


FIG. 23 RESOLVED PULSE SEPARATION

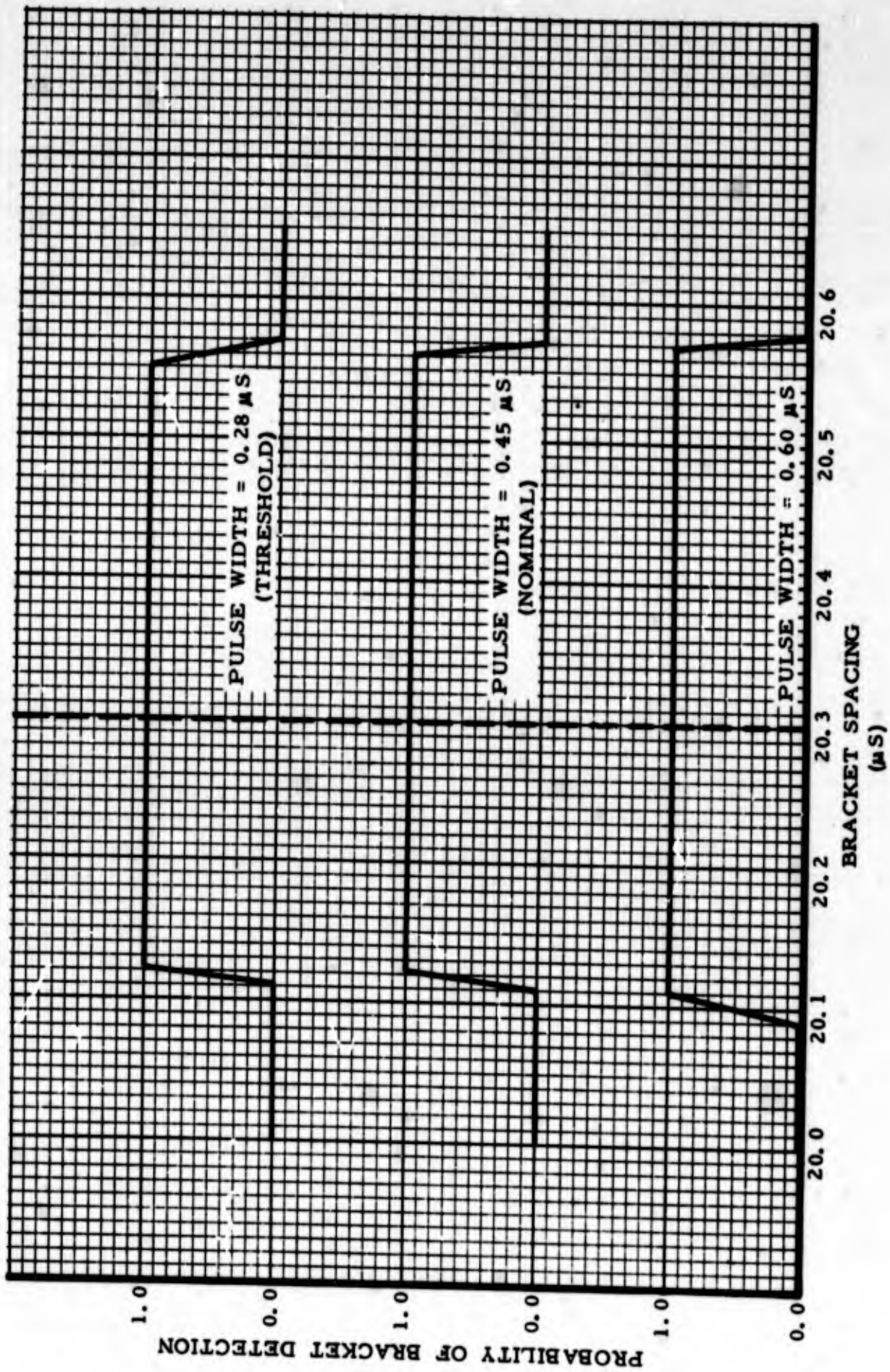


FIG. 24 BRACKET DETECTION CHARACTERISTICS

manner giving rise to a rapid succession of such pulse pairs. The process of investigation into the true origin of the received pulse trains is described further in later sections.

### Target Detection

Description - Each mode A/3 bracket detection pulse is temporarily stored in a ferrite core memory (Memory I) for the statistical target detection process. The location in memory at which the pulse is stored represents the range of the aircraft which generated the reply. Each interrogation period is divided into discrete 1/4 nmi range cells. When an interrogation is initiated, each range cell is sequentially addressed from 0 to maximum range (200 nmi for the ARSR-2) so that when a bracket detection occurs, an indication is made in the range cell that is addressed at that instant. This particular range cell is the first element of an eleven bit shift register called the sliding window. The information stored in this shift register represents the mode A/3 bracket detections that have or have not occurred at this specific range cell during the last eleven interrogation periods. If a mode A/3 bracket detection occurs, a "one" is shifted in. If a bracket detection does not occur, a "zero" is shifted in. Each time the latest mode A/3 bracket detection for that specific range is shifted into the register (sliding window), the oldest is shifted out and lost. If no mode A/3 bracket detection occurs due to a "miss" or the end of the target run length, "zeros" are shifted in.

For each range cell during each mode A/3 interrogation period, the contents of the register (sliding window) are inspected and summed in a Digital-to-Analog Converter as shown in Figure 25. The sum voltage is applied to the Beacon Leading Edge Analog Slicer and the Beacon Trailing Edge Analog Slicer where it is compared to a switch selected threshold level. When the number of "ones" in the sliding window equals the switch settings, an output signal is produced, indicating that the beacon target leading edge or trailing edge has been detected. The logic is such that a target leading edge signal is produced before the beacon trailing edge signal.

When  $T_L$  has been reached, the target is considered detected and is given the status of "in process." When  $T_T$  has been reached, the target is declared complete and the information concerning the target is transferred out.

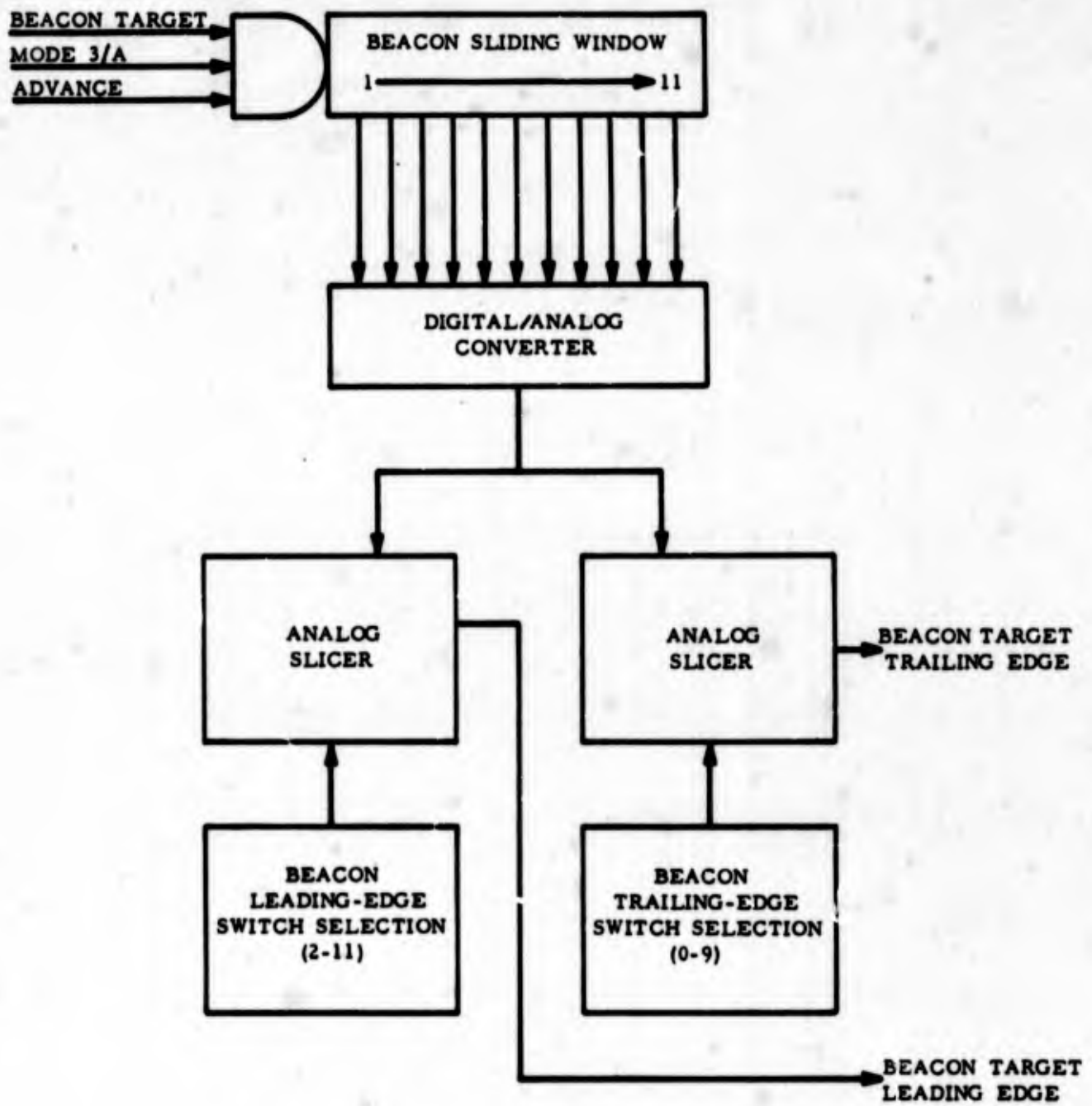


FIG. 25 BEACON SLIDING WINDOW BLOCK DIAGRAM

### Probability of Detection with Controlled Inputs

A. Test Procedure - The DTGTS was used to generate a continuous succession of beacon targets to be applied to the RVDP input. These targets all occurred at the same range. An average fruit density of 100,000 random replies per antenna scan was also produced and mixed with the target input signal. This fruit density represents the maximum density that the processor is required to handle as measured at the Elwood site. A more detailed discussion of the beacon fruit environment at the Elwood site is contained in Appendix VI.

Target run length (RL) settings of 30 and 45 were used. The random-gating function of the DTGTS was used to randomly inhibit single replies within the target run length. For various settings of the random gating, the number of replies of the run length allowed at the DTGTS output was counted. The ratio of total replies at the DTGTS output to the run length setting represents the Target Reliability (TR).

A mode interlace of 1:1:1 (A/3, C, 2) was used throughout the test.

The number of targets generated by the DTGTS and the number of targets declared by the RVDP were counted to obtain probability of detection.

B. Test Results - The curves of Target Reliability versus Probability of Detection for  $T_L$ 's equal to 6, 7, 8, and 9 are shown in Figure 26. These curves resulted from using target run lengths of 30 and 45. A run length of 30 represents a minimum target and a run length of 45 represents an average target for a system whose antenna rotation rate is 6.25 revolutions per minute and whose interrogation rate is 360 per second. For comparison the statistically-derived theoretical curve for run length 33 is also shown for each setting of  $T_L$ .

### On-Line Tests of Probability of Detection

A. Test Procedures - A test aircraft was flown along a selected radial that was relatively clear of other traffic. An altitude of 26,000 feet was selected to insure that the aircraft was always within line-of-sight of the beacon antenna. As soon as the aircraft was identified and had attained the assigned altitude, data collection

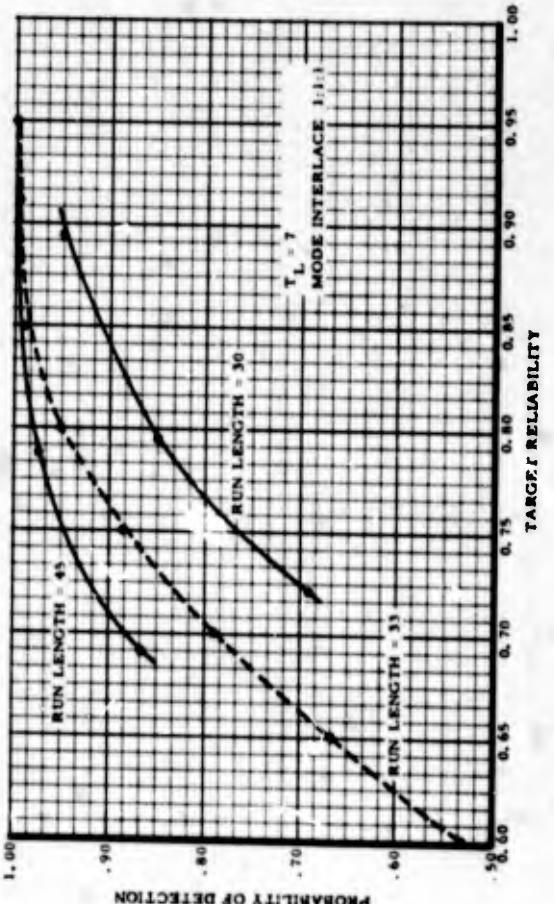
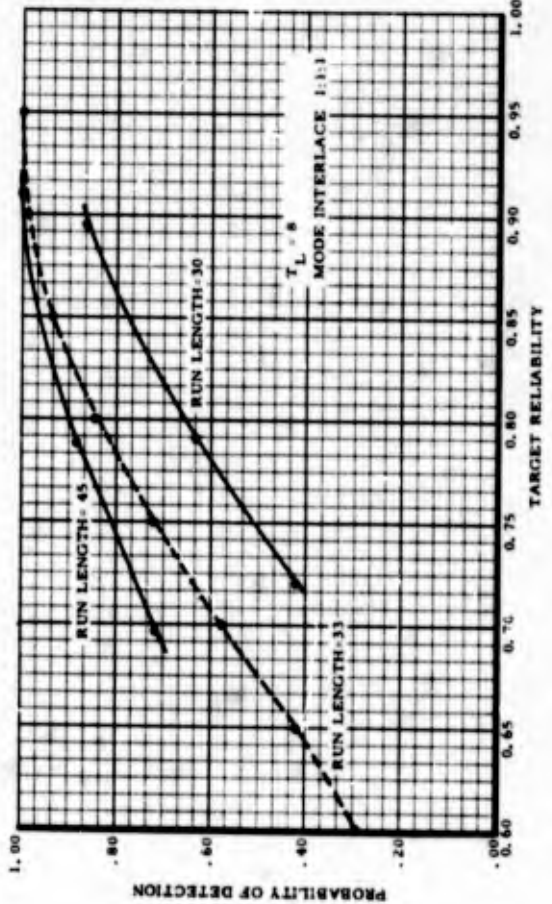
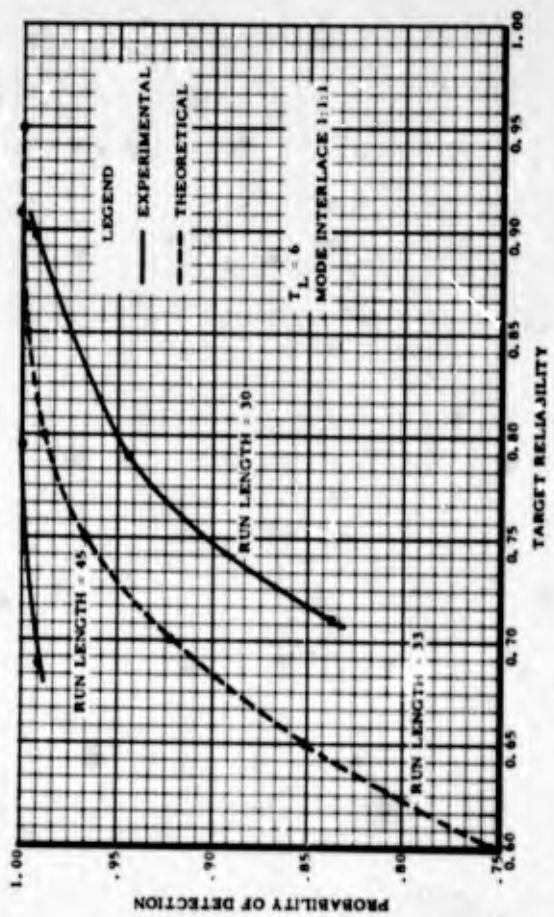
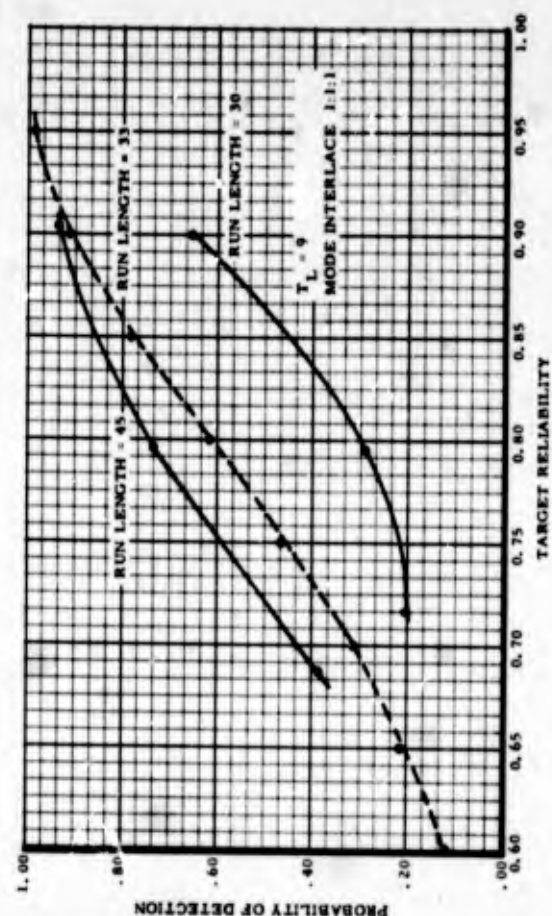


FIG. 26 BEACON PROBABILITY OF DETECTION

began. Air Traffic Control specialists observed the beacon replies on both digital and video displays, and a "hit" or "miss" was recorded each antenna scan. This was continued to maximum range (200 nmi). A  $T_L=6$  was chosen for the flight tests based on the static  $P_D$  test results and the fruit density measurements at Elwood described in Appendix VI.

Descriptions of the flight test configuration and the test flight procedures are contained in Appendix IV.

B. Test Results - The percentage of scans in which a target was detected by ATC specialists, during the dynamic tests, was tabulated for each 10-mile increment to indicate the probability of detection as the aircraft approached the maximum range of the radar facility. The percentage for each 10-mile increment is shown in Figure 27. As indicated, the digital channel produced a higher probability of detection than the video channel.

Figure 28 is a photograph of the 200 nmi range digital display which can be compared with Figure 29, a photograph of the 200 nmi range video display taken at the same time.

#### False Target Detection

A. Test Procedure - An average density per scan of randomly distributed beacon replies (fruit) was generated and used as the RVDP input. With each  $T_L$  setting, the number of beacon targets declared by the RVDP was recorded each antenna scan for 100 scans. This was repeated for several settings of average fruit density and for several values of  $T_L$ . The tests were performed using an interlace ratio of 1:1:1 (modes A/3, C, and 2).

B. Test Results - Figure 30 shows the results of the tests with  $T_L$  settings of 5 through 8, respectively. The Fruit Count Per Scan is an average count of the randomly distributed beacon replies for 100 scans of the antenna. The Average False Targets Per Scan that were detected by the RVDP for the various fruit densities are shown as the solid-line curve on each figure. The dashed-line curve is the statistically-derived theoretical curve for the conditions and  $T_L$  setting that exist for each test.

For  $T_L = 5, 6, \text{ and } 7$ , the experimental value of average false targets per scan for a given fruit density is less than expected when compared with the theoretical curve. This can be attributed to an element of radial correlation that exists in the generation of random fruit. The theoretical curve is based on the assumption

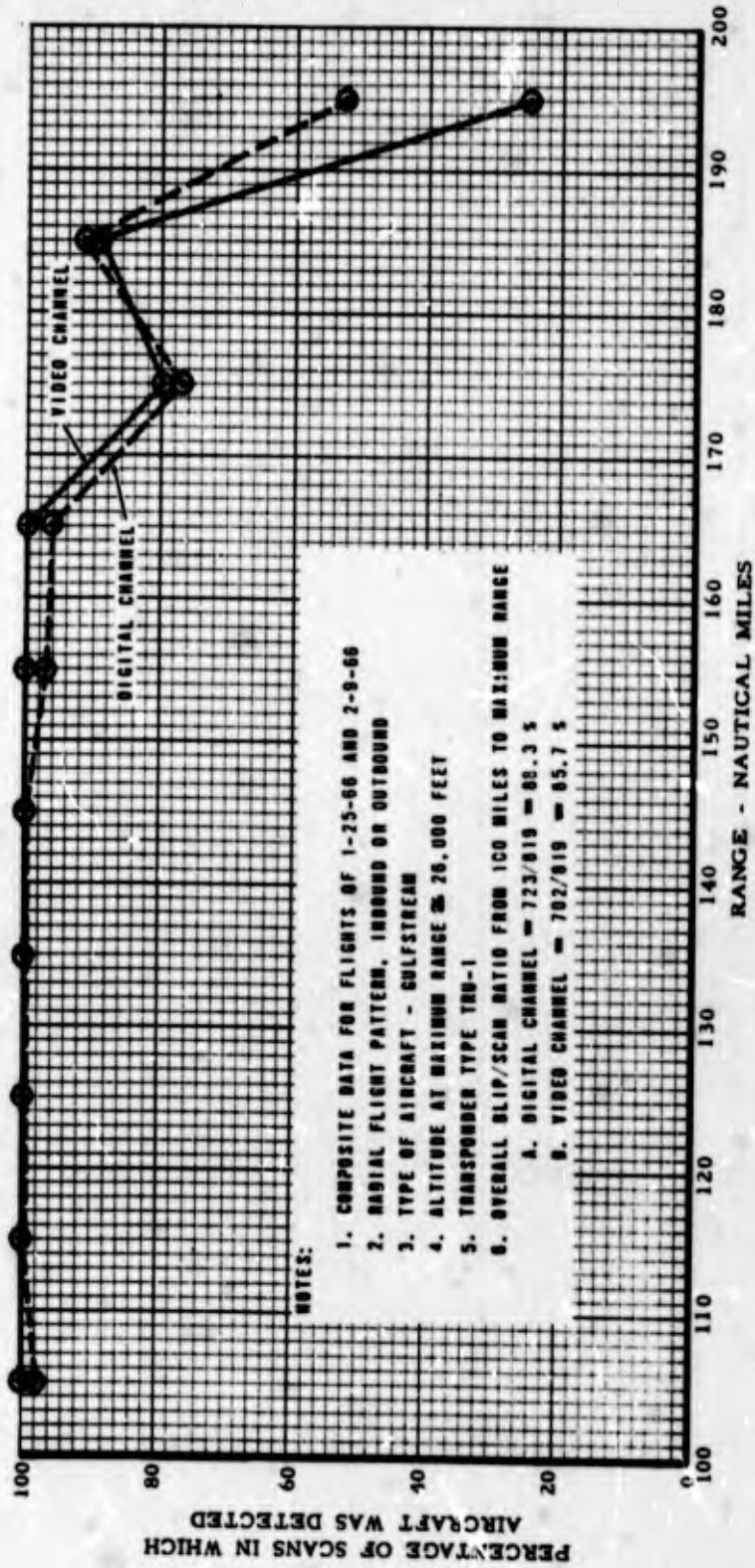


FIG. 27 BEACON SENSITIVITY AT MAXIMUM RANGE

PROJECT NO.  
231-001-01X  
DIGITAL CHANNEL  
DATE: 2/28/66  
BEACON

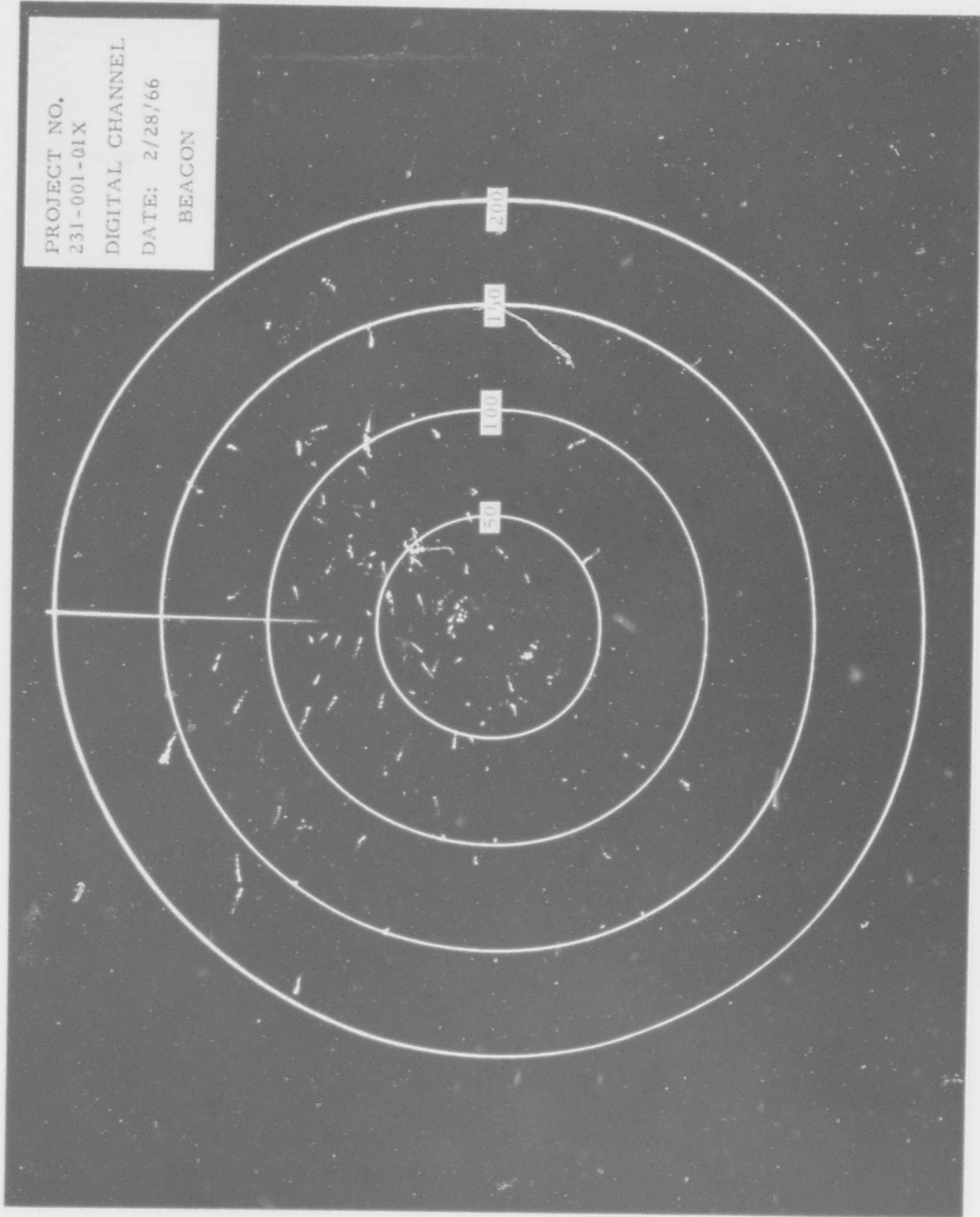


FIG. 28 DIGITAL CHANNEL DISPLAY PRESENTATION (200 MILE RANGE)  
- BEACON

PROJECT NO.  
231-001-01X  
VIDEO CHANNEL  
DATE: 2/28/66  
BEACON

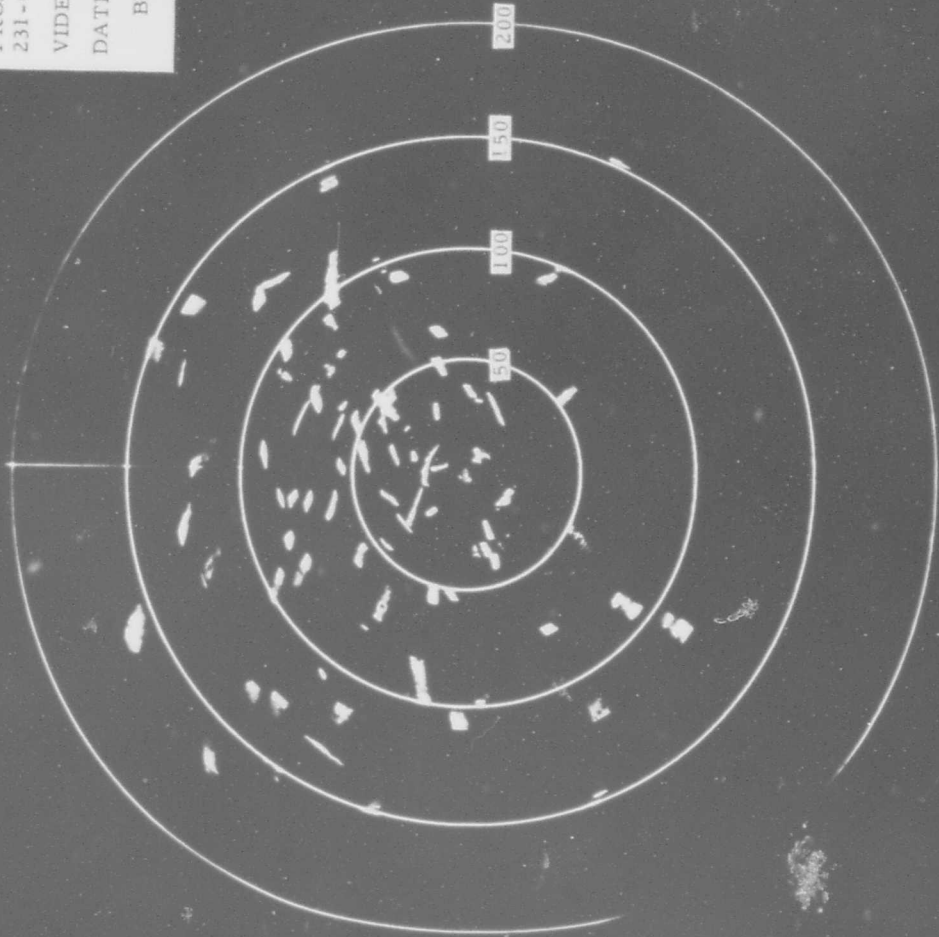


FIG. 29 VIDEO CHANNEL DISPLAY PRESENTATION (200 MILE RANGE)  
- BEACON

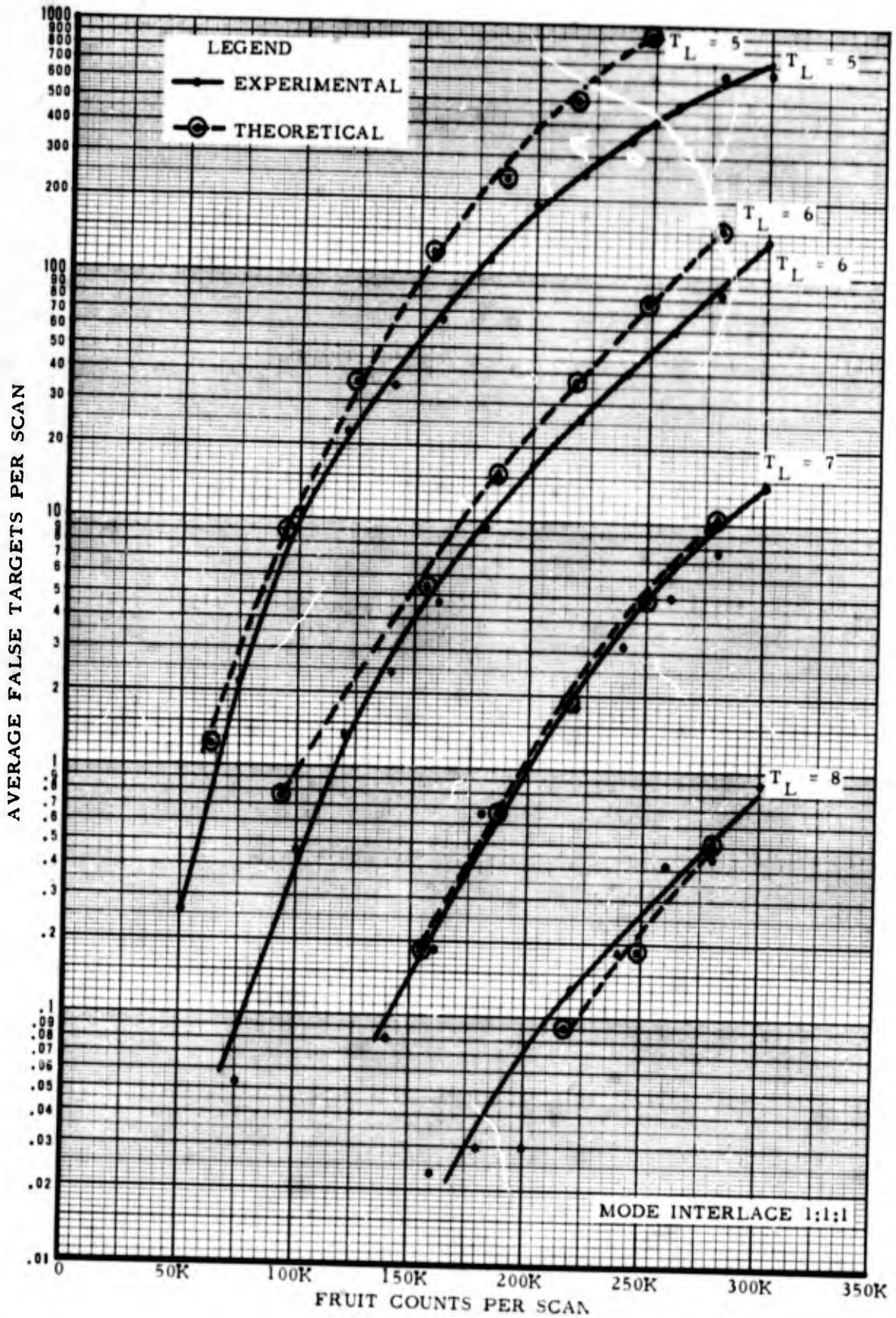


FIG. 30 BEACON FALSE TARGET DETECTION

that the distribution of non-synchronous beacon bracket detections are truly random. These random bracket detections are, of course, caused by a random distribution of non-synchronous replies or fruit. No radial or azimuth correlation of the random fruit is assumed in the theoretical case. In the experimental case and, in fact, in the live beacon environment an element of radial correlation exists which tends to reduce the probability of false target detection. This range correlation is caused by the fact that in the experimental tests a beacon code, rather than just bracket pulses, was used when generating the random beacon replies. When two replies occurred adjacent to each other in range, a third or phantom bracket detection could occur due to two code pulses at the proper spacing. These phantom bracket detections were counted as part of the total when the average fruit count per scan was obtained. Thus, some of the fruit counts per scan were radially correlated. Since the sliding window detection method of the RVDP requires azimuth correlation of bracket detections, less of the total per scan was available for detection due to the element of radial correlation.

Since codes are used in the live beacon environment, the experimental data obtained in this test are more representative of the average false targets per scan detected in a live environment of random distributions of non-synchronous replies.

Some data were obtained using a  $T_L$  setting of 9. The average false targets per scan were insignificant with values less than 0.01 for average fruit counts above 240,000 per scan. No false targets were detected below 240,000 per scan in this test.

#### Radar Reinforced Beacon Targets

A. Test Procedure - When both primary radar returns and beacon replies from the same aircraft are processed, only one output message will be prepared if there are no target splits and if the primary radar and beacon returns are processed concurrently. Within this single beacon message is a bit that signifies when the message has been reinforced by a primary radar return. One of the project objectives was to determine how well the primary radar and beacon returns from the same aircraft are correlated.

Data collected during the accuracy test flight of February 11, 1966, were reduced to determine the percentage of antenna scans that resulted in a radar reinforced beacon message when both primary radar and beacon returns were being processed.

Since non-correlation of beacon and primary-radar returns is a function of the delay tolerance in the airborne transponder, an additional check was made on correlation of returns from all aircraft, in the surveillance area, which were detected by both the beacon and primary radar detectors.

B. Test Results - For a total of 208 antenna scans during the accuracy flight, the following results were obtained:

184 (88.5%) reinforced radar-beacon targets

9 (4.3%) non-correlated targets, i. e., non-reinforced beacon targets with a primary radar target in an adjacent range cell

3 (1.4%) misses, both primary radar and beacon

12 (5.8%) primary radar targets only with no associated beacon targets

Since none of the nine non-correlated returns were separated in azimuth, the azimuthal alignment of the beacon and primary radar antenna was satisfactory. Lack of correlation in range is most likely due to variations in the delay of the transponder reply. The specification for variations in the delay of transponder replies is plus or minus one-half microsecond,<sup>7</sup> which is more than sufficient to cause the beacon target to be detected in a separate range bin from the primary radar target when the aircraft is close to a range bin interface.

The check of correlation of returns from beacon-equipped aircraft in the surveillance area produced similar results. From a total population of 326 targets (ten antenna scans) detected by both the beacon and primary radar detectors, only eight targets (2.45%) were non-correlated.

These results indicate that the present tolerance on airborne transponder delay produces an acceptable level of correlation between beacon and primary radar returns in an enroute-type (1/4 nmi range cells) RVDP.

Code Detection: Each beacon reply consists of a pair of bracket pulses spaced 20.3 microseconds apart, and between the two bracket pulses are 13 data pulse positions spaced in multiples of 1.45

- - - - -

7

Reference 7

microseconds. In a given reply, a pulse can occur in any position. An additional pulse position exists in which the Special Position Identification (SPI) pulse can occur. The SPI pulse follows the leading edge of the second bracket pulse (F2) by 4.35 microseconds. All the details of an idealized pulse train reply are described in Appendix V.

### Code Sampling

A. Description - After quantizing, the beacon reply video is applied to the SPI Delay Line and the Main Decoding Delay Line as shown in Figure 31.

The code sampling and garble sensing functions of the RVDP are initiated when bracket detection occurs. At this time, the bracket detection pulse is sent to Memory 1 for the statistical target detection process and to the Transfer Control circuitry. The Transfer Control allows the bracket detection pulse to strobe the SPI Delay Line and Main Decoding Delay Line contents into Buffer Register 1. At the same time the beacon range count is also applied to Buffer Register 1. This range will serve as the address when the information is to be stored in Memory 2. The mode during which the reply code was received is also stored in the buffer register so that the code data will be stored in the proper portion of the Memory 2 word. If Buffer Register 2 is unoccupied, the data are immediately transferred to Buffer Register 2 and kept there until garble sensing is completed. This leaves Buffer Register 1 available for another reply train which may be caused by a second aircraft in close proximity to the first.

B. Performance - The code sampling characteristics of the RVDP are shown in Figure 32. Each code pulse was varied one at a time, ahead of and behind its nominal position. The pulse position from F1 for 0% and 100% pulse acceptance is shown for:

1. Code pulse width at 0.30 microseconds (lower threshold for 100% quantizer detection)--curve A
2. Code pulse width at 0.45 microseconds (nominal) --curve B
3. Code pulse width at 0.60 microseconds --curve C

The nominal position and the 0.1 microsecond point ahead of and behind each code pulse are indicated.

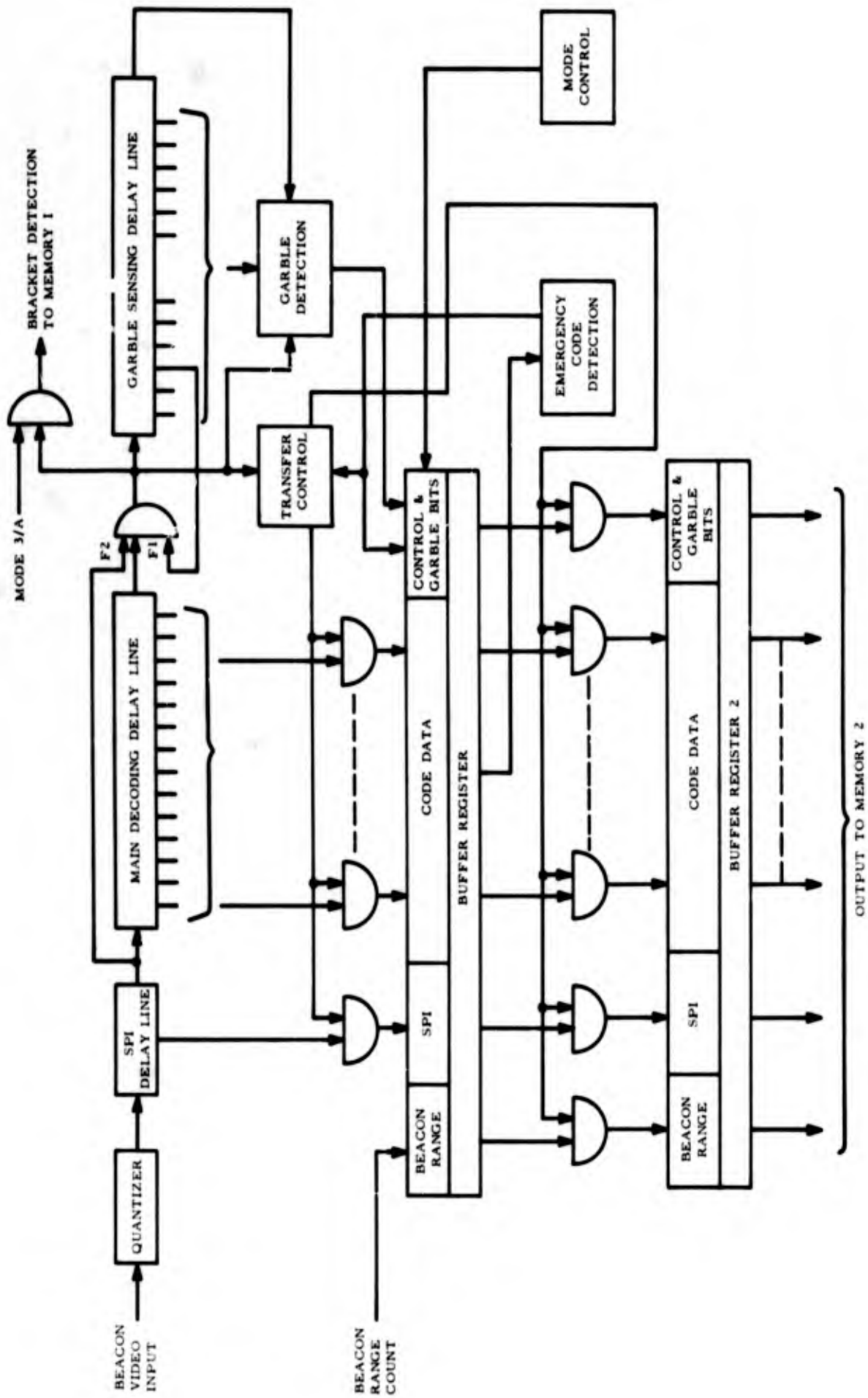


FIG. 31 BEACON REPLY PROCESSING BLOCK DIAGRAM

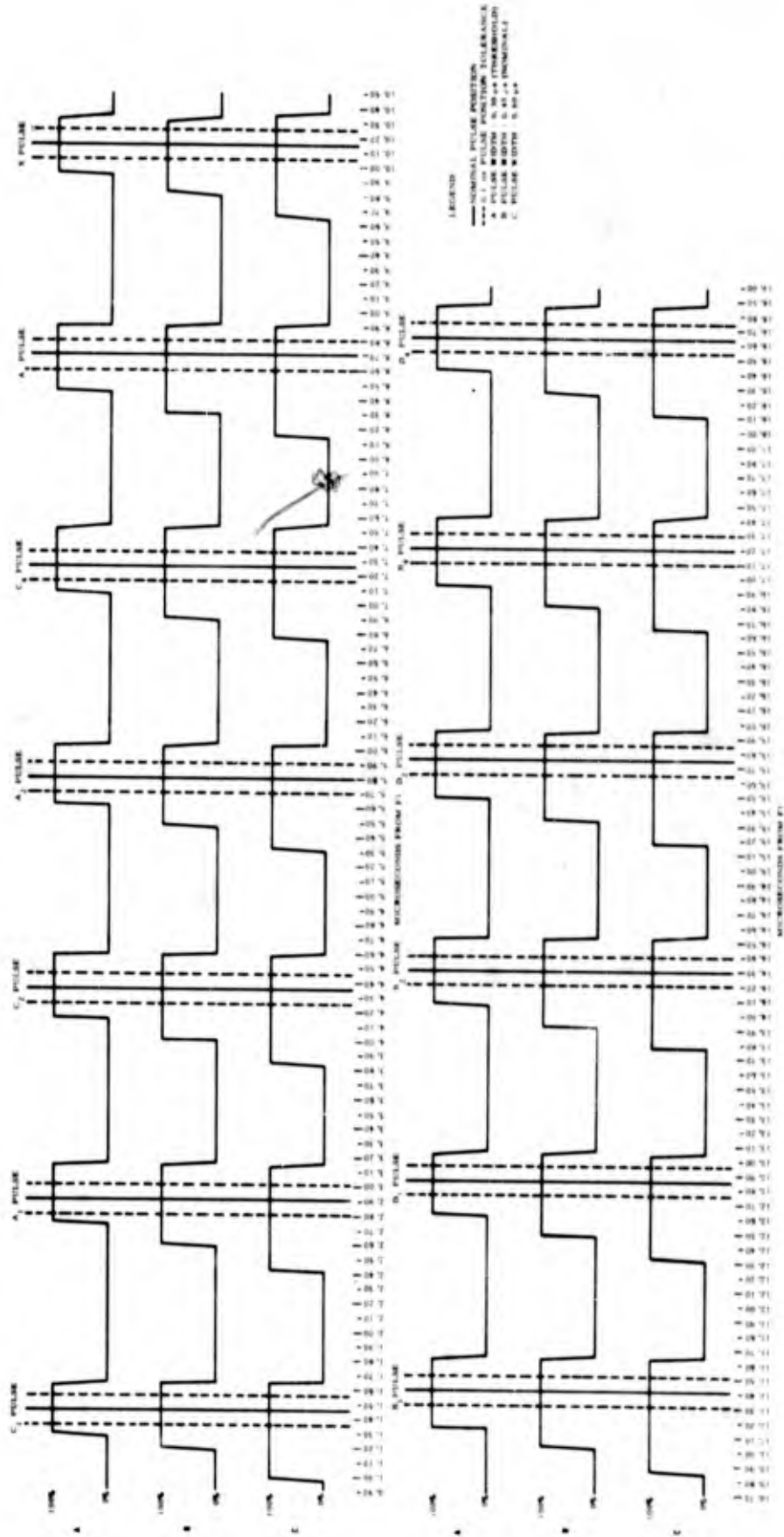


FIG. 32 BEACON CODE ACCEPTANCE ZONES

As pulse width is increased, the acceptance zone also increases. However, the increase is only in the direction ahead of nominal position. A limit exists behind nominal position, and this limit is determined by the fixed delay that occurs between the leading edge of the F1 pulse and the generation of the strobe pulse used for code sampling. Since the nominal position of all code pulses is referenced to the F1 pulse, the strobe always occurs at the same time after nominal pulse position. It was also found that the position of the pulse acceptance zones did not vary with varying bracket spacing. Figure 33 shows the pulse acceptance zone for the SPI pulse. The nominal position and the 0.1 microsecond point ahead of and behind are indicated. As in the case of the code pulses, the acceptance zone increases as the pulse width is increased. However, the position of the acceptance zone is dependent on the bracket spacing. This is because the detection of the SPI pulse is made with reference to the F2 pulse.

### Garble Sensing

A. Description - A garble condition is said to exist if the code pulses of one reply train overlap into the code pulse positions of a second reply train such that the ownership of one or more code pulses is not apparent. This condition will usually give rise to false reply trains if the spacing of any two pulses resulting from the garble situation is the same as bracket spacing. Thus, a false bracket detection would occur.

The garble sensing function is initiated by a bracket detection pulse applied to the Garble Sensing Delay Line. Each 1.45 microsecond interval of time after bracket detection, the bracket detection gate is examined for coincidence indicating potential garble. When the bracket detection pulse appears at the output of the Garble Sensing Delay Line, a garble bit is set in the buffer register if a potential garble were discovered.

The presence of an SPI pulse in the reply train will not be seen as a potential garble since, at 4.35 microseconds after bracket detection, the bracket coincidence detector is inhibited for one pulse-sampling period.

B. Performance - Two targets, both consisting only of bracket pulses, were adjusted for complete overlap. One target was then continuously moved out in range until a change in status, such as garble or interleave, occurred for either target. The F1-to-F1 leading

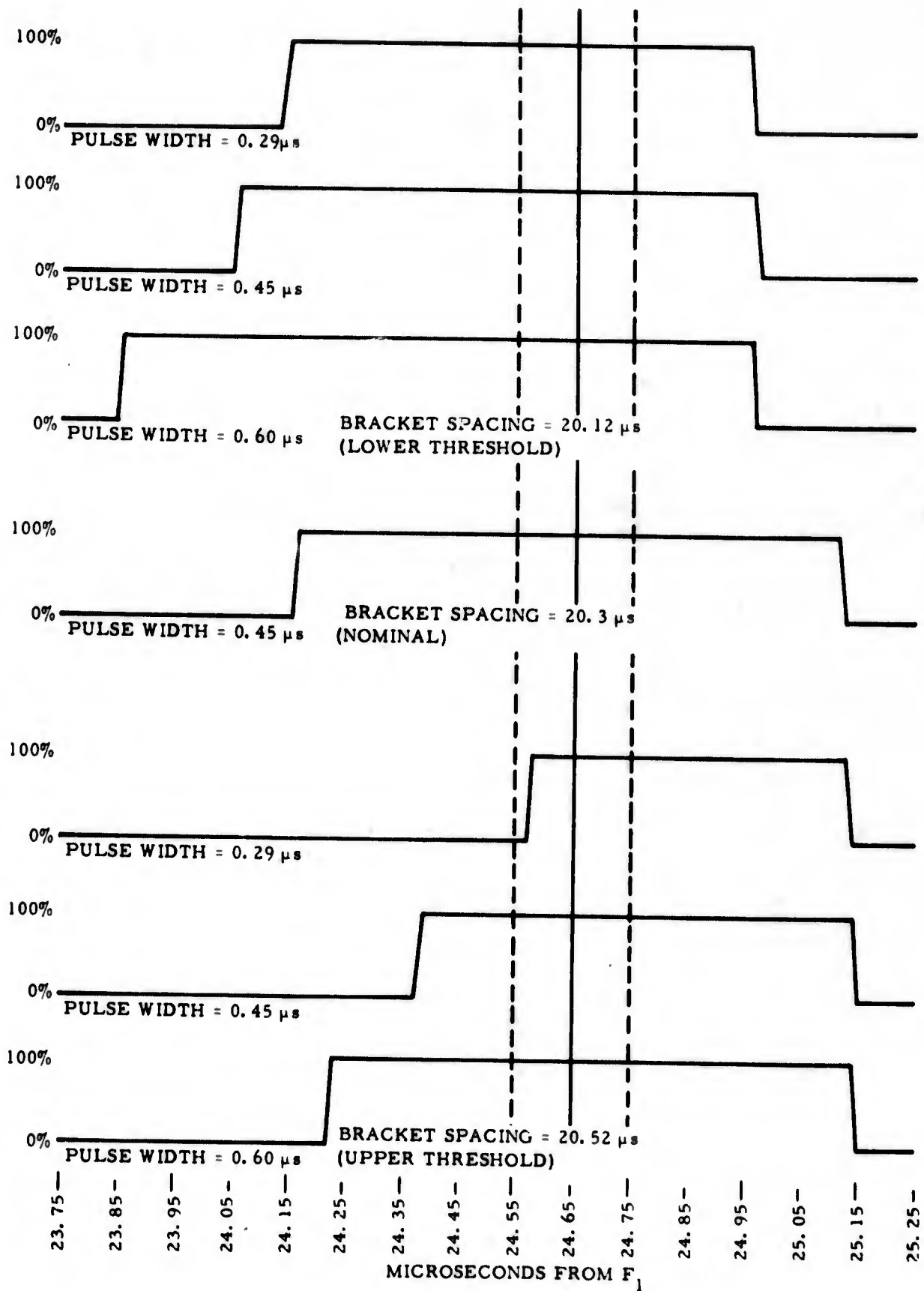


FIG. 33 SPI PULSE ACCEPTANCE ZONE

edge spacing between the two targets was measured at each change of status. The separation was increased until both targets were always resolved.

The zones of interleave, garble, not-garble, and target-not-declared are shown in Figure 34 for the case where two targets of brackets only were used. Target "A" indicates the target closer in range and Target "B" indicates the target being moved out in range. The symbols used to describe the various conditions that exist from overlap to complete separation are also shown in Figure 34. The spaces where no symbols are used are the zones of interleave; that is, both targets are declared and not garbled.

The test was repeated using a code  $7777 + X + \text{SPI}$  as one target and only bracket pulses for the second target. The code  $7777 + X + \text{SPI}$  was moved out in range to obtain the change in status points. At each change of status the F1-to-F1 spacing was measured until the F1 pulse of the code  $7777 + X + \text{SPI}$  overlapped the F2 pulse of the brackets. From this point on, the F2-to-F1 spacing was measured at each change of status.

Figure 34 shows the zones of interleave, garble, not-garble, and target-not-declared for the case where Target "A" consisted of brackets only and Target "B" consisted of code  $7777 + X + \text{SPI}$ .

Except for a small zone at approximately 8 microsecond spacing, there exists an A-NG (Target A not garbled), B-ND (Target B not detected) condition from 4.16 microseconds to the point where F1 of Target "B" overlaps F2 of Target "A." The "B" target is not declared at all in this zone. This is probably due to the fact that since Target "B" contains all possible code pulses, every position of Target "B" provides a code pulse in the SPI detection zone of Target "B." This is considered the overlap position in the upper chart. Target "B" is moved farther in range continually, and the situations that occur are shown in the upper chart.

### Emergency Code Detection

A. Description - Emergency or communications failure reply codes (7700 or 7600) receive a priority status in the RVDP since the detection of such in Buffer Register 1 prevents further garble updating. A special set of gates is arranged to detect these two reply code trains. When either of these codes is detected, the priority status is indicated by setting a bit in the control portion of the Buffer Register.

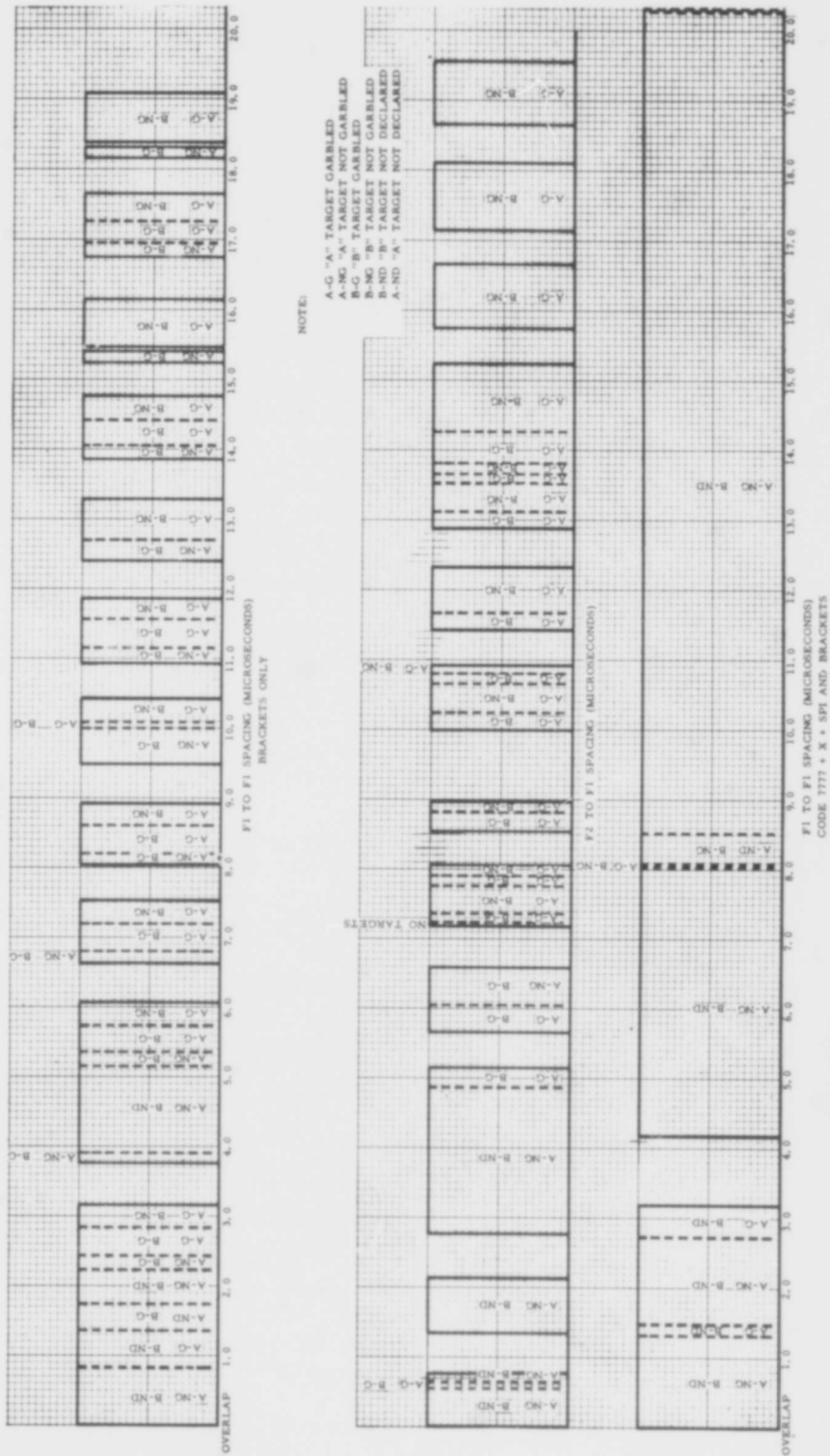


FIG. 34 BEACON CODE GARBLE SENSING ZONES

B. Performance - Tests were conducted to determine the detection limits of each pulse position within the emergency codes and the conditions under which the emergency indications are inhibited. Each pulse of a mode A/3 code 7700 and code 7600 was varied in position to determine its detection zone. These zones are shown in Figure 35 and they represent the zone within which a particular pulse is accepted 100% of the time if it lies wholly within the indicated zone. Nominal pulse widths of 0.45 microseconds were used for this test.

An interfering pulse was mixed with the emergency codes and its position was varied from ahead of the emergency code through the code train to behind the emergency code. The zones where the emergency indication was inhibited 100% of the time are also shown in Figure 35. Here again, the interfering pulse must lie wholly within the inhibit zone for 100% inhibit.

There are no inhibit zones outside the framing pulses. This indicates that a false emergency indication can occur when the pulses of an interfering code train complement a second code train to fill in the missing pulses to form an emergency code. The interfering pulses must, of course, lie within the detection zones of the missing pulses of the code train being complemented.

It must be re-emphasized that the emergency indication discussed is the control bit that is set in the buffer register as a result of the detection of an emergency code. This does not imply that the final validated code will be an emergency code.

### Code Validation

A. Description - Beacon code information for mode A/3 mode C, and mode 2 is validated by comparing the presently-received code with the previously-stored code. Control bits in the message label are set upon successful validation for each mode. The codes are stored in a 1024-address, random-access, ferrite-core memory 2 at the range at which the bracket detection occurred. To facilitate memory 2 processing, the beacon code is accompanied by control bits indicating the mode of reply (A/3, C, or 2), the condition of the code (garbled or not), its special status as an emergency code (code 7600 or 7700), and the presence or absence of the SPI pulse.

The beacon code and its associated control bits are written into memory 2 by transferring the beacon range at which the

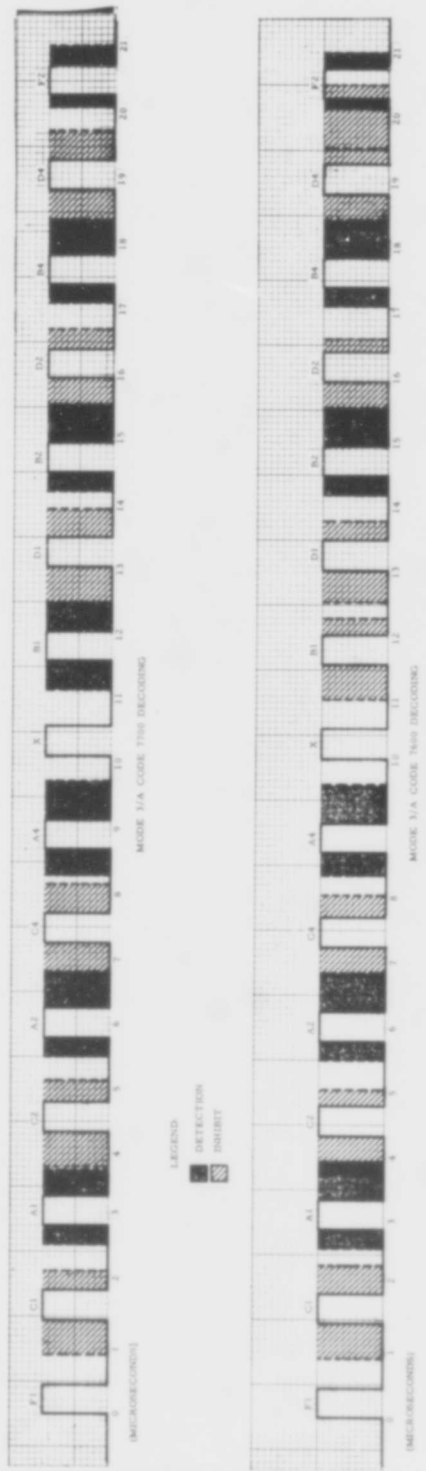


FIG. 35 EMERGENCY CODE DETECTION/INHIBIT ZONES

bracket detection occurred in the memory 2 random-access address register and the code and control bits into the memory 2 information register. A memory 2 write cycle is then initiated to store the information in the memory 2 stack. Conversely, to read from the memory 2 stack (the processed beacon code corresponding in range to the "beacon-target-complete" status bit stored in memory 1) the memory 1 address (range) must be transferred to the memory 2 address register. A memory 2 read cycle then fetches the processed beacon code to the memory 2 information register, making the code available to the output message assembler.

B. Performance - The DTGTS was used to trigger beacon replies for each mode from a beacon code generator. Various fruit densities were generated and mixed with the beacon replies and applied to the input of the RVDP.

Each target output message from the DTG was printed out. Various combinations of code content within the message and code validation indications in the message label were counted.

The test was performed with the following operating conditions:

1. Run length: 45
2.  $T_T$ : 2
3. Mode interlace: 1:1:1 (A/3, 2, C)
4.  $T_L$ : 7 and 9
5. Target reliability (TR): 0.7 and 1.0
6. Fruit density: 0 to 200,000 per scan
7. Code validation for each mode is begun at  $T_L$

Figure 36 represents probabilities for all possibilities of correct or incorrect code validated and not validated for the total population. For a specific set of test conditions, the sum of all four probabilities for each data point will be unity.

The probability of correct code validation versus fruit density is shown for each test condition. With higher  $T_L$  settings, the probability of validation of correct codes decreases. With lower values of target reliability, the probability of validation of correct codes decreases.

The probability of the occurrence of correct code reported but not validated versus fruit curves indicates that the attempt

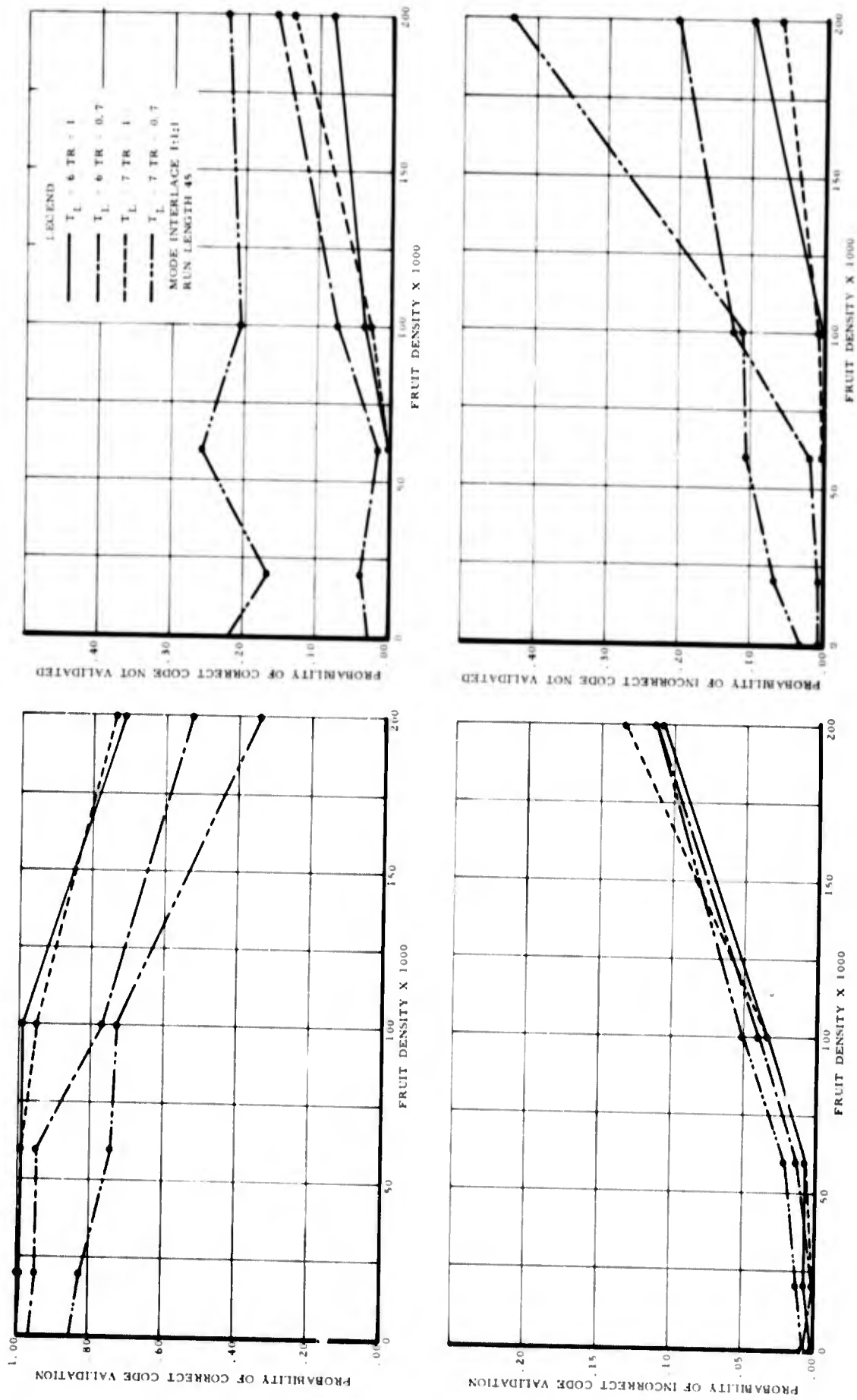


FIG. 36 BEACON CODE VALIDATION AS A FUNCTION OF FRUIT DENSITY

to validate the replies available was not successful. The last reply code that was received was correct but not validated.

The values of probability of the occurrence of incorrect code validation versus fruit density are, in general, lower than the probability of the occurrence of incorrect codes not validated. This is as expected.

During the collection of data for the code validation test, it was noted that a significant number of false SPI pulses occurred in a fruit environment. The data were tabulated and reduced, and Figure 37 shows the probability of declaring a false SPI pulse on Mode A/3 replies versus fruit density. The values obtained are considerably higher than desired. This is due to the fact that the SPI pulse is not validated. A single pulse detected in the SPI position is sufficient to report an SPI pulse as part of the output message.

#### On-Line Tests of Code Detection

A. Test Procedure - A test aircraft was flown along a selected radial to maximum range (200 nmi) at an altitude of 26,000 feet to insure that the aircraft was always within line-of-sight of the beacon antenna. As soon as the aircraft was identified and had attained the assigned altitude, data collection began.

Three mode interlace with a ratio of 1:1:1 (A/3, C, 2) was used by the beacon interrogator. However, the test aircraft was not equipped to reply to mode 2 interrogation. The mode A/3 and mode C replies were received and applied to the input to the RVDP. Output messages were recorded on magnetic tape. The data were later reduced and analyzed with a computer.

The threshold at which validation begins is, in the RVDP, the same as  $T_L$ . A  $T_L$  of six was used throughout the test flights. This value was chosen as a result of fruit density tests described in Appendix VI.

B. Test Results - The curves for probability of validation for mode A/3 and mode C as a function of range are shown in Figures 38 and 39, respectively. Curves for both correct-code-validated and incorrect-code-validated are shown. The data were grouped into 20 nmi segments for data reduction and presentation. For a limited time during the test flights, the mode A/3 emergency code 7700 and the communication failure code 7600 were transmitted by the aircraft. Of 26 total antenna scans, 84.6% were correctly validated, 11.5% validated with an incorrect code, and 3.8% were reported correctly but not validated.

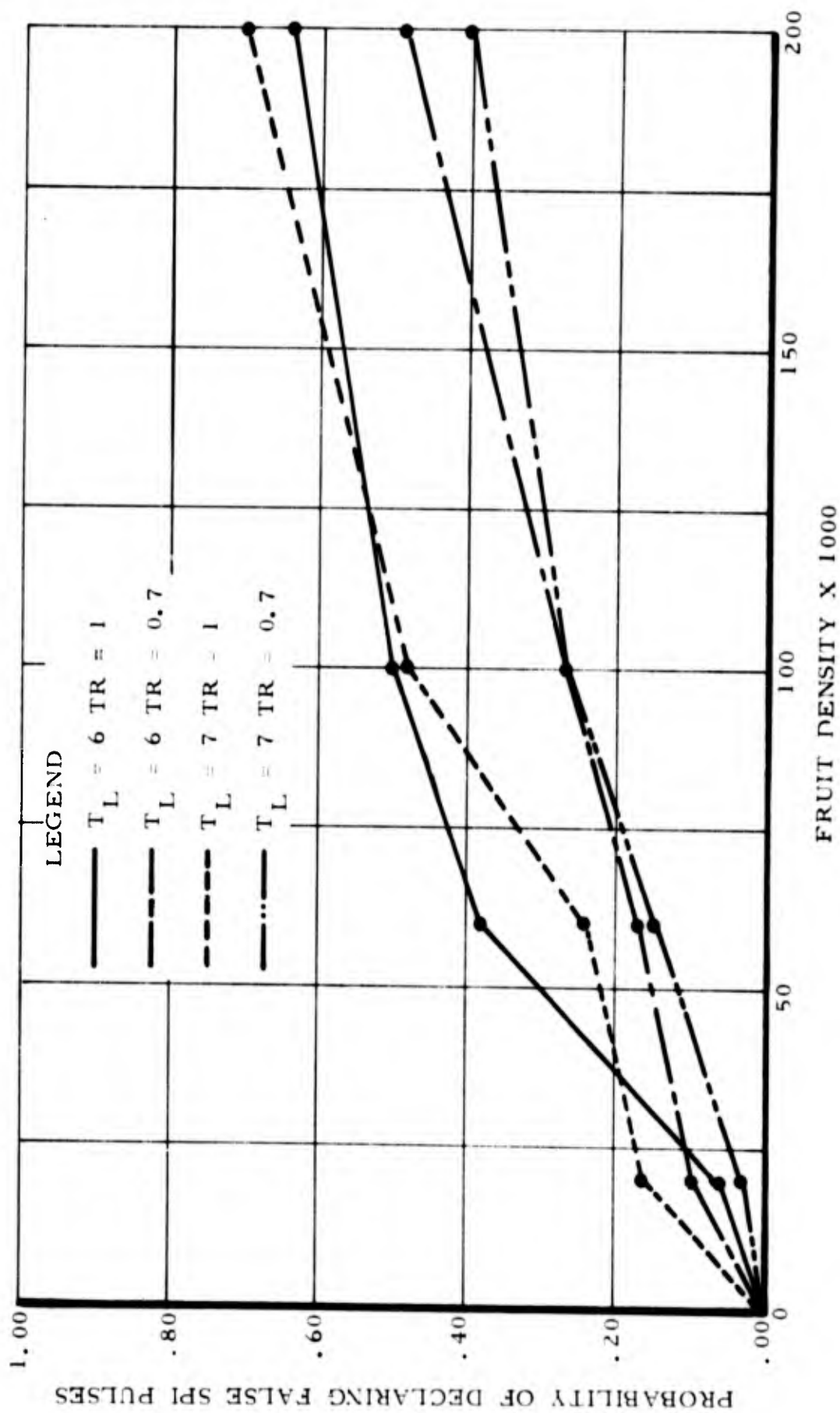


FIG. 37 PROBABILITY OF DECLARING FALSE SPI PULSES

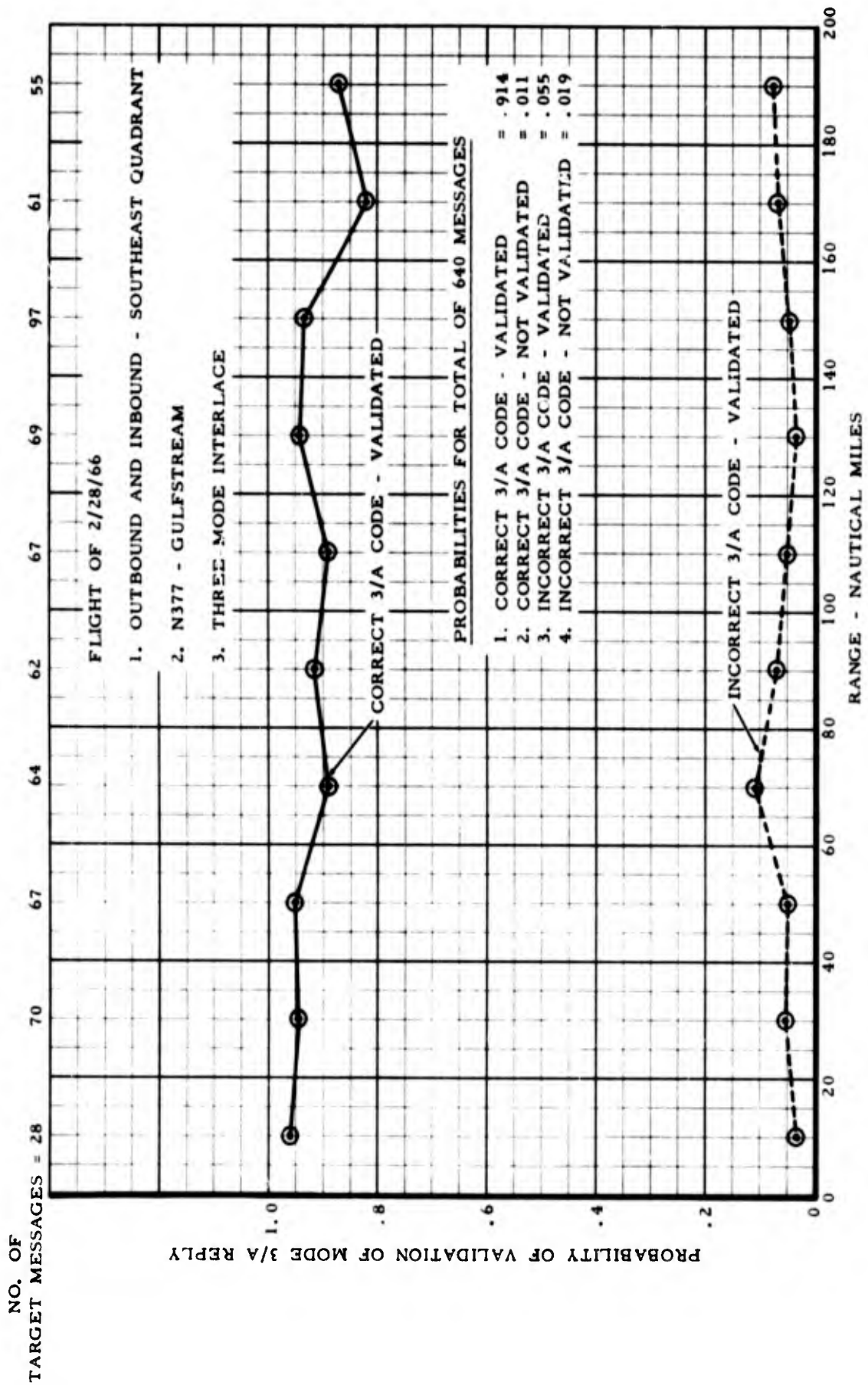


FIG. 38 RESULTS OF CODE VALIDATION TESTS FOR MODE A/3 INTERROGATIONS

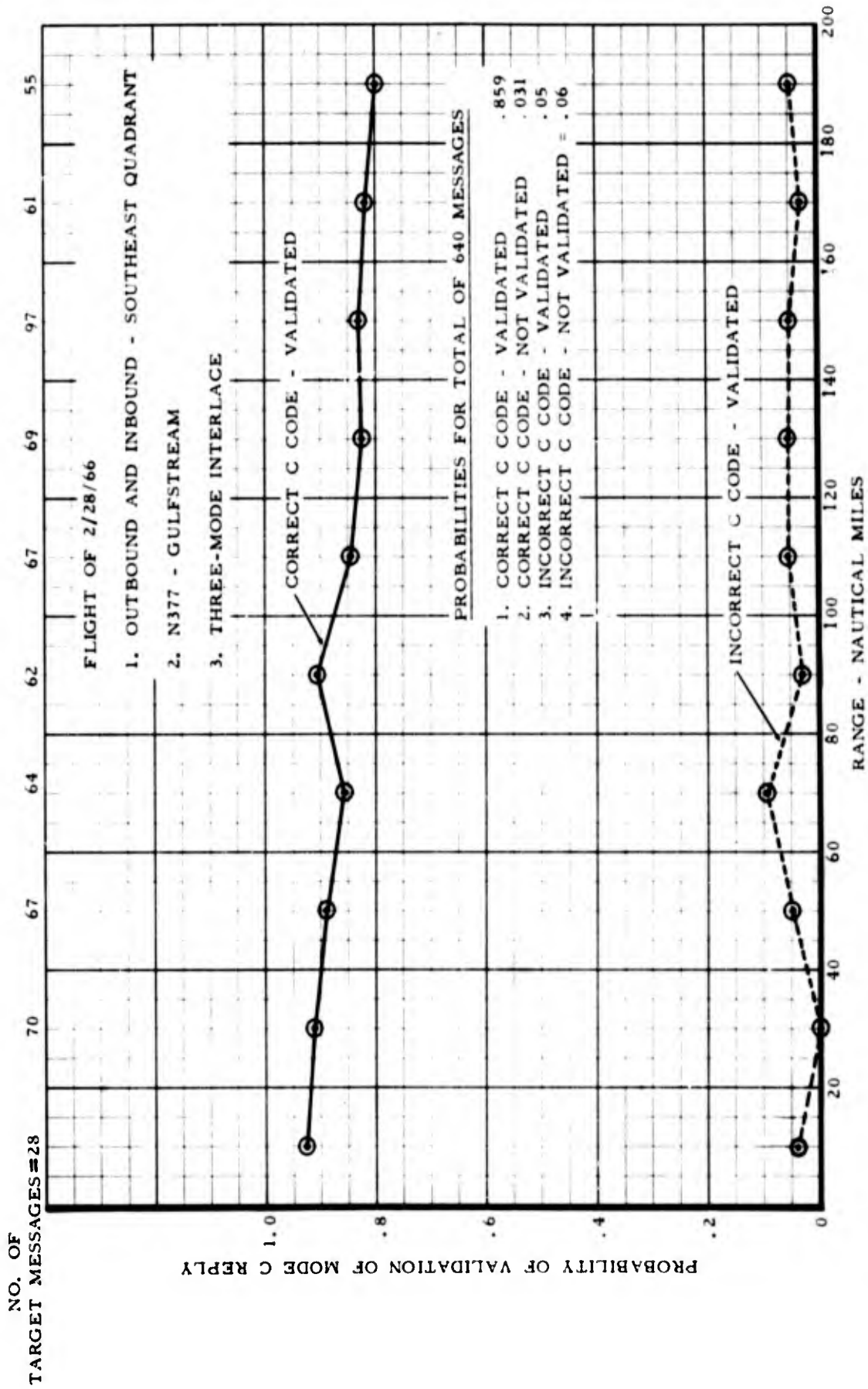


FIG. 39 RESULTS OF CODE VALIDATION TESTS FOR MODE C INTERROGATIONS

During the entire code validation tests, no validated false emergency code (7700) or false communication failure code (7600) was reported.

RVDP Performance Using Defruited Beacon Video: The RVDP was designed to detect beacon targets and successfully extract code information with input video signals consisting of a mixture of synchronous and non-synchronous (fruit) beacon replies. This, of course, requires that the proper settings of statistical detection in the RVDP have been made for the beacon system and environment in question. It was found that a statistical detector such as the sliding window detector is particularly suited to a system where target reliability will average less than unity.

The question then arose as to how this type statistical detector would perform with input video signal that has most of the non-synchronous replies removed with the use of defruiting equipment. The following two tests were performed and the results are shown.

Probability of Detection - The DTGTS was used to generate a continuous succession of beacon targets. These targets all occurred at the same range. An average fruit density of 100,000 random replies per antenna scan was also produced and mixed with the target signal. The composite signal was then applied to the input of a storage tube defruiter adjusted for normal operation, and the output of the storage tube defruiter was applied to the RVDP input.

Target RL settings of 30 and 45 were used. The random-gating function of the DTGTS was used to randomly inhibit single replies within the target run length. For various settings of the random gating, the number of replies of the run length allowed at the DTGTS output was counted. The ratio of total replies at the DTGTS output to the run length setting represents the Target Reliability (TR).

A mode interlace ratio of 1:1:1 (A/3, C, 2) was used throughout the tests.

The number of targets generated by the DTGTS and the number of targets declared by the RVDP were counted to obtain probability of detection.

The curves of Target Reliability versus Probability of Detection for  $T_L$  equal to 6, 7, 8, and 9 are shown in Figure 40. These

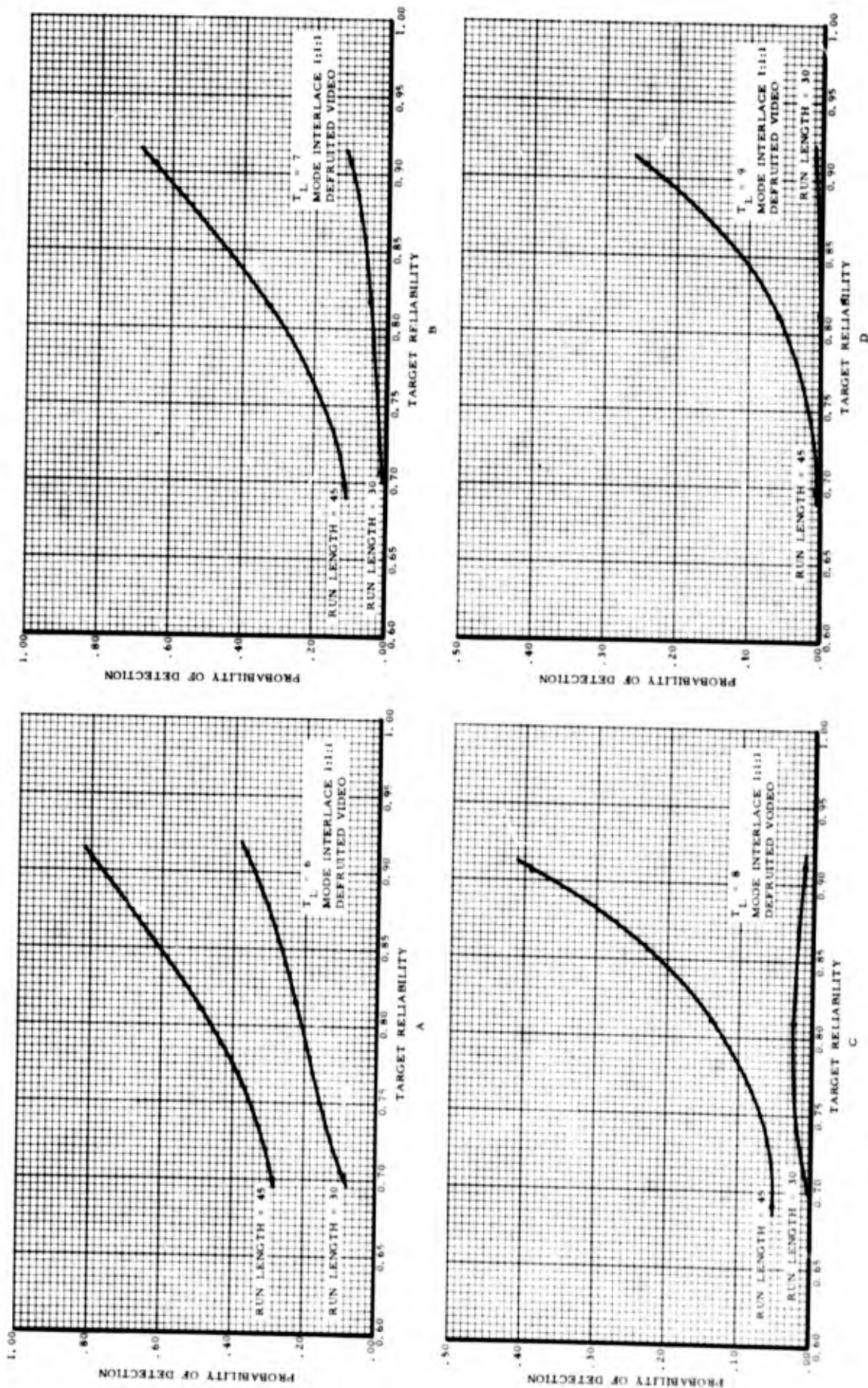


FIG. 40 BEACON PROBABILITY OF DETECTION USING DEFRAITED VIDEO

curves resulted from using test target run lengths of 30 and 45. A run length of 30 represents a minimum target and a run length of 45 represents an average target for a system whose antenna rotation rate is 6.25 revolutions per minute and whose interrogation rate is 360 per second.

As expected, the probability of detection for each setting of  $T_L$  is less than the same settings would produce using undefruited video input. Using defruited video, the effective TR is actually less than the TR specified in the test as the signal is applied to the beacon receiver. The operation of the defruiter is such that the last reply that occurs on each mode is stored in the defruiter and, since no additional reply is received for comparison to the stored reply, it is lost. Therefore, even with TR=1, one less reply on each mode is applied to the RVDP input from the defruiter output. When a TR less than one occurs for each miss that occurs during the target run length, an additional reply is lost in the defruiter.

Code Validation - The DTGTS was used to trigger beacon replies for each mode from a beacon code generator. Various fruit densities were generated and mixed with the beacon replies and applied to the input of the RVDP through the beacon receiver. A storage tube defruiter was used to provide the defruited video input.

Each target output message from the DTG was printed out. Various combinations of code content within the message and code validation indications in the message label were counted.

The test was performed with the following operating conditions:

1. Run length: 45
2. Mode interlace: 1:1:1 (A/3, 2, C)
3.  $T_L = 6$ ,  $T_T = 2$
4. Target reliability (TR): 0.7 and 1.0
5. Fruit density: 0 to 200,000 per scan
6. Code validation for each mode is begun at  $T_L$ .

A  $T_L$  of 6 was selected for this test as an attempt to provide a compromise setting for both defruited and undefruited video. It is not an unreasonable setting for both videos and provides data which can be used for relative comparisons.

Figure 41 represents probabilities for all combinations of correct code validated and not validated and incorrect code validated and not validated for the total population. For a specific set of test conditions, the sum of all four probabilities for each data point is unity. The curves representing the RVDP code validation performance using undefruited video with  $T_L = 6$  are repeated in Figures 41 and 42 for convenience in comparing results.

The probability of the occurrence of correct code validation versus fruit density is shown in Figure 41A with the defruiter in (defruited video) and the defruiter out (undefruited video). With  $TR = 1$  there is essentially no difference in the probability of the occurrence of correct code validation with defruited and undefruited video. However, with  $TR = 0.7$  there is a difference. This is due to the fact that with the defruiter in, the effective  $TR$  is actually less than 0.7. The  $TR$  specified in the test is the  $TR$  as the target is applied to the receiver. The operation of the defruiter is such that the last reply that occurs on each mode is stored in the defruiter and, since no additional reply is received for comparison to the stored reply, it is lost. Therefore, even with a  $TR = 1$ , one less reply on each mode is applied to the RVDP input from the defruiter output. When a  $TR$  less than one occurs for each miss that occurs during the target run length, an additional reply is lost in the defruiter. It is quite possible that, if enough replies for each mode were available, validation would ultimately occur. This is evidenced by Figure 41B which shows that a high probability of the occurrence of correct code not validated occurs for defruited video with  $TR = 0.7$ . Figure 41B also shows that defruited and undefruited video at  $TR = 1.0$  and undefruited video at  $TR = 0.7$  produce very similar results.

Figure 41C shows that a higher probability of the occurrence of incorrect-code validation occurs with undefruited video. This is partly due to the fact that garble situations that occur may not always be indicated as garble. When an SPI pulse (false or valid) is detected as part of a code train, certain garble situations that may be present are not indicated and an incorrect code may be stored in memory. Usually, when a garble is detected, the code is destroyed. The SPI pulse detection can prevent this since an ambiguity exists between the presence of an SPI pulse and a garble situation. This method of operation would be acceptable if the probability of declaring false SPI pulses were very low. However, this is not the case as shown in Figure 42. An excessive number of false SPI pulses are declared. This number can be considerably reduced by validating the SPI pulse.

Figure 41D shows the probability of the occurrence of incorrect codes not validated. These curves are as expected in view

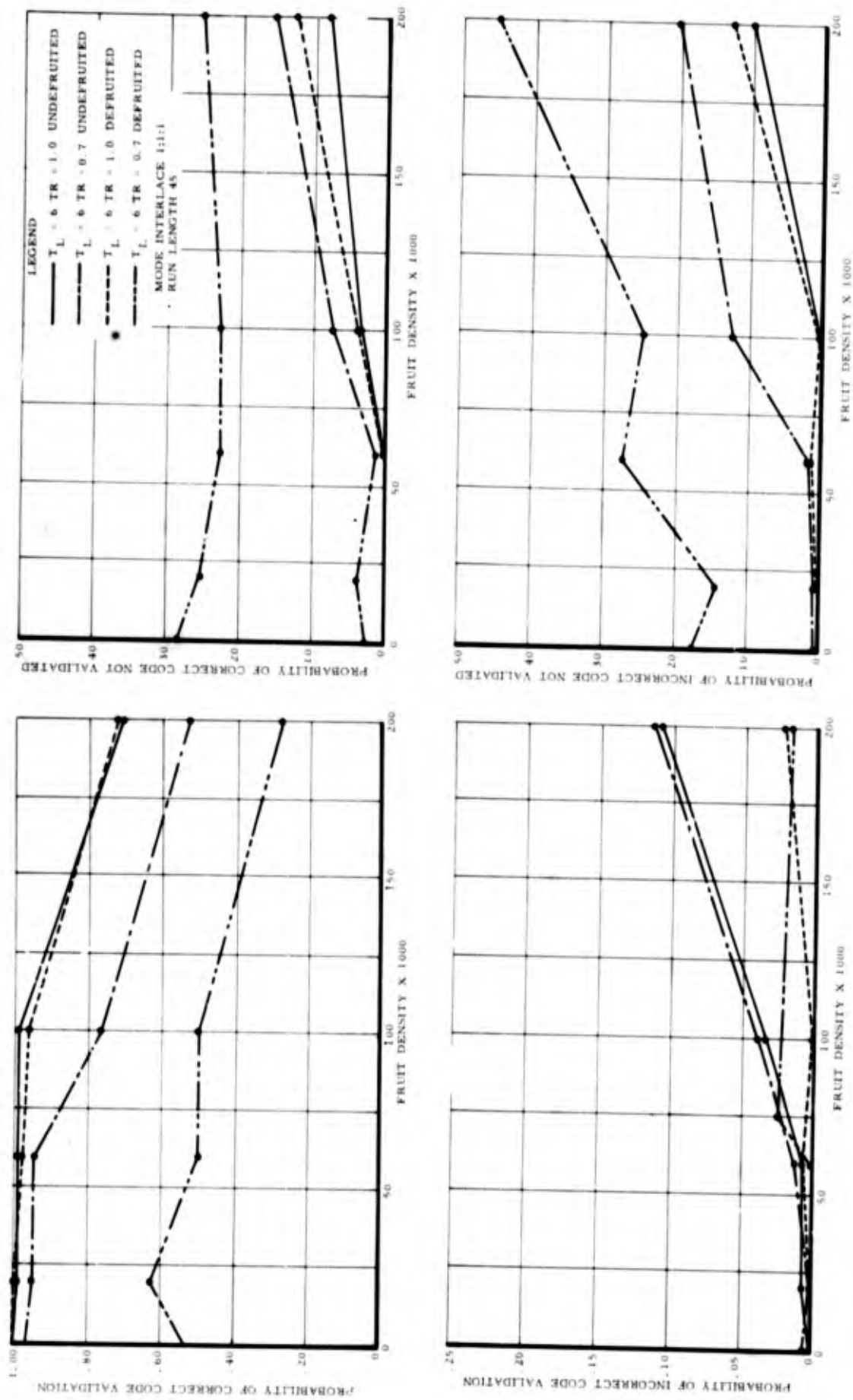


FIG. 41 BEACON CODE VALIDATION USING NORMAL AND DEFRUITED VIDEO

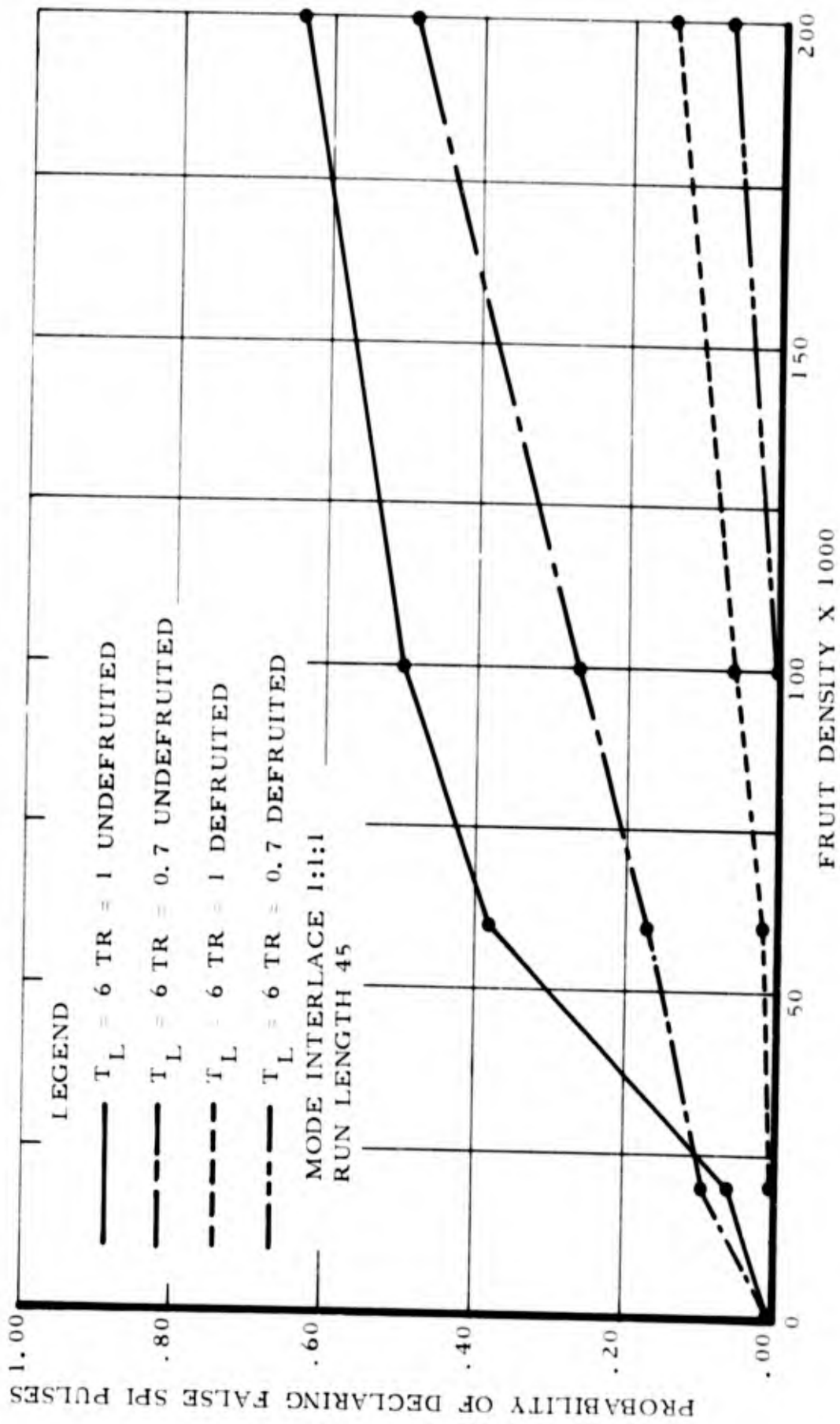


FIG. 42 PROBABILITY OF DECLARING FALSE SPI PULSES USING NORMAL AND DEFRUITED VIDEO

of the previously described curves. They simply indicate all remaining incorrect codes that were not validated.

### Mode Generation and Detection

Description - The RVDP has the capability to internally generate Modes A/3, 2, and C interrogation pulse pairs for use by a beacon ground station transmitter. In addition, the side lobe suppression pulse can also be included for external use.

During internal mode of operation, the RVDP generates the beacon interrogation pulse pairs in an interlace pattern selectable on the mode interrogation control panel. The available interlace sequences are as follows:

1. 0 through 4 mode A/3 interrogation followed by:
2. 0 through 4 mode 2 interrogations followed by:
3. 0 through 4 mode A/3 interrogations followed by:
4. 0 through 4 mode C interrogations followed by recycling

While generating interrogation triggers for external use, applicable mode control signals for use by the RVDP also are generated.

To generate the interrogation pulses, a decoded output of the search range counter to be gated into the mode interrogation delay line is enabled. The desired settings of the mode interrogation switches control the preset of the mode interrogation repeat register; this permits advance of the mode interrogation register by the decoded range count. The interrogation register outputs are used to gate the delay line outputs to a pulse shaper and to the output line driver. The side lobe suppression pulse, as mentioned previously, also is generated two microseconds after pulse P1. A detailed description of the interrogation pulse pairs is contained in Appendix V.

Performance - The mode-selector switches were used to generate the various interrogation pulse pairs and combinations of interlace ratios. It was verified that the combinations did indeed occur, and the measured pulse parameters were as follows:

	Mode 3/A	Mode 2	Mode C
Pulse Amplitude (volts)	17.50	17.00	17.00
Pulse Width (microseconds)	0.83	0.81	0.82
Pulse Rise Time (microseconds)	0.06	0.06	0.06
Pulse Decay Time (microseconds)	0.12	0.12	0.12
Jitter	0.06	0.06	0.06
Pulse Separation (microseconds)			
P1 to P2	2.02	2.06	2.03
P1 to P3	8.06	5.06	21.04

When externally generated pulses are used to trigger the beacon equipment, the pulses are supplied to the RVDP on two lines and are decoded for internal control. The interrogation pulses are gated from the input line receivers to the mode-interrogation delay line. Taps on the delay line are used to check for a P1 pulse that occurs 5, 8, or 21 microseconds before the P3 pulse for detecting beacon mode processing in accordance with the mode detected. The interrogation interlace for the mode triggers is established by the ATCBI-3 equipment when generated externally.

### Accuracy

The accuracy of the RVDP pertinent to its use as a component of the National Airspace System (NAS) is a function of the primary radar and beacon systems supplying the inputs to the RVDP and may be determined only by observing actual aircraft targets in a live environment. Tests with controlled inputs were conducted to determine to what extent the RVDP itself could contribute to system error.

Accuracy Checks with Controlled Inputs: Range and azimuth accuracies of the primary radar and beacon detectors were measured statically through the use of test target signals. The static tests were performed to investigate how certain processor peculiarities might affect the system accuracy. The range accuracy static tests were performed to check the accuracy of the range clock and to investigate the effect of receiver noise and beacon fruit on range accuracy. The azimuth accuracy static tests were performed to check the amount of azimuth bias produced by the sliding window detector and to investigate the effect of receiver noise and beacon fruit on azimuth accuracy.

### Primary Radar Azimuth Accuracy

A. Test Procedure - The primary radar static azimuth accuracy tests were conducted with the RVDP leading edge threshold

at 6 and the percent noise setting at 4%. A strong test target (14 dB above MDS) was inserted into the radar waveguide. The target messages reported by the RVDP were recorded with  $T_L - T_T$  (sliding window leading edge threshold minus trailing edge threshold) settings of 2 and 5.

B. Test Results - There is an expected difference between the actual center azimuth and that reported by the RVDP due to the run length stretching effect of the sliding window.\* The test results are shown in Figure 43(a). Each distribution represents 240 data samples. It can be seen that the mean azimuth bias is within one ACP\*\* of that which was calculated. This bias is of no concern in an operational environment since it would be corrected with the azimuth counter preset provided in the equipment. The range of data is as expected: + 1 ACP, due to the fact that the number of ACP's per scan do not equal the number of triggers per scan; and + 2 ACP's, when the effect of noise hits adding to either end of the target run length is included.

#### Beacon Azimuth Accuracy

A. Test Procedure - The beacon static azimuth accuracy tests were conducted with the RVDP leading edge threshold at 7 and a 1:1:1 (A/3, 2, C) mode interlace ratio. The DTGTS (described in Appendix IV) was used to generate the test signals and the fruit for this test. The target messages reported by the RVDP were recorded for each combination of the following conditions:

1. Fruit density: 0 and 100,000 per scan
2. Target Reliability: 1.0 and 0.7
3.  $T_T$  setting: 2, 3, and 4

B. Test Results - The test results are shown in Figures 43(b) to (e). Each distribution represents 200 data samples. The azimuth bias is considerably greater than the primary-radar azimuth bias because of the three-mode interlace.\*

Figure 43(b) represents the ideal situation of no fruit and a target reliability of 1.0. Figure 43(c) shows the distributions of azimuth bias for a fruit density of 100,000 replies/scan and a target reliability of 1.0. As expected, the spread of the distribution is greater

\* See Appendix VII

\*\* 1 ACP represents 0.088 degrees

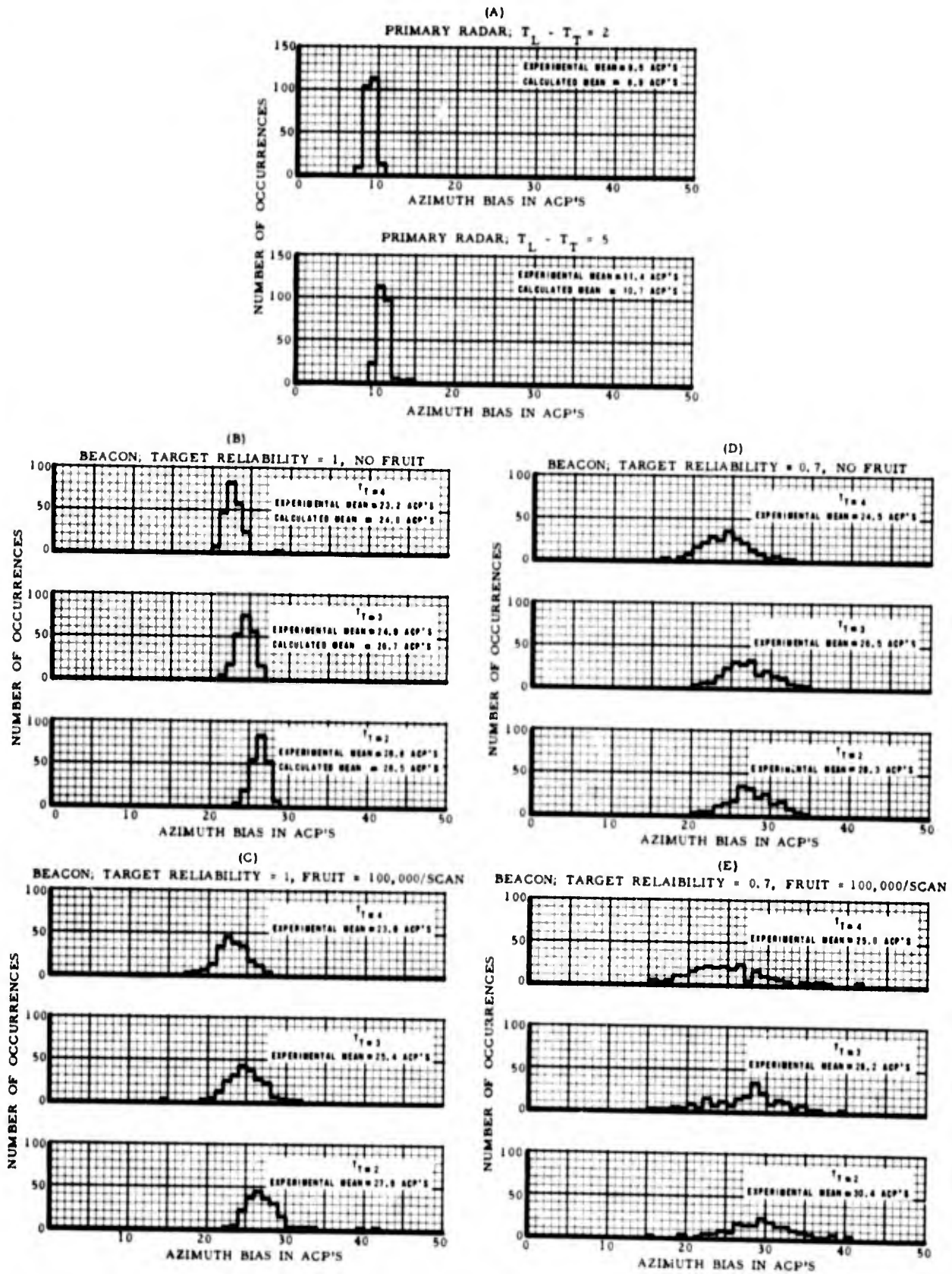


FIG. 43 RVDP AZIMUTH BIAS

due to the fruit environment. The experimental mean changed very little. This is also expected since fruit could add to either end of the target run length.

Figure 43(d) shows the distributions of azimuth bias for a zero fruit density and a target reliability of 0.7. The distribution spreads have increased due to the missing replies in the target run length of 0.7 target reliability. The means have also increased. This is as expected since the missing replies will always cause the RVDP declared azimuth to shift farther in azimuth from the actual target run length center.

Figure 43(e) shows the distributions of azimuth bias for a fruit density of 100,000 per scan and a target reliability of 0.7. This situation represents a worst case in distribution spread and bias shift.

#### Primary Radar Range Accuracy

A. Test Procedure - The primary radar static range accuracy of the RVDP was tested by generating two targets at the same azimuth and at nominal ranges of 50 and 150 nmi. The actual and reported ranges of these targets were then compared.

The RVDP internal test target generator was set for one nmi. These test-target pulses triggered a digital delay generator (Hewlett-Packard 218) whose delays were set for 600 and 1800 microseconds. The delayed pulses were used to modulate an RF signal generator, the output of which was applied to the radar waveguide. The signal generator power was adjusted to 12 dB above radar MDS and the RVDP percent noise setting was set for 8 percent. The resulting target messages were recorded for 10 scans. Both delays were increased 32 times in 0.2 microsecond steps; the RVDP output messages were observed for approximately 10 scans each time.

B. Test Results - The resulting range distributions associated with delay for the first eleven range increases are shown in Figure 44.

After adding the 1 nmi test target delay and 2.6 microseconds (for line delay, RF generator and receiver delay) to the 600 and 1800 microsecond delays from the pulse generator, the total delays from RVDP search zero range count are 49.753 nmi (614.96 microseconds) and 146.841 nmi (1814.96 microseconds). As can be seen from Figure 44, the initial reported ranges are 49 13/16 (49.812 nmi) and 146 14/16

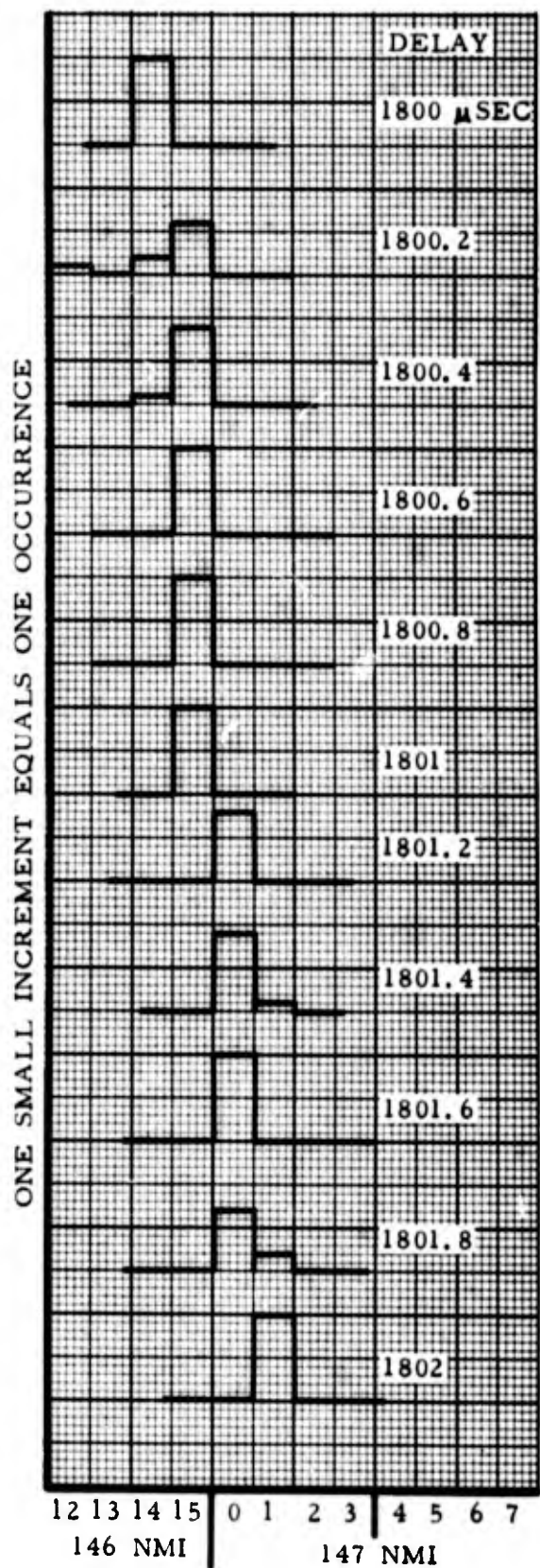
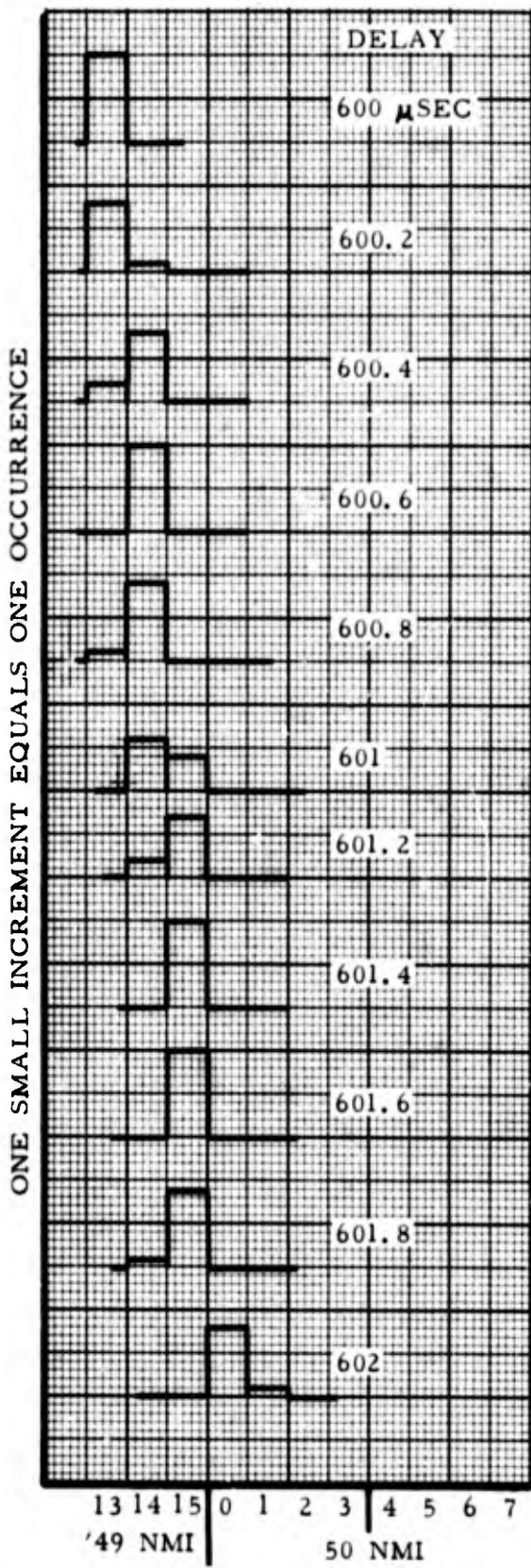


FIG. 44 DISTRIBUTIONS OF DECLARED RANGE

(146.875) nmi. The deviations between the expected and reported ranges are 0.059 and 0.034 nmi, respectively. These deviations are less than the 1/16 nmi precision of the RVDP. The small difference in these deviations at widely-separated ranges shows negligible error in RVDP master clock frequency.

Figure 44 shows that the target report distributions cross 1/16 nmi interfaces for approximately every 0.8 microsecond change in target position as expected and that there are very few target reports whose range accuracy was declared on a noise hit.

#### Beacon Range Accuracy

A. Test Procedure - The test procedure for the check on beacon range accuracy was similar to that for the primary radar range-accuracy check. Nominal ranges of 10 and 100 nmi were selected for the beacon targets.

B. Test Results - Because of the lack of noise in the beacon system as opposed to the primary radar system, the distributions were not plotted. The difference between reported range and actual range as a function of actual range is shown in Figure 45 for the target at 10 nmi and Figure 46 for the target at 100 nmi. The dotted lines which are extended to the limits of the 1/16 nmi range increment generate a saw-tooth function which is a characteristic of quantizing error. The mean error was found to be 0.01 nmi at both 10 and 100 nmi, which again indicates a high degree of linearity in the RVDP master clock.

The test was repeated with a fruit density of 100,000 per scan. Only 1.2 percent of the reported ranges were in error by as much as 1/16 nmi due to range accuracy being declared on a noise hit.

On-Line Accuracy Tests: The purpose of the accuracy tests was to obtain error distributions for the RVDP and to determine the correct value to use as a preset for the RVDP azimuth counters. During all testing the azimuth counter presets were zero. The RVDP range alignment had been accomplished statically with test signals. During all accuracy tests, the ACP's were obtained from the ACP generator (SG-135) that was installed on the pedestal of the ARSR-2 antenna which was aligned to magnetic north (-9.6 degrees from true north).

#### Range and Azimuth Accuracy

A. Test Procedure - Accuracy of the RVDP for range and

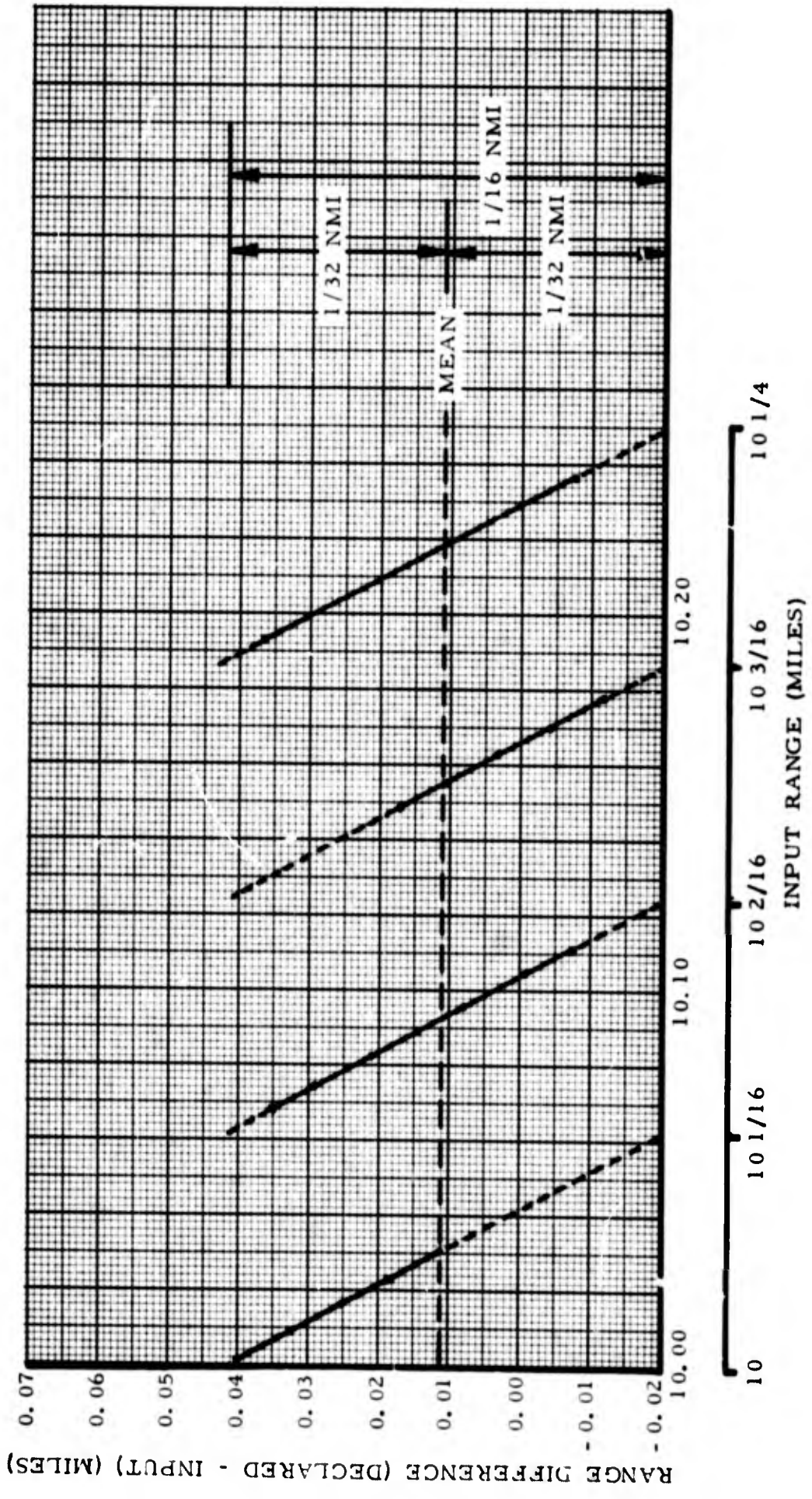


FIG. 45 BEACON DECLARED RANGE DIFFERENCE (SHORT RANGE)

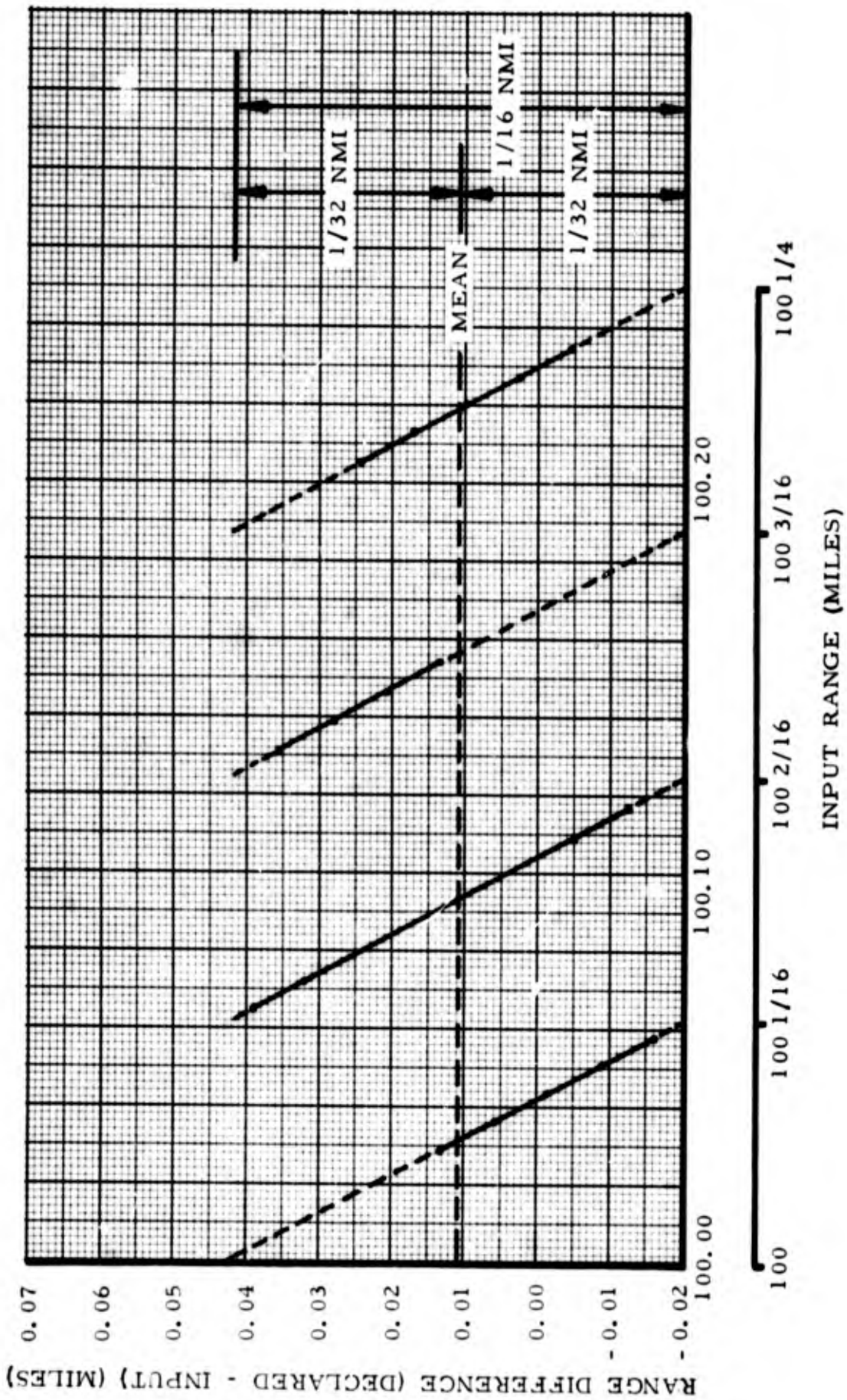


FIG. 46 BEACON DECLARED RANGE DIFFERENCE (LONG RANGE)

azimuth was determined by comparison of the aircraft position data in each RVDP message (DRG output) with the aircraft position data reported by the Extended Area Instrumentation Radar (EAIR) facility. (The EAIR is one of the range instrumentation systems employed at NAFEC and is described in Appendix IV.) The actual comparison was done by an IBM 7090 computer. Aircraft flight procedures used during the accuracy measurements are described in Appendix II.

B. Test Results - RVDP target-position data are shown in Table II. As shown for the flight of February 11, 1966, the mean value for the reported azimuth difference was -1.728 degrees for primary radar and -3.067 degrees for beacon. Therefore, -20 ACP's ( $1.728/0.088$ ) is the azimuth counter preset value for primary radar, and -35 ACP's ( $3.067/0.088$ ) is the azimuth counter preset value for beacon. Range alignment was considered satisfactory since, for both primary radar and beacon, the mean range error was less than  $1/16$  nmi ( $0.0625$  nmi).

Distributions of the range accuracy data obtained on February 11, 1966, for primary radar and beacon are shown in Figure 47. Distributions of azimuth accuracy data obtained on February 11, 1966, for primary radar and beacon are shown in Figure 48.

Accuracy as a Function of Range - To ascertain if the range and azimuth error varied as a function of range from the ARSR-2 facility, the inbound flight data (DRG output) of January 25, 1966, (beacon) and February 8, 1966, (primary radar) were grouped into 20-mile increments. The statistics for these grouped data, which are shown in Figure 49, do not indicate any definitive pattern insofar as target-position reporting being a function of the range from the facility. It should be noted that, in almost every case, the dispersion of data (standard deviation) was greatest at the minimum and maximum ranges.

**TABLE II**  
**RVDP ACCURACY DATA**

Date of Flight	No. of Samples	RANGE ERROR		AZIMUTH ERROR	
		Mean (Nautical Miles)	S. D. **	Mean*	S. D. ** (Degrees)
<b><u>BEACON ONLY</u></b>					
1/25/66	590	0.084	0.165	2.922	0.254
2/9/66	318	0.032	0.101	2.930	0.214
2/11/66	196	0.007***	0.055	3.067***	0.356
<b><u>PRIMARY RADAR ONLY</u></b>					
2/8/66	374	0.211	0.102	1.638	0.272
2/11/66	354	0.057***	0.096	1.728***	0.233
<b><u>PRIMARY RADAR AND BEACON</u></b>					
2/11/66	163	0.019	0.030	1.694	0.105

\* Referenced to magnetic north

\*\* One standard deviation

\*\*\* Values used in determining preset values for range and azimuth counters

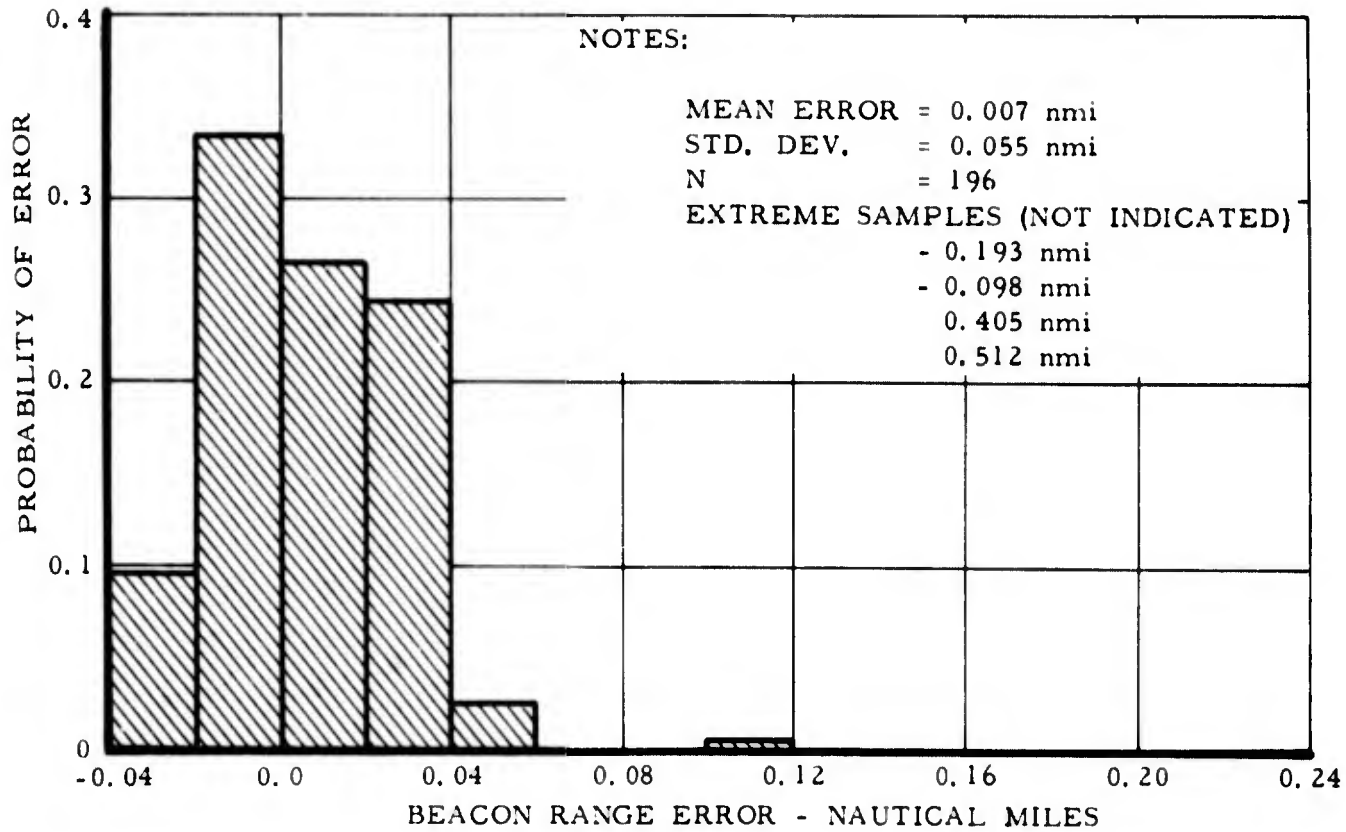
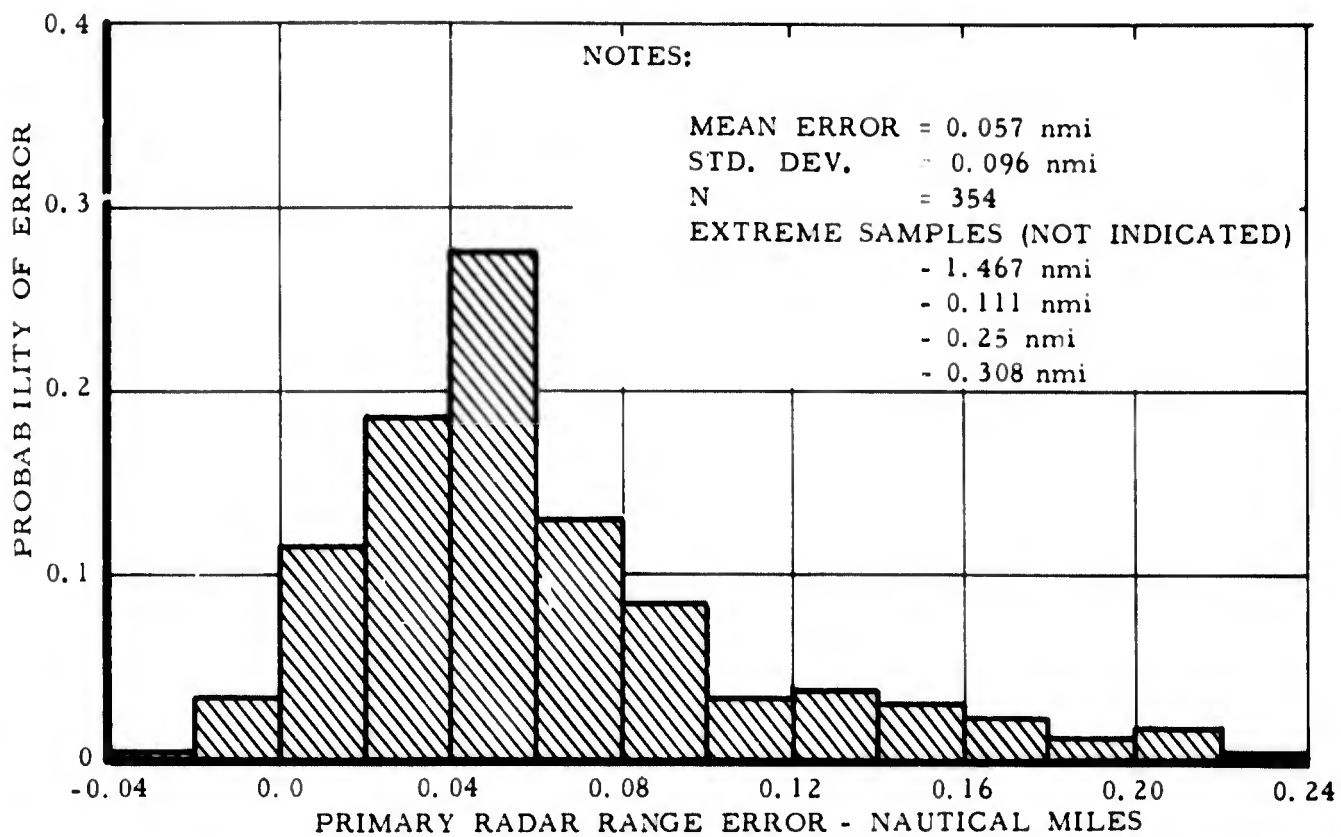


FIG. 47 DISTRIBUTIONS OF RVDP RANGE ERRORS

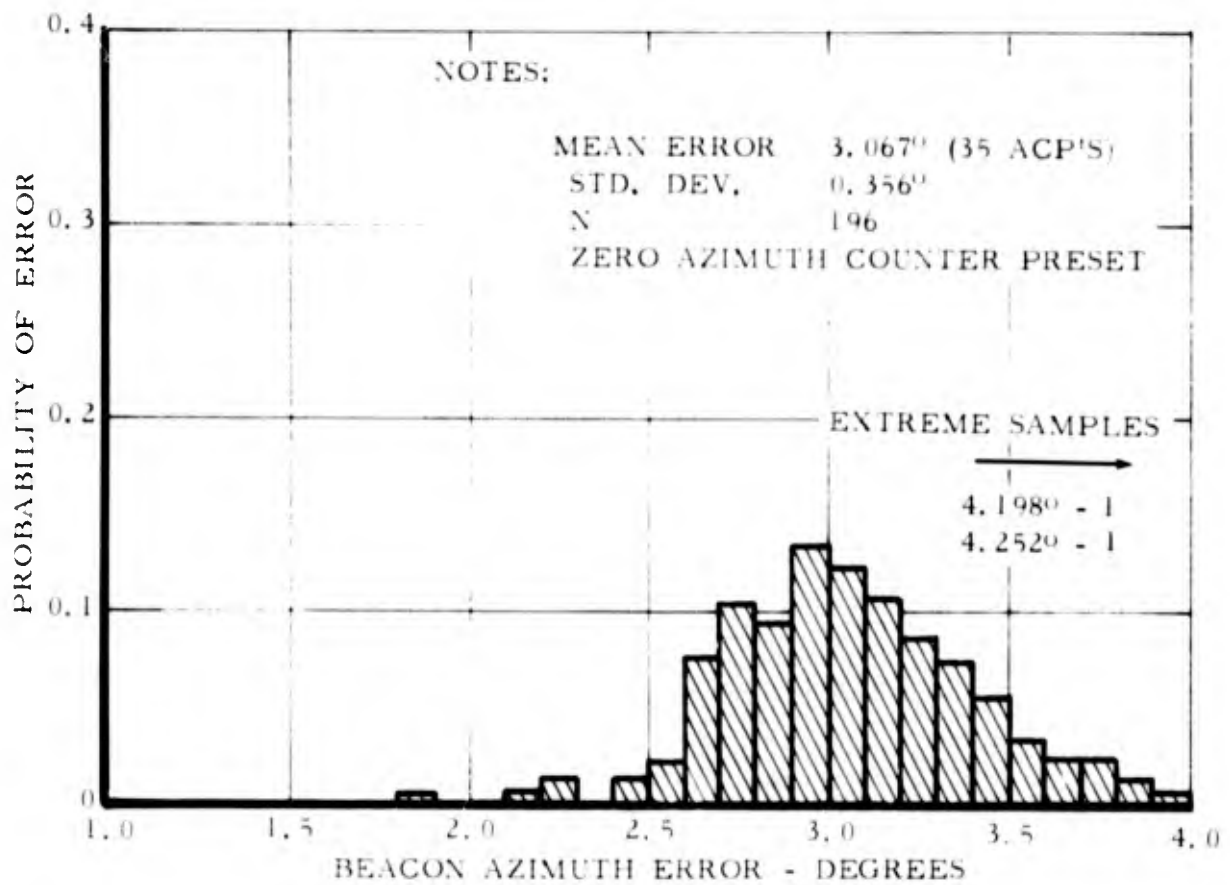
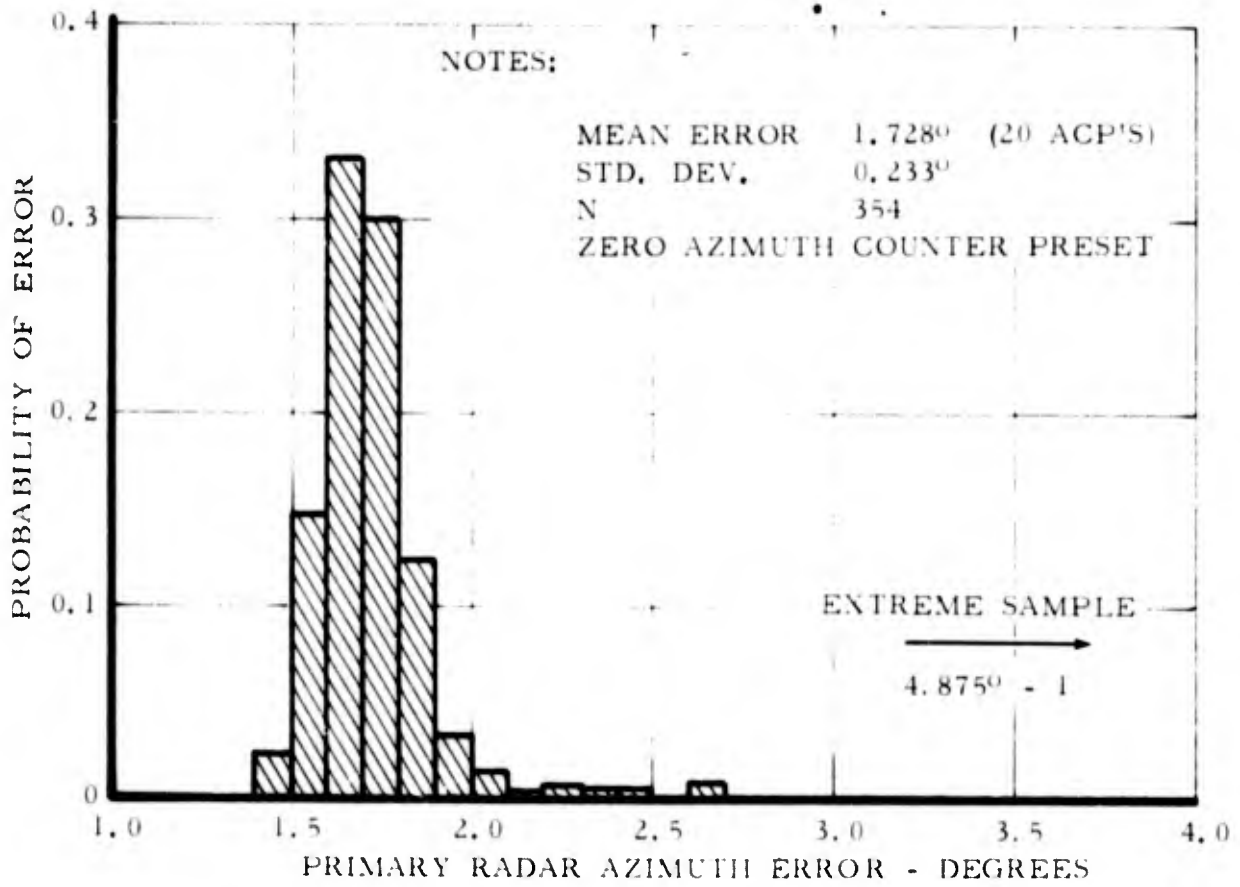


FIG. 48 DISTRIBUTION OF RVDP AZIMUTH ERRORS

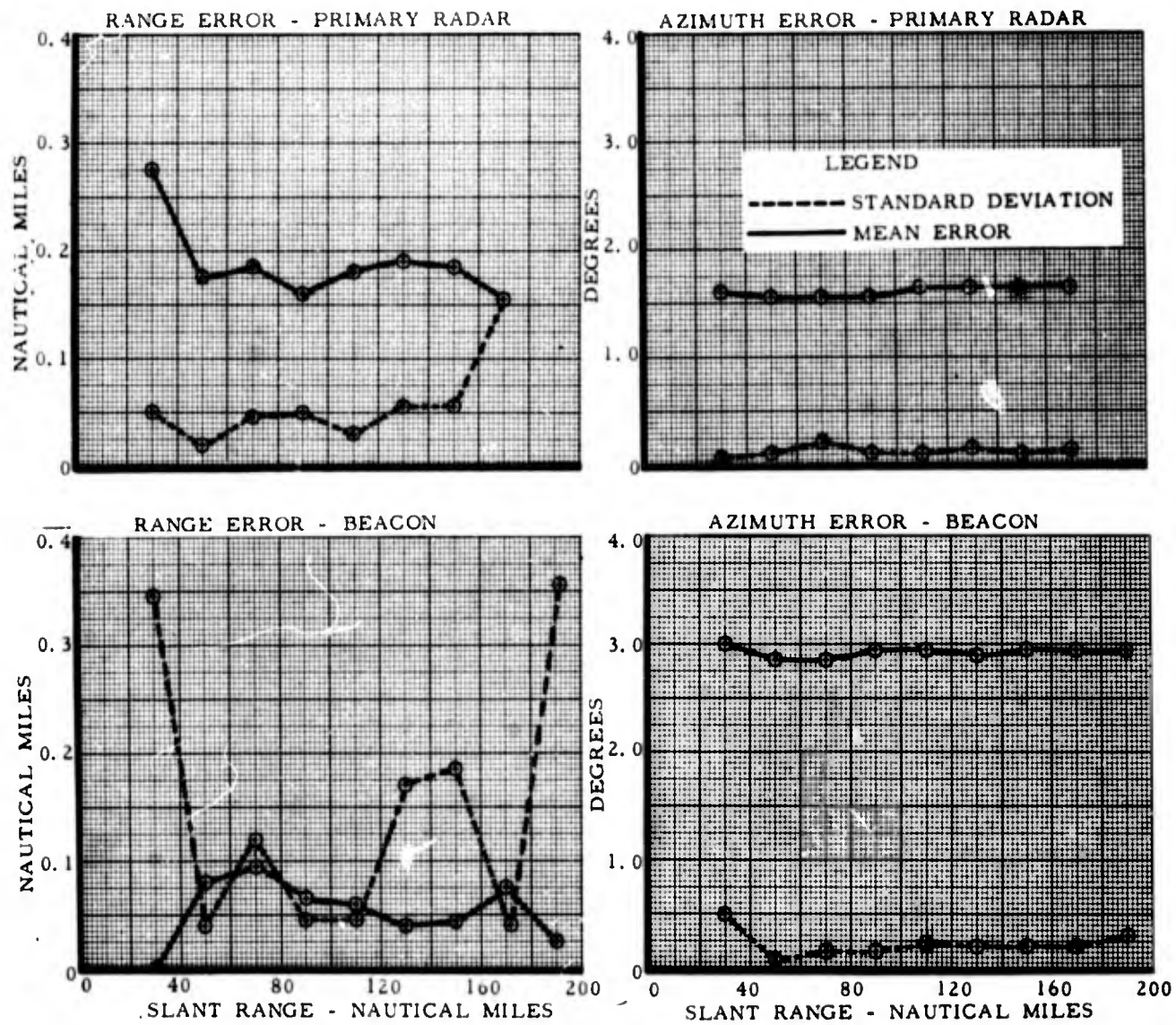


FIG. 49 RVDP ACCURACY AS A FUNCTION OF RANGE

## Resolution

The resolution capability of the RVDP pertinent to the actual minimum aircraft separation distance required that would result in a discrete target being detected for each aircraft is a function of the primary radar and beacon systems supplying the inputs to the RVDP as well as the RVDP itself. These tests were accomplished with actual aircraft in a live environment. Range and azimuth resolution checks were performed with controlled inputs to determine the effect of the RVDP itself on system resolution.

Resolution Checks with Controlled Inputs: The range and azimuth resolution capability of the primary radar and beacon detectors was measured statically through the use of test signals. Range resolution tests checked the operation of the range discrimination modification\* and azimuth resolution tests checked the stretching effect of the sliding window detector.

### Azimuth Resolution

A. Test Procedure - Primary radar azimuth resolution was statically tested by inserting two 14 dB test targets into the waveguide at the same range. While observing the test target pair on the RAPPI monitor, the initial azimuth separation was decreased until the resolution threshold was approached. Then, the number of resolved occurrences in 20 scans was observed each time the azimuth separation was decreased by one radar trigger period until the targets were 100% unresolved.

Data were taken for five target-detection parameter combinations as shown in Table III. This table also shows the minimum azimuth separation for resolution, which is a function of target run length and trailing-edge threshold\*\* only.

TABLE III  
AZIMUTH RESOLUTION TEST CONDITIONS

RVDP Settings			$T_T$ (triggers)	Target Run Length (triggers)	Calculated Minimum Azimuth Separation for Resolution	
$T_L$ (triggers)	$P_N$	$T_L - T_T$ (triggers)			(triggers)	(degrees)
6	4%	2	4	16	25	2.6
6	4%	5	1	16	28	2.9
6	4%	2	4	10	19	2.0
7	8%	2	5	16	24	2.5
7	8%	5	2	16	27	2.8

\* See Appendix II

\*\* See Appendix VII

B. Test Results - Figure 50 shows the percent of resolved occurrences versus azimuth separation in triggers. If noise were not present, the curves of Figure 50 would all be step functions with the break occurring at the calculated minimum azimuth separation indicated in Table III. With noise in the system, noise hits will, on occasion, occur between the two targets and cause them to become unresolved. The binomial distribution may be used to calculate the probability that a sufficient number of noise hits will occur to cause the targets to become unresolved. The azimuth resolution curves of Figure 50 are plotted from calculated data while the data points shown are the results of the measurements.

A similar static test was performed to check beacon azimuth resolution. The results were consistent with the theoretical values calculated from the expressions derived in Appendix VII. Since the checks were made without a fruit environment, the results were deterministic rather than probabilistic as was the case for the search tests.

#### Range Resolution

A. Test Procedure - To statically test primary-radar range resolution of the RVDP, two RF test targets were generated at the same azimuth and at a nominal range of 50 nmi--separated by 1 nmi. The test target power was 14 dB above that required for minimum discernible signal, and the pulse widths were 3.5 microseconds (the width of typical returns from large aircraft targets as observed on an "A" scope). The range of the farthest target was decreased in 0.7 microsecond steps until the targets were coincident. Then the range of this target was increased in 1.4 microsecond steps until a 1 nmi separation was again established. Each time the separation was changed, the RVDP output was monitored for five scans.

B. Test Results - Figure 51 shows the 5-scan mean difference in reported ranges versus target separation in microseconds or nautical miles. This figure shows that reported separation decreases linearly as range separation decreases until the target pulses merge (at 3.5 microsecond separation). At this time a range split occurs and the reported separation remains constant as the true target separation is decreased. When the target separation decreases to the point where the combined pulse width is less than that required for a range split (nominally, 4 microseconds), the farthest target disappears and the function decreases to zero.

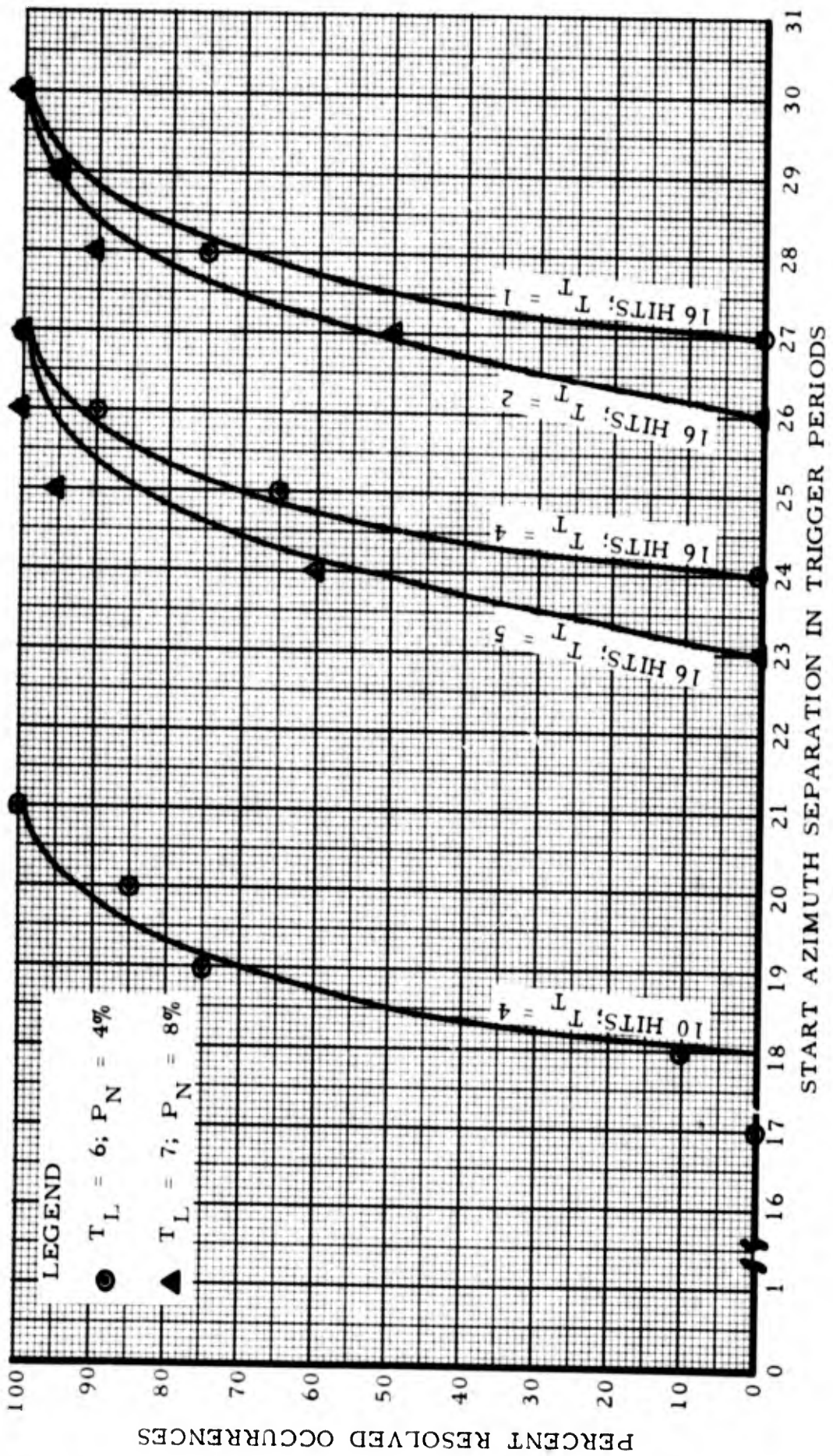


FIG. 50 PRIMARY RADAR AZIMUTH RESOLUTION

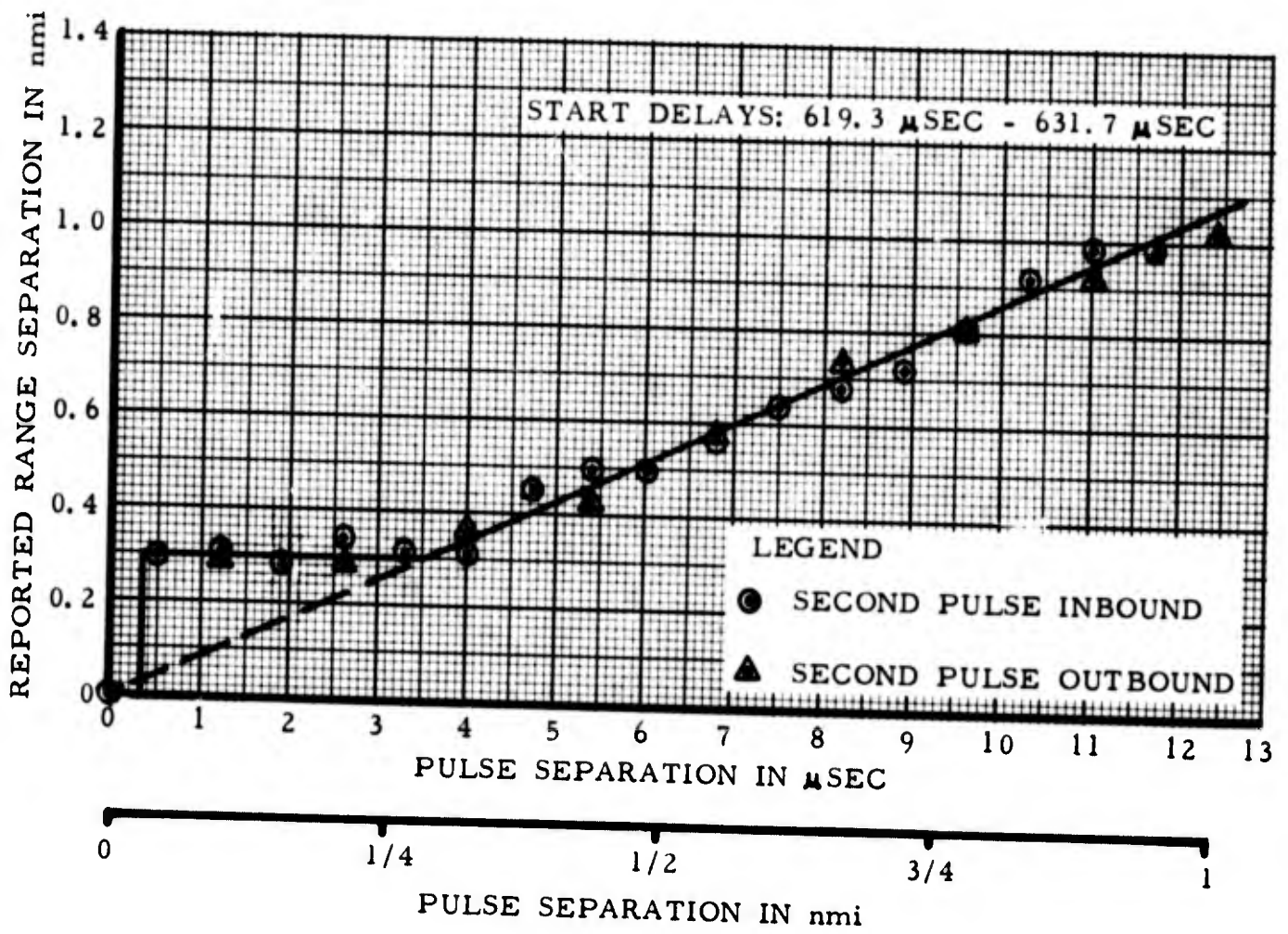


FIG. 51 REPORTED VS. ACTUAL PULSE SEPARATION

It can be seen that the search range resolution of this system is a matter of definition; i. e. , whether the target pair is considered unresolved when their reported ranges no longer indicate the true separation, or when the second target disappears. If the second definition is used, the RVDP is able to resolve targets in range even though their signal returns overlap.

Beacon range resolution was also tested by decreasing the range separation between two test targets at the same azimuth. The pulse width of the beacon signal was 0.5 microseconds and, therefore, range resolution should be primarily a function of the 3.1 microsecond range cell. Beacon range resolution was found to vary from 1/4 nmi to 1/16 nmi, depending on the relative position of the first target within its own range cell.

### On-Line Resolution Tests

Test Procedure - The flight test laboratory described in Appendix IV was used to collect the on-line resolution data. While observing the displays, ATC specialists recorded the number of targets that were displayed for two test aircraft proceeding along a radial (range resolution) or along an arc (azimuth resolution). To eliminate the effect of trail data, the scan converters for both the digital channel and the video channel were adjusted so that the displayed targets were erased within one antenna-scan period.

Aircraft-separation data during these dual-aircraft flights were collected by observance of the range-tracker indicator panel (Appendix IV) installed in the trailing aircraft. During each antenna scan, the observed aircraft separation value was transmitted to the control/display area to enable recording concurrently with the collection of display-resolution data.

In addition to the use of the Atlantic City VORTAC facility by both aircraft, the trailing aircraft was vectored by the NAFEC Test Control Facility to assure that both aircraft were proceeding along the same arc during the azimuth-resolution tests. Aircraft flight procedures specified the desired aircraft separation during each radial or orbital flight pattern.

### Test Results

A. Range Resolution - The capability of the ATC specialist to detect two targets, as a function of aircraft separation during the radial

flights, is shown in Figure 52 for primary radar and Figure 53 for beacon. As indicated in these figures, the required aircraft separation that resulted in two targets being displayed for 80% of the antenna scans was between 0.5 and 0.6 miles for the video channel and between 0.6 and 0.7 miles for the digital channel. The difference between the two channels was attributed to the resolution of the display subsystem (RBDE-5) since the diameter of the "dot" on the digital-channel display was greater than the width of the "slash" on the video-channel display at the instant of writing on the scan-converter tube.

To exclude the limitation due to the resolution of the RBDE-5 subsystem, an analysis of the RVDP messages (DRG output) generated during each scan for the test aircraft was performed. For primary radar returns, two messages were generated for 80% of the antenna scans when the aircraft separation was between 0.2 and 0.3 miles (Figure 52). For beacon, the 80% point was reached when the aircraft separation was 0.4 miles (Figure 53).

B. Azimuth Resolution - The capability of the ATC specialist to detect a target for each aircraft, as a function of azimuth separation between the test aircraft, is shown in Figure 54 for primary radar and beacon.

For primary radar, the digital channel resolution (80% point) was between 4.5 and 5.0 degrees, as compared to a 3.0 to 3.5 degree value for the video channel.

For beacon, the digital channel resolution was considered as being between 7.5 and 8.0 degrees, as compared to a 6.5 to 7.0 degree value for the video channel. The 80% point for resolved radar beacon targets on the digital channel was not reached since the required separation was greater than the range capability of the range-tracker equipment that was installed in the aircraft.

For both primary radar and beacon, the azimuth resolution results were considered adequate in view of system theory. For example, the primary radar sliding window requires a total of 8 misses to clear the 13-bit sliding window of "hits" from one aircraft (prior to declaring  $T_T$ ) before receiving "hits" from the second aircraft.

During the reduction of azimuth resolution data, only those antenna scans were considered that resulted in an RVDP target message (DRG output) for each test aircraft, and each message reporting

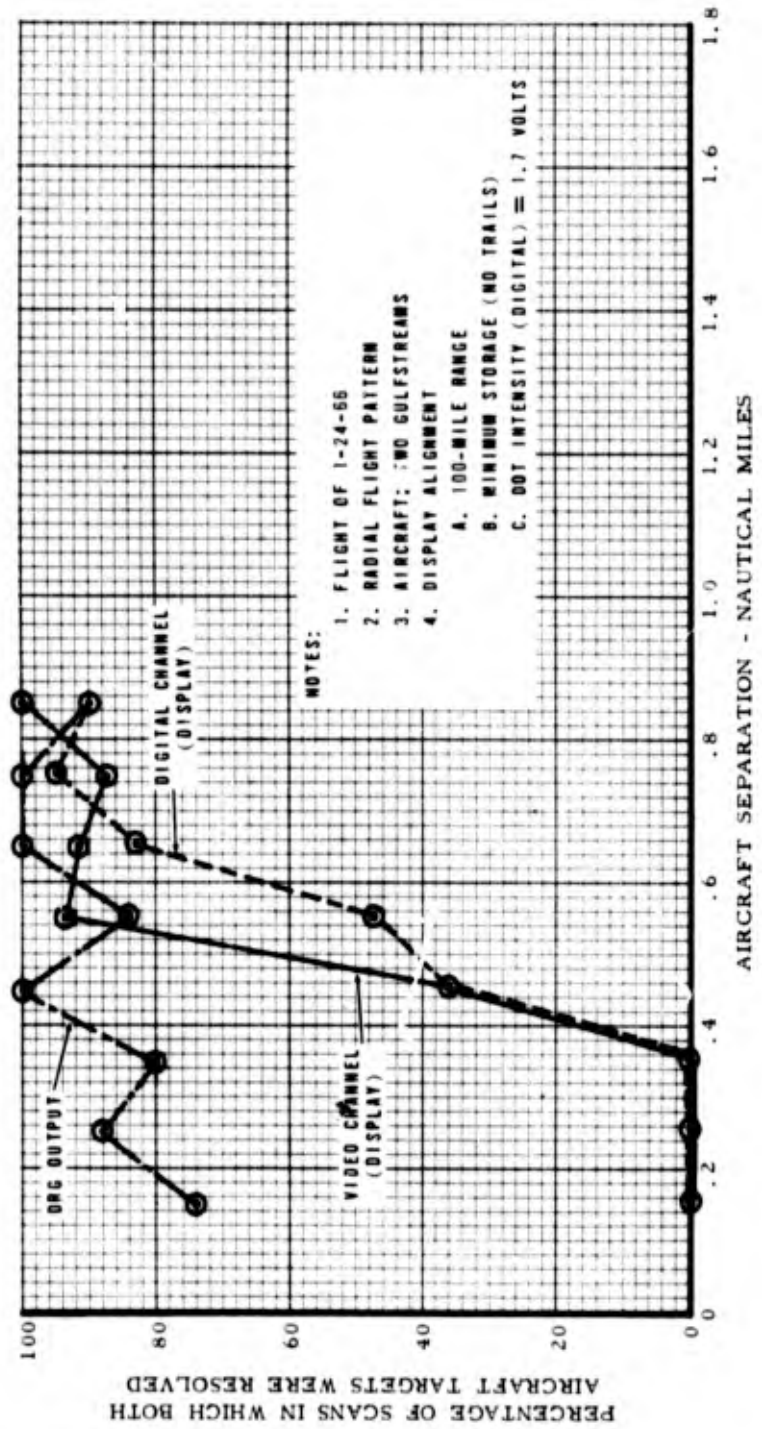


FIG. 52 RANGE RESOLUTION FOR PRIMARY RADAR

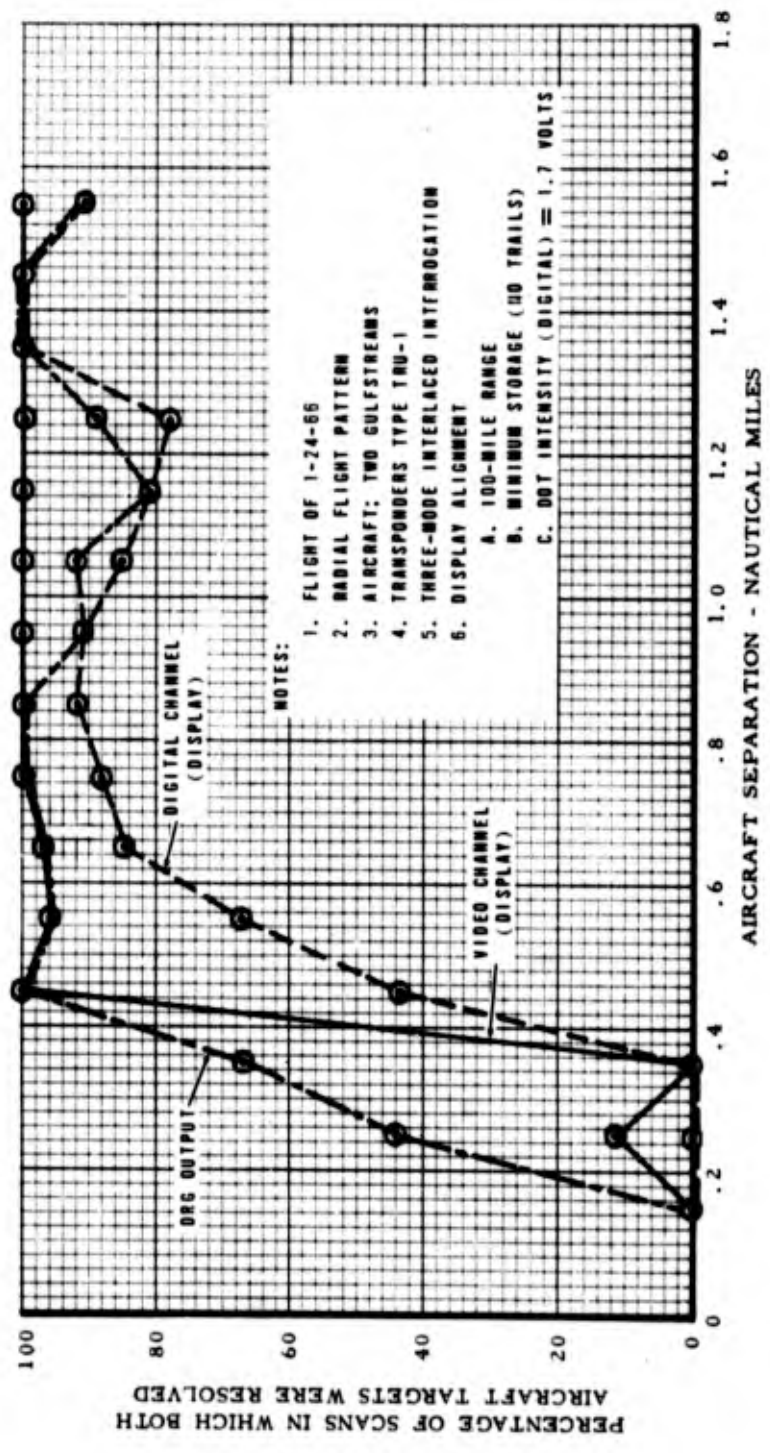


FIG. 53 RANGE RESOLUTION FOR BEACON

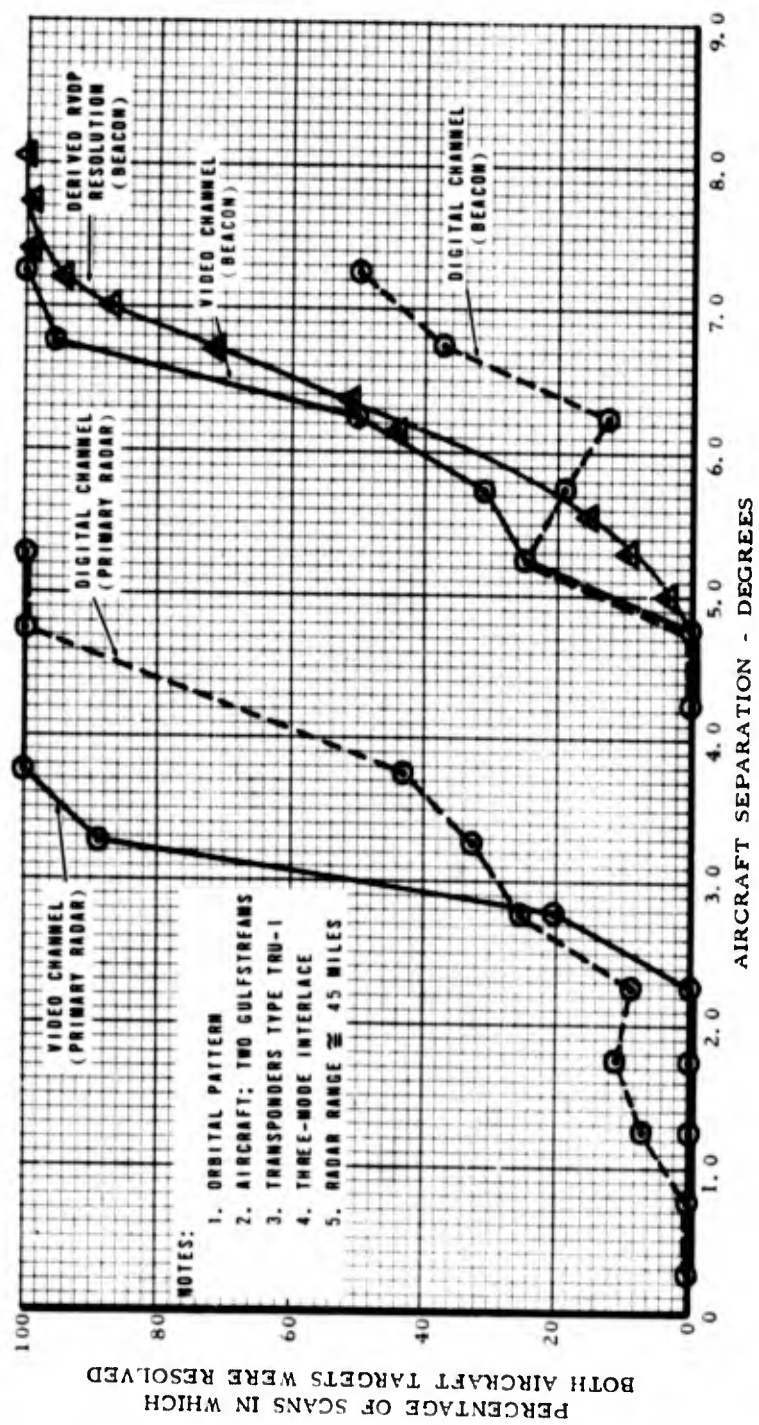


FIG. 54 AZIMUTH RESOLUTION - PRIMARY RADAR AND BEACON

the range of each aircraft within the same RVDP range cell. This definition was necessary to eliminate the effect of the range resolution capability of the RVDP. However, this placed a limitation in the amount of usable data since it became essential that both aircraft had to be at the same range from the radar facility. For example, during the azimuth resolution flight for primary radar, RVDP messages were obtained for 609 antenna scans. Of this total, resolved-target messages were obtained for 468 antenna scans, indicating the resolution capability of the RVDP when both range and azimuth resolution were considered. However, only 22 resolved-target messages were obtained that could be considered independent of the range resolution capability of the RVDP. To supplement the beacon azimuth resolution test data, a beacon azimuth resolution curve was derived from a population of beacon target run lengths (width of actual beacon returns in radar triggers). The resulting derived curve shown in Figure 54 represents beacon targets from the entire range coverage of the beacon facility and each data point represents an average population size of 420. The method of deriving resolution from target run length is described in Appendix VII.

The difficulty in obtaining azimuth resolution measurements that were independent of the range resolution capability of the RVDP indicates the overall resolution capability is primarily a function of range resolution. This characteristic becomes more apparent when a longer storage time is used for the RBDE-5 scan converters since two aircraft would have to remain within 1/4 mile (slant range from the radar facility) of each other to avoid being resolved over a period of several scans. The overall resolution capability of the digital channel is depicted in Figure 55, which can be compared to the resolution capability of the video channel (Figure 56).

Target Split Rate: In detection systems such as the RVDP, changes in the detection criteria which improve target resolution result in an increase in the split rate for single targets. A range split occurs when the radar return from an aircraft is so wide as to be quantized and detected in more than one range cell. An azimuth split occurs if, after trailing edge detection ( $T_T$ ), sufficient hits are received that can cause leading edge threshold detection ( $T_L$ ) a second time during the scanning period.

Test Procedure - RVDP messages (DRG output) that were obtained during the single aircraft flights were analyzed to determine the number of splits that occurred.

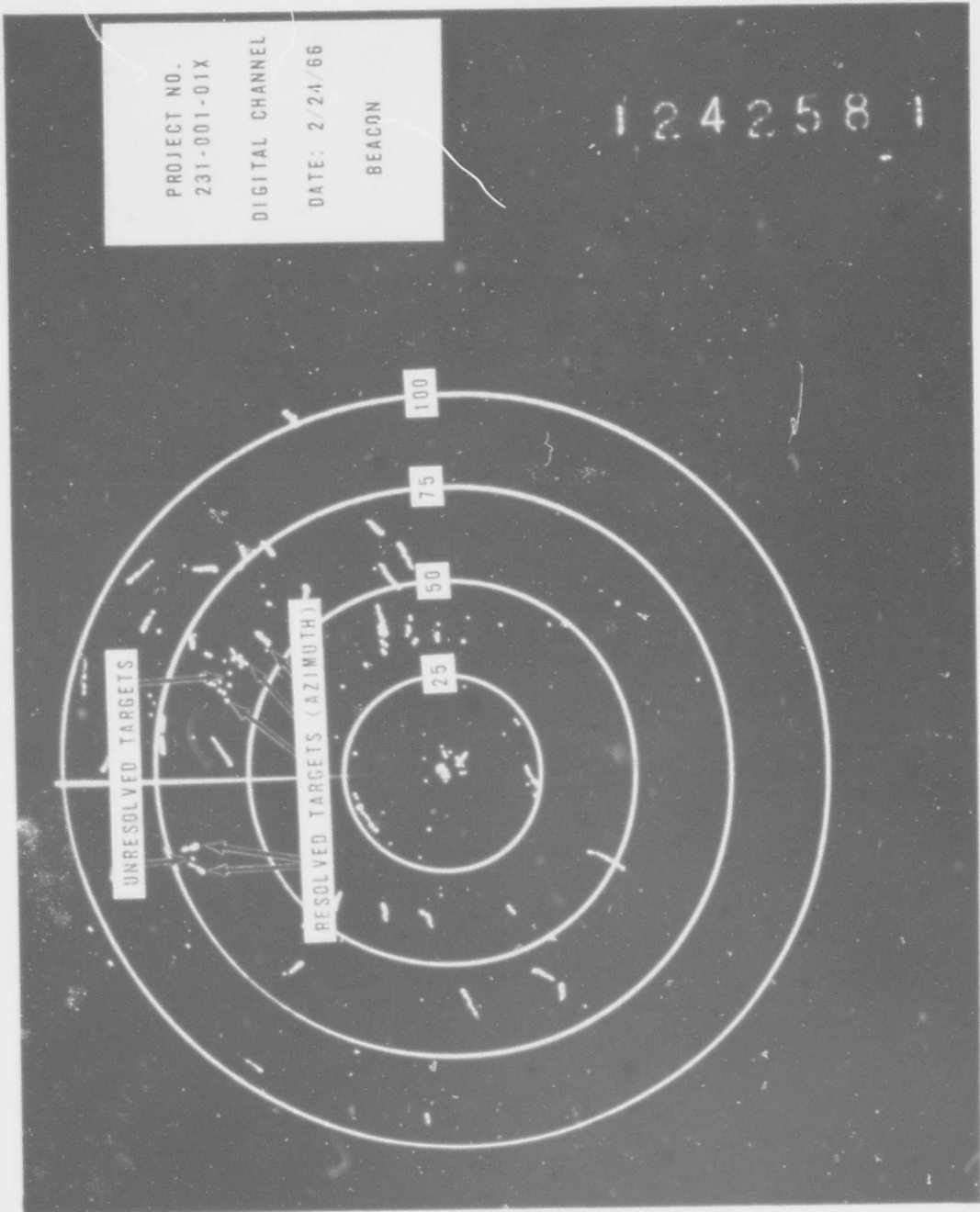


FIG. 55 DIGITAL CHANNEL DISPLAY PRESENTATION - BEACON

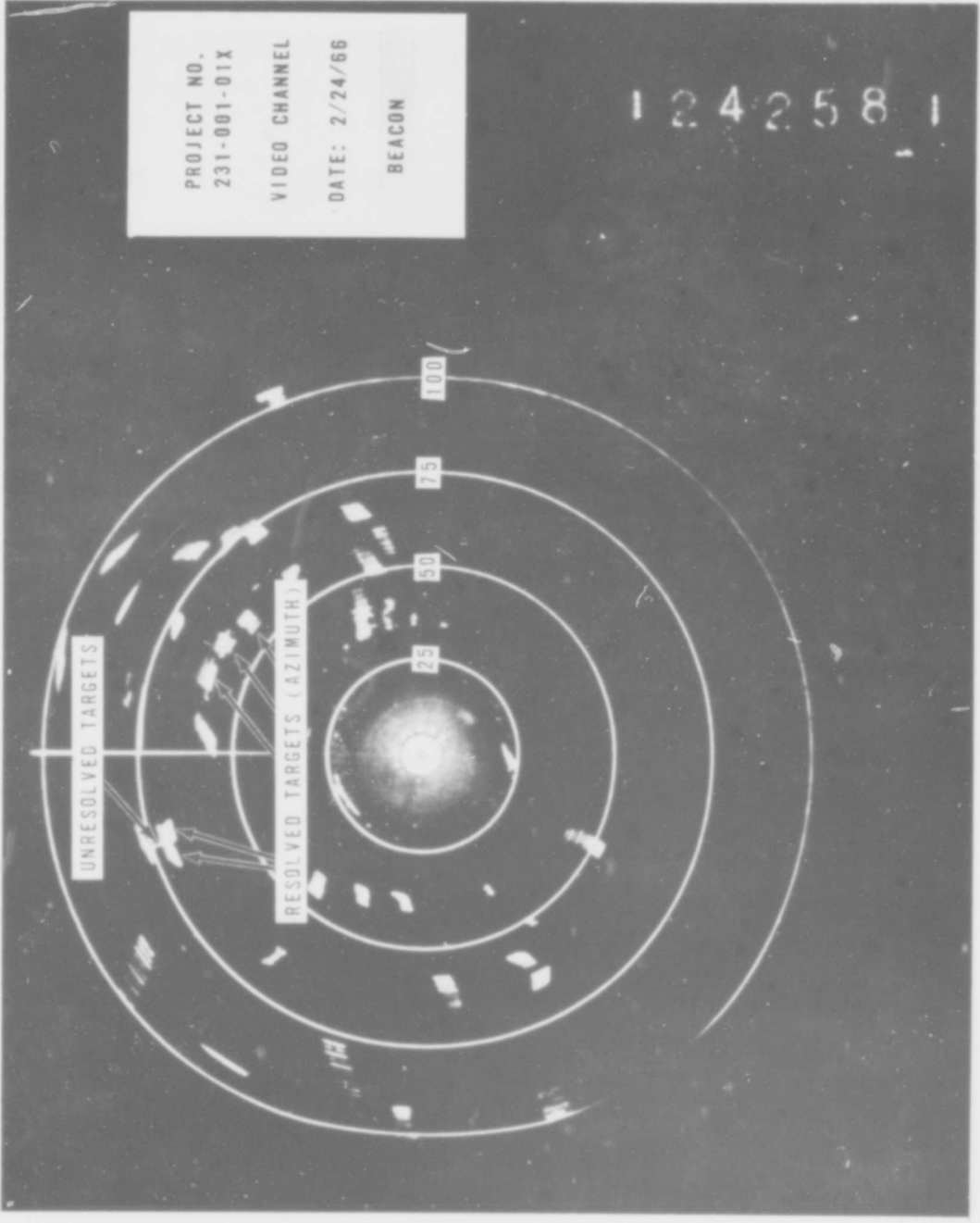


FIG. 56 VIDEO CHANNEL DISPLAY PRESENTATION - BEACON

Test Results - For a total of 1,382 primary radar messages that were analyzed, there were 30 (2.17%) splits and eight (0.58%) duplicate messages. The duplicate messages that were presented were not considered splits since both messages had exactly the same reported range and azimuth.

For a total of 1,634 beacon messages that were analyzed, there were 11 (0.67%) splits and 11 (0.67%) duplicate messages.

### Data Transfer Capacity

Target messages were transmitted from the radar/RVDP site to the point of use via three class 4A telephone lines and their associated modems (Lenkurt type 26B). The performance of the data transfer system is the subject of a separate report.<sup>8</sup>

Message Transfer Rate: Each of the three telephone lines was driven at a 2400-bit-per-second rate for a total data transfer capacity of 7200 bits per second. An RVDP message, for primary radar only, consisted of 52 bits, and a beacon message (or a combined beacon and primary radar message) consisted of 91 bits. Between each message is a 13-bit idle character which, when added to the message bits, resulted in a transfer requirement of 65 bits or 104 bits for each message. Thus, the message capacity of the data transfer system was a maximum of 1060 primary radar target messages of 665 beacon target messages per 9.6 second scan period of the radar. These transfer rates are maximum transfer rates and the transmission of map messages, status messages, etc., would correspondingly reduce the capacity for transfer of target messages.

Normally, a mixture of beacon and primary radar messages would be transferred, and the maximum message capacity under such conditions would be of most interest. Assuming 200 beacon target messages are to be transferred per scan, a maximum of an additional 740 primary radar messages could be transferred for a total of 940 messages per scan.

Test Procedure - During many of the flight tests, especially when weather clutter was present, a count of total messages processed per scan was maintained at the output of the RVDP.

Test Results - Data on message counts per scan obtained at the output of the RVDP are presented as histograms in Figure 57. Under

- - - - -

<sup>8</sup> Reference 8

NOTE:  
N = TOTAL SCANS

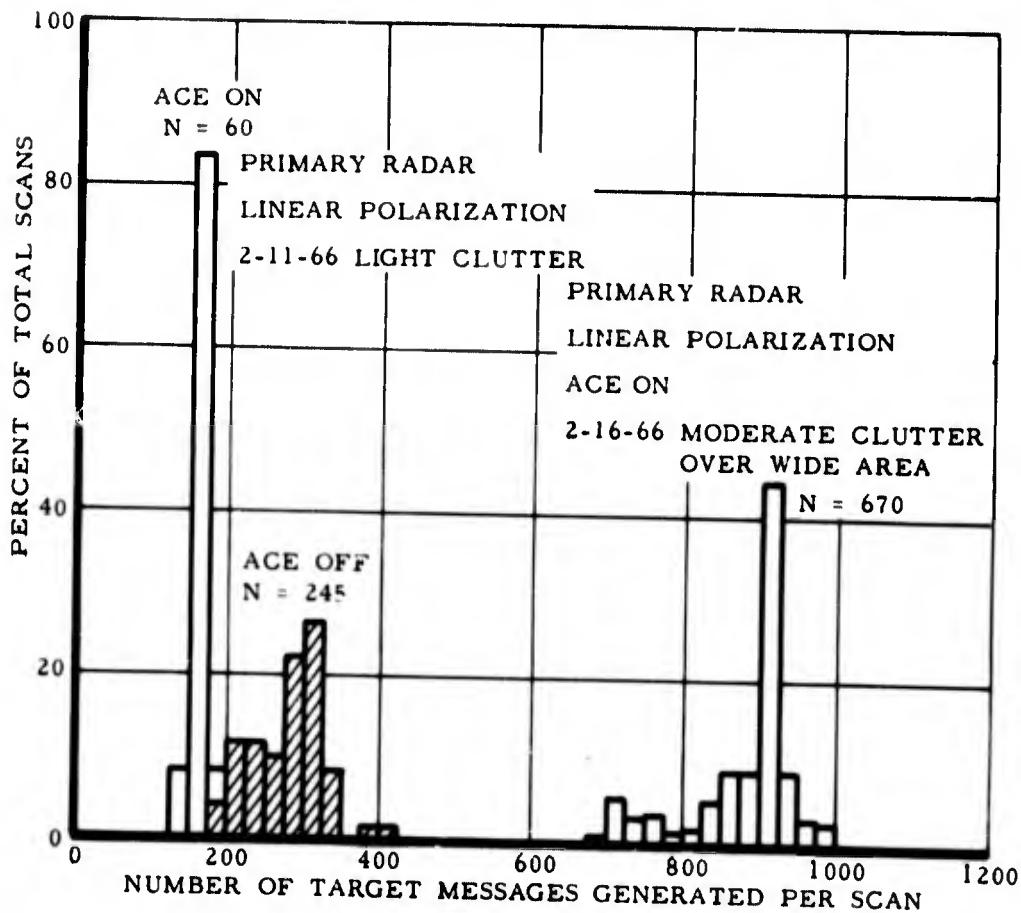
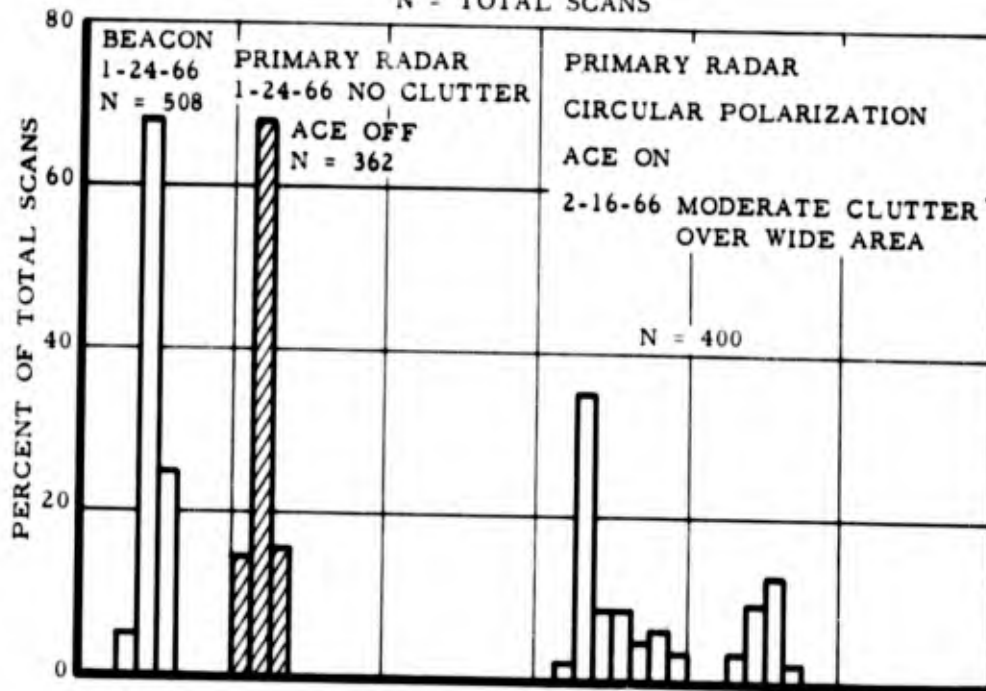


FIG. 57 DISTRIBUTIONS OF MESSAGE TRANSFER RATES

conditions of light clutter and no clutter, the message transfer rate remained well within the capacity of the data transfer system. However, when the clutter extended over a significant portion of the surveillance area as it did on February 16, 1966, the maximum capacity of the data transfer system was approached.

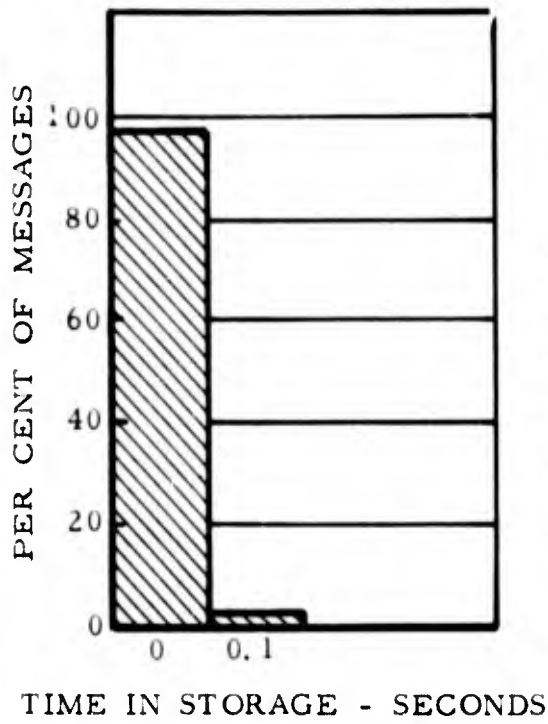
When ACE was not employed during weather clutter tests, the number of messages that were processed did, on occasion, exceed the maximum capacity of the data transfer system. At no time during weather-clutter tests did an overload condition exist in the data transfer system when the ACE function was on.

Message Time-In-Storage: A time-in-storage is computed for all beacon and search messages in the DTG. When the message is read from memory to be placed in the output register, the time-in-storage word is added. The time-in-storage, which is in 0.1 second increments, is also compared to a constant number equal to 1/2 of the time of one antenna scan. If the OVER 1/2 SCAN INHIBIT function is enabled, and the 1/2 scan comparator circuit determines that a target has been held in the memory for more than 1/2 scan, the message is obsolete and is destroyed by resetting the output register in which it is held unless one of the emergency beacon codes (7600 or 7700) is present. If the OVER 1/2 SCAN INHIBIT function is not enabled, the message is transmitted.

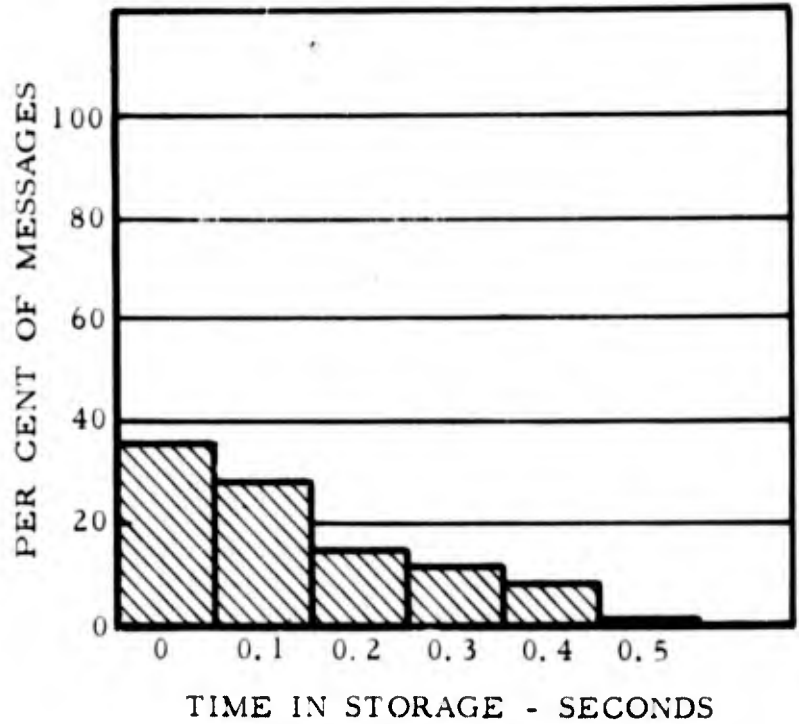
Test Procedure - The time-in-storage information was extracted from recorded flight test data for periods of time that represented different message rates. The OVER 1/2 SCAN INHIBIT function was disabled.

Test Results - The time-in-storage distributions that resulted from four message rates are shown in Figure 58. Under conditions of no clutter (Figure 58a), very few messages encountered delay in output processing. In light clutter conditions (Figure 58b), more messages are delayed but the percentage of messages delayed and the amount of time-in-storage is not significant when compared to the 1/2 scan time.

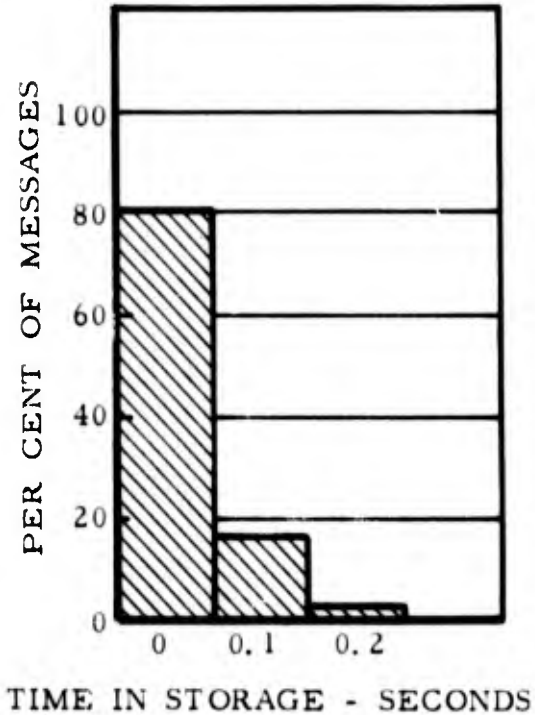
Figure 58c shows the time-in-storage distribution that resulted from a heavy clutter condition with ACE on. In this case the average message rate is close to the maximum message handling capability of the system. Under these conditions the percentage of messages delayed increased further, but here again, this percentage and the amount of time-in-storage of the delayed messages is not significant. This indicates that as long as the message rate remains



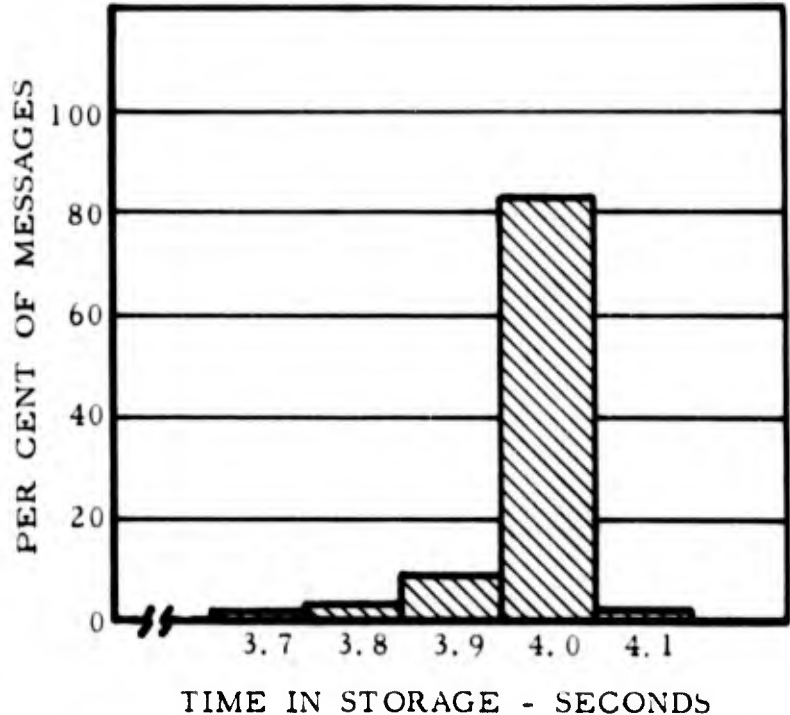
(a)  
287 MESSAGES PER SCAN



(c)  
970 MESSAGES PER SCAN



(b)  
583 MESSAGES PER SCAN



(d)  
1,092 MESSAGES PER SCAN

FIG. 58 DISTRIBUTIONS OF MESSAGE TIME-IN-STORAGE

below an overload condition, as will always be the case with ACE on, message delay in transmission will not be excessive.

Figure 58d shows the time-in-storage under conditions of clutter which extended over a significant portion of the surveillance area with ACE off. An overload condition occurs and the maximum message transfer capacity or saturation of the system is reached. In addition, since messages are being generated faster than they are transmitted, the time-in-storage also approaches the maximum value.

It must be pointed out that the maximum time-in-storage and maximum messages per scan indicated in Figure 58d do not exactly agree with the predicted values for the system. This was investigated and it was found that an adjustment in the time-in-storage circuitry had been inadvertently changed, thus producing the difference. This small difference does not affect the validity of the data.

## SUMMARY OF RESULTS

1. The primary radar quantizer reference level control system maintained the proper probability of quantizing under normal conditions and prevented 100% quantization in simulated clutter tests.
2. Aircraft target run length distributions indicate that suppressing targets with run lengths greater than 37 would not degrade target detection while suppressing targets with run lengths less than 5 would cause fewer than 10% of the target returns from 150 to 200 miles to be lost. Run length distributions of clutter targets indicate that 55% to 70% of clutter returns would have been suppressed with these run length criteria.
3. For any fixed false target rate, the maximum primary radar detection sensitivity was achieved with a leading edge threshold ( $T_L$ ) of 7.
4. With a leading edge threshold ( $T_L$ ) of 7 and a percent noise setting ( $P_N$ ) of 7%, the primary radar probability of false alarm was  $10^{-6}$  with receiver noise only as an input.
5. The sensitivity at maximum range was equivalent for RVDP processed video and unprocessed video (PPI display) for both primary radar and beacon.
6. The ability of ATC specialists to track aircraft through weather clutter was essentially the same whether they used the displayed output of the RVDP or a normal radar PPI display.
7. The Automatic Clutter Eliminator (ACE) performance indicated that the probability of false alarm due to clutter was limited to approximately  $10^{-3}$ . The false alarm rate in clutter was not adjustable and no optimization of the balance between sensitivity and false alarm rate in clutter was possible. The Common Digitizer (AN/FYQ-40) will have selectable clutter false alarm rates.
8. Pulse detection performance in the beacon quantizer was such that all reply pulses whose parameters complied with established specifications were quantized. The rise time criterion was, however, responsible for rejecting some closely-spaced pulses.
9. The statistical detection of beacon targets performed as theoretically predicted. In all fruit densities tested it was possible to maintain a low probability of false alarm through proper selection of the leading edge threshold ( $T_L$ ).

10. The size of the beacon code pulse acceptance zones was a function of pulse width. A 0.3 microsecond code pulse was rejected when on the order of 0.2 microsecond away from its nominal position, while a 0.6 microsecond code pulse was not rejected until it was over 0.5 microsecond from its nominal position.
11. During flight tests in the fruit environment that exists in the Elwood area of coverage, 88% of the beacon code replies were properly detected and validated. In tests with simulated fruit densities of 100,000 per scan the percentage of beacon code replies which were properly detected and validated was 78% when the target reliability was 0.7 and the leading edge threshold was 6. The code validation threshold ( $T_V$ ), the number of hits required in the beacon sliding window before the code validation process was initiated, was slaved to the leading edge threshold ( $T_L$ ). Thus, it was not possible to simultaneously optimize the target detection and code detection processes. The Common Digitizer (AN/FYQ-40) will have a separate code validation threshold control.
12. The probability of declaring a false SPI pulse was 27% in a simulated fruit density of 100,000 per scan when the target reliability was 0.7 and the leading edge threshold was 6. This is caused by the wide SPI pulse acceptance zones and the fact that SPI pulse validation is not performed.
13. The use of defruited beacon video in the RVDP resulted in a lower probability of target detection and probability of correct code detection than the use of undefruited beacon video. This difference was greatest for targets with low target reliability. With the use of defruited video, a lower leading edge threshold would produce acceptable probabilities of target detection and correct-code detection, but the probability of azimuth splits would increase appreciably.
14. The standard deviations of the RVDP range and azimuth error distributions were approximately 0.1 nmi and  $0.25^\circ$ , respectively.
15. Aircraft separation required for a 50% probability of range resolution by the RVDP was approximately 0.3 mile for beacon and less than 0.2 mile for primary radar. Aircraft separation required for a 50% probability of azimuth resolution by the RVDP was approximately  $7^\circ$  for beacon and  $3^\circ$  for primary radar at a range of 45 nmi. While the azimuth resolution capability of the RVDP may seem poor, it must be pointed out that the limitation in azimuth resolution only applies when the two aircraft in close proximity are within the same range cell. During flight tests it was very difficult to obtain azimuth resolution data since the test aircraft were seldom in the same range cell.

16. The overall target split rate of the RVDP was 2.17%.

17. During tests in weather clutter conditions the data transfer rate approached, but never exceeded, the maximum capacity of the data transfer system and as long as maximum capacity is not exceeded, excessive message time-in-storage will not occur.

## CONCLUSIONS

1. Modifications to the RVDP units at Elwood and Suitland are required prior to integration into the NAFEC System Support Facility for the National Airspace System (NAS) for operational testing as a component of that facility.
2. The primary radar quantizer and the threshold switching technique employed in the RVDP operated satisfactorily.
3. The primary radar target detection process, including the Automatic Clutter Eliminator (ACE), performed in a satisfactory manner and as theoretically expected.
4. The beacon quantizer and statistical detector operated satisfactorily and as theoretically expected.
5. The size of the beacon code pulse acceptance zones is a function of pulse width and can become too wide to maintain an acceptable degree of accuracy in code pulse sampling and garble sensing in a high fruit environment.
6. The performance of code validation was satisfactory in the normal live fruit environment that exists in the Elwood area of coverage. The performance was not acceptable in extremely high simulated fruit densities. An excessive number of false SPI pulses were detected.
7. The use of defruited beacon video degraded the performance of the RVDP.
8. The accuracy and resolution of the RVDP are satisfactory.
9. The capacity (7200 bits per second) of the data transfer system is satisfactory.

## RECOMMENDATIONS

It is recommended that:

1. The RVDP units at Elwood, New Jersey, and Suitland, Maryland, modified as below, be integrated into the NAFEC System Support Facility for the National Airspace System (NAS) for operational testing as a component of that facility.

a. Modifications to the RVDP at Elwood, New Jersey, and the RVDP at Suitland, Maryland:

(1) The function generator be modified to allow selection of probability of false alarm in clutter of  $10^{-3}$ ,  $10^{-4}$ ,  $10^{-5}$ , and  $10^{-6}$ .

(2) The size of beacon code pulse detection zones be fixed (not pulse width sensitive) and limited to a zone which would allow the code pulse to be detected 0.2 microsecond ahead of and behind nominal position.

(3) A separate control for selection of code validation threshold be incorporated to permit the optimum selection for the environment within which the system is to operate.

(4) Validation of the reception of SPI pulse be performed in the same way as the other code pulses.

b. Modifications to the RVDP at Suitland, Maryland:

(1) An adjustable range discrimination capability be provided for the primary radar quantizers.

(2) Run length discrimination logic be added to the primary radar detector.

(3) The beacon sliding window be changed from two 3-bit, mode-sensitive sliding windows (for modes A/3 and C) to one 11-bit sliding window sensitive to mode A/3 only.

2. The following procedures for setting the detection threshold be followed:

- a. The primary radar leading-edge detection threshold ( $T_L$ ) be set at 7.
  - b. The percent noise ( $P_N$ ) be set at 7%. This setting may be adjusted to achieve the desired false alarm rate with the transmitter turned off.
  - c. The run length discriminator minimum be set at 5 and the maximum set at 37.
  - d. The optimum beacon leading edge criteria ( $T_L$ ) be established at Elwood by adjusting the  $T_L$  until the desired false target rate due to non-synchronous and near synchronous fruit is achieved. Periodic checks are required as the fruit environment changes. This procedure should also be followed at any site where a digitizer is to be used.
  - e. The rise time criterion in the beacon quantizer be removed to prevent complete rejection of partially-overlapped pulses whose composite rise time is greater than the criterion.
3. Defruited beacon video not be used in the RVDP.
  4. Future azimuth resolution specification for digitizers be based on the measured run length distribution rather than the arbitrary 3 dB points on the antenna gain pattern.

## REFERENCES

1. Final Report, FAA Contract ARDS-549, "Techniques and Cost of Radar Remoting," July 1962.
2. Final Report, FAA Contract ARDS-628, "Comparative Cost Analysis of Microwave and Wireline Radar Remoting Techniques," March 1963.
3. Federal Aviation Agency, "Principles for Digitizing and Narrow Band Remoting of Radar and Radar Beacon Information," Selection Memorandum No. 26, September 1964.
4. Chapman, Clifford, "Dynamic Tests of the Radar Video Data Processor (RVDP)," National Aviation Facilities Experimental Center, Federal Aviation Agency, Atlantic City, N. J., Memorandum Report, May 26, 1966.
5. Swerling, Peter, "The Double Threshold Method of Detection," Rand Corp., RM-1008, December 17, 1952, ATI No. 210454.
6. Rice, S. O., "Mathematical Analysis of Random Noise," Bell System Technical Journal, Vols. 23 and 24. (Also available in "Selected Papers on Noise and Stochastic Processes," edited by Nelson Wax, Dover Publications Inc., N. Y., 1954).
7. Federal Aviation Agency, "U. S. National Standard for Common System Component Characteristics for the IFF Mark X (SIF)/Air Traffic Control Radar Beacon Systems SIF/ATCRBS" - Amended December 27, 1963.
8. Turner, Vaughn E., and Jefferson, Francis W., "Investigation of Off-the-Shelf Modem Equipment, NAS Point-to-Point Data Transfer," Systems Research & Development Service, Federal Aviation Agency, Report No. RD-65-90, July 1965.

## ACKNOWLEDGMENT

Acknowledgment is made to the following key personnel for their contributions to the project effort in the test and evaluation of the RVDP.

1. Mr. Karl Burkard, project engineer, for directing most of the tests of the primary radar detection functions of the RVDP and for his contribution in the preparation of this report.
2. Mr. Clifford Chapman, project engineer, for directing flight test portion of this project and for his contribution in the preparation of this report.
3. Mr. Joseph Voisich, principal engineer, for guidance in project management and assistance in coordinating the many facets of the test effort.
4. Mr. Lawrence Casarow, former project manager, for directing the project effort from its early planning phase through the beginning of the data collection phase.
5. Messrs. Oliver P. Carlson, Stanley E. Ware, Michael S. Hulse, and Van T. Mason, project technicians, for their persistence and conscientious effort in data collection.
6. Messrs. Daniel W. Riley and Norman Watts, project computer programmers; Mr. Theodore W. Rundall, ATC Specialist; Mr. Raymond E. Murray, Radar Facility Manager; and the flight-test support personnel from the Technical Facilities Division for their cooperation and assistance during the test program.

## APPENDIX I

### RADAR VIDEO DATA PROCESSOR (RVDP) - SYSTEM DESIGN

#### Purpose of RVDP

The Radar Video Data Processor (RVDP) accepts search radar (primary radar) and radar beacon (secondary radar) video information; detects the presence of radar and/or beacon targets; determines target position in azimuth and range; validates beacon mode A/3, C, and 2 replies; correlates radar and beacon information for the same target; and furnishes one target message per target per scan. It performs these functions in the presence of noise, clutter, and most friendly or intentional interference. The target message always contains range and azimuth data, and in some cases it may also contain target reply-code information. Non-target report messages indicating system status and operating mode are also supplied. Both target and non-target messages are suitable for narrow-band transmission to remote centers for further processing. Various fixed, automatic, and manual mapping functions augment statistical processing of radar video.

#### Inputs to RVDP

The RVDP is completely compatible with the full complement of FAA primary and secondary radars. It accepts antenna synchro signals, master trigger (pre-trigger), and normal and MTI video from Air Route Surveillance Radars (ARSR-1A, ARSR-2) or Airport Surveillance Radars (ASR-2, modified; ASR-3, modified; and ASR-4, ASR-5, ASR-6).

The RVDP also accepts mode triggers and beacon video from the Air Traffic Control Beacon Interrogator (ATCBI-2; ATCBI-3, modified) and Beacon Video Test Set. Fixed-map inhibit signals are obtained from standard FAA Video Mapping Units.

#### Outputs from RVDP

The RVDP Data Transmission Group (DTG) provides messages to the Central Computer Complex (CCC) and Digital Filter Group (DFG) in the local RVDP configuration, or to the specified modems for narrow-band transmission to the Data Receiving Group (DRG) in the remote RVDP configuration. Serial data transfers from the DTG to the transmitting modem and from the receiving modem to the DRG are controlled by modem-generated clock pulses.

The parallel, 6-bit-plus-parity data transfer to the CCC from either the local DTG or the DRG is controlled by RVDP-ready/CCC-received logic. Data transfer to the DFG is bit-serial controlled by an RVDP clock.

### Description of Equipment

The RVDP (Figure 1-1) processes the radar inputs to produce target report messages. The RVDP operating modes are manually selected on the equipment control panels.

By treating the RVDP in terms of the functional capabilities of each of the equipment groups (Figure 1-2), an orderly progression of the processing functions can be traced, and the relationships between the various equipment groups can be established.

Monitor and Azimuth Generator (MAG): The Azimuth Data Converter (ADC) receives dual-speed antenna synchro signals from the ASR or ARSR radar, quantizes them into 4096 azimuth change pulses per scan, provides a "north" reference pulse once per scan, and drives a synchro resolver to produce sine and cosine components from the PPI sweep generators. The Monitor is a RAPPI/PPI CRT display which permits observation of target processing in the PPI mode and of completed targets as they are transmitted in the RAPPI mode. For the RAPPI mode, digital-to-analog coordinate converters provide beam deflection.

Basic Group (BG): The Basic Group provides those functions fundamental to target detection; namely, timing, quantizing, and processor monitoring. The BG comprises the four sub-groups discussed below.

1. Azimuth, Range, and Timing Group (ARTG) - The range clock in the ARTG provides basic timing for all RVDP logic, properly synchronized with radar zero range. After proper presetting, the search azimuth and beacon azimuth counters provide a count of the azimuth change pulses. Search azimuth counters feed the PMG to establish test-target azimuth and initiate the sector mapping criteria, and feed the CPG for search radar azimuth calculation. Beacon azimuth counters feed the PMG to establish beacon test-target azimuth, and the CPG for beacon-only target azimuth calculation. The ARTG is designed to utilize azimuth-change and scan-reference pulses generated by the MAG or supplied from an external source such as a pedestal-mounted SG-135 pulse generator.

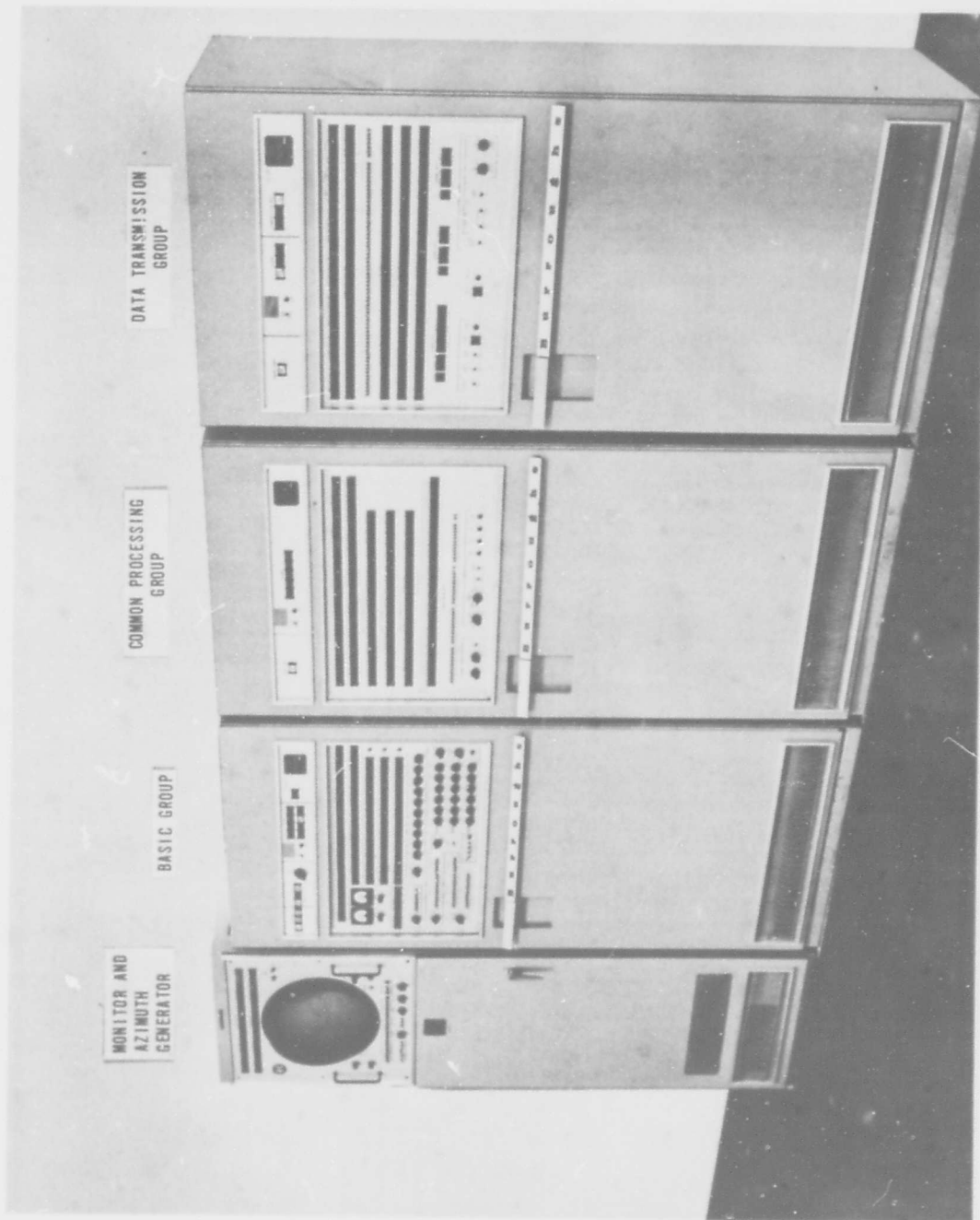


FIG. 1-1 RADAR VIDEO DATA PROCESSOR

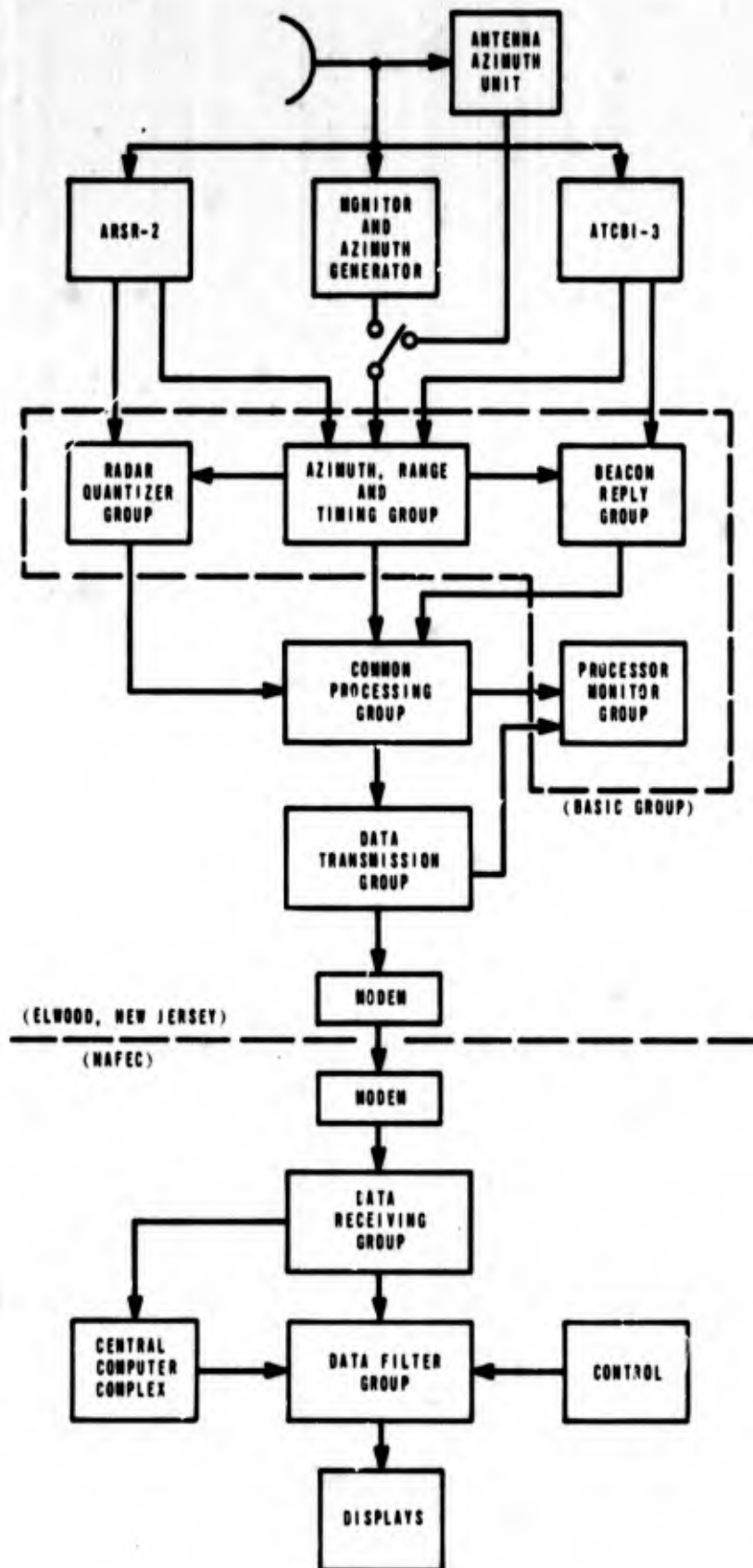


FIG. 1-2 BLOCK DIAGRAM OF THE RADAR VIDEO DATA PROCESSING SYSTEM

2. Radar Quantizer Group (RQG) - The Radar Quantizer Group quantizes normal and MTI radar video. The clip level is normally maintained constant with respect to the long-term average video noise level but is modified by ambient clutter density. Clutter is reduced through a unique set of functions called Automatic Clutter Elimination (ACE), which regulates the target detection process. These regulatory functions include target detection threshold controls based on manual mapping criteria, automatic mapping in areas of extremely heavy clutter, and inhibition of the detection processes based on range-limit and fixed-map signals.

3. Beacon Reply Group (BRG) - The Beacon Reply Group detects and processes valid beacon reply code trains. Serial pulse trains are quantized and applied to decoding delay lines. Proper coincidence of a pair of bracket pulses establishes bracket detection and initiates data code sampling, beacon range assignment, and tests to determine the garble status of the detected reply. Mode A/3 bracket coincidence pulses are sent to the CPG for detection of beacon targets. Double pulses are generated for display on the PPI monitor. Reply codes (modes A/3, C, and 2) are transferred to the CPG for storage and code validation. As in the RQG, fixed-map inputs and beacon range-limit gates can be used to inhibit reply code processing.

4. Processor Monitor Group (PMG) - The Processor Monitor Group enables local or remote control of RVDP processing functions and generates indications of system status. The processing function control includes:

Manual mapping controls for three independently selected range and azimuth sectors

Search and beacon range limit controls (On/Off)

Fixed and auto-map outline, and system status message generation

On-Off control of fixed, auto, and manual map functions

Transmission of fixed map outline messages

Selection of local/remote controls

Beacon and search test-target generation

**Common Processing Group (CPG):** The Common Processing Group statistically detects targets, accepting the following as inputs: quantized video from the Radar Quantizer Group (RQG), bracket coincidence from the Beacon Reply Group (BRG), test video from the Processor Monitor Group (PMG), and clock pulses and azimuth and range counts from the Azimuth, Range, and Timing Group (ARTG). Each target so detected is processed to generate a target report message combining search and beacon data. The target message is transferred to the Data Transmission Group (DTG) for storage and transmission. Detection and message preparation functions are summarized below.

1. **Search Target Detection** - Search target processing involves statistical detection in a 13-bit sliding window detector, center azimuth computation, and target range-accuracy determination. The target detection criterion (minimum number of hits at a given range over thirteen trigger periods required for detection) in the sliding window detector is normally determined by a manual switch setting. In clutter conditions the target detection criterion is determined automatically by the Automatic Clutter Eliminator (ACE).

2. **Beacon Target Detection** - Beacon target processing is similar to that for search targets. Beacon target detection is based on statistical detection of mode A/3 bracket coincidences detected at a given range on successive mode A/3 interrogations. Detection is accomplished in an eleven-bit sliding window. Code validation of replies to mode A/3, C, and 2 interrogations and center azimuth computation are also performed in the CPG.

3. **Target Message Preparation** - Upon completion of the detection processes, search and beacon reply data are correlated in range and combined into a single target report message for transfer to the DTG. The reports are stored in the DTG until called for transmission, either to the CCC and DFG directly or via a data link and the DRG.

**Data Transmission Group (DTG):** The Data Transmission Group provides the buffer storage between the CPG and the CCC and DFG. This storage is required because the instantaneous message generation rates of the RVDP exceed the average message acceptance rate of the intermediate telephone channel transfer system. The DTG stores completed target reports, map outline messages, and system status messages. When a message-transfer request is received, the oldest message in storage is retrieved and placed in an output shift register.

prior to transfer to the requesting equipment. During transmission and under control of the requesting equipment (modem, or CCC), parity is added to each information field. The DTG also furnishes formatted target position reports and map outline messages to the RAPPI monitor for display.

Data Receiving Group (DRG): Remotely located RVDP's communicate with the NAS complex (CCC and DFG) by a DTG/Modems/DRG data link. The DRG at the receiving terminus (Figure 1-3) accepts recovered clock and data pulses from the data modems and provides an output interface to the CCC and DFG. The DRG recognizes valid messages received on any of its nine channels, determines the type of message so as to route it to the proper equipment (CCC, DFG, or local RAPPI Monitor associated with the DRG), checks the parity of each field in the message, and transfers the message to the proper output device in the required transfer mode. As an auxiliary function, the DRG provides a reverse communication link whereby a remote RVDP may be controlled via the DRG from the NAS complex.

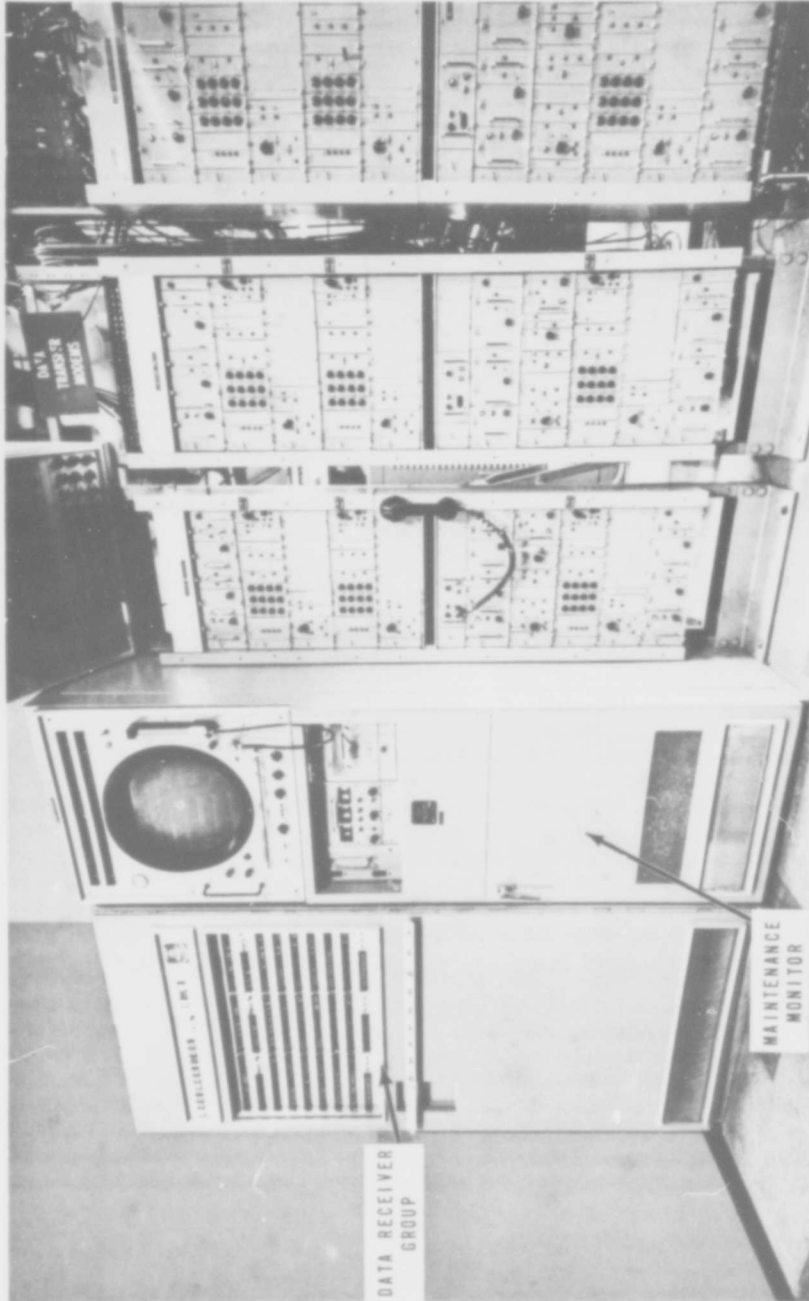


FIG. 1-3 DATA RECEIVING FACILITY

## APPENDIX II

### MODIFICATIONS TO THE RVDP

The modifications performed by the contractor to make the RVDP more closely resemble the CD are described completely in Section X of Instruction Manual - Radar Video Data Processors. These modifications were:

1. Operational Evaluation Modification (This allowed the print out of selected target messages at the DRG RAPPI.)
2. Run Length Discrimination Modifications
3. 11-Bit Beacon Sliding Window Modifications
4. Beacon Trigger Interrogation Decoding and Trigger Generation Modifications
5. Mode 2 Processing Modifications

In addition to these modifications a total of 32 modifications were incorporated in the RVDP at Elwood, N. J., during the test program. Twenty-eight of these modifications were accomplished to facilitate data collection and reduction. The majority of these were removed at the conclusion of the test program. The remaining four modifications were incorporated to improve the performance of the RVDP and will remain in it. A brief description of these modifications follows:

1. Range Discrimination Modification (#7)

This modification was found necessary to reduce target range splitting (the declaration of two or more targets in consecutive memory range cells because of excessive widths of received radar video pulses).

Range discrimination is implemented by the insertion of a seven-bit range clocked shift register between the video slicer output and the video hit flip flop. The outputs of the register are combined in an 'OR' configuration to inhibit the input to the video hit flip flop during eight clock periods (3.09 microseconds) subsequent to a radar pulse return that satisfies the quantizing minimum-width criterion. Since the return must have a width of at least one clock period (.386 microsecond) to satisfy the quantizing minimum-width criterion, the inhibit signal lasts

for eight clock periods, and two more clocks are required to initiate another hit, the minimum time required between the declaration of range for one target and declaration of range for the next target is eleven clock periods (11/32 nmi or 4.25 microseconds). The radar-return pulse-width criteria for a single processed target are then established at .386 to .772 microsecond (minimum) and 4.25 to 4.636 microseconds (maximum). The one clock period ambiguity in each of these figures arises due to the return-pulse leading edge phasing with respect to the clock pulses.

## 2. Beacon Fine Delay Alignment Modification (#13)

In order to process beacon code and altitude information, two separate memories are used in the Common Processing Group. Memory I (detection memory) contains the target-status bits and range/azimuth information, while Memory II (code processing memory) contains identification code and altitude information. These two portions of a beacon message must be inserted at identical addresses (ranges) of their respective memories; otherwise, a "Determined False Target" signal is generated to clear the information.

Line-up of the two memories is normally effected by presetting the beacon range counter until the beacon information is inserted at the same address in both memories.

This line-up technique was limited to increments of one master-clock period, however, and smaller inherent propagation delays of the system would allow information at a range near a Memory I address interface to be inserted in a cell adjacent to that of Memory II, and the information was discarded.

In the modified circuitry a finely-incremented (50 nanosecond) delay line is used to delay beacon bracket detector pulses prior to storage in Memory I so that the difference in propagation time for the signal applied to both memories can be made an exact multiple of one master clock period. Precise alignment is then possible by presetting the beacon range counter.

## 3. Modification to Prevent Validation of Beacon Messages Prior to Leading Edge Detection (#15)

The unmodified beacon validation process was completely independent of the beacon target-detection process and merely required that two successive ungarbled code trains be received. As a result, unrelated,

near-synchronous codes could be validated. This information was held in memory until a beacon target was detected at the same address, at which time the validated unrelated code could be erroneously transferred out as the information associated with that particular target.

This modification was designed to prevent final validation of beacon targets until beacon target-detection logic had detected a target at the same address at which the code train information appeared.

The modification is implemented by clearing Memory II of old information at the time of beacon leading edge declaration and allowing the Beacon Reply Group (BRG) buffer register access to Memory II only on subsequent triggers until the target is completed or until the code is validated. Since the aircraft is nearer the center of the interrogator beam during this period, a much higher probability of correct validated code association is achieved.

#### 4. Lead Edge Range Accuracy Modification (#28)

Target range accuracy reporting in the RVDP is accomplished by inserting the information from a two-bit range accuracy register into Memory I. This register indicates the relative range of a detected target within one memory range cell in one-quarter cell increments:

00 - 1st quarter cell (1/16 nmi)

10 - 2nd quarter cell (1/8 nmi)

01 - 3rd quarter cell (3/16 nmi)

11 - 4th quarter cell (1/4 nmi)

Prior to this modification the range accuracy register was continually updated upon the receipt of range accuracy "hits" provided by four range accuracy flip flops, which were gated with memory clock pulses to indicate the proper quarter of the cell during which the hit occurred.

Since range accuracy logic is completely independent of target-detection logic, and statistical detection requires the target to be out of the antenna beamwidth long enough to reduce the number of "ones" in the sliding window sufficiently to meet the trailing edge criterion there was a high probability that from the time a target leaves the beam, until trailing edge is declared, quantitized radar receiver noise and/or unrelated beacon brackets will "update" the range-accuracy register to an erroneous setting.

In the modified range accuracy logic, either beacon leading edge or primary radar leading edge signals are gated in an "and" configuration with Memory I range accuracy addressing logic as a condition to insert accuracy information into Memory I. Updating of Memory I accuracy information is then inhibited for the remainder of the target run length and is not enabled until the next beacon or search leading edge detection. This configuration insures the sampling of range accuracy information during the time the target is well into the radar antenna beamwidth, thereby greatly reducing the probability of associating erroneous range-accuracy data with the processed target.

## APPENDIX III

### RVDP MAINTAINABILITY AND AVAILABILITY

#### Maintainability of the Elwood RVDP

The RVDP that was installed at Elwood, New Jersey, was not used for availability data collection because, in the course of testing, it was continually being modified for different test configurations. However, at the conclusion of the test and evaluation program, the maintenance log was reviewed and the following summary of maintenance problems with the RVDP was extracted. The maintenance time expended during the project, exclusive of the implementation of modifications, may be grouped into three categories: (1) minor failures, (2) wiring and/or logic discrepancies, and (3) catastrophic failures.

Minor Failures: It is felt that the occurrence of minor component failures was relatively infrequent considering the complexity of the processor and the rigorous experimentation to which it was exposed. The majority of these failures were the result of inadvertent short circuits between pins of printed circuit connectors during trouble shooting by maintenance personnel.

Other minor failures were caused by site power failure and erroneous connections of temporary jumper wires used during the installation or removal of a modification.

Wiring and/or Logic Discrepancies: Discrepancies of this category were the most difficult to detect and diagnose. Symptoms caused by a missing or extraneous connection were so subtle as to avoid detection for extended periods of time. The following three problems were brought to light during the intensive flight data collection and reduction program:

1. Beacon targets were not being processed during the length of two memory range cells. The condition recurred every eight miles in range. Search targets processed normally. This beacon processing problem persisted for approximately two months prior to the discovery of its cause, a missing wire in the Common Processing Group on December 22, 1965. Apparently, this wire had inadvertently been removed along with some temporary wiring which had been used for data-collection purposes.

2. Wrong range-accuracy bits were being assigned radar and beacon targets. The cause was found to be a transposition of the least significant and most significant range accuracy signals entered

in the Common Processing Group output register. While trouble shooting this problem, the need for a design change became apparent. The time of target range accuracy determination was changed from target trailing edge to target leading edge, thereby enhancing system range accuracy. This design change is described more completely in Appendix II, "Modifications to the RVDP."

3. Beacon targets would not transfer to the CPG output register until one more beacon hit than was prescribed by the beacon leading edge criterion switch was received. Trouble shooting this problem was facilitated by the NAFEC Beacon Test Target Generator. The cause of this problem was found to be a wiring error in the Beacon Code Validation modification.

Catastrophic Failures: Catastrophic failures are defined herein as those which rendered the entire site inoperable due to a multiplicity of component failures. Three such failures were recorded during the period of this report:

1. High voltage arcing in the area of the bleeder resistors used for focus and brightness control of the RAPPI/PPI Monitor caused multiple semiconductor failures in the associated video and sweep circuits. Although protective circuits were installed, trouble recurred on four different occasions. Length of time to repair has been decreased significantly by the substitution of repairable sweep amplifier circuits for the original non-repairable (potted) type. No permanent cure has been found for the basic problem, however.

2. Wholesale destruction of transistors contained on the "Memory Core Read Driver" and "Memory Core Write Driver" logic cards occurred when power was applied to the Common Processing Group while the "Core Memory Switch" logic cards were removed. While troubleshooting an undervoltage fault indication in the cabinet power supplies, groups of logic cards were removed in an effort to reduce the power supply load. Instructions to maintenance personnel relating the hazards of operating read or write drivers without the associated "Memory Switch" has prevented recurrence of this trouble.

3. A short circuit between the +15 volt and +30 volt power buses in the Data Transmission Group caused the Power Supply Fault Control to shut down the entire cabinet. Since each cabinet power supply is connected to several hundred card locations, trouble shooting was lengthy and tedious. The cause of this trouble was subsequently determined to be a +30 volt power bus ribbon shorting to the adjacent pin (+15V) of a logic-card socket.

### Availability Data for Suitland RVDP

A procedure to obtain availability data consisted of recording each outage and the duration of each outage that occurred on the RVDP that was installed at Suitland, Md. The data are limited to the extent that the study was related to component availability since this equipment was not in operational use and did not have the modifications that were installed in the RVDP at Elwood, N. J.

Copies of the FAA "Maintenance Log of Electronic Facilities" (Form FAA-406c) were forwarded periodically to the project manager at NAFEC and, in addition, a memo was prepared by personnel at Suitland, Md., in reference to each RVDP outage. This memo outlined the reason and duration of each outage. From this information, the number and duration of all outages were tabulated (Table I).

Data recording began from the start of 24-hour operation on June 7, 1965, at 0800 through June 7, 1966, at 0800. This represents one year of operation (8760 hours). During this period, outage time that was not chargeable to the RVDP was 81.4 hours, resulting in a total scheduled operating time of 8678.6 hours. Using this scheduled operating time and the data shown in Table I, a summary of availability data for the Suitland RVDP was obtained (Table II). As indicated in Table II, availability data were calculated for two conditions: (1) when all RVDP equipments were considered and (2) when all, except the RAPPI/PPI monitor unit, were considered. The reason for including availability data for condition 2 was because the RAPPI/PPI monitor is used primarily for maintenance and does not affect the target detection function of the RVDP.

TABLE I

Outage No.	Date	Time	Unit	RVDP Outage Time (hrs)
1	6/25/65	1315	Core Memory Switch	3.40
2	7/19/65	1315	RAPPI/PPI	10.33
3	8/2/65	1230	Monitor Alarm	3.75
4	8/3/65	0845	Monitor Alarm	5.75
5	8/18/65	0915	DTG/CPG	2.25
6	9/21/65	0930	DTG	0.08
7	10/4/65	1357	RAPPI/PPI	5.67
8	10/8/65	1508	RAPPI/PPI	2.72
9	10/12/65	1300	RAPPI/PPI	2.18
10	10/27/65	1005	CPG	1.42
11	11/1/65	0830	RAPPI/PPI	3.08
12	11/14/65	0330	Memory 1A	2.50
13	11/23/65	1415	Servo Alarm	0.08
14	12/3/65	1005	MODEM	1.42
15	12/7/65	0935	MODEM	0.17
16	12/8/65	1025	DTG	4.60
17	12/28/65	0905	MODEM	0.70
18	1/4/66	1000	Basic Group	0.70
19	1/11/66	1435	Basic Group	5.00
20	1/20/66	0830	RAPPI/PPI	11.00
21	1/26/66	0830	RAPPI/PPI	4.20
22	2/2/66	1050	CPG	4.20
23	2/4/66	1400	Basic Group	2.70
24	2/21/66	0850	RAPPI/PPI	2.50
25	4/1/66	1430	CPG	1.50
26	4/4/66	1100	CPG	1.50
27	4/25/66	0835	BRG/RQG	6.50
28	5/3/66	0820	ADC Unit	4.70
29	5/20/66	1320	BG	1.46

TABLE II

SUMMARY OF AVAILABILITY DATA FOR RVDP AT SUITLAND, MD.

Condition 1: (RVDP, including RAPPI/PPI unit)

1. Total number of failures = 29
2. Total outage time from failures = 96.06 hours
3. Total operating time = 8582.54 hours
4. Mean time between failures = 295.95 hours
5. Mean time to repair = 3.31 hours
6. Availability =  $\frac{295.95}{295.95 + 3.31} \times 100 = 98.9\%$

Condition 2: (RVDP, excluding RAPPI/PPI unit)

1. Total number of failures = 21
2. Total outage time from failures = 54.38 hours
3. Total operating time = 8624.22 hours
4. Mean time between failures = 410.68 hours
5. Mean time to repair = 2.59 hours
6. Availability =  $\frac{410.68}{410.68 + 2.59} \times 100 = 99.4\%$

**BLANK PAGE**

## APPENDIX IV

### TEST ENVIRONMENT

#### Inputs to the RVDP

##### ARSR-2 Primary Radar

###### General Information

Location	
Latitude	39° 35' 19.0"
Longitude	74° 41' 56.0"
Ground elevation above mean sea level	119 feet

###### Transmitter

Frequency band	L-band
Frequency range	1280 to 1350 megacycles
Power output	
Peak power	5.0 megawatts
Average power	10.0 kilowatts
Pulse width	2.0 microseconds
Pulse repetition frequency	
Average	360 pulses per second
Staggered	315, 360, and 420 pulses per second
Duty cycle	.00068

###### Receiver

Sensitivity in decibels below 1 milliwatt	106 to 110 (MTI video) 107 to 111 (normal video) 111 to 115 (integrated normal video)
Noise figure	10 decibels
IF bandwidth	30.0 megacycles
Video bandwidth	3.0 megacycles
Automatic frequency control	Yes
Automatic gain	Yes
Sensitivity time constant	Yes
Fast time constant	Yes
First MTI blind speed	560 knots

### Data Outputs

Video	Moving target indication (MTI) Normal
Synchro	Integrated normal 1 speed and 36 speed

### Coverage and Accuracy

Maximum range	200 nautical miles (radar)
Maximum target altitude	80,000 feet
Azimuthal coverage	360 degrees
Accuracy and resolution	
Range accuracy	3.0 percent of range
Range resolution	1 percent of range in use
Azimuthal resolution	2.0 degrees

### Antenna

Scan rate	6 r/min (cw)
Gain	34.3 decibels
Polarization	Linear and circular
Reflector type	Cosecant-squared
Beamwidth at half-power points	
Horizontal plane	1.2 degrees $\pm$ 0.1 degree
Vertical plane	3.75 degrees $\pm$ 0.1 degree

### Data Transfer System

Microwave transmission link  
to Building 149

## ATCBI-3 - Beacon Interrogator

### Transmitter

Power output (adjustable)	+ 18 dbw to +35 dbw
Normal operating frequency	1030 $\pm$ 0.2 megacycles
Interrogation RF pulse pair spacing	
Mode 1:	3.0 $\pm$ 0.1 microseconds
Mode 2:	5.0 $\pm$ 0.1 microseconds
Mode A/3:	8.0 $\pm$ 0.1 microseconds
Mode B:	17.0 $\pm$ 0.1 microseconds
Mode C:	21.0 $\pm$ 0.1 microseconds
Mode D:	25.0 $\pm$ 0.1 microseconds

Selectable mode interlace configurations (any mode can represent X, Y or Z)	Continuous interrogation on X Continuous interrogation on Y Continuous interrogation on Z X Y X Y etc. X Y Z X Y Z etc. X X Y X X Y etc. X X Y X X Z X X Y X X Z etc.
Interrogation rate	360 per second
RF pulse width	0.8 $\pm$ 0.1 microsecond
RF pulse rise time	0.05 to 0.1 microsecond
RF pulse decay time	0.2 microsecond maximum
Maximum duty cycle	0.3%
Transmitter modulation delay	0.8 microsecond maximum
Second interrogation pulse (P3) Delay with respect to beacon synchronization pulse	33.0 to 110 microseconds continuously variable
RF side lobe suppression	Pulse characteristics equal to those of interrogation pulses
Pulse (switch selectable feature) SLS trigger timing	Succeeds first interrogation pulse by 1.6 to 2.4 microseconds

#### Receiver

Receiver type	Superhetrodyne
Normal operating frequency	1090 megacycles center frequency
IF amplifier mid-frequency	59.5 $\pm$ 0.5 megacycles
Overall bandwidth at -3 dB points	8 megacycles minimum
Overall bandwidth at -40 dB points	18 megacycles maximum
Image response	90 dB below center frequency response
Overall receiver noise figure	10 dB (maximum)
Tangential sensitivity	-87 dBm minimum (at equipment antenna terminal)
IF gain control methods	Manual and Sensitivity Time Control circuit (present STC curve is a -40 dB curve)
Receiver delay	0.5 microsecond maximum

Antenna

Type	L-band broadside co-linear array
Scan rate	6 r/min.
Azimuthal coverage	360 degrees
Gain	21.5 dB
Horizontal beamwidth at half-power points	2.35 degrees

Data Transfer System

Microwave transmission link  
to Building 149

## Special Instrumentation

In the RVDP test program several unique test instruments were used (some developed especially for the project). A brief description of each of these is included in this section.

Digital Target Generator Test Set: The Digital Target Generator Test Set (DTGTS) will accept range and azimuth reference pulses from radar or radar-beacon equipments or other external equipments and generate up to three independently variable, digitally-controlled groups of triggers which simulate radar returns from three radar targets. The output triggers simulating each target are selectively gated by using an interlace feature incorporated in the DTGTS or randomly gated by using an external noise source. Provisions are also made for sequentially increasing the range of the output triggers for one of the targets in discrete steps, thus simulating radar beacon replies that are near-synchronous. The DTGTS also has the capability of generating non-synchronous triggers from an external noise source. The simulated targets are identified as the "X" target, the "Y" target or the "Z" target. A functional block diagram is shown in Figure 4-1 and a photograph is shown in Figure 4-2.

An azimuth reference pulse, which occurs once each scan of the antenna, is required to establish azimuth timing with the DTGTS. The range reference pulse, which occurs once each range period, is required to establish range timing and to provide azimuth increments within the DTGTS.

Master Clock - The master clock provides the timing increments for the range counters. The DTGTS can operate with an external clock or it can generate its own range increments provided by a 1/512 nmi increment crystal-controlled oscillator.

Target Azimuth Switches - The azimuth start position of each target is controlled by its associated target azimuth switches. The increments of azimuth used are the interrogation periods of the radar or beacon system of interest. The numerical setting of the thumbwheel switches represents the number of interrogation periods that occur after the azimuth reference pulse before the first "hit" of the target appears.

Target Range Switches - The range position of each target is controlled by its associated target range switches. The numerical setting of the thumbwheel switches read directly in nautical miles with 1/16 nautical mile as the smallest increment of variation.

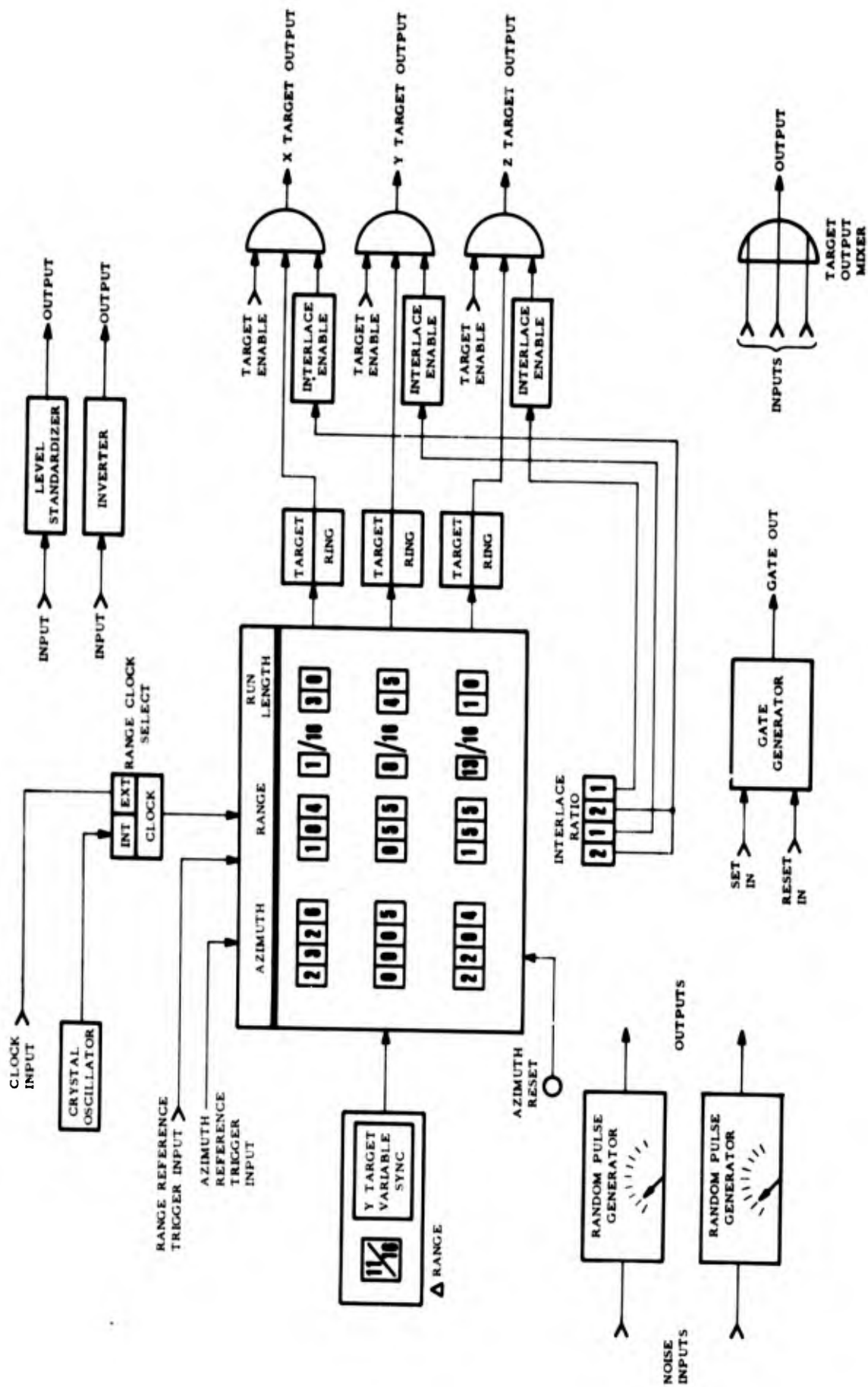


FIG. 4-1 DIGITAL TARGET GENERATOR TEST SET  
FUNCTIONAL BLOCK DIAGRAM

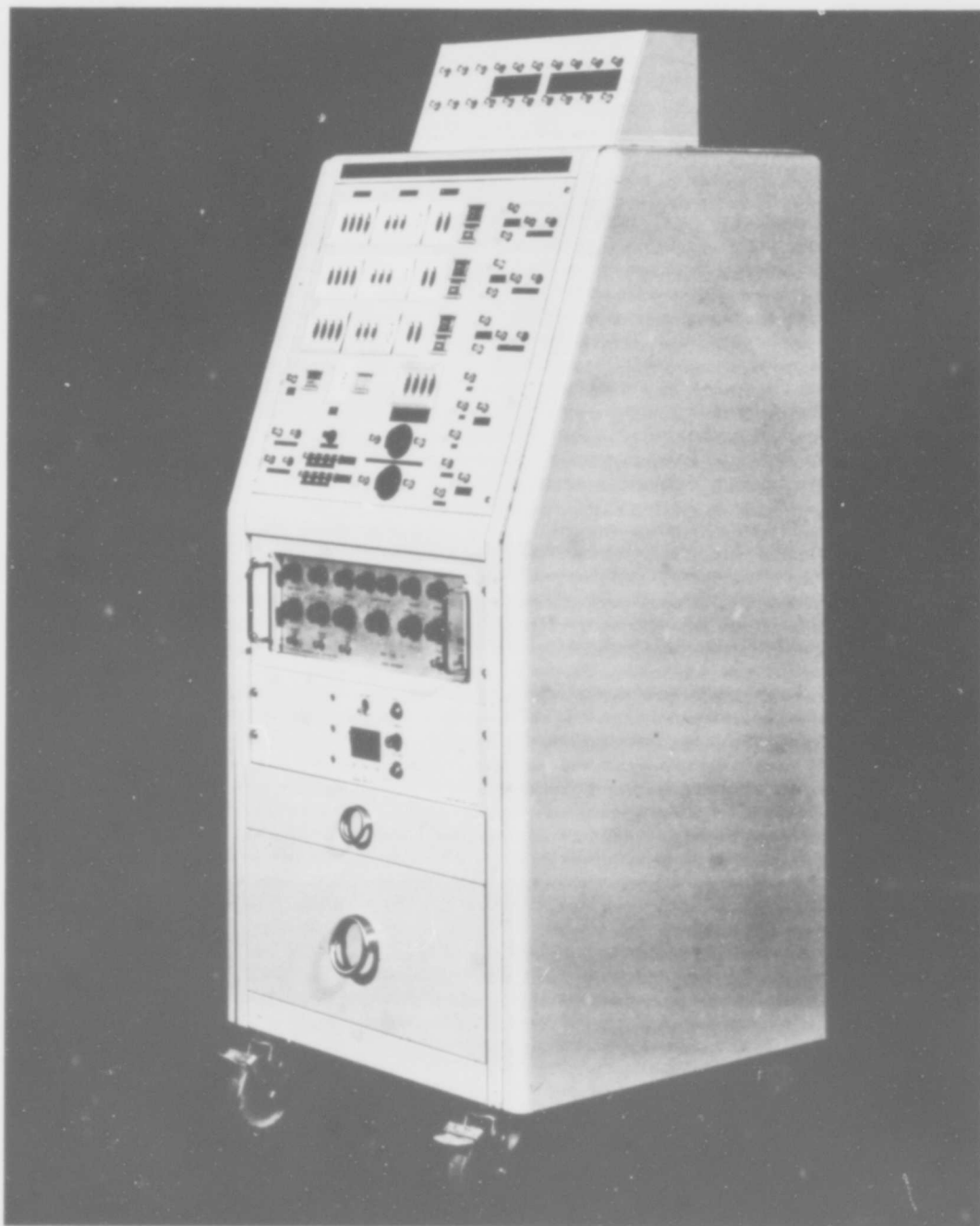


FIG. 4-2 DIGITAL TARGET GENERATOR TEST SET

Target Run Length Switches - The run length or number of hits for each target is controlled by its associated target run length switches. The numerical setting of the thumbwheel switches represents the number of consecutive interrogation periods during which a target output pulse will be produced. These hits will occur at the selected range and the first hit will occur at the selected azimuth.

A two-position function switch is associated with the controls for each target. The TARGET position of the switch allows the normal target output to occur with the selected run length. The RING position produces a target output pulse every interrogation period at the selected range for the entire 360° of antenna rotation.

Target Output - The target output signal is a series of pulses which simulate a radar target or can be used to trigger a beacon code generator which would simulate a beacon target. One pulse appears each interrogation period at the range selected on the target range switches. The first pulse appears at the azimuth selected on the target azimuth switches and pulses continue to appear consecutively until the selected run length has been reached.

The Target Enable inputs associated with each target output provides for the random gating of the target output to simulate the random "holes" that occur in actual beacon replies, gating the target output to follow an externally generated beacon mode interlace pattern, or any other desired gating function.

Interlace Ratio Switches - A separate set of thumbwheel switches controls the interlace ratio with which each target can be generated. The sequence of the switches is XYXZ, with X, Y, and Z each representing one of the trigger or target generator outputs. Any ratio in any combination up to 9999 can be produced with this configuration. For example, when a ratio of 2:1:2:1 is selected, two X-triggers, then one Y-trigger, then two more X-triggers, then one Z-trigger are produced and the pattern is repeated for as many times as required to complete the selected run length.

Random Pulse Generator - As a separate function, the DTGTS can also produce a variable number of triggers which occur at random and are not in synchronism with the system timing. This is accomplished by connecting a noise generator to the noise input which is connected to a Schmitt trigger circuit. The noise-level control varies the noise level into the Schmitt trigger circuit input to produce the desired average number of random triggers at the random trigger output. The random output triggers can be applied to a beacon code generator to

produce code trains, thus creating a controlled environment of non-synchronous replies or fruit. They can also be gated with the trigger output to produce a target reliability less than one.

Gate Generator - The gate generator is a flip flop whose set and reset input and whose set output is brought out to front panel jacks.

Variable Synchronism - The Y target has the additional capability of producing triggers whose ranges increase from one interrogation period to the next by a selected increment. The starting range and azimuth and the run length are still controlled by the thumbwheel switches. The range increment can be varied with a thumbwheel switch (Y RANGE ADVANCE) in 1/16 nautical mile steps from 1/16 nautical mile to 15/16 nautical mile. This condition produces the effect of a target in near synchronism with the interrogation rate and the degree of synchronism can thus be predetermined.

Video Mixer - This circuit is a three-input diode mixer or "OR" gate for negative triggers (0V to -6V). This allows mixing all three trigger outputs to produce a single output to trigger a beacon code or signal generator.

Auxiliary Jack Panel - The Auxiliary Jack Panel contains inverters, with which a signal can be changed to opposite logic levels, and level standardizers, which are used to convert any other logic levels to the logic levels used in the DTGTS (0V and -6V).

Variable Pulse Generator - A variable pulse generator, EH Model 139, is part of the DTGTS. This unit has the capability of producing pulses with continuously variable frequency, amplitude, rise time, decay time, width, delay and baseline offset.

Beacon Reply Counter: The Beacon Reply Counter (BRC) is a device which can count beacon replies each interrogation period and provide a direct recording of the distribution of the occurrence of the beacon replies. The replies counted can be synchronous or non-synchronous (fruit) or a combination of both. Decoded replies or raw video pulses can be counted. The output recording is an analog representation of counts per interrogation.

Referring to the Block Diagram of Figure 4-3, a radar pre-trigger or a beacon sync trigger or any other range-reference trigger is applied to the Beacon Decoder.

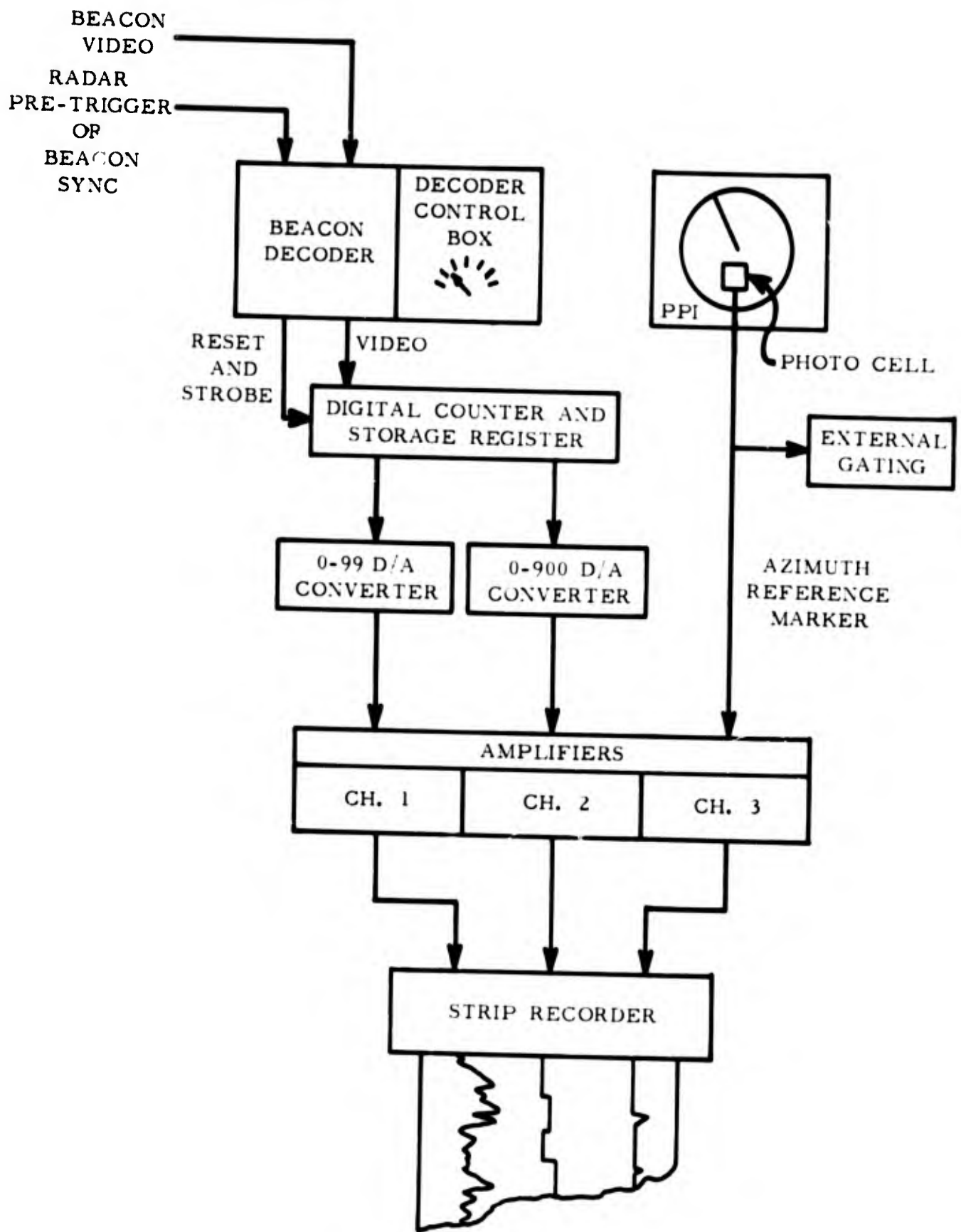


FIG. 4-3 BEACON REPLY COUNTER BLOCK DIAGRAM

Beacon video is also applied to the Beacon Decoder. With the use of the Decoder Control Box, any one of several decode functions can be performed. The decoder can be set to produce a single pulse output for each bracket decode; or it can be set to produce a single pulse when any particular beacon code has been decoded; or it can be set to simply pass on the raw video as it was received.

When a pre-trigger occurs at the beginning of an interrogation period, a strobe gate is generated which disables the input to the counter. At the end of the strobe gate, a pulse is generated which resets the entire counter. After the reset, the input to the counter is enabled and each pulse from the video output of the Beacon Decoder is counted. It continues to count until the next pre-trigger occurs at which time the strobe gate is again generated to disable the counter input. An even more important function of the strobe gate is to strobe the contents of the counter, in parallel, into a storage register. This storage register will hold the count until it is changed at the end of the next interrogation period. As previously described, the counter itself is reset at the end of the strobe gate.

The first two decades of the storage register, representing counts from 0 to 99, are connected directly to a Digital-to-Analog (D/A) Converter. The third decade of the storage register, representing counts from 0 to 900 in steps of 100, is connected to a separate D/A Converter. Each of the analog voltages is amplified separately and applied to a strip recorder which produces a calibrated record of the count. The hundreds digit is recorded separately from the units and tens so that the unit counts are discernible on the output recording.

An Azimuth Reference Marker is necessary and can be provided externally or it can be derived from a photo cell placed on the face of the cathode ray tube of a Plan Position Indicator as shown in the block diagram. Each time the sweep scans past the photo cell, the Azimuth Reference Marker is generated. This is recorded directly at the output or used to control the counter input. An auxiliary function of the Azimuth Reference Marker is to activate a relay once each antenna scan. This relay can be used to trigger a scope camera or any other external device requiring azimuth reference information.

The configuration described provides a recording of the beacon replies received each interrogation period. For each revolution of the antenna, the recording shows the azimuthal distribution (of the beacon replies) that exists.

An accumulation function can be actuated by push-button. This function provides an accumulation of the beacon reply counts each interrogation period for each antenna revolution. Distribution information can also be extracted from this kind of recording. The accumulation is performed by inhibiting the reset function and gating the input to the counter with the Azimuth Reference Marker. The counter is held reset until the Azimuth Reference Pulse occurs, at which time the reset is removed and the counter input is enabled. The counter functions until the Azimuth Reference Marker again occurs and the counter is reset and disabled. The recording produced is an accumulation of beacon replies for exactly one antenna revolution.

The counter/recorder configuration is easily calibrated. A CALIBRATE push-button control connects the pre-trigger input to the counter. The reset function is inhibited but the strobe gate is still generated. The net result is that the counter will count through its entire capacity (0 to 999), being strobed after each count and continue to repeat the cycle. The output recording shows two staircase functions, one composed of unit counts from 0 to 99 and the other composed of hundred counts from 0 to 900. These can be calibrated on the output recording by adjusting the gain of the amplifiers.

Digital Data Recorder: The Digital Data Recorder accepts RVDP output data in digital form from the Data Transmission Group (DTG) and provides a magnetic tape recording which can be used to produce a hard copy print-out. The system also has a direct print-out capability limited to one test target per scan without the necessity of intermediate magnetic-tape recording. The system block diagram is shown in Figure 4-4.

The Record Group has the direct interface with the DTG. When activated, clock pulses are supplied to the DTG for shifting data into the Record Group. These data are then recorded on magnetic tape.

The Playback Group accepts the stored data from the magnetic tape readout and separates each portion of the message into registers in preparation for decoding and programming. To do this, decode functions for message types are performed. The message types are beacon, search, system status, map outline, or special character. It is at this point where specific message types can be selected for print-out.

In the Beacon and Search Programmer, each portion of the message is decoded and the signals to initiate print-out of the decoded

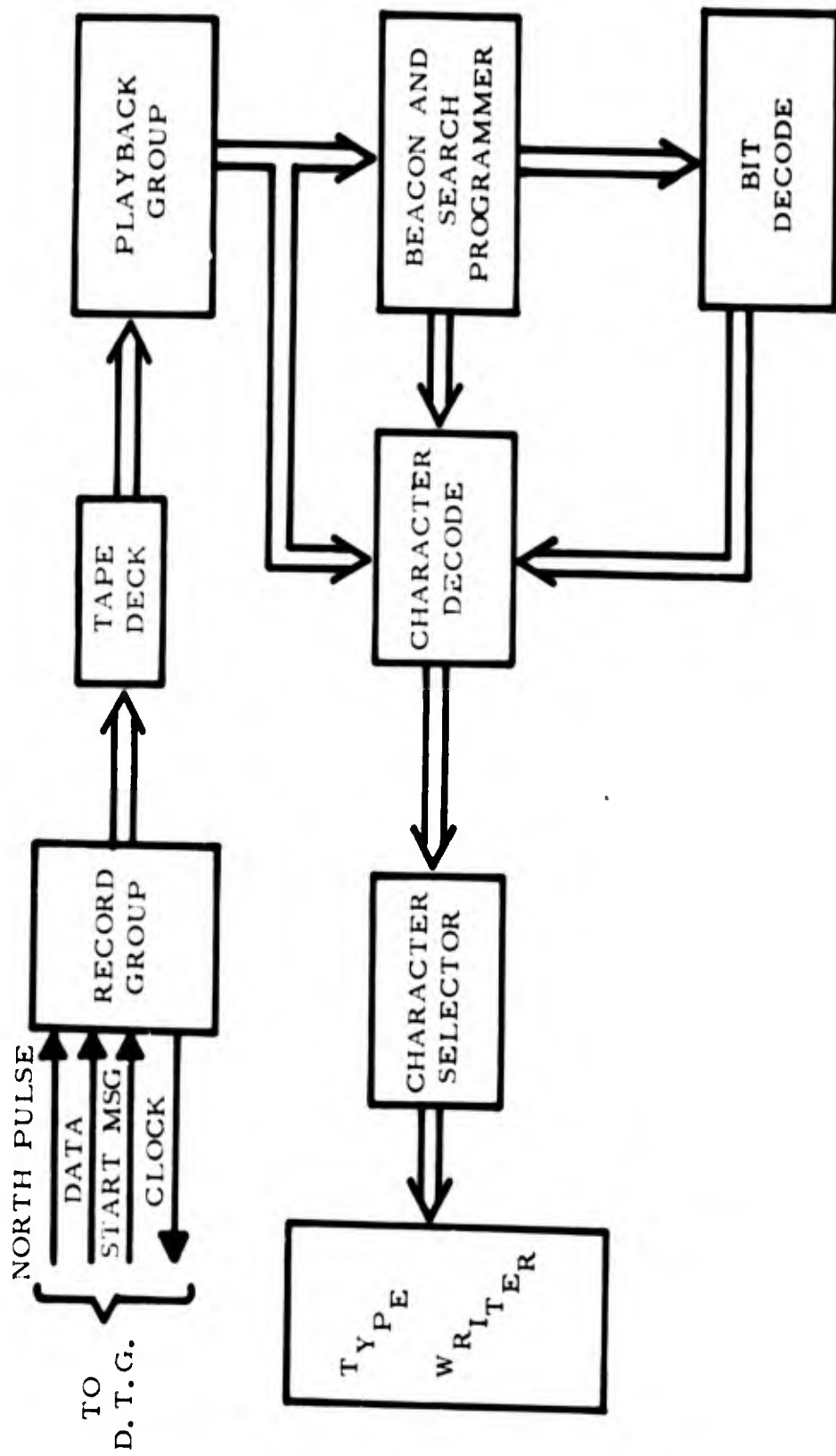


FIG. 4-4 DIGITAL DATA RECORDER BLOCK DIAGRAM

information are generated. The decode function also includes parity checks of the message as it is received and processed.

The Bit Decode and Character Decode are actually part of the Beacon and Search Programmer. The Beacon and Search Programmer provides all the control functions such as character selection and timing for message decode while the Bit Decode and Character Decode perform the actual decode functions for the information contained in the message. Specific beacon codes can be selected for print-out.

The Character Selector provides the interface between the decoded information and the typewriter. The proper keys are activated in response to received decoded signals.

Range Tracker Equipment: The range tracker was an interrogator-transponder system that was used to measure the slant-range separation between two aircraft during the range and azimuth-resolution tests. The system consisted of an ARN-21B interrogator, an APR-9 receiver, and the ranging and tracking portions of a prototype radar system that were installed in one aircraft; and a modified APX-6 transponder that was installed in another aircraft. A photograph of the interrogator/receiving/tracking portion of the system is shown in Figure 4-5.

The ARN-21B interrogator transmitted a pair of pulses that were received by the APX-6 transponder, which had been modified to shape the video pulses and alter the time interval between the pulses as required by the decoder. This modification enabled the APX-6 to respond to the leading edge of the second ARN-21 pulse. Upon receiving the reply pulse from the APX-6, the APR-9 receiver provided a video pulse to the range-tracking circuits of the AN/BPN-1 tracker. The time interval between the second ARN-21B pulse and the video pulse at the APR-9 was used to measure the range between the two aircraft. A flip-flop circuit was used in conjunction with a blocking oscillator to permit the second pulse of the ARN-21 pulse pair to provide the synchronizing pulse to the tracking equipment. The range-track and range-delay units, originally part of a ground-based missile guidance system, provided a two-scale time-measuring system. Coarse range measurements were made by use of range marks having a spacing of 10 nautical miles; and a phantastron-type delay circuit was used to obtain fine range measurements between the range marks. Error signals from a time discriminator were used to control a servomotor that provided automatic range tracking. Range was read as a function of the servomotor shaft which was coupled to numerical counters at the photopanel.

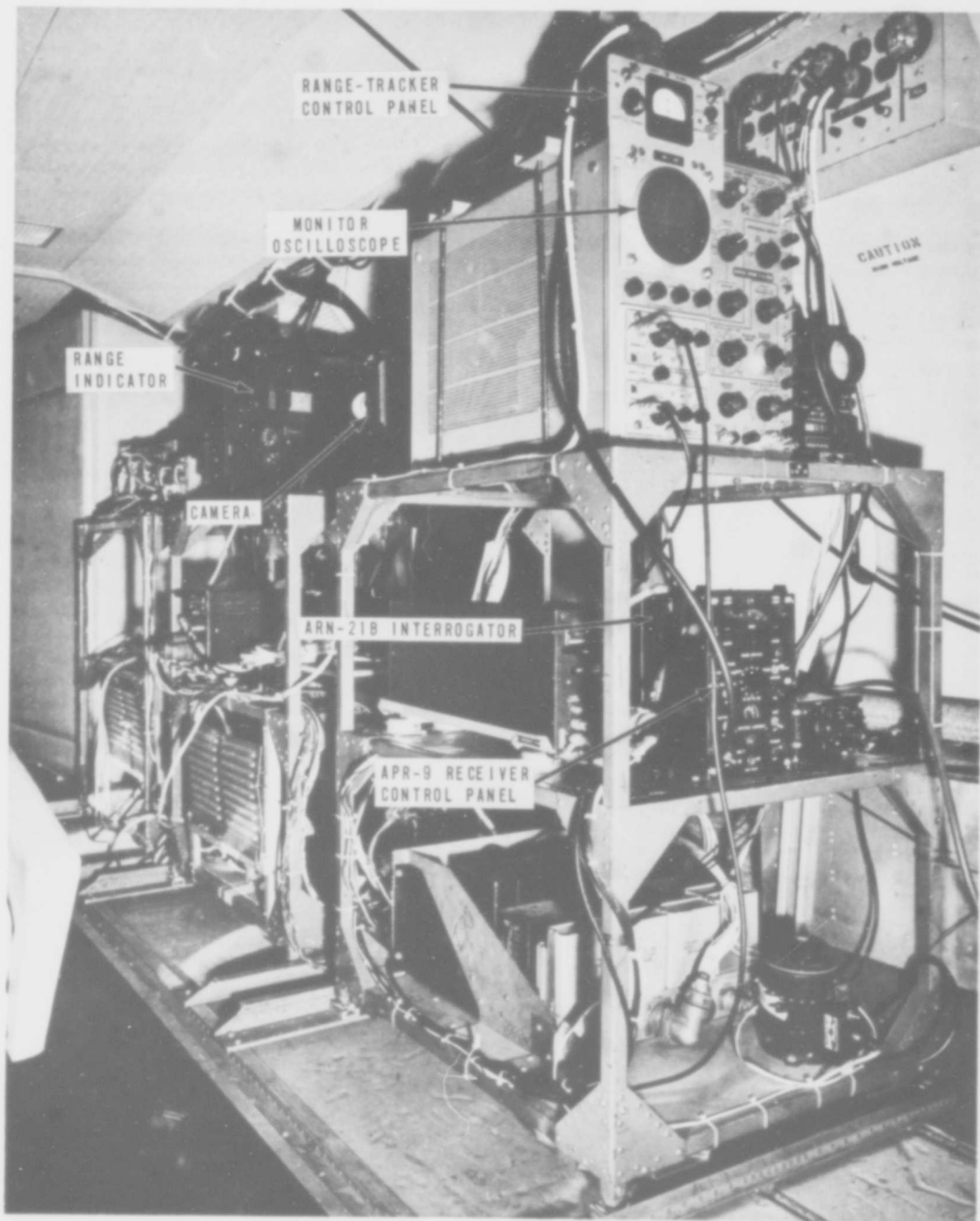


FIG. 4-5 RANGE TRACKER EQUIPMENT

Calibration of the equipment was accomplished using the Phototheodolite system at NAFEC. The rms error in slant range of the calibration runs made on January 28, 1963, ranges from approximately +15 feet for the run made at the nominal 1/2 nautical mile range to approximately +70 feet for the run made at the nominal 4 nautical mile range.

### Support Facilities

Extended Area Instrumentation Radar (EAIR): The EAIR facility at NAFEC was used to obtain target position data which constituted the reference when determining the range and azimuth accuracy as reported by the RVDP.

The EAIR facility is comprised of a Precision Instrumentation Radar, Polar to Cartesian Coordinate Converter, X-Y, X-H Plotting Board, Digital Data Computer, and a Magnetic Tape Recorder. The Precision Instrumentation Radar is capable of automatic tracking of a specific target and provides the slant range, azimuth angle, and elevation angle of the target. The specified slant-range accuracy is 20 yards and the specified azimuth angle accuracy is within 0.2 mil (0.011 degrees). Time-of-day data were recorded simultaneously with target-position data on magnetic tape in a format that was compatible for processing by an IBM 7090 computer.

Computation Facility: The RVDP messages obtained at the output of the DRG were recorded on magnetic tape by a general purpose digital computer (Computer Controls Corporation, Type DDP-24). This computer was part of a simulated radar digitizer system which provided an output compatible for processing by an IBM 7090 computer. The NAFEC time-of-day reference was also recorded to permit time correlation, later, when comparing target-position data, as reported by the RVDP, to target-position data that were obtained by the EAIR facility.

Track Analysis and Display Program (TAD) - The TAD program was used to extract specific RVDP messages from the magnetic tape recording performed by the general purpose digital computer. The TAD program is a modified version of a computational system (STARE) that was developed by MITRE for use in the evaluation of the FST-2 radar digital detector.

The TAD program (written for the IBM 7090 computer) is capable of displaying the recorded output of the RVDP plus certain

light gun switches on an IBM 780 Cathode Ray Tube. The operator can select appropriate light gun switches to perform desired data editing and track selection. The selected data are available for print-out or for further computer processing at the termination of the TAD program.

RVDP-EAIR Comparison Program - Further analysis of RVDP messages was accomplished by an IBM 7090 program which compared the target-position data within each RVDP message to the target-position data reported by the EAIR facility. For each RVDP message, a printout indicated the difference between RVDP and EAIR in reporting the range and azimuth of the target. For all messages that were selected by the TAD system, the program provided statistical summary data, i. e., number of samples, mean deviation, and standard deviation of the RVDP messages.

Flight Test Laboratory: To obtain a display of targets associated with the RVDP messages, the output of the DRG was applied to Radar Bright Display Equipment (RBDE-5) via a Data Filter Group (DFG):

The DFG was designed to provide an ATC specialist with the means to identify radar targets (based on beacon-reply codes) and inhibit information not desired at the operational displays. During this project, utilization of the DFG was limited to its coordinate-conversion function, which changed the digital Rho-Theta message into a digital X-Y message.

The RBDE-5 equipment converted the digital X-Y message received from the DFG to analog X-Y voltages for deflection of the write beam of the scan converter tube. The output of the RBDE-5 (TV scan) was displayed on two 22-inch displays and one 16-inch display in the flight test laboratory. The 22-inch displays were observed by ATC specialists during the sensitivity and resolution tests. The 16-inch display was equipped with 35-millimeter cameras to obtain photographs that could be analyzed to obtain accuracy data.

Adjacent to each of the above displays was an equivalent-size display which presented radar data that had been remoted via the Radar Microwave Link (RML-4). Figure 4-6 is a photograph of the control/display area and Figure 4-7 is a block diagram showing the data collection points.

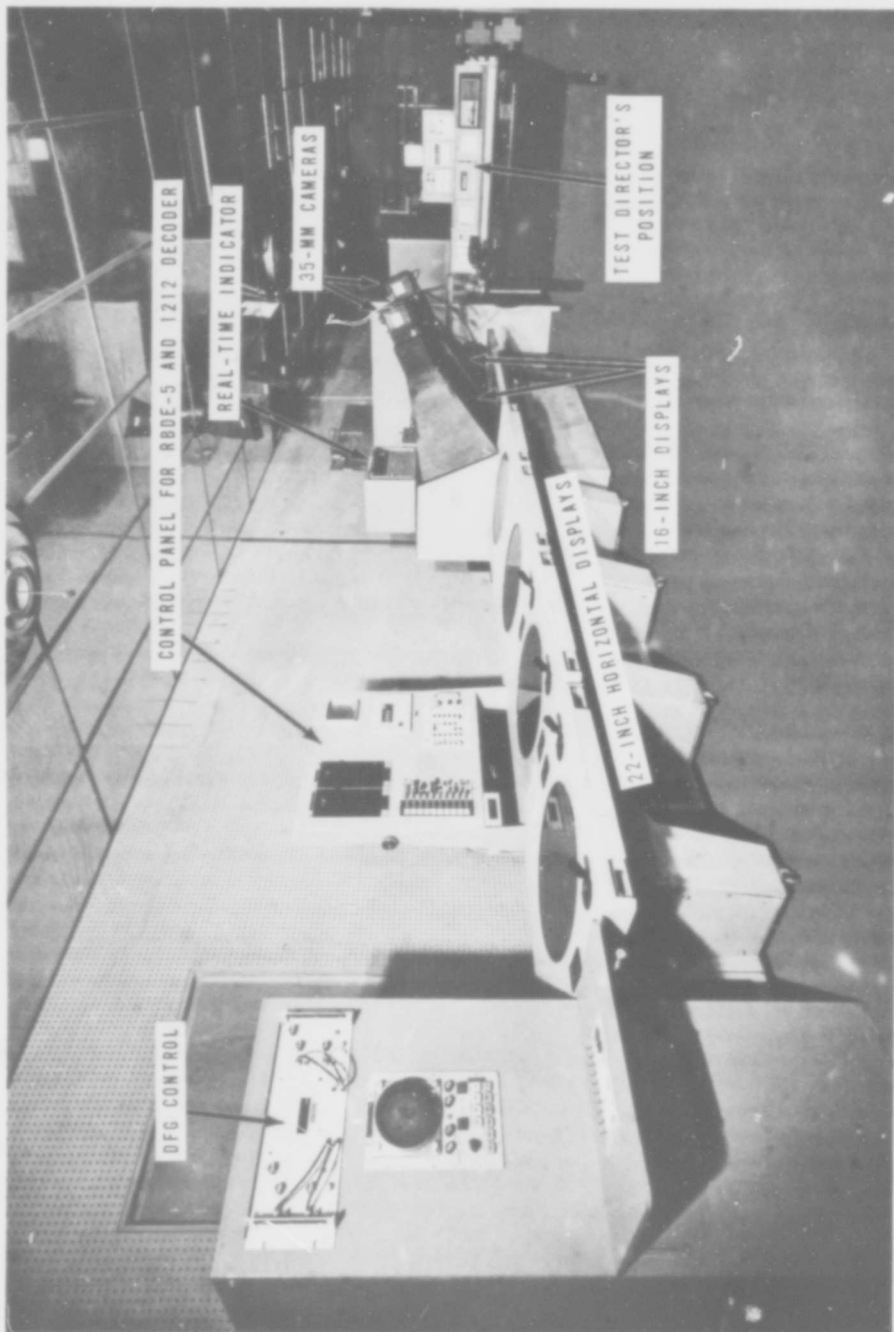


FIG. 4-6 PHOTOGRAPH OF CONTROL/DISPLAY AREA

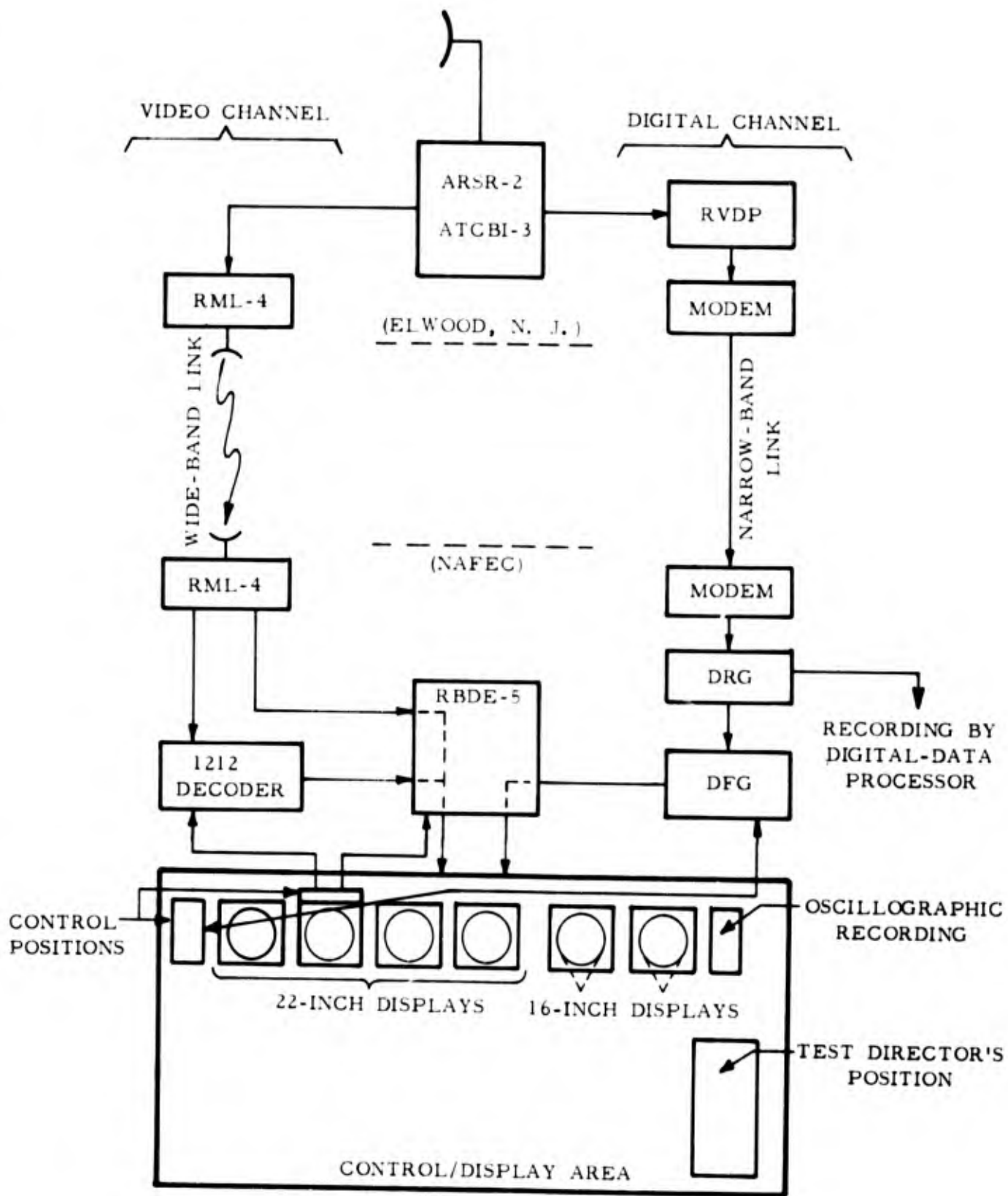


FIG. 4-7 BLOCK DIAGRAM OF THE DIGITAL CHANNEL, THE VIDEO CHANNEL, AND THE DATA COLLECTION POINTS FOR FLIGHT TESTS

The flight test laboratory also contained the remote-control positions for equipment associated with the digital and video channels. Communications to the radar site, NAFEC test-control laboratory, and the computer data-collection facility were available from this flight test laboratory.

### Test Flight Procedures

1. **Date of Flight:** January 24, 1966  
**Purpose:** Range Resolution  
**Aircraft:** N376 and N377  
**Route:** Shuttle on the ACY 154 radial, between the ACY 40 -mile and 70-mile DME fixes.  
**Procedure:** N376 follows N377 throughout the flight at distances specified during pilot briefing (0.15 to 1.25 nmi)  
**Altitude:** N377; 15,000 feet. N376; approximately 500 feet below N377 for each mile of separation between aircraft.  
**Mode A/3 Reply Code:** N376; 0622. N377; 0644.
  
2. **Date of Flight:** January 25, 1966  
**Purpose:** Probability of Detection; Radar Beacon  
**Aircraft:** N377  
**Route:** Shuttle on the SIE 142 radial between ARSR-2 ranges of 200 and approximately 140 miles  
**Altitude:** 26,000 feet  
**Mode A/3 Reply Code:** 2144 and 1144
  
3. **Date of Flight:** February 3, 1966  
**Purpose:** Azimuth Resolution; Primary Radar  
**Aircraft:** N376 and N377  
**Route:** Shuttle on the ACY 35-mile DME arc between the ACY 120 and 180 radials  
**Procedure:** N376 follows N377 throughout the flight at distances specified during pilot briefing. (0.9 to 2.8 nmi)  
**Altitude:** N377; 15,000 feet. N376; approximately 500 feet below N377 for each mile of separation between aircraft.  
**Mode A/3 Reply Code:** N376; 0622. N377; 0644.

4. Date of Flight: February 7, 1966  
 Purpose: Azimuth Resolution; Radar Beacon  
 Aircraft: N376 and N377  
 Route: Shuttle on the ACY 35-mile DME arc between the ACY 120 and 180 radials.  
 Procedure: N376 follows N377 throughout the flight at distances specified during pilot briefing (0.9 to 10.6 miles).  
 Altitude: N377; 15,000 feet. N376; approximately 500 feet below N377 for each mile of separation between aircraft.  
 Mode A/3 Reply Code: N376; 0622. N377; 0644.
5. Date of Flight: February 8, 1966  
 Purpose: Probability of Detection; Primary Radar  
 Aircraft: N377  
 Route: Shuttle on the SIE 142 radial between ARSR-2 ranges of 200 and approximately 140 miles  
 Altitude: 26,000 feet  
 Mode A/3 Reply Code: 0644
6. Date of Flight: February 9, 1966  
 Purpose: Probability of Detection; Primary Radar and Radar Beacon  
 Aircraft: N376  
 Route: Shuttle on the ACY 140 radial between ARSR-2 ranges of 200 miles and approximately 140 miles.  
 Altitude: Run #1: Outbound 28,000 ft.; Inbound 27,000 ft.  
 Run #2: Outbound 26,000 ft.; Inbound 25,000 ft.  
 Run #3: Outbound 26,000 ft.; Inbound 27,000 ft.  
 Run #4: Outbound 27,000 ft.; Inbound 26,000 ft.  
 Mode A/3 Reply Code: 0622
7. Date of Flight: February 11, 1966  
 Purpose: Accuracy; Primary Radar and Radar Beacon  
 Aircraft: N247  
 Route: Radials and arcs southeast of ACY between the ACY 154 and 110 radials, at various ranges to a maximum of 80 miles from ACY.  
 Altitude: 15,000 feet  
 Mode A/3 Reply Code: 0433

8. **Date of Flight:** February 28, 1966  
**Purpose:** Code Validation, Radar Beacon  
**Aircraft:** N376  
**Route:** Shuttle on the ACY 140 radial between  
ARSR-2 ranges of 200 and approximately  
140 miles  
**Altitude:** 26,000 feet  
**Mode A/3 Reply Code:** 0622

NOTES:

1. **Aircraft:** N376 - Grumman Gulfstream (G159)  
N377 - Grumman Gulfstream (G159)  
N247 - Convair (ET-29C)
2. **Navigation Aids:** ACY - Atlantic City, N. J. (VORTAC)  
SIE - Sea Isle City, N. J. (VORTAC)
3. **All directions and radials are referenced to magnetic north; all distances are in nautical miles. All altitudes in oceanic area were in reference to standard altimeter setting of 29.92" Hg.**

## APPENDIX V

### BEACON SYSTEM DESCRIPTION

The Air Traffic Control Radar Beacon System consists of airborne transponders and an interrogator, which may or may not be associated with, or slaved to, a primary surveillance radar. In operation, an interrogation pulse-group transmitted from the interrogator-transmitter unit, via a directional interrogator-antenna assembly, triggers each airborne transponder located in the direction of the main beam, causing a multiple-pulse reply group to be transmitted from each transponder. These replies are received by the ground interrogator-receiver. Measurement of the round-trip transit time determines the range to the replying aircraft while the mean direction of the main beam of the interrogator-antenna, during the reply, determines the azimuth. The nature of the multiple-pulse reply provides individualized information pertaining to the responding aircraft.

#### The Interrogation Function

The interrogation consists of two transmitted pulses designated P1 and P3. An additional pulse, P2, is transmitted via an omni-directional antenna immediately following the first interrogation pulse P1. The P2 pulse is used for amplitude comparison with the P1 pulse by the transponder to prevent side-lobe interrogation. The interrogation pulse pair interval and the relative position of the P2 pulse are shown in Figure 5-1. Also shown are the relative signal levels and coverage for side-lobe suppression.

#### The Reply Function

The beacon reply function employs a signal composed of two framing or bracket pulses spaced 20.3 microseconds measured leading edge to leading edge at the .5A points described in Figure 5-2. Between the two bracket pulses are 13 data-pulse positions, spaced in multiples of 1.45 microseconds. In a given reply, a pulse can occur in any position. An additional pulse position exists in which the Special Position Identification (SPI) pulse can occur. The SPI pulse follows the leading edge of the F2 bracket pulse by 4.35 microseconds, with a tolerance of  $\pm 0.1$  microsecond in respect to the leading edge of any other pulse in the train.

An idealized pulse-train reply is shown in Figure 5-2. Pulse spacing, pulse shape, and pulse designations are illustrated.

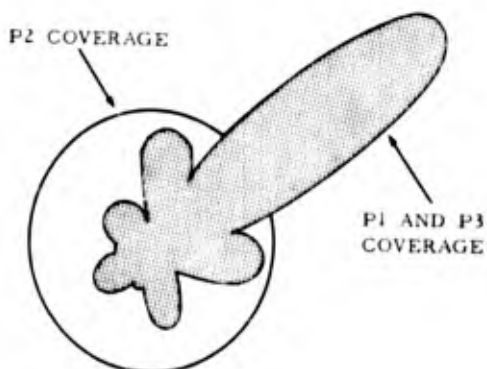
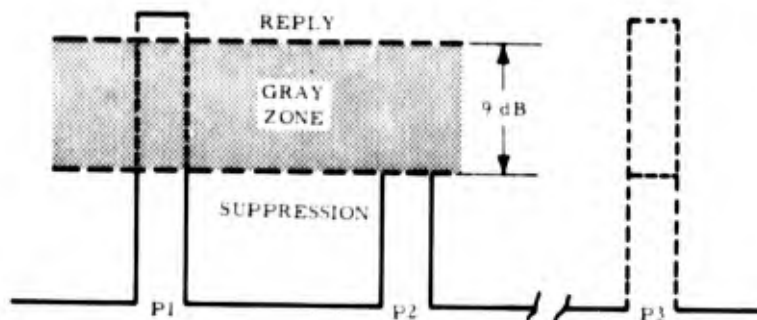
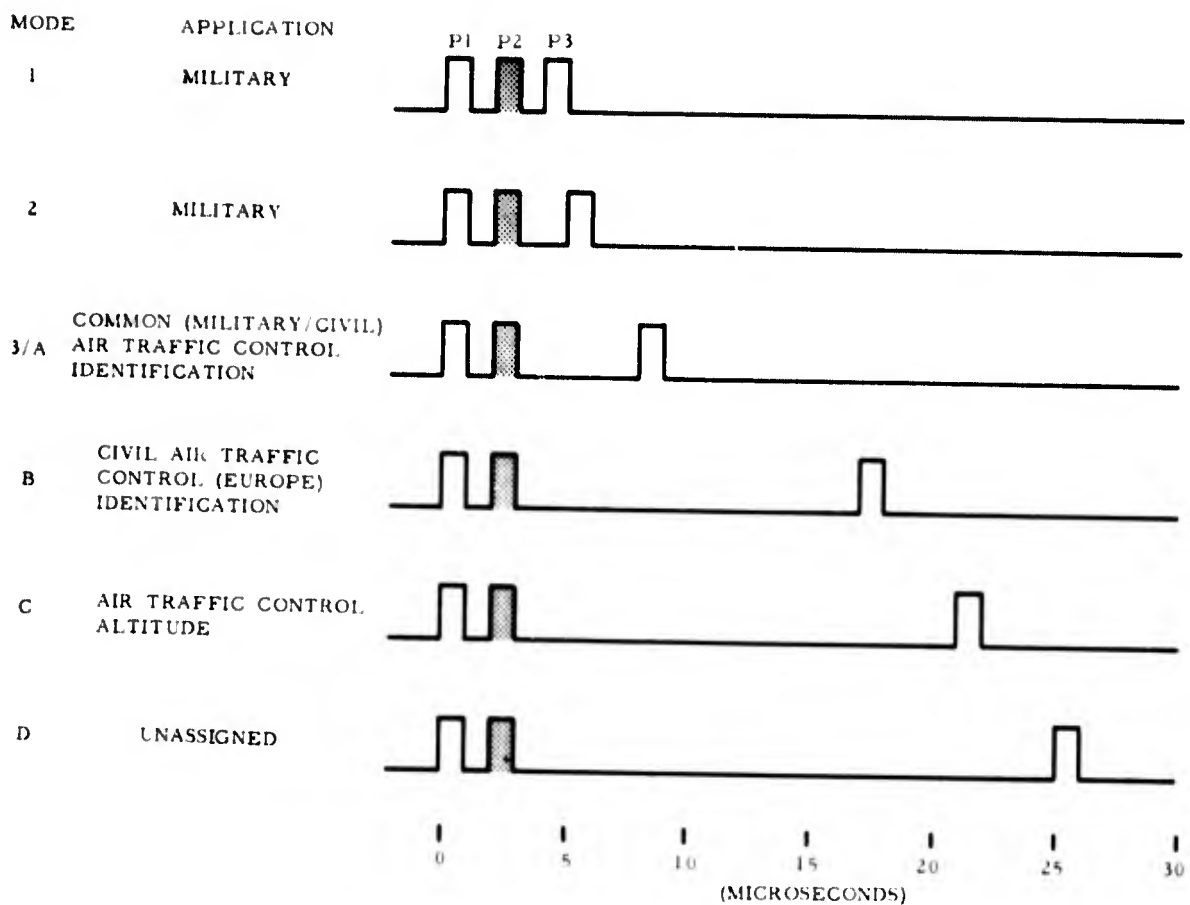


**FIG. 5-1 BEACON INTERROGATION PULSE PAIR INTERVALS AND SIDE LOBE SUPPRESSION OPERATION**



Transponders respond to the various interrogation pulse pairs, or modes, but not all transponders are equipped to respond to all modes. The modes of interest in the RVDP are: mode 2, mode A/3, and mode C. Mode 2 is the military Mark X (SIF) mode. Mode A/3 is a type of identification mode to which either civil (mode A) or military (mode 3) transponders can reply. Mode C is the altitude interrogation mode. The form of the data received from either a mode 3 or a mode A transponder is the same except for the emergency and IDENT replies. An SPI pulse may be included in the reply received during mode A/3 interrogations. In mode A replies, the SPI pulse is present when the IDENT switch on the aircraft transponder is depressed. In mode C replies, the SPI pulse position is used as a code-pulse position.

An IDENT reply from some military transponders is represented by two identity code-pulse trains containing the same code. The first bracket pulse of the second pulse train appears in the SPI pulse position of the first pulse train; i. e., the first bracket pulse of the second pulse train occurs 4.35 microseconds after the second bracket pulse of the first pulse train, measured from leading edge to leading edge.

Mode A/3 Replies: In mode A/3 replies, A, B, C and D denote octal numbers, with A as the most-significant digit and D the least-significant digit. The number A (in octal code) is equal to the sum of the subscripts of the "A" pulses which are present for any given reply. For example:

1. Code 3600 would consist of information pulses A1, A2, B2, B4. No "C" or "D" pulses would be present.
2. Code 2157 would consist of pulses A2, B1, C1, C4, D1, D2, D4.

Two of the mode A/3 code designations are reserved for special purposes: 7700 is designated "Emergency" reply and 7600 is designated "Radio Communication Failure." The emergency reply from military transponders is represented by four pulse trains of the same code. The first pulse train of the group may sometimes be code 7700. The first bracket pulse of the second, third, and fourth pulse trains appears in the SPI pulse position of the first, second, and third pulse trains, respectively; i. e., the first bracket pulse train occurs 4.35 microseconds after the second bracket pulse of the preceding pulse train, measured from leading edge to leading edge.

Mode 2 replies: The military mode 2 replies have the same form of pulse position and designation as mode A/3. However, the grouping for octal decoding is not the same. The presence of the "X" pulse in mode 2 replies designates a special military function.

Mode C replies: Mode C is the altitude interrogation mode. Only those transponders having the capability can reply to this interrogation mode with altitude reporting. In mode C replies, the height reply data are in ICAO automatic pressure-height transmission code. The code consists of two sections, coarse and fine. The coarse section indicates altitude up to 126,500 feet, in 500-foot increments and is a reflected code. The fine section increases resolution up to 100 feet. Aircraft transponders may reply in the 500-foot increment code or the 100-foot increment code.

**BLANK PAGE**

## APPENDIX VI

### BEACON FRUIT ENVIRONMENT

To test the RVDP using controlled simulated beacon input signals, it was necessary to produce these input signals in a simulated environment that resembled the actual environment as closely as possible. The environment, within which valid beacon replies are present, consists of non-synchronous (fruit) replies of various densities. The previous method of measuring the amount of fruit that exists in the coverage area of a site was to count the number of replies (non-synchronous) each revolution of the antenna. From this a figure of "fruit density per scan" was obtained. Although this kind of information may have some limited use, it is not adequate to fully describe the live environment that exists and may, in some cases, be quite erroneous. The occurrence of fruit is not evenly distributed over the area of coverage, as counts per scan implies, but is concentrated in specific areas. The heaviest concentrations usually appear around airports and along heavily-traveled airways. Figure 6-1 shows this tendency of fruit concentration in specific areas. The total fruit count shown is 15,212.

The importance of information on the distribution of fruit and the density in specific areas is clear when the data-handling capability of the processor is considered. The processor must be capable of handling the highest target and fruit density that can occur at a site. This highest density cannot be obtained by counting fruit per scan because this number does not represent the highest density that occurs within the coverage of the antenna.

The Beacon Reply Counter (BRC) was designed and built to count beacon replies each interrogation period and provide a direct recording of the distribution of the occurrence of the beacon replies. The replies counted can be synchronous or non-synchronous or a combination of both. Decoded replies or raw video pulses can be counted. When reference is made to fruit counts in this report, this implies that bracket-decoded non-synchronous replies are counted. The output of the BRC is an analog representation of counts per interrogation. The BRC is described in detail in Appendix IV.

Recordings of bracket-decoded undefruited video (targets and fruit) and bracket-decoded defruited video (targets only) distributions were obtained at the Elwood, N. J., ATCBI-3 site for a twenty-day period.

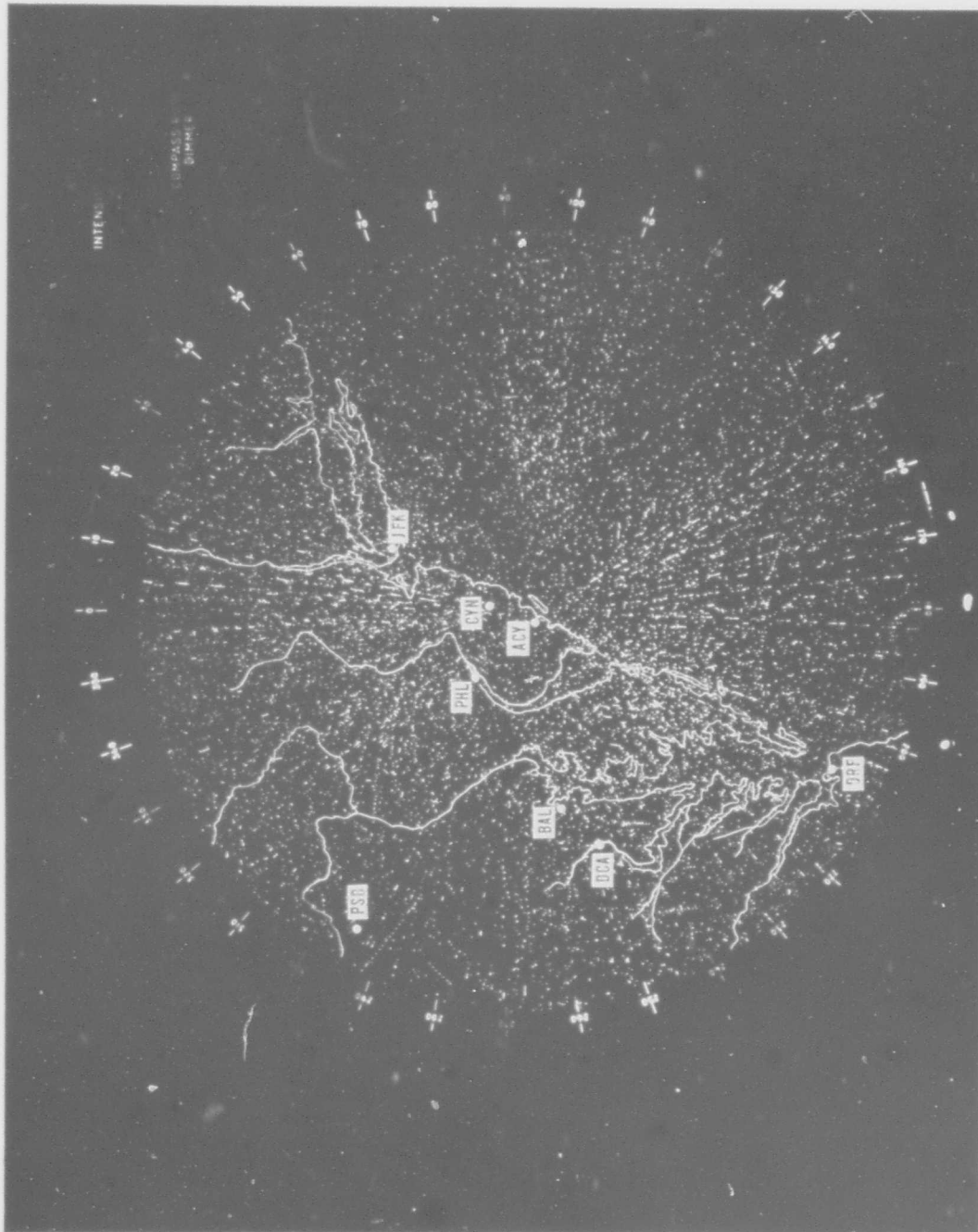


FIG. 6-1 FRUIT ENVIRONMENT IN THE AREA OF COVERAGE FOR ELWOOD, N. J.

These recordings include periods of peak traffic. Figure 6-2 shows one of the azimuthal distributions of defruited and undefruited video obtained during the twenty-day period. The BRC was taken to Palermo Air Force Station, located approximately 16 miles southwest of NAFEC, where recordings were made to verify the counts and distributions that were obtained at Elwood. Figure 6-3 shows one of the distributions obtained at Palermo.

Figure 6-4 shows the average of the distributions of undefruited video at Elwood for the twenty-day period.

It is quite evident from Figures 6-2, 6-3 and 6-4 that the highest concentrations of targets and fruit occur in the vicinity of airports and along airways.

The highest count of bracket-decoded undefruited video for a four-degree sector (effective beam width) that was recorded during the entire test period was 956. This represents the highest density of beacon replies that the processor would have had to handle. This density, integrated over the entire scan, would represent 86,040 replies per scan. Therefore, when the simulated environment was produced for beacon testing of RVDP, an average fruit density of approximately 100,000 replies per scan was generated so that the simulated environment would resemble the highest density encountered at the site.

It was also determined from the fruit count data that during the test flights a beacon target leading edge criteria  $T_L$  setting of 6 was to be used. This would provide a high probability of detection and probability of code validation, while maintaining a low probability of false-target detection.

#### Near-Synchronous Replies

At various times during the test period an input signal consisting of fruit only (no interrogations) was applied to the RVDP. The output was monitored for the appearance of false targets that were declared. Whenever a false target occurred, recordings of the azimuthal distribution of fruit were made. The recordings were then analyzed to determine the fruit density within a four-degree sector centered about the azimuth at which the false target was declared.

It was determined that the fruit densities that were recorded at the azimuth of the false targets were not high enough to produce false targets

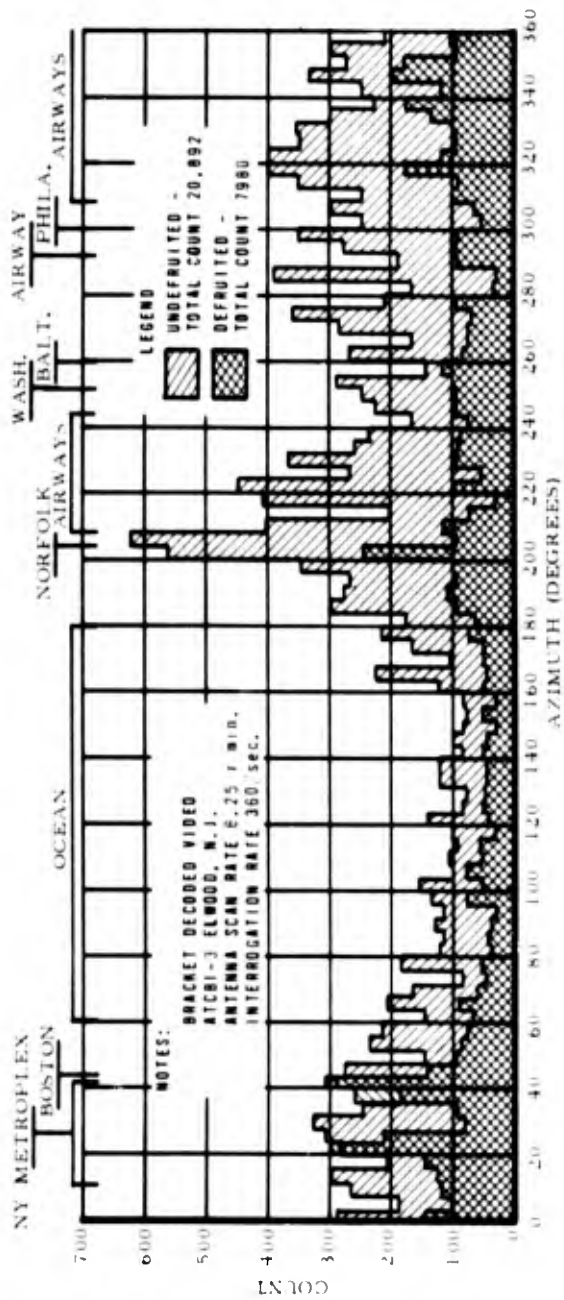


FIG. 6-2 AZIMUTHAL DISTRIBUTION OF BEACON REPLIES AT ELWOOD, N. J.

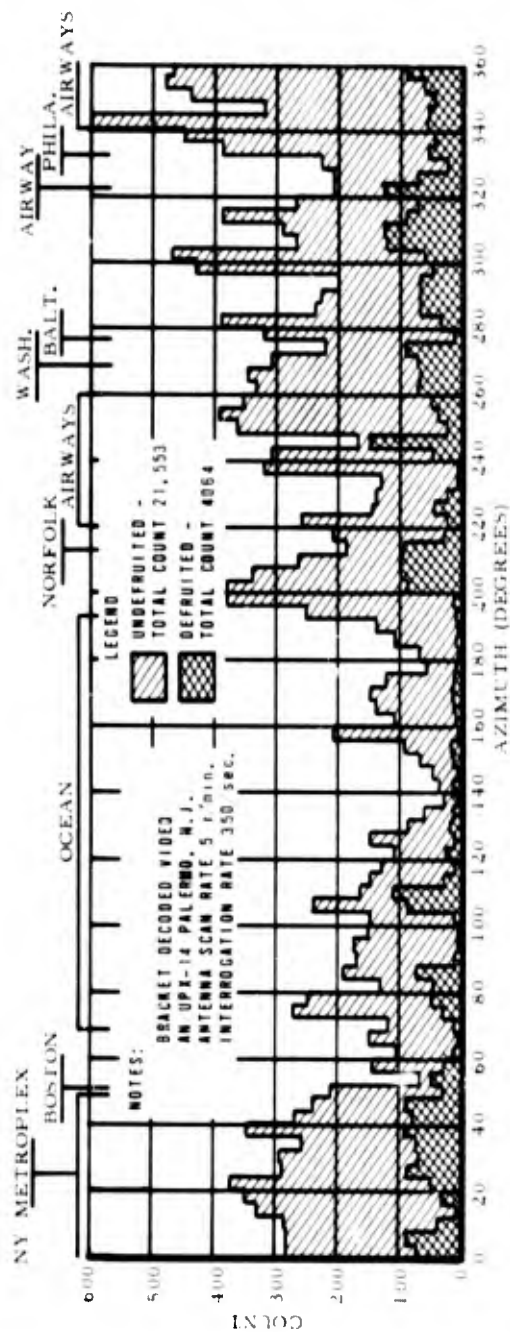



FIG. 6-3 AZIMUTHAL DISTRIBUTION OF BEACON REPLIES AT PALERMO, N. J.

NOTES:

BRACKET DECODED VIDEO  
 ATCBI-3 ELWOOD, N. J.  
 AVERAGE OF 20-DAY PERIOD  
 ANTENNA ROTATION 6.25 r/min.  
 INTERROGATION RATE 360/sec

LEGEND

 UNDEFRUITED -  
 TOTAL COUNT 18,322

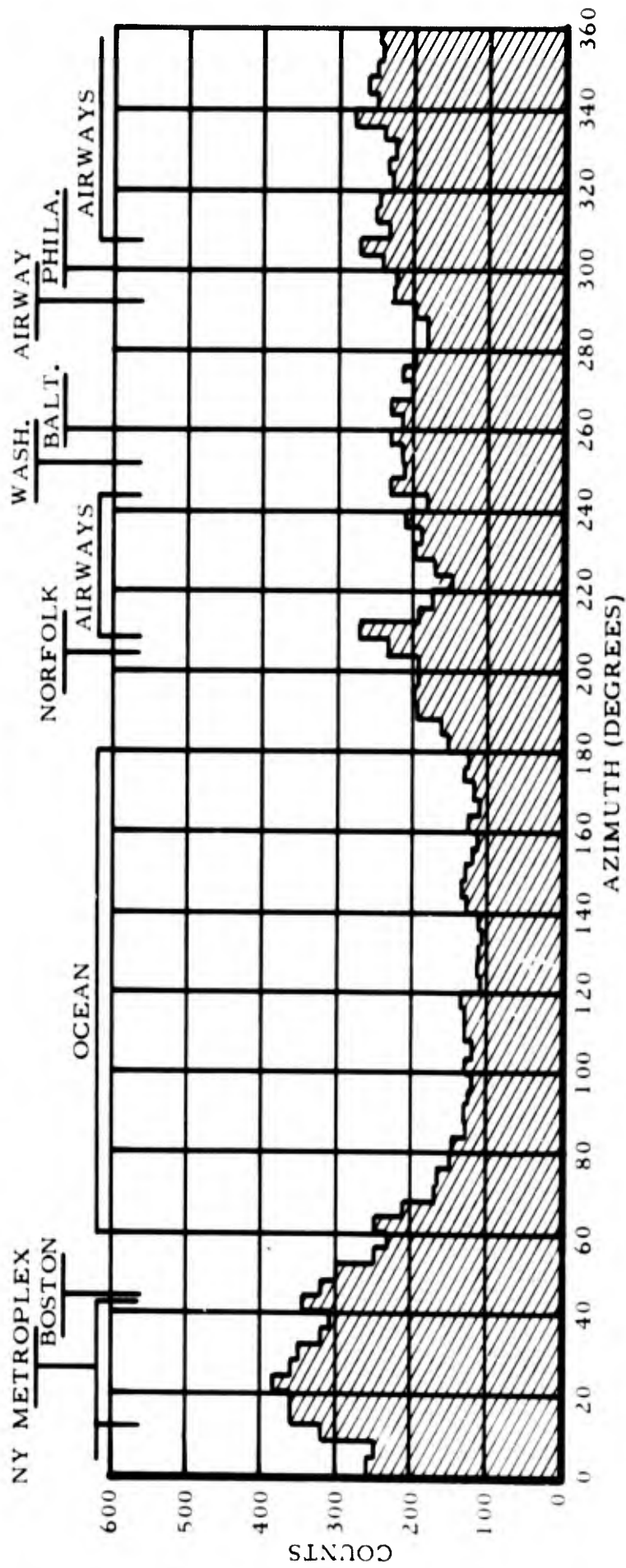


FIG. 6-4 AVERAGE AZIMUTH DISTRIBUTION OF BEACON REPLIES  
 AT ELWOOD, N. J.

if the fruit were assumed to be randomly distributed. However, as shown in Figure 6-1, this is not always the case. Near-synchronous targets appear and can sometimes be near enough in synchronism to be detected as a synchronous target. The data showed that the false targets were declared in low and high-fruit densities alike. No direct relationship could be determined between the occurrence of a false target and the density of fruit in the area within which it was declared. This supports the theory that they were produced as a result of near synchronism rather than a high density of randomly-distributed fruit.

## APPENDIX VII

### DERIVATION OF AZIMUTH BIAS AND RESOLUTION EQUATIONS

#### Target In-Process Run Length

Due to the run length stretching effect of the sliding-window detector, the target run length and the RVDP in-process run length are not identical.

Consider what happens at the output of the D/A converter where the hits in the sliding window are added. Figure 7-1 shows that the hits begin to accumulate

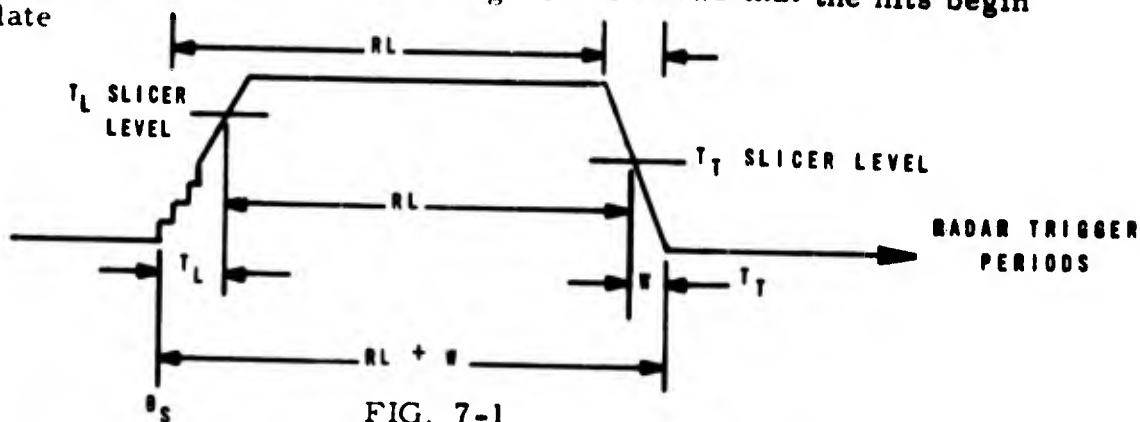


FIG. 7-1

in the sliding window at  $\theta_s$ , the start azimuth of the target. When the window is full, the D/A converter output remains constant until, at the end of the target run length (RL), zeros are shifted into the sliding window. At this time the hits in the sliding window begin to decrease until the window is empty and the D/A converter output falls to zero. At the time the  $T_L$  slicer reference is exceeded, the target is declared in-process and this bit is reset when the D/A converter output falls below the  $T_T$  slicer level. The RVDP azimuth calculation process and the run-length discrimination function utilize this in-process run length (rl). From Figure 7-1, it can be seen that

$$RL + W = T_L + rl + T_T, \quad (1)$$

where  $W$  = sliding window size. This expression may be solved for either the target run length (RL) or the in-process run length (rl) to convert from one quantity to another for any given window size and combination of leading and trailing edge parameters.

#### Azimuth Bias

While the actual target center azimuth in radar trigger periods is:

$$\theta_A = \theta_S + (1/2) RL, \quad (2)$$

the center azimuth reported by the RVDP ( $\theta_R$ ) occurs at the center of the in-process run length. Therefore,

$$\theta_R = \theta_S + T_L + 1/2 rl \quad (3)$$

Substituting from equation (1),

$$\begin{aligned} \theta_R &= \theta_S + T_L + (1/2) [RL + W - T_L - T_T] \\ \theta_R &= \theta_S + (1/2) RL + (1/2) W + (1/2) T_L - (1/2) T_T \end{aligned} \quad (3a)$$

From equations (2) and (3a), one can see that there is a difference between the reported center azimuth and the true target center azimuth.

This bias is:

$$\begin{aligned} \text{AZIMUTH BIAS} &= \theta_R - \theta_A \\ &= \theta_S + (1/2) RL + (1/2) W + (1/2) T_L - (1/2) T_T - \theta_S - (1/2) RL \\ \text{AZIMUTH BIAS} &= (1/2) [W + (T_L - T_T)] \end{aligned} \quad (4)$$

Thus, this bias is independent of geographical sector or the actual target run length.

#### Conversion from Radar Triggers to Azimuth Change Pulses

The foregoing discussion has been entirely in terms of radar trigger periods. The azimuth of a target is reported in Azimuth Change Pulses (ACP's), and the in-process run length count is maintained in ACP's, while the detection process and actual target run length are in terms of radar-trigger periods. Azimuth change pulses are pulses which are generated every 1/4096 antenna rotation and have a fixed relationship to radar trigger periods only if the radar antenna rotation speed is constant. The ARSR-2 antenna at the Elwood, N. J., site was protected by a radome and did rotate at a constant speed. The number of radar triggers counted per antenna rotation was 3,452. This count was found to be consistent throughout the test period.

In-process run length (equation 1) in ACP's is:

$$rl = K_1 [RL + W - T_L - T_T] \quad (5)$$

where  $K_1 = \frac{\text{ACP's per scan}}{\text{triggers per scan}}$

For the Elwood, N. J., site

$$K_1 = \frac{4096}{3452} = 1.186$$

Likewise, azimuth bias (equation 4) in ACP's is:

$$\text{Azimuth Bias} = (1/2) K_1 [W + (T_L - T_T)] \quad (6)$$

#### Azimuth Resolution

The condition for azimuth resolution is based on the premise that the first hit of the second target must not come before the first target is declared complete. Therefore,

$$\theta_{S2} - \theta_{S1} > RL + W - T_T \quad (7)$$

or, from (5)

$$\theta_{S2} - \theta_{S1} > T_L + \frac{rl}{K_1}$$

is a condition for azimuth resolution. This expression may also be used to define resolution in terms of the difference in center azimuth of two targets with identical run lengths.

#### Effect of Beacon Mode Interlace

Up to this point, it was assumed that the system was processing search or beacon single mode interrogation information.

Hits are transferred to the beacon sliding window only during primary (A/3) mode interrogation periods.

If a 3-mode interlace ratio (1:1:1) is used, the contents of the sliding window build up one third as rapidly as for single mode as shown in Figure 7-2.

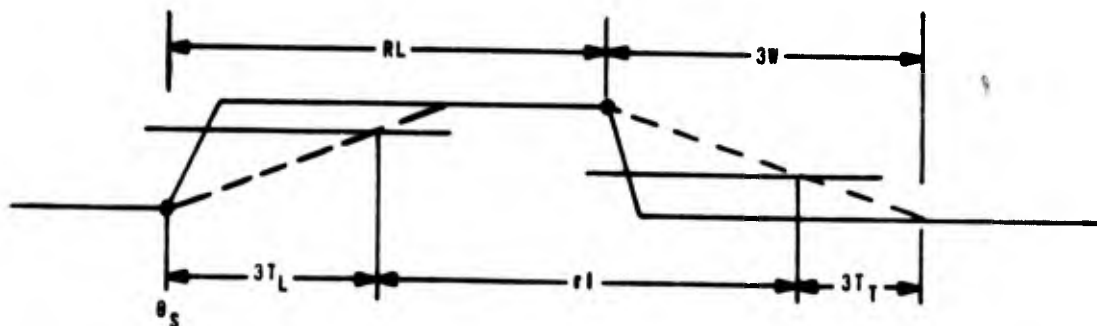


FIG. 7-2

Similar derivations lead to the following expressions:

$$rl = K_1 [RL + K_2 (W - T_L - T_T)] \quad (8)$$

$$\text{BIAS} = (1/2) K_1 K_2 [W + T_L - T_T] \quad (9)$$

$$\theta_{S2} - \theta_{S1} = \frac{RL + K_2 [W - T_T]}{rl} \quad (10)$$

where:

$$K_2 = \frac{\text{total no. of interrogations/mode interrogation cycle}}{\text{no. of primary mode interrogations/interrogation cycle}}$$

e. g.  $K_2 = 3$  for 3 mode (A/3:C:2)

$$K_2 = \frac{3}{2}$$
 for 2 mode (A/3:A/3:C)

$$K_2 = 2$$
 for 3 mode (A/3:C:A/3:2)

etc.

These derivations also hold true for the case where the target run length is less than the sliding window size.

It should be noted that all three quantities, azimuth bias in particular, vary with mode interlace ratio. Therefore, different azimuth presets are required when mode interlace configuration is changed.